A novel role for CaMKIIδ in modulating vascular inflammation in young and aged aortae

A thesis presented by

Claire McCluskey

In fulfilment of the requirements for the degree of

Doctor of Philosophy

September 2017

Acknowledgments

Firstly, I wish to thank my supervisor Dr. Susan Currie for her continuous support, patience and encouragement throughout my PhD. I can't emphasise enough how much I appreciate all that you have done for me – I really couldn't have asked for a better mentor. I would also like to offer my sincere gratitude to Dr. Andy Paul for always offering words of advice and reassurance over the last four years.

Special thanks also to Margaret MacDonald for her technical assistance with the *in vivo* work and for generally being a friendly face to turn to when I needed one! I'd also like to mention Graeme Mackenzie and all of the other technical staff who have continuously helped me throughout my PhD. Also, to Mark MacAskill and Adrian Thompson from Edinburgh University – thank you for your expert training and knowledge in helping me obtain my echocardiography measurements.

I could not have completed my PhD without all of the love and support from my family and friends. I would like to particularly mention my parents who have always encouraged me throughout my studies, even when things have been tough. I would mention all of my brothers and sisters individually but that list would be too long! You have all been so supportive though and I'm eternally grateful for that. I have made a number of good friends since starting my studies in SIPBS. One person who deserves a huge mention is Samantha White. We both started this journey together and I genuinely do not think I could have finished it without you! You are like an extension of my right arm now and I'm so happy that I've made a best friend for life! My other SIPBS 'bestie' who I owe a lot to is Nicola Woods – we kept each other sane even when we were experiencing 'overwhelming' moments and just wanted to cry in the toilets! You always offered me words of advice and helped keep me motivated but most importantly, we got to plan our weddings together during coffee breaks (before either of us were even engaged!)

Finally, my most important thank you goes to my fiancé Ross. You've put up with a LOT of tears and near-nervous breakdowns over the last four years, not to mention all of the practice presentations I've made you sit through in our living room. You have

been continuously supportive, reassuring and are most understanding best friend anyone could have - even if you do think CaMKII is grown in a test tube!

I dedicate this thesis to you all!

Publications

McCluskey, C. & Currie, S (2017) Alterations in endothelial calcium/calmodulin dependent protein kinase II during ageing may contribute to vascular dysfunction. *Mech. Ageing Devpt.* (In preparation/submitted)

Martin, T. P., McCluskey, C., Cunningham, M. R., Beattie, J., Paul, A & Currie, S (2017) CaMKIIδ interacts directly with IKKβ and modulates NF-κB signalling in adult cardiac and vascular cells. *J. Mol Cell Cardiol* (submitted).

McCluskey C., MacDonald M. & Currie S. (2017) Ageing of the vascular endothelium: a novel role for CaMKII delta? *Heart* 103, S2, A2

McCluskey, C., Paul, A. & Currie, S (2016) Calcium/calmodulin-dependent protein kinase II delta – does ageing mirror disease in the cardiovascular system? *FASEB J*, 30, no. 1, 767.3

Salleh M.M., McCluskey C., Bushell T.J. & Currie S. (2016) Inositol trisphosphate receptor contribution to ventricular cardiac fibroblast function in healthy and hypertrophied mouse hearts. *Faseb J. 30, no.1, 1178.2*

McCluskey, C., Paul, A. & Currie, S (2015) Pro-inflammatory signaling in vascular endothelium: a novel role for CaMKIIδ in ageing. *Heart 101* (Suppl 4) A100-A101.

Salleh, M. M., McCluskey, C., Bushell, T. J. & Currie, S (2014) CaMKIIδ modulates intracellular release and cell proliferation in adult cardiac fibroblasts. *Heart 100* (Suppl 4) A16.

Poster Communications

Experimental Biology Annual Meeting, San Diego, 2016. McCluskey, C., Paul, A. & Currie, S. Calcium/calmodulin-dependent protein kinase II delta – does ageing mirror disease in the cardiovascular system?

Scottish Cardiovascular Forum Annual Meeting, Belfast 2016. McCluskey, C., Holland, I., McCormick, C., MacDonald, M. & Currie, S. Assessing functional and phenotypic alterations in the aged heart and vasculature.

Scottish Cardiovascular Forum Annual Meeting, Edinburgh 2015. McCluskey, C., Paul, A. & Currie, S. Pro-inflammatory signalling in vascular endothelium: A novel role for CaMKII in ageing?

British Society for Cardiovascular Research Annual Meeting, Manchester 2015. McCluskey, C., Paul, A. & Currie, S. Pro-inflammatory signaling in vascular endothelium: a novel role for CaMKIIδ in ageing.

British Society for Cardiovascular Research Annual Meeting, Reading 2014. Salleh, M. M., McCluskey, C., Bushell, T. J. & Currie, S. CaMKIIδ modulates intracellular release and cell proliferation in adult cardiac fibroblasts.

Oral Communications

Scottish Cardiovascular Forum Annual Meeting, Glasgow 2016. McCluskey, C., MacDonald, M. & Currie, S. Ageing of the vascular endothelium: a novel role for CaMKII?

Table of Contents

Chapter 3: Investigating an interaction between CaMKIIδ and NF-κB signalling in endothelial cells 70

Chapter 4: Ageing – cardiovascular and endothelial cell dysfunction 119

Chapter 5: Alterations in CaMKII and NF-κB signalling with Ageing 162

List of Figures

Chapter 1

Chapter 2

Chapter 3

Chapter 4

Chapter 5

List of Tables

Abbreviations

32^P	Phosphorus-32
AGEs	Advanced glycation end products
AIP	Autocamtide II-related inhibitory peptide
Ang-II	Angiotensin-II
ARD	Ankyrim repeat domain
ATP	Adenosine triphosphate
AV	Atrioventricular
AW	Anterior wall
BAFF	B cell activating factor
BSA	Bovine serum albumin
Ca^{2+}	Calcium ion
CaM	Calmodulin
CAM	Cellular adhesion molecule
CaMKII	Calcium/calmodulin-dependent protein kinase II
cAMP	Cyclic adenosine monophosphate
CARMA	Caspase recruitment domain-controlling protein
CD45	Leukocyte common antigen
CF	Cardiac fibroblasts
cGMP	Cyclic guanosine monophosphate
CICR	Calcium induced calcium release
CO	Cardiac output

COX-2	Cyclo-oxygenase-2
CRP	C reactive protein
CVD	Cardiovascular disease
DAPI	4', 6-diamidino-2-phenylindole
DCFDA	2', 7' – dichlorofluorescein duacetate
dH_2O	Distilled water
DNA	Deoxyribonucleic acid
DTT	Dithiothreithol
EC	Endothelial cells
ECC	Excitation-contraction coupling
ECGS	Endothelial cell growth supplement
ECL	Enhanced chemiluminescence
ECM	Extracellular matrix
ED	Endothelial dysfunction
EDD	Endothelium-dependent dilation
EDTA	Ethylenediaminetro-acetic acid
EGTA	Ethyleneglycol-bis-(β-aminoethylether)-N, N'-tetracetic acid
eNOS	Endothelial nitric oxide synthase
E-Selectin	Endothelial leukocyte adhesion molecule
ETC	Electron transport chain
FBS	Foetal bovine serum
FCS	Foetal calf serum

FITC	Fluorescein isothiocyanate
FS	Fractional shortening
GAPDH	Glyceraldehyde-3-phosphate dehydrogenase
H_2O_2	Hydrogen peroxide
HEPES	4-(2-hydroxyethyl)-1-piperazineethanesulfonic acid
HF	Heart failure
HR	Heart rate
HRP	Horseradish peroxidase
HUVECs	Human umbilical vein endothelial cells
ICAM-1	Intercellular adhesion molecule-1
IgG	Immunoglobulin
IKK	Inhibitory-κB kinase
IL-1β	Interleukin-1β
IL-4	Interleukin-4
IL-6	Interleukin-6
iNOS	Inducible nitric oxide synthase
IκBα	Inhibitory kappa β alpha
KCl	Potassium chloride
LPS	Lipopolysaccharide
LTCC	L-type Ca2+ channels
LVEDD	Left ventricular end diastolic dimension
LVESD	Left ventricular end systolic dimension

MCP-1	Monocyte chemoattractant protein-1
Met	Methionine
Mg^{2+}	Magnesium ion
MI	Myocardial infarction
Na+	Sodium ion
Na3VO4	Sodium orthovanadate
NaCl	Sodium chloride
NADPH	Nicotinamide adenine dinucleotide phosphate
NaH_2PO_4	Sodium dihydrogen orthophosphate
NEMO	Nuclear factor kappa B essential modulator
NF-κB	Nuclear factor kappa B
NIK	Nuclear factor kappa B inducing kinase
NO	Nitric oxide
NOX	NADPH-oxidase complex
O_2	Oxygen
O_2^-	Superoxide anion
ONOO-	Peroxynitrite
PBS	Phosphate buffered solution
PCNA	Proliferating cell nuclear antigen
PECAM	Platelet endothelial cell adhesion molecule
PKA	Protein kinase A
PKC	Protein kinase C

PLA	Proximity ligation assay
Pp65	Phosphorylated p65
PW	Posterior wall
PWDM	Pulsed wave Doppler mode
PWV	Pulse wave velocity
RHD	Rel-homology domain
ROS	Reactive oxygen species
RyR	Ryanodine receptor
SA	Sinoatrial
SDS	Sodium dodecyl sulphate
Ser	Serine
ShARM	Shared ageing research models
SMC	Smooth muscle cells
SPR	Surface plasmon resonance
TAD	Transcription activation domain
TAK-1	TGF-β-activated kinase
TBARS	Thiobarbituric acid reactive substances
TBHP	Tert-Butyl hydrogen peroxide
TBST	Tris buffered saline, tween
TGF-β	Transforming growth factor-β
Thr	Threonine
TNF-α	Tumour necrosis factor-alpha

TRITC   Tetramethylrhodamine isothiocyanate

VCAM-1   Vascular cell adhesion molecule-1

VTI   Velocity time integral

vWF   Von Willebrand factor

WH   Whole homogenate

Abstract

Ageing presents as the greatest risk factor for development of cardiovascular disease. Calcium/calmodulin dependent protein kinase IIδ (CaMKIIδ) is well established as playing a fundamental role in normal cardiac function, as well contributing to the pathophysiology of heart disease. A similar role for CaMKIIδ in the vasculature remains elusive. Furthermore, very little is known of whether this enzyme contributes to cardiovascular pathology associated with ageing.

Oxidative stress and chronic inflammation are both key features of the ageing process and are underpinned predominantly by the development of vascular endothelial dysfunction. Nuclear Factor kappa B (NF-κB) pro-inflammatory signalling is a key modulator of endothelial dysfunction and in recent years has been shown in the heart to be regulated by CaMKIIδ. The precise mechanisms by which CaMKIIδ exerts these effects on NF-κB signalling remain poorly understood and a comparable link has yet to be recognised between both pathways in the vascular endothelium.

This study has used a combination of *in vitro* and *in vivo* techniques to focus on (i) identifying a link between CaMKII and NF-κB signalling in vascular endothelial cells, (ii) characterising a chronic inflammatory and stressed phenotype in parallel with cardiovascular dysfunction in aged rats, and (iii) assessing alterations in both CaMKII and NF-κB signalling during ageing. Importantly the study has focused on vascular endothelial cells, providing novel insight into the role of CaMKIIδ in these cells during their dysfunction with ageing. A novel direct interaction between CaMKII and NF-κB signalling has been demonstrated at the level of inhibitory-κB kinase β (IKKβ) using proximity ligation assay (PLA) technology. Aged animals displayed visible signs of both cardiac and vascular dysfunction and this correlated with enhanced inflammation and oxidative stress. Interestingly, both CaMKIIδ and NF-κB signalling were both altered specifically at the level of the endothelium with ageing and therefore may both contribute to endothelial dysfunction. Future work should be performed to investigate the interaction between CaMKIIδ and NF-κB in the endothelium in more detail. By specifically targeting the protein-protein interaction between CaMKII and IKKβ, inflammation associated with endothelial dysfunction may be reduced and restoring

the balance in activity of both pathways could also reduce or prevent the progression of other age-related conditions.

Chapter 1: Introduction

1.1 The process and different theories of ageing

Ageing is a universal, multidimensional process for all eukaryotes and is characteristically described in humans as a time-dependent progressive accumulation of changes and decline in physiological functions, causing an individual to become more susceptible to disease and death (Harman, 1981). The rate at which an organism ages is to some extent regulated by genetics, which is evident by the fact that longevity differs between species and between individual members of a species (Harman, 1956). Mean longevity in humans, which is defined as the mean life expectancy at birth of individuals in a given species (Vina et al., 2007), has increased dramatically in the past few decades. This is primarily due to the discovery and development of vaccines, antibiotics and generally better control of infectious diseases and improved understanding of illnesses. In spite of this, when experiments have been performed in laboratory animals, where manipulations such as dietary supplementation of vitamins and induction of physical exercise have been used, this has been successful in increasing mean longevity; however maximal longevity is still significantly lower than that of humans (McCay et al., 1935; Walford et al., 1995), thus, highlighting the importance of species differences when it comes to ageing.

Other important non-biological factors such as environmental influences can also contribute to reduced or improved lifespan of a species (Lavrovsky et al., 2007). Ageing alone is now considered the greatest risk factor for the development of many diseases including cardiovascular diseases (CVD), cancer, diabetes, arthritis and neurological disorders; all of which increase exponentially with advanced age. However, conditions such as these have higher prevalence in certain geographical areas suggesting a link between premature ageing (as a result of disease) and environment. Epidemiology studies show that the incidence of CVD is significantly higher in countries of the developed world such as the United Kingdom and is in fact accountable for 45% of all deaths in Europe regardless of age in these areas (Bhatnagar et al., 2016). Furthermore, the prevalence of CVD in such countries is becoming more common in younger people than previously, therefore highlighting the fundamental significance of lifestyle and environmental factors that contribute to the development of age-associated diseases. These are not new findings however, as it has been well

known for some time that factors such as poor diet and lifestyle choices correlate with the development of those age-related conditions listed above. As such, not only is it of key importance that an attempt to improve the public awareness of the effects such environmental factors can have on ageing; it is also imperative that a clear understanding of the intrinsic pathophysiological process underpinning ageing itself is met. This will allow for a better understanding of the combined effects of both external and internal factors and the development of novel interventional treatments for the reduction and/or prevention of the disorders mentioned, mediating the overall promotion of good health in the aged individual.

1.1.1 The oxidative stress theory of ageing

Understanding the complex intrinsic theory of ageing has been the subject of extensive speculation for a number of decades, with considerable evidence now supporting a vast number of theories behind the process. The most widely known theory of ageing was first proposed by Harman (1956) – The Free Radical Theory of Ageing. This postulated that the presence of free radicals within the body, produced during normal metabolic processes, have deleterious effects on cells and tissues and thus, induce the physiological changes associated with ageing. Since this concept was first introduced, a substantial amount of evidence has now been published to support this notion and to provide a more in-depth understanding of it.

The oxidative stress theory of ageing is an expansion of the free radical theory and proposes that endogenous reactive oxygen species (ROS) are toxic free radicals that are the primary causal factor responsible for the variety of macromolecular oxidative modifications observed during the ageing process (Csiszar et al., 2008; Singh & Newman, 2011). At adequate concentrations, ROS play important roles in various cellular processes including cell signalling and homeostasis. They mediate signal transduction cascades and function to reversibly oxidise/reduce protein cysteine thiol groups as molecular on/off switches; thus are regarded as essential for the regulation of the metabolome (Linnane et al., 2007; Jenny, 2012). At increased levels, under normal conditions, ROS may be neutralised by intracellular antioxidants and enzymes,

for example superoxide dismutases, catalase and peroxiredoxins (Buffenstein et al., 2008). However, when levels rise above physiologically typical concentrations, incomplete neutralisation of ROS may prevail consequently causing oxidative damage to cellular constituents, e.g. DNA, lipids and protein damage (Buffenstein et al., 2008). There is an abundance of evidence supporting this theory in animal models, where it has been reported that aged animals show a higher index of oxidation than young and furthermore, they accumulate greater levels of oxidised proteins, DNA and lipids (Sohal et al., 1993). Additionally, studies have also demonstrated that administration of antioxidants significantly improves average lifespan in various animal models (Vina et al., 1992; Sadowska-Bartosz & Bartosz, 2014). These combined findings overall suggest that improving lifespan is not only attributable to resistance against oxidative stress, but also dependent upon specific manipulation of the antioxidant pool which is modified with ageing (as will be discussed in the next section).

1.1.1.1 Sources of reactive oxygen species

There are many sources of ROS within a cell (Figure 1.1), however mitochondrial production is by far the greatest. During aerobic metabolism, the production of ROS by the electron transport chain (ETC) in the mitochondria during oxidative phosphorylation is an inevitable by-product (Buffenstein et al., 2008). This is due primarily to the fact that during this process, electrons are regularly lost during their transfer between ETC complexes and can thereby react with molecular oxygen (O_2) to form ROS (Morgan & Lui, 2011). Approximately 1-2% of all O_2 used by the mitochondria in mammals is accountable for the production of ROS (Vina et al., 2007) which has led to further expansion of the oxidative stress theory and the development of the mitochondrial theory of free radicals in ageing (Turrens, 2003). This suggests that cellular senescence associated with ageing is caused primarily by ROS affecting the mitochondrial genome in post-mitotic cells. Since mitochondria from post-mitotic cells use O_2 at high rates (Terman et al., 2010), they produce more ROS as a by-product which consequently can overwhelm the antioxidant cellular defences and thereby lead to oxidative stress. This has been supported by numerous studies in the

literature, including one particular experiment in which isolated mitochondria from fibroblasts of aged rats were injected into those of young rats. Interestingly, they observed that the cells from young animals that received 'old' mitochondria, rapidly entered senescence (Corbisier & Remacle, 1993), thus strongly proving that mitochondrial ROS plays an important role in ageing.

There are also various enzymes within cells which mediate the production of intracellular ROS, in particular the phagocytic nicotinamide adenine dinucleotide phosphate (NADPH)-oxidase complex, NOX2 (gp96). It functions by using NADPH to transfer electrons inside the cell and to reduce cellular O_2 to superoxide anions ($O_2^{\cdot}$) which can contribute to the oxidation of proteins such as that observed with ageing (Brown et al., 2009; Lambeth et al., 2004; Quinn et al., 2006). Superoxide is also classically produced as a means of defence against pathogens, where it is converted to the microbicidal compound hypochlorous acid (HOCl) by enzymes superoxide dismutase and myeloperoxidase (Quinn et al., 2006). However, during this normally pro-cell survival process, some ROS can leak out from the phagosome to the cytosol, thus contributing to a stressed cell phenotype (Morgan & Lui, 2011). As the incidence of infection and disease exponentially increases with advanced age, defence mechanisms against such invading pathogens are also markedly enhanced, thus the likelihood of increased ROS leakage from cells is high. Additionally, $O_2^{\cdot-}$ production has also been shown to be capable of reacting with the naturally occurring vasodilator nitric oxide (NO), consequently causing toxic peroxynitrite anion ($ONOO^-$) formation (Beckman et al., 1993). As well as triggering oxidative damage to cells, this scavenging of NO also leads to reduced NO-mediated vasodilation, thus having a detrimental impact on the vascular system which has indeed been demonstrated to be negatively affected in older individuals (Csiszar et al., 2008) as will be discussed in more detail later in this chapter.

In addition to superoxide anions, another particularly important free radical thought to play a role in ageing is hydrogen peroxide (H_2O_2). H_2O_2 is also produced during mitochondrial respiration by the ETC during the reaction of $O_2^{\cdot-}$ with water (H_2O) to form the highly oxidative molecule that it is. A number of studies have shown that levels of H_2O_2 increase substantially with ageing (Cavazzonia et al., 1999; Sohal &

Sohal, 1991) and importantly, that this is predominantly attributed to damaged mitochondria (Sohal & Sohal, 1991). One particular investigation reported that these enhanced levels of H_2O_2 detected with ageing also correlated with cellular senescence and increased expression of thiobarbituric acid reactive substances (TBARS) (a well-known marker for oxidative stress) (Conti et al., 2015); thus suggesting a key role for this free radical in contributing to the oxidative damage and modifications to cells with advanced age.

It has been suggested that a weakened antioxidant defence may also be a contributing factor to the overall increase in oxidative conditions with ageing (Buffenstein et al., 2008). As previously mentioned, ROS may be neutralised by intracellular antioxidants under normal conditions. However, if the generation of free radicals exceeds the protective effects of antioxidants, this can contribute to oxidative damage which accumulates as we age. It has been reported that enhanced mitochondrial activity with ageing (which leads to superoxide anion production) also correlates with a burdened antioxidant system, primarily caused by reduced activity of endogenous antioxidant enzymes; reduced biokinetics of antioxidant metabolism; and reduced bioabsorption of antioxidants (Poljsak & Milisav, 2013). Thus, the resulting overall outcome is an alteration in redox homeostasis, which ultimately underpins the oxidative stress theory.

Respiration

- $O_2^{\cdot -}$ & H_2O_2 production by ETC of mitochondria

Enzymes:

- NADPH oxidase
- Xanthine Oxidase
- Nitric Oxide Synthase
- Lipoxygenase

ROS
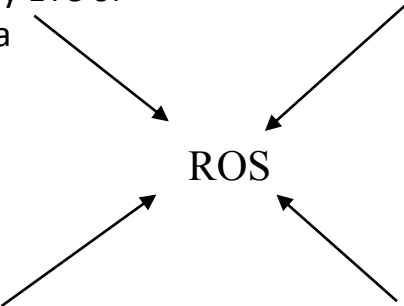
Respiratory burst

- Neutrophil production & release of ROS during immune response

Peroxisomes

- Breakdown of LCFA by β-oxidation

Figure 1.1: Different sources of intracellular ROS production. The mitochondria are a major source of ROS ($O_2^{\cdot -}$, superoxide; H_2O_2, hydrogen peroxide) primarily through leakage of electrons from Complexes I and III during respiration. ROS are also produced by numerous enzymes, predominantly NADPH oxidase; during host immune response as a by-product of respiratory burst and in peroxisomes during the breakdown of long chain fatty acids (LCFAs).

1.1.2 Chronic inflammation and ageing

There is now a large amount of evidence suggesting that ageing is associated with the persistence of a chronic low grade inflammatory phenotype. This has led to the development of the 'inflammaging' theory of ageing where it has been postulated that this increase in inflammation, despite being low level, significantly increases the risk of illness and/or death within the aged population (Csiszar et al., 2008; Edirisinghe & Burton-Freeman, 2014).

Under normal conditions, the inflammatory cascade is initiated in response to trauma or infection at a local, cellular level. A number of key cells and mediators are activated to help clear the body of invading pathogens and instigate recovery, including macrophages and monocytes, and the production of key cytokines, tumour necrosis factor (TNF)-α and interleukin (IL)-1β (Gabay & Kushner, 1999). These mediators are responsible for progressing the response to a systemic level, which involves multiple organs (Jenny, 2012). During infection or disease, this inflammatory reaction is acute and is accompanied by heat, redness, pain and swelling. These symptoms normally pass quickly as the inflammatory response rapidly clears the infection/necrosis. However in the ageing context, the inflammation observed is chronic but predominantly low-grade therefore symptoms are normally sub-clinical. The response is indeed mediated by the same effectors as those listed above during an acute reaction, however the outcome differs significantly (Tracy, 2003).

Chronic inflammation as a function of ageing has been well demonstrated across a wide range of studies. One of the most prominent biomarkers for this inflammatory phenotype in the aged individual is an increase in circulating pro-inflammatory cytokines. The elderly population express a 2-4 fold elevation in levels of inflammatory cytokines such as TNF-α, IL-6 and IL-1β even in the absence of any pathophysiological ailment (Bruunsgaard & Pedersen, 2003; Singh & Newman, 2011); where those who age 'successfully' are likely to have lower levels of these pro-inflammatory markers (Akbaraly et al., 2013). TNF-α is a pro-inflammatory cytokine of the acute phase response and is therefore known to play an essential role in the initiation of the inflammatory cascade as mentioned above. One particular study by

Bruunsgaard et al., (1999) confirmed an increased concentration of serum TNF-α among centenarians when compared to younger control groups and this was associated with the prevalence of Alzheimer's disease and atherosclerosis, both age-related conditions. Raised plasma concentrations of IL-6 in aged subjects have also been shown by various studies in both animals and humans (Akbaraly et al., 2013; Cohen et al., 1997; Ershler et al., 1993). This cytokine has been demonstrated to be particularly relevant to ageing outcomes as it has a direct effect on the brain and skeletal muscles (Barbieri et al., 2003). Consequently, high levels of IL-6 correlate with age-associated phenotypes such as type 2 diabetes, CVD and brain atrophy (Akbaraly et al., 2013). Similarly, IL-1β has also been shown to play a key role in promoting inflammation during ageing (Deten et al., 2005) and is specifically thought to be involved in contributing to age-associated conditions of the cardiovascular system such as myocardial infarction (MI) and atherosclerosis (Dinarello, 2006).

1.1.2.1 Mechanisms of inflammation with ageing

Numerous mechanisms have been proposed as causative factors for the chronic inflammation associated with ageing. As well as playing a central role in oxidative damage, ROS (primarily H_2O_2) have also been implicated in mediating the production of various pro-inflammatory molecules (Lavrosky et al., 2000). This has led to the concept of the "molecular inflammatory process" in ageing, which was first introduced by Chung et al., (2002). This concept proposes that altered redox-sensitive cellular signalling pathways cause molecular activation of pro-inflammatory genes which subsequently leads to an inflammatory phenotype across tissues and organs, a process which is exacerbated over time (i.e. ageing) (Chung et al., 2006). An abundance of evidence now supports this theory and links together both oxidative stress and inflammation theories of ageing, where mitochondrial ROS has been shown to both activate and be activated by pro-inflammatory cytokine signalling (Hughes et al., 2005; Zinovkin et al., 2014; Zhang & Gutterman, 2007).

In addition to this, dysfunction of the endocrine system is apparent with increased age, where sex steroid production is most notably affected (Singh & Newman, 2011). Sex

hormones can modulate the production of inflammatory cytokines, which has been demonstrated in numerous studies. One particular investigation showed that IL-6 and other pro-inflammatory cytokines were significantly increased in post-menopausal women (Endrighi, Hamer & Steptoe, 2016). Similar findings were also reported in aged men, where an inverse relationship existed between testosterone and inflammatory markers (Maggio et al., 2006).

The accumulation of functional decline in multiple systems that present with ageing and the overall decrease in strength, physical function and weight, cause an individual to become increasingly frail with old age (Fried et al., 2001). It has been demonstrated that an association exists with frailty and inflammation in ageing, even in the absence of other common age-related conditions (Walston et al., 2002). Thus, the cumulative effects of all of the above components form a complex interplay and the basis for ageing. With a steady rise in our ageing population and the inevitable burden on healthcare and social services that this brings, it has become increasingly important to promote healthy ageing. Given the role that inflammation and oxidative stress play in ageing, could it be that therapeutic targeting of these processes may prove beneficial?

1.4 Current methods for researching ageing

Research in ageing is now a very popular area due simply to the fact that people are now generally living significantly longer than they once did. Over the past few decades, as technology and resources have improved, rapid advances in the mechanisms that control different processes of ageing including cell proliferation, differentiation and survival are leading to new insights into the regulation of ageing. By understanding the complicated intrinsic mechanisms of the ageing process, opportunities may arise that allow routes for prevention or at least reduction of the physiological and pathological changes that occur with advanced age.

1.2.1 In vitro models

Many *in vitro*-based approaches have been used to investigate ageing. Cells growing in culture can be serially passaged to replicate a senescent phenotype, similar to that of aged cells. Cellular senescence is a hallmark of ageing and refers to the process of cells eventually losing their ability to divide. Initial experiments by Hayflick and colleagues (1965) showed that normal cells in culture also exert this limited capacity to divide and therefore could represent as a much simpler and less expensive means of researching the ageing phenomenon (Hayflick, 1965). The key question which accompanies this now well-used method however, is how does this translate *in vivo*? Various markers of senescent cells have been identified in those cells grown in culture and serially passaged, including dysfunctional telomeres, altered gene expression and lack of DNA replication, shown by the presence of proteins such as proliferating cell nuclear antigen (PCNA) (Collins & Mitchell, 2002; Campisi & Fagagna, 2007). These senescence-associated markers have also been identified *in vivo* and it has been reported that cells which express one or more of these markers are relatively rare in young organisms but do increase with advanced age (Campisi & Fagagna, 2007), thus showing a translation. Characteristic morphological alterations also accompany this replicative senescence approach, including increased cell size, number of multinucleated cells, number of vacuoles within the endoplasmic reticulum and cytoplasm of the cells, and the development of large lysosomal bodies; all processes believed to occur during cellular ageing *in vivo* (Cristofalo & Pignolo, 1993). However, these events have been found to vary widely depending on the study, species and tissue. Importantly, a fundamental issue of using this *in vitro*-based approach is that it only models a very limited aspect of ageing. Despite providing valuable mechanistic insight into the cellular senescent component of ageing, it is limited in that it does not completely replicate *in vivo* biology. Cells grown in culture differ hugely than those in an intact organism in terms of growth and metabolic needs (Phipps et al., 2007). The commonly used 10-fold dilution of serum in cell culture media contains substantially lower concentrations of protein than is normally found in extracellular tissue fluids *in vivo* (Rubin, 1997). Furthermore, using such an approach does not account for the numerous other reasons as to why we age, including the

chronic inflammatory component. Thus, a more beneficial and realistic approach to investigate the complex process of ageing may be to use animal models.

1.2.2 Animal Models

The most scientifically accurate and relevant method for investigating the complex ageing process would of course be to use human studies, however a major drawback of doing so is the impracticality due to the long life span of humans. Ethical issues are also a fundamental shortcoming in terms of studying particular organs and harvesting tissue. Furthermore, the fact that the genetic and environmental factors may vary too much between individuals may be a cause for concern (Solleveld and Hollander, 1984). In spite of this, numerous studies have indeed been conducted in humans with regard to investigating ageing, where centenarians have provided useful insight particularly into differences in expression of certain genes involved in 'successful' ageing (Wheeler & Kim, 2011). Such studies are however expensive and extremely time-consuming therefore there are now numerous pre-clinical animal models employed as an alternative means for investigating *in vivo* ageing and the associated pathophysiologies.

A key issue with animal models for studying ageing is that one has to establish what defines an animal as aged and how does this correlate with ageing in humans? Solleveld and Hollander (1984) stated that an aged animal is "one which is past the 50% survival age derived from a population which has a more or less rectangular survival curve and in which the pathological changes are characterised by multiple lesions." Although long-living species may be more appropriate models for human ageing, for example the naked mole rat which has a lifespan of around 28 years (Buffenstein, 2005), rodents (in particular mice and rats) have also been identified as useful animals for ageing research. These animals are used widely throughout laboratory research to study various disease processes, including ageing as they have several advantages: (i) they have moderately short lifespans (in comparison to humans), (ii) the relatively low costs of housing and feeding and (iii) the availability of genetically defined strains and stocks. These animals have much shorter lifespans than humans as they have a very fast rate of ageing. This has been attributed to the

fact that rodents have greater levels of ROS generated from aerobic metabolism and display lower antioxidant defences at younger ages than humans (Buffenstein, 2005). They also show increased expression of various age-associated genes correlating with what is observed in humans (Koks et al., 2016). As a result, these animals can be used for ageing research simply by calculating what age corresponds to an aged human. Numerous studies have provided evidence to suggest that a typical laboratory rat which corresponds to approximately 70-75 human years is around 2 years old and that a 3 month old rat corresponds to 15-20 human years, i.e. a young human which would be used as a control in ageing studies (Sengupta, 2013). Overall, this makes investigating the complex processes involved during ageing less complex, time-consuming and more cost-effective than human studies. Furthermore, the introduction of ShARM (shared ageing research models) has allowed the acceleration of such pre-clinical ageing research in animals by facilitating the sharing of resources and costs among research communities; thus providing a simpler means for investigating ageing *in vivo*. Importantly, given the fact that many diseases including CVD, cancer and diabetes are all age-related; the future of research specifically into such pathophysiologies may also require models in aged animals instead of young (as they are more commonly performed in at present). This would ultimately provide better translational findings to the clinic and therefore the development of better therapeutic interventions for such conditions.

1.5 Ageing of the Cardiovascular System

1.3.1 Physiology of the heart

The human heart serves to pump blood through the vessels of the circulatory system and to all areas of the body, thus providing them with oxygen, nutrients and removing any metabolic waste. In mammals, the heart is divided into four chambers: the upper left and right atria and two lower chambers referred to as the right and left ventricle. The left ventricle (LV) is responsible for pumping the oxygen-rich blood into the systemic circulation via the aorta. It is therefore the thickest of the hearts' chambers

given the crucial role it plays and receives a large amount of research interest in terms of cardiac function and dysfunction.

The rhythmic contractions of the heart muscle (myocardium) are under the control of the sinoatrial (SA) node and are fundamental to controlling sufficient cardiac output (CO). The SA node generates spontaneous electrical impulses (or action potentials) through the atria, causing them to simultaneously contract in a coordinated wave-like manner and forcing blood into the ventricles. This electrical impulse then subsequently strikes the atrioventricular (AV) node and propagates to the Purkinje fibres, via the Bundle of His, causing ejection of the blood into the aorta and pulmonary artery. These set of events which lead to ventricular contraction of the myocardium are known as systole. Immediately after each systole, the heart ventricles relax during diastole, allowing the chambers to re-fill with blood again before the trigger of another action potential. In addition to this electrical excitation of the myocardium, the heart will not contract unless a subset of events, known as excitation-contraction coupling (ECC) is initiated. This fundamental process is regulated by the ubiquitous second messenger calcium (Ca^{2+}) and was first established by the classic experiments of Ringer (1883), where he demonstrated that the frog heart would not contract in the absence of extracellular Ca^{2+}. This regulated Ca^{2+} cycling occurs within the electrically excitable muscle cells of the heart known as cardiomyocytes. ECC begins with depolarisation of the myocytes which subsequently induces an influx of Ca^{2+} via voltage-sensitive L-type channels (LTCC). This inward current of Ca^{2+} further promotes the release of Ca^{2+} from intracellular stores within the sarcoplasmic reticulum via activation of the ryanodine receptors (RyR) in a process termed Ca^{2+}-induced Ca^{2+} release (CICR), thus raising the overall cytoplasmic Ca^{2+} levels (Maier & Bers, 2002). The intracellular Ca^{2+} ions can now readily bind to the Ca^{2+}-sensitive myofilament subunit, troponin C and thus, mediate contraction of the myocardium during systole. Relaxation of the heart during diastole is associated with lowering the levels of cytosolic Ca^{2+} (Vander et al., 1998). As a result, altered Ca^{2+} signalling has been at the forefront of research in cardiac function and dysfunction.

1.3.2 Cardiac dysfunction with ageing

CVD remains as the leading cause of mortality in the aged population (North & Sinclair, 2012). In terms of heart health, advanced age is associated with complex alterations to the cardiac structure and function. Similar to that observed in the diseased phenotype, ageing alone has been shown to induce some level of LV hypertrophy (Olivetti et al., 1991) and changes in cardiac shape from elliptical to spherical have been reported (Goldspink et al., 2003). Fibroblast proliferation is apparent and collagen deposition more prominent, with an increase in cross-linking between adjacent fibres, leading to a rise in fibrotic tissue and stiffening of the heart muscle (Horn & Trafford, 2016; North & Sinclair, 2012). Although cardiomyocyte numbers decrease as a result of apoptosis, they become somewhat enlarged in shape, thus contributing to the hypertrophied state of the myocardium. As would be expected with an alteration in cardiomyocyte phenotype, altered Ca^{2+} handling is also apparent with ageing as it is during disease. Evidence suggests that altered Ca^{2+} homeostasis is linked to the oxidative stress component of ageing (Ureshino et al., 2014) and that there is a marked loss of CICR during ageing, which leads to 'leaky' Ca^{2+} spark activity in the cardiomyocytes themselves (Weisleder & Ma, 2008). In spite of this, the dysregulation of Ca^{2+} signalling during ageing is not as well studied as it is in models of cardiac disease.

The overall changes in cardiac wall thickness and shape have important implications for wall stress and contractile efficiency (Strait & Lakatta, 2012) and therefore contribute to the general dysfunctional state of the myocardium with ageing. The aged heart shows a decline in CO with a less efficient response to increased workload and negative effect on heart rate (HR) (Christou & Seals, 2008; Kostis et al., 1982). This is primarily due to physiological changes occurring at the level of the SA node, including fat accumulation and loss of pacemaker cells (Cheitlin, 2003). It has been reported that by the age of 75, only 10% of the number of cells at the SA node seen in young adults remain present (Strait & lakatta, 2012). In combination with the other structural changes listed, including hypertrophy and fibrosis, this ultimately causes slowed propagation of electrical impulses throughout the heart during ageing.

Ageing of the myocardium is also associated with enhanced inflammation and oxidative stress, similar to that observed in animal models of hypertrophy and heart failure (HF). Given that pathological remodelling occurs in the aged heart, where collagen and fat deposition are increased and the development of ischaemic or necrotic tissue accumulates (Biernacka & Frangogiannis, 2011; Horn & Trafford, 2016; Kwak, 2013), it is not surprising that an inflammatory response is activated as a form of host defence. Studies in mice have shown that cardiac fibrosis and diastolic dysfunction associated with ageing correlate with increased myocardial expression of monocyte chemoattractant protein (MCP)-1/CCL2, IL-4, IL-13 and CD45+ myeloid derived fibroblasts (Biernacka & Frangogiannis, 2011). In humans, it has also been suggested that MCP-1/CCL2 plays a key role in ischaemic cardiac fibrosis associated with ageing (Cieslik et al., 2011). Furthermore, a recent study provided evidence that specific immune cell populations are increased in aged myocardial tissues, including CD4$^+$ T lymphocytes (Ramos et al., 2016). Aged mice have elevated levels of activated CD4$^+$ T cells in the heart draining lymph nodes compared to young, therefore confirming activation of inflammatory signalling is a key feature of the ageing heart, even in the absence of previous myocardial damage.

Evidence suggests ROS are also increased in the aged myocardium. In the heart, mitochondria provide the primary source of energy that fuels the contractile apparatus (Chaudhary, El-Sikhry & Seubert, 2011). As discussed in Section 1.1.1.1, mitochondrial function declines with age and as a result, enhanced ROS production by the ETC is evident, therefore mediating cellular damage by oxidative stress. Studies have shown that ROS levels are amplified in aged hearts and are in fact predominantly responsible for the loss of cardiomyocytes seen with ageing of the heart (Hafner et al., 2010). Furthermore, increased protein and lipid oxidation are both evident in aged hearts, despite enhanced antioxidant concentrations also being reported (Marin-Garcia et al., 2013). This suggests that the compensatory mechanisms of antioxidants are not sufficient in neutralising the increased levels of ROS and therefore a pro-oxidant environment develops within the aged heart.

1.3.3 The vascular system

The vasculature refers to all of the blood vessels within the body, including arteries and veins that supply organs and tissues with oxygen, vital nutrients and are involved in the elimination of waste products. Ageing has a remarkable effect on the vascular system leading to a heightened risk for the development of diseases of the vasculature, including atherosclerosis, hypertension and arterial fibrillation (Lakatta & Levy, 2003). The health of both vascular and cardiac systems are not mutually exclusive however, as each system greatly affects the other (as one would expect) given their overall general functions. Despite this, most research focuses primarily on either the heart or the vasculature and therefore the link between diseases (and ageing) of both systems is often overlooked. There are a wide range of factors that contribute to ageing-associated cardiac dysfunction but arterial dysfunction appears to be crucial (Seals et al., 2011).

The main artery within the body is the aorta which is responsible for carrying blood away from the heart, extending down the abdomen where it can then distribute oxygenated blood to all other parts of the body. The aorta is the most extensively studied arterial blood vessel in vascular research as it is by far the largest and contributes significantly to vascular pathogenesis, particularly during atherosclerosis. Each blood vessel, including the aorta is made up of three distinctive layers as depicted in Figure 1.2. These include the tunica adventitia, tunica media and tunica intima. The adventitia is predominantly made up of flexible fibrous tissue, containing elastin and collagen to provide structure to the vessel (Sherwood, 2003). The tunica media, which lies in the middle of the vessel wall, consists of smooth muscle cells (SMCs) and controls vessel diameter and therefore, blood pressure, by contracting or relaxing. The innermost layer around the vessel lumen is the tunica intima and is made up of a monolayer of endothelial cells (ECs) which act as an interface between the circulation and vessel tissue. This single cellular layer of cells is often referred to as the endothelium and has received a large amount of attention in the area of cardiovascular research over the years, given its role in regulating vascular function and dysfunction by numerous mechanism
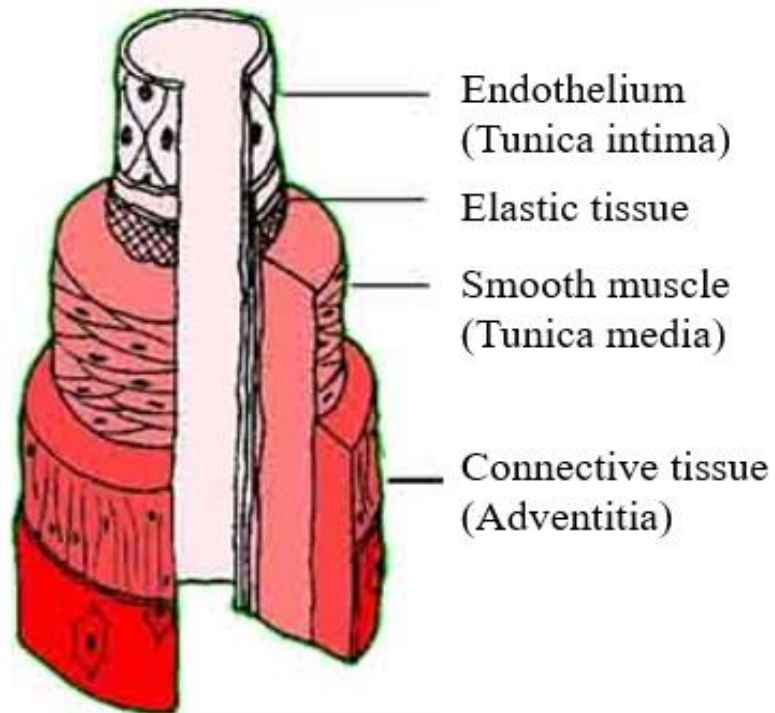
Figure 1.2 Illustration of arterial structure. The tunica intima consists of a single monolayer of endothelial cells which are in direct contact with the arterial lumen. The tunica media contains smooth muscle cells with a layer of elastin between joining with the tunica intima to provide structure to the vessel. The adventitial layer is predominantly made up of loose connective tissue.

1.3.3.1 The Endothelium of the vasculature

The healthy endothelium is a simple monolayer of ECs which line the interior surface of blood vessels. It plays a key role in vascular function as the ECs themselves are in direct contact with circulating blood, therefore are able to respond to various physical and chemical signals. As a result, these cells mediate a wide range of processes including vascular tone, SMC proliferation, cellular adhesion and vessel wall inflammation (Deanfield et al., 2007; Kadl & Leitinger, 2005; Pate et al., 2010). They act as a semi-selective barrier between the vessel lumen, connecting the circulating blood and the surrounding tissues; therefore their health is vital in terms of mediating the controlled passage of nutrients, oxygen and immune cells into and out of the bloodstream.

Early experiments conducted by Furchgott and Zawadzki (1980) were the first to demonstrate the presence of an endothelium-derived relaxing factor, which was later found to be nitric oxide (NO). NO is generated from L-arginine in the ECs by the action of the enzyme endothelial NO synthase (eNOS) (Forstermann & Munzel, 2006). Once produced, NO can then readily diffuse from the endothelium to the vascular SMCs of the tunica media to subsequently activate guanylate cyclase, leading to cyclic guanosine monophosphate (cGMP)-mediated vasodilation (Deanfield et al., 2007; Widmaier et al., 2007). Thus, despite the SMCs themselves being responsible for mediating contraction (vasoconstriction) and relaxation (vasodilation) of the blood vessels; it is in fact the ECs which play a crucial role in modulating the release of mediators required to carry out such functions. The frictional force of the blood in a vessel (shear stress) is an activator of eNOS in normal physiology (Versari et al., 2009). Shear stress is sensitive to alterations to CO (Corson et al.,1996) and therefore connects cardiac function with vascular responses. One example is the production of endothelial-derived NO (Davies, 2007). ECs in their healthy form provide a smooth surface for the vessel thereby reducing the turbulence of blood flow. This, in combination with the release of NO maintains the vascular wall in a quiescent state by inhibiting events such as inflammation and cellular proliferation (Deanfield et al., 2007). These cells are not unresponsive however, as upon endothelial activation this quiescent state is altered to one with an increased inflammatory profile, where

expression of cytokines, chemokines and cellular adhesion molecules (CAMs) are all up-regulated (van der Loo et al., 2009). Endothelial activation is also associated with variations in the secretion of autocrine/paracrine factors which are fundamental to the inflammatory response (Csiszar et al., 2008) and will be discussed in more detail below.

1.3.4 The aged vasculature

1.3.4.1 Endothelial dysfunction

Endothelial dysfunction (ED) occurs when the loss of proper endothelial function prevails and a pro-inflammatory, pro-oxidant and hyperactive phenotype develops (Figure 1.3). ED is a hallmark of most vascular diseases and is considered as a key early event in the development of atherosclerosis and coronary artery disease (Deanfield et al., 2005). ED is also a key feature of the ageing process and is likely related to the increased ROS levels seen during ageing, (Donato et al., 2007; van der Loo et al., 2000). Interestingly, during ED eNOS can switch phenotype to generate further ROS. This is termed eNOS uncoupling and results in superoxide and H_2O_2 formation within the ECs, further potentiating the pro-oxidant environment associated with ageing. This also subsequently diminishes the generation of NO (North & Sinclair, 2012) and therefore dysregulation of vasoconstriction and vasodilation becomes a feature of the aged vasculature. ECs become less sensitive to shear stress with advanced age, and therefore, the overall net outcome is a significant reduction in protective NO mediated endothelium-dependent dilation (EDD) (North & Sinclair, 2012).

ED leads to increased expression of various pro-inflammatory cytokines and adhesion molecules. This consequently triggers enhanced endothelial-leukocyte interactions and when coupled with the augmented permeability, significantly amplifies inflammatory cell migration and tissue damage (Lerman & Zeiher, 2005). A number of well-characterised circulating molecules have been associated with age-associated ED, including VCAM-1, ICAM-1 and E-Selectin (Ridker et al., 2004; Rifai & Ridker, 2002). Additionally, it has been reported that with ED as the endothelial barriers

become more porous, there is increased migration of vascular SMCs into sub-endothelial spaces, where they deposit extracellular matrix (ECM) proteins that consequently result in intimal thickening (North & Sinclair, 2012). Senescence of ECs can indeed occur in environments where there is a sustained increase in ROS and inflammatory signalling. In such cases, the ECs lose integrity and can eventually detach from the wall into the circulation (Woywodt et al., 2002). This can occur during ageing as a result of the chronic low grade inflammatory and pro-oxidant phenotype, and has been demonstrated by increased levels of endothelial microparticles derived from senescent and apoptotic cells from aged individuals (Deanfield et al., 2007).
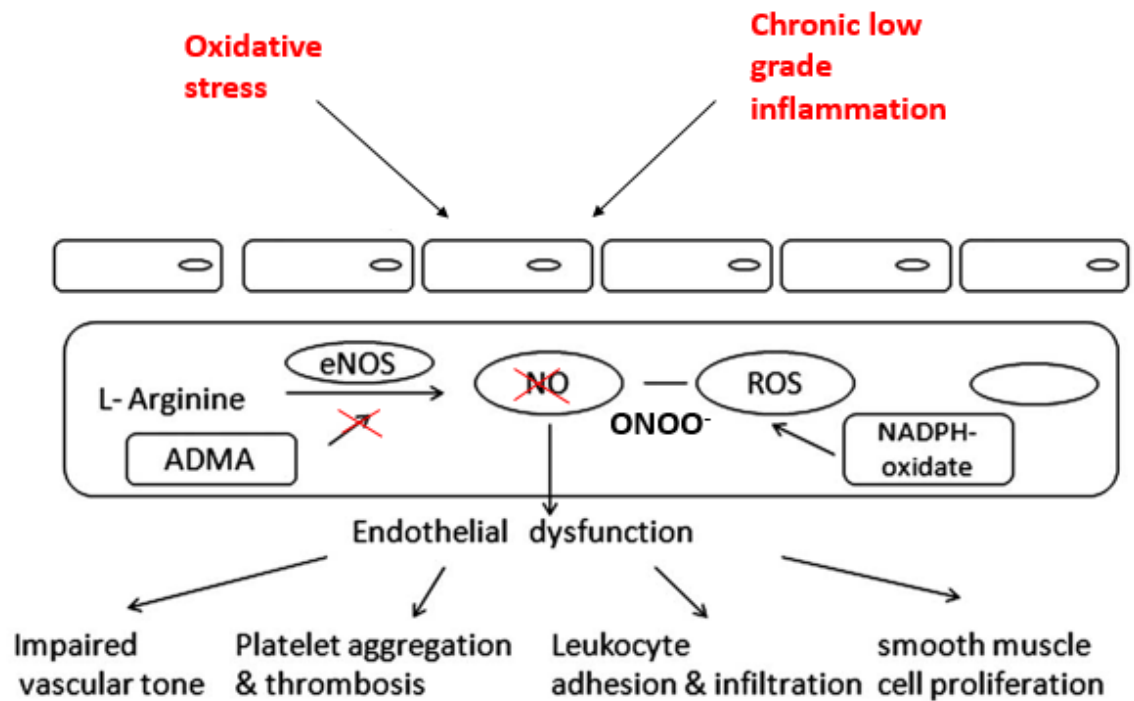
Figure 1.3 Consequences of endothelial dysfunction with ageing. Increased oxidative stress and chronic inflammation in the aged vascular system leads to a series of events within the endothelial cell, causing endothelial dysfunction. Increased production of ROS by NADPH mediates peroxynitrite anion (ONOO⁻) formation. Endothelial nitric oxide synthase (eNOS) 'uncoupling' leads to scavenging of nitric oxide (NO). Ablated asymmetric dimethylarginine (ADMA) interference with L-arginine also results in reduced production of NO, overall contributing to reduced vasodilation/impaired vascular tone. Leukocyte adhesion & filtration is increased due to up-regulated expression of cell adhesion molecules. Smooth muscle cell proliferation and hypertrophy is also augmented causing intimal thickening and the likelihood of platelet aggregation & thrombosis development is high. (Adapted from Lu et al., 2014).

1.3.4.2 Structural changes to the vasculature during ageing

As well as the dysfunctional endothelium, ageing of the vasculature is also associated with various structural alterations to the vessel itself. The lumen becomes somewhat enlarged and thickening of the vessel wall develops which, coupled with the reduced EDD, promotes vascular stiffness (Izzo & Shykoff, 2001). Such changes have been well documented in the aorta itself (Ferrari et al., 2003) and have been associated with an enhancement in pulse wave velocity (PWV). Progressive dilation and elongation of the aorta also develops with advanced age, where it has been reported that the volume of the thoracic aorta can increase up to 4-fold between the ages of 30 and 80 human years (Lakatta et al., 1987). A reduction in the amount of elastic tissue is also a major causal factor for the development of these changes, in combination with increased collagen deposition. Furthermore, fibrosis, fragmentation of elastin filaments, calcification and formation of advanced glycation end-products (AGEs) are all fundamental characteristics of the aged vasculature (Seals et al., 2014); as well as the deposition of intraluminal fatty streaks – a hallmark for the development of atherosclerotic plaques (Fernandez-Ortiz, Badimon & Fuster, 1999). As a direct result of the decrease in vascular distensibility, arterial pulse pressure increases, which is secondary to increased systolic pressure (Lakatta et al., 1987). During diastole the aged aorta does not dilate as well as a younger counterpart, as a consequence of the aortic elastic tissue and smooth muscle not being able to sustain a forward blood flow. This ultimately puts a larger amount of pressure on the LV during systole (O'Rourke, 1982). All of these structural and functional modifications have been confirmed *in vivo* by echocardiography and clinically, these changes result in an augmented systolic pressure which may lead to increased risk for the development of ailments such as atherosclerosis, hypertension and atrial fibrillation (Lakatta & Levy, 2003), all of which are age-related pathophysiologies.

1.4 Introduction to the nuclear factor kappa B signalling pathway

The pro-inflammatory nuclear factor-κB (NF-κB) family of proteins have been shown to potentiate the development of ED and subsequent chronic inflammation of the

vasculature during ageing (Chung et al., 2002; Donato et al., 2007; Ungvari et al., 2007). Importantly, this has been shown in humans to be predominantly caused directly by the increased ROS observed with ageing (Donato et al., 2007; Pierce et al., 2009). Thus NF-κB may serve as the key link connecting both oxidative stress and inflammation pathways observed with advanced age, as will be discussed later in this chapter.

NF-κB was first discovered in 1986 by Baltimore and his colleagues, where it was initially identified as playing a fundamental role in regulating immunoglobulin G (IgG) gene expression within B lymphocytes. NF-kB is a nuclear factor that binds selectively to the κ light-chain enhancer, covering the DNA sequence 'GGGACTTTCC' (Sen & Baltimore, 1986). This early work originally alleged NF-κB to be specific to B lineage cells only, however this transcription factor is now recognised as being expressed in virtually all cell types and is today, one of the most intensively studied cellular signalling pathways (Gamble et al., 2011). The NF-κB signalling pathway is activated by numerous stimuli, including a variety of pro-inflammatory cytokines, growth factors, ROS and viral proteins (Chen & Grenne, 2004). It regulates various genes involved in cell survival and apoptosis (Li et al., 2004) as well as inflammatory genes which play a central role in the innate and adaptive immune response (Valen et al., 2001a). NF-kB is also known to be active in a range of diseases including cancer, arthritis, asthma and importantly, CVD (Baldwin, 2001).

1.4.1 The NF-κB family

NF-κBs are a family of Rel proteins, of which there are five members: p65 (RelA), RelB, c-Rel, p50/p105 (NF-κB1) and p52/p100 (NF-κB2). They are structurally related eukaryotic transcription factors that mediate signalling from the cell surface to regulate target genes within the nucleus via interior signalling platforms (Gamble et al., 2011). The NF-κB complex, which consists of a heterodimer of p50 and p65 subunits (Chen & Grenne, 2004), binds to κB sites within the promoters of a variety of genes and regulates their transcription through the recruitment of co-activators and

co-repressors (Basak & Hoffman, 2008). Each NF-κB member contains a highly conserved N-terminal Rel-homology domain (RHD) which allows the protein to undergo nuclear localisation and DNA binding. This domain is also responsible for association with the inhibitory kappa B (IκB) family of cytoplasmic proteins which retain NF-κB in its inhibitory state until activated (Ghosh & Karin, 2002). The p65, Rel B and c-Rel subunits also contain C-terminal transcription activation domains (TAD-1 and TAD-2) which are required for transcriptional activation of certain genes (van der Heiden et al., 2010). Both p50 and p52 lack these TAD's and therefore may repress transcription unless they are associated with an NF-κB member that contains a TAD or with other proteins capable of recruiting co-activators (Hayden & Ghosh, 2008).

1.4.2 Activation of the NF-κB signalling pathway

Under resting conditions the NF-κB dimer is retained within the cytoplasm through an interaction with various inhibitory proteins. The family of IκB's consists of five members: α, β, γ, ε and ζ. Other proteins which also exist and can inhibit NF-κB activity include Bcl-3 and two NF-κB precursor proteins (p100 and p105) (Basak & Hoffman, 2008; Hayden & Ghosh, 2008). These inhibitory proteins all contain an Ankyrin repeat domain (ARD) which masks NF-κB DNA binding and their nuclear localisation signal (Van der Heiden et al., 2010). In response to cell stimulation, proteolysis of the inhibitors occurs via two distinctive signalling pathways: the canonical and the non-canonical pathway and NF-kB is activated. Stimulation of both pathways ultimately leads to transcription of divergent subsets of pro-inflammatory genes as discussed below.

The canonical pathway of NF-κB utilises an inhibitory-κB kinase (IKK) complex consisting of two catalytic subunits, IKKα and IKKβ, in composite with an essential regulatory subunit, NF-κB essential modulator (NEMO) or IKKγ (Poyer et al., 2000). Upon cell stimulation by pro-inflammatory cytokines such as TNF-α and IL-1β, various adapter proteins are recruited, including TNF-receptor associated factors (TRAFs) (Gamble et al., 2011). This facilitates the recruitment of pivotal enzymes, including TGF-β-activated kinase (TAK1) and ERK kinase kinase 3 (MEKK3), which

can then phosphorylate and activate IKKβ at Ser177 and Ser181 (Shmidt et al., 2003). Activation of IKKβ allows subsequent phosphorylation of IκBα at Ser32 and Ser36, which targets it for rapid polyubiquitination followed by proteolytic degradation through the 26S proteasome (Zandi et al., 1997). The now activated NF-κB complex can then release itself from IκBα and translocate to the nucleus where it binds to specific κB sites to regulate transcription of many genes that encode for proteins which are central to the inflammatory response. These include TNF-α, IL-1β, IL-6, adhesion molecules (intercellular adhesion molecule-1 (ICAM-1), vascular cell adhesion protein-1 (VCAM-1), E-Selectin) and enzymes inducible nitric oxide synthase (iNOS) and cylclo-oxygenase -2 (COX-2) (Chung et al., 2002), all of which are known to be up-regulated during ED (Figure 1.4).

The non-canonical pathway ultimately leads to transcription of genes encoding processes such as B cell maturation and lymphoid organogenesis (Gamble et al., 2012). This pathway is activated by stimuli including lymphotoxin-β and B cell activating factor (BAFF), resulting in activation of the NF-κB-inducing kinase (NIK). This can then subsequently phosphorylate IKKα at Ser 176 and Ser 180 (Hayden & Gosh, 2008), rendering IKKα now active to phosphorylate p100 and lead to ubiquitination and proteolytic processing to p52. The active p52/RelB heterodimer translocates to the nucleus where it regulates specific gene transcription as described above (Figure 1.5).
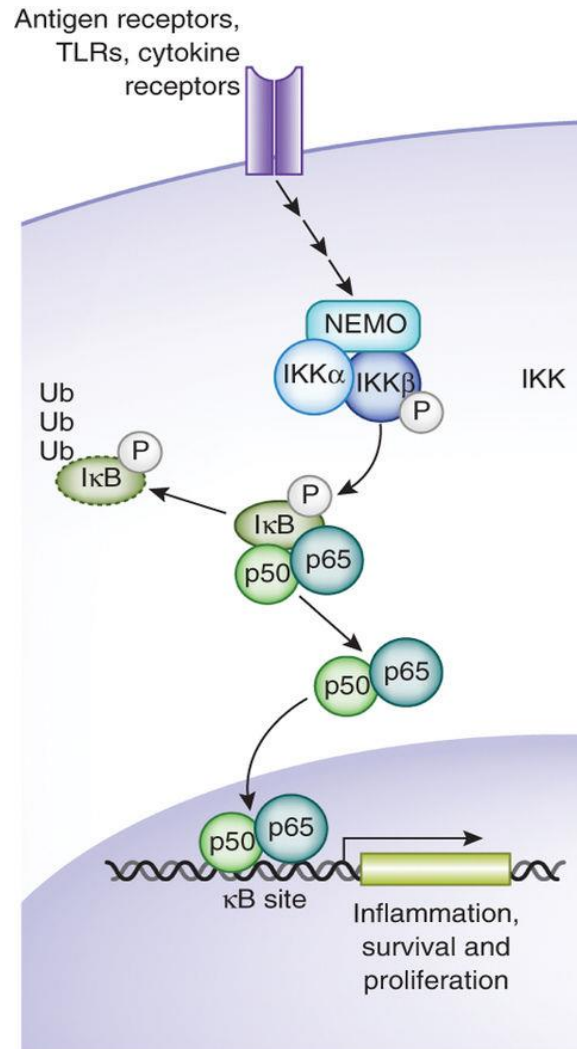
Figure 1.4 Canonical pathway of NF-kB activation. Activation of canonical signalling is induced by signals including antigens, toll-like receptor (TLR) ligands and cytokines (TNF-α and IL-1β). This causes activation of the IKKβ subunit of the IKK complex, mediated by a wide variety of signalling adapters including TRAF and TAK1). IKKβ phosphorylation of classical IκB proteins bound to the NF-κB dimer p50-p65 induces ubiquitination (Ub) of the IκB and proteasome-induced degradation. NF-κB can now enter the nucleus and bind specific κB DNA sites to mediate gene transcription encoding functions such as inflammation and cellular proliferation. (Gerondakis et al., 2013).
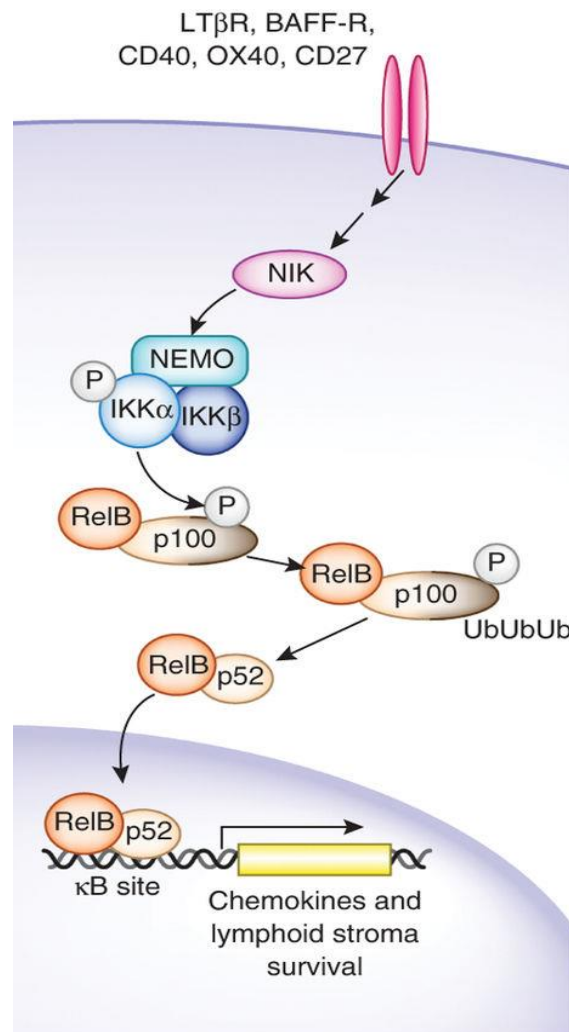
Figure 1.5: Non-canonical pathway of NF-kB activation. Activation of this pathway is induced by stimuli including lymphotoxin-β LTβ) and B cell activating factor (BAFF) binding their receptors (R). This causes NIK to activate IKKα, which then phosphorylates p100, triggering proteosomal processing and ubiquitination (Ub) required for the activation of p52-RelB dimers. These dimers then translocate to the nucleus to modulate gene transcription via binding to κB sites. (Gerondakis et al., 2013).

1.4.3 Involvement of NF-κB in development of endothelial dysfunction during ageing

As well as activation of NF-kB pro-inflammatory signalling by stimulation with circulating cytokines, there is now a vast amount of evidence to show that increased oxidative stress can also stimulate this pathway (D'Angio and Finkelstein, 2000; Haddad et al., 2000). Depending on the context, ROS can both activate and inhibit NF-κB signalling (Morgan & Lui, 2011) and as such, this results in a high degree of complexity comprising ROS interactions with various components of the signalling cascade. A number of studies have shown that ROS, in the form of H_2O_2, can activate the IKK complex and therefore lead to enhanced pro-inflammatory canonical NF-κB signalling. This has been proposed to be largely due to dimerization of IKKγ/NEMO through the formation of disulphide bonds between Cys54 and Cys347 (Herscovitch et al., 2008). Other studies have also shown that ROS can mediate the phosphorylation of RelA (p65), thus enhancing downstream signalling and translocation to the nucleus, potentiating pro-inflammatory gene transcription further. Moreover, adding to the difficulty of defining the specific function of ROS in terms of mediating NF-κB activity, it is now understood that many of these interactions occur in a cell-specific manner. Interestingly, ECs have been shown to exhibit ROS-mediated NF-κB activation (Brar et al., 2003).

Donato et al., (2007) were the first group to report an increase in NF-κB pro-inflammatory signalling during ageing within human vascular aortic ECs. Importantly, this age-associated increase in NF-κB expression and activation was positively related to an increase in several markers for oxidative stress, including EC nitrotyrosine, NADPH oxidase and xanthine oxidase, as well as impaired EDD. Furthermore, they demonstrated that increased nuclear translocation of NF-κB was associated with a decrease in expression of IκBα within these human vascular ECs (Donato et al., 2009). These findings highlight the significant role that canonical activation of NF-κB plays in contributing to the ED observed with advanced age via ROS signalling. Conversely, enhanced expression of NF-κB within vascular ECs could also be the result of oxidative stress, as NF-κB has the capability to both stimulate the production of, and

be stimulated by ROS (Brar et al., 2002; Brar et al., 2003). Taking all of this into account, the precise reason as to why both oxidative stress and chronic inflammation theories of ageing are linked can be demonstrated. Under normal physiological conditions (i.e. in healthy, young adults) NF-kB signalling is transient and short-lived and any activation of pro-inflammatory genes is terminated quickly due to controlled regulation of the pathway (Chung et al., 2006). However, if the activation signal persists, e.g. during the ageing process where there is a sustained increase in circulating levels of ROS and cytokines; continuous activation of the NF-kB signalling cascade could prevail and the outcome would be a chronic inflammatory phenotype. This therefore suggests a central role for NF-kB in the regulation of inflammatory processes during ageing via ED (Helenius et al., 1996; Korhonen et al., 1997).

1.4.4 NF-κB as a therapeutic target

In addition to ED associated with ageing, NF-κB signalling has also been implicated in mediating dysfunction of the vasculature associated with disease e.g. atherosclerosis and hypertension (Gareus et al., 2008). Furthermore, there is a plethora of evidence connecting activation of NF-κB to hypertrophic remodelling of myocardial tissue (Anderson et al., 2011; Kashiwase et al., 2005). As a result, targeting NF-κB activity has been proposed as an effective therapeutic approach for the treatment of such conditions. However, NF-κB also has an essential part to play in the resolution phase of inflammation and in tissue repair (Ghosh and Hayden, 2008). Eradicating NF-κB activity may be beneficial in one cell type but may have detrimental consequences in others. The therapeutic potential of treating inflammatory-based conditions (including ageing) may therefore lie in improved understanding of how NF-κB activation is regulated in specific cell types and in development of strategies aimed at reducing rather than abolishing NF-κB actions. This could be achieved by targeting specific regulation of part of the larger NF-κB signalling network. Specifically, inhibition of a modulator of NF-κB activity could dampen the overactive inflammatory signalling without compromising the host defence response (Rahman & Fazal, 2011).

1.4.5 Ca^{2+}-dependent modulation of NF-κB signalling

Ca^{2+} is known to be important in the regulation of NF-κB (Hughes et al., 1998). This was initially identified by the analysis of NF-kB activation in response to T-cell stimulation (Mattila et al., 1990) and since then, the role of Ca^{2+} in activating upstream and/or downstream targets in the NF-κB signalling cascade of virtually all cell types has been explored. Anderson and his colleagues have examined these key signalling components for an extensive period of time and in 2011, raised the hypothesis that the enzyme Ca^{2+}/calmodulin-dependent protein kinase II (CaMKII) may be the fundamental link between altered Ca^{2+} signalling and inflammation associated with myocardial infarction (MI), via NF-κB signalling (Singh & Anderson, 2011). Interestingly, there is extensive evidence indicating that a defect in the regulation of intracellular Ca^{2+} plays a role in the diseased vasculature, for example Ca^{2+} levels have been reported to be elevated in aortic SMCs of spontaneously hypertensive rats (Tostes et al., 1997). NF-κB signalling is also well established as playing a fundamental role in dysfunction of the vasculature (Gareus et al., 2008). However, it remains elusive whether a similar link also exists between altered Ca^{2+} signalling pathways and NF-κB in the vascular setting.

1.5 Introduction to CaMKII

CaMKII is a multi-functional protein kinase of about 50-60kDa, which was first highlighted for its dependence on Ca^{2+}/Calmodulin (CaM) binding for activation (Schulman & Greengard, 1978). CaM is a principal intracellular Ca^{2+}-binding protein expressed in all eukaryotic cells. It functions within cells as an intermediate protein that transduces Ca^{2+} signals by binding Ca^{2+} ions. Upon Ca^{2+}-binding, CaM undergoes a conformational change enabling it to interact with various target proteins (Hughes et al., 1998) and mediate cellular processes such as inflammation, apoptosis and SMC contraction (Hughes et al., 1998; James et al., 1995).

CaMKII modulates a variety of intracellular Ca^{2+}- dependent signalling processes such as neuronal plasticity, learning and memory, ion channel/receptor activation, muscle

contraction, cell secretion and gene expression. Modulation of these processes primarily occur due to CaMKII-mediated phosphorylation of a variety of target proteins (Colbran, 2004; Hudmon and Schulman, 2002; Soderling et al., 2001). The ability of CaMKII to modulate such a diverse range of functions may be down to the existence of a family of CaMKII isoforms, all of which are derived from four closely related genes (α, β, γ and δ). The expression of α and β subunits are normally restricted to neuronal tissue, whereas δ and γ subunits are present in various tissues, including the heart (Anderson, 2005). The δ isoform is constitutively expressed in the heart (Edman & Schulman, 1994), where it is now known to be present in both cardiomyocytes and cardiac fibroblasts (CFs) (Cai et al., 2008). Here, CaMKIIδ can present as various alternatively spliced variants, predominantly δ_2 and δ_3. There is now a significant amount of evidence for the involvement of CaMKIIδ in mediating normal cardiac function and dysfunction, and for augmented CaMKIIδ expression and activity in structural heart disease (Anderson, Brown & Bers, 2011; Currie, 2009; Martin et al., 2014). This is underpinned by the fact that CaMKIIδ plays a well-established role in modulation of cardiac contractility and may have a possible part to play in regulating hypertrophic gene transcription (Ramirez et al., 1997), inflammation and fibrosis (Anderson, Brown & Bers, 2011). Furthermore, studies have revealed that selective inhibition of CaMKIIδ activity, can significantly improve myocardial function in failing hearts (Sossalla et al., 2010).

More recently, the δ isoform was also discovered to be the dominant subunit of CaMKII found within ECs of the CVS, however it is the δ_6 splice variant which is expressed at higher levels compared with the more common δ_2 and δ_3 in heart (Wang et al., 2010). This variant has been shown to play a fundamental role in mediating thrombin-induced EC barrier dysfunction (Wang et al., 2010), however the overall role of CaMKIIδ in ECs of the vasculature still remains fairly elusive. Several groups have reported that CaMKII signalling may contribute to vascular pathologies, such as atherosclerosis. However, these emerging discoveries have only been shown in arterial SMCs, where CaMKII has been identified as playing a key role in SMC proliferation, hypertrophy, migration and contraction (Marganski et al., 2005; Maione et al., 2017; Singer et al., 2012).

1.5.1 Structure and activation of CaMKII by autophosphorylation

Each CaMKII subunit consists of a highly conserved N-terminus catalytic domain (approx. 280 amino acids) and a C-terminus association domain (150-220 amino acids) that flank a regulatory domain (approx. 40 amino acids) (Anderson, 2005). The regulatory domain contains a pseudo-substrate and a CaM-binding region that coincide to mediate responses to changes in cytoplasmic Ca^{2+} levels, i.e. the frequency, amplitude and duration of Ca^{2+} transients (Anderson, 2007; Zhang & Brown, 2004). CaMKII remains inactive under resting conditions, where the presence of this auto-regulatory domain restricts substrates from binding to the catalytic domain in the absence of Ca^{2+}/CaM. This is achieved through an interaction of the catalytic with the regulatory domain at threonine 286/287 (Thr286/287) (Erickson et al., 2008). Upon binding of Ca^{2+}/CaM, the subsequent conformational change causes relief of this autoinhibition, rendering the enzyme active (Hudmon & Shulman, 2002). In this activated state, adenosine triphosphate (ATP) and CaMKII substrates have access to the catalytic domain of the kinase for subsequent enzymatic catalytic activities (Hudmon & Shulman, 2002). The initial increase in Ca^{2+}/CaM which enables activation of CaMKII is initiated by various factors which cause stress to cells, for example in cardiac tissue where ischaemia and hypertrophy mediate activation (Anderson, 2007). Maximal activity of CaMKII is observed following Ca^{2+}/CaM binding and under sustained Ca^{2+}/CaM binding, the enzyme can lock itself in the activated state by autophosphorylation at Thr286/287. This is primarily due to the now negatively charged phosphate preventing re-association of the catalytic domain (Hudmon & Shulman, 2002). This autophosphorylation event initiates a 1000-fold increase in the affinity for Ca^{2+}/CaM within the regulatory domain and prolongs the Ca^{2+}/CaM stimulated activity of CaMKII (Skelding & Rostas, 2009), thus resulting in Ca^{2+}/CaM – independent (autonomous) activity, i.e. the enzymatic activity of CaMKII is retained even in the absence of bound Ca^{2+}/CaM (Anderson, 2007; Hudmon & Shulman, 2002; Zhang & Brown, 2004) (Figure 1.6).
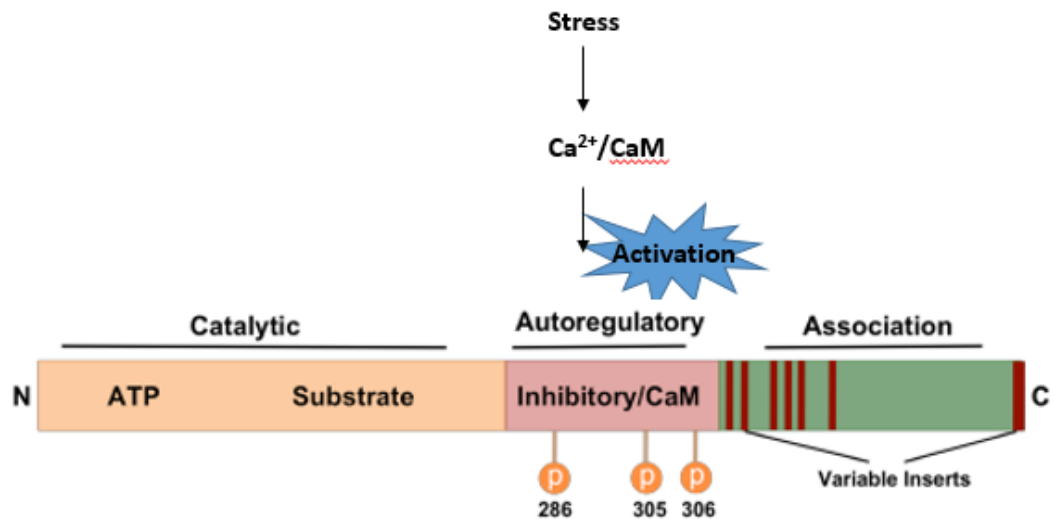
Figure 1.6 Activation of CaMKII by autophosphorylation. CaMKII becomes active following Ca^{2+}/CaM binding, relieving the autoinhibition of the enzyme enforced by the autoregulatory domain. Subsequent autophosphorylation at Thr286/287 within the regulatory domain leads to sustained activation of CaMKII, even in the absence of Ca^{2+}/CaM. (Adapted from Colbran, 2004).

1.5.2 Activation of CaMKII by oxidation

In more recent years, studies have discovered that under pro-oxidant conditions CaMKII activity may also be increased (Erickson et al., 2008; Zhu et al., 2007). This suggests that oxidative stress signals within the cell can modulate downstream Ca^{2+}-mediated cellular responses. This phenomenon was originally highlighted in a study showing that H_2O_2 treatment of T lymphocyte cells mediated activation of CaMKII, independent of Ca^{2+} signalling (Howe et al, 2002). The precise mechanisms by which ROS could mediate activation of CaMKII remained unclear, until experiments performed in the Anderson lab (Erickson et al., 2008) provided novel data to suggest this ROS-dependent, Ca^{2+}-independent CaMKII activation was initiated by modification of paired methionine residues M281/282 on CaMKII. It was also reported that CaMKII activation by either autophosphorylation or oxidation required the enzyme to be initially 'opened' by Ca^{2+}/CaM binding, thus enabling access to the autoregulatory domain for either mechanism of activation to occur. Similar to autophosphorylation, oxidation can prevent subsequent interaction of the autoinhibitory region with the catalytic domain, providing sustained Ca^{2+}-independent activation of CaMKII (Erickson et al., 2008) (Figure 1.7). As discussed earlier, elevated levels of ROS have been demonstrated in various models of cardiac disease, including MI and link to this mode of CaMKII activation in the heart (Kinugawa et al., 2000) and HF (Maack et al., 2003). In spite of this, it remains unclear whether similar modifications occur within the diseased vasculature. Furthermore, to date no one has yet investigated CaMKII expression in the aged cardiovascular setting. As outlined in Section 1.1, ageing is the single greatest risk factor for the development of CVD (North & Sinclair, 2012) and given the significantly enhanced levels of circulating ROS associated with advanced age, the potential for altered CaMKII activity (via increased oxidation) within aged individuals is strong.
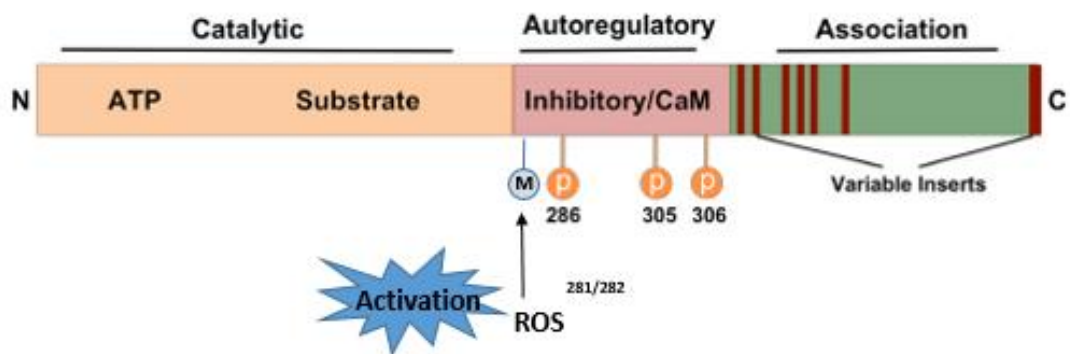
Figure 1.7 Activation of CaMKII by oxidation. ROS can mediate CaMKII activation by oxidation of methionine residues 281/282 in the autoregulatory domain of the enzyme. Similar to autophosphorylation, oxidation can prevent subsequent interaction of the autoinhibitory region with the catalytic domain, providing sustained Ca^{2+}-independent activation of CaMKII. (Adapted from Colbran, 2004).

1.6 Interaction between CaMKIIδ and NF-kB signalling

CaMKII has been established as a regulator of NF-κB activity in a variety of cell types, including T cells, neurones and cardiomyocytes (Hughes et al., 2001; Jang et al., 2001; Meffert et al., 2003; Singh & Anderson, 2011). Particular attention has been paid to the role of CaMKII in myocardial function and pathophysiology (Anderson, Brown & Bers, 2011; Currie, 2009). Studies have reported that both CaMKIIδ expression and CaMKII activity are increased in hypertrophied and failing hearts (Kirchhefer et al., 1999; Martin et al., 2014; Sossalla et al., 2010) and that selective inhibition of CaMKIIδ improves myocardial function in failing human hearts (Sossalla et al., 2010), thus underpinning the pivotal role that this enzyme plays in CVD progression. Importantly, evidence presented by various research groups has identified that CaMKIIδ mediates cardiomyocyte hypertrophy and cardiac inflammation via activation of the NF-κB signalling pathway (Singh & Anderson, 2011). This was initially established when it was discovered that in post-MI cardiomyocytes, NF-κB activity (and associated inflammation) was increased and that this correlated with up-regulated CaMKIIδ expression (Singh et al., 2009). It was proposed that CaMKII could modulate the NF-κB signalling pathway at different levels of the cascade, as it appeared to affect different proteins within the canonical pathway of activation depending on cell type (Singh & Anderson, 2011). For example, in T cells inhibition of CaMKII eliminated the 12-myristate 13-acetate (PMA)-induced phosphorylation and degradation of IκB, however TNF-α-induced IκB degradation was not affected (Hughes et al., 2001). Additionally, CaMKII has also been shown to activate NF-κB signalling in T lymphocytes indirectly via caspase recruitment domain-containing protein (CARMA 1) phosphorylation (Ishiguru et al., 2006). In spite of this, the exact mechanism by which the δ isoform of CaMKII modulates the NF-kB signalling pathway remains elusive. Work by our own research group has provided novel evidence to suggest that CaMKIIδ may specifically interact with IKKβ within the NF-kB signalling cascade (Martin, 2011). This work was predominantly carried out in CFs and showed that LPS-induced IκBα degradation was inhibited in the presence of the selective CaMKII inhibitor autocamtide-2-related inhibitory peptide (AIP). Further analysis using recombinant proteins and Surface Plasmon Resonance (SPR)

technology revealed that the δ isoform of CaMKII could specifically interact with IKKβ, but not IKKα or IKKγ (NEMO) of the IKK complex involved in the canonical pathway of NF-κB activation. This is an important step towards understanding how CaMKIIδ may modulate NF-κB activation and associated inflammation in the heart. It remains unclear though whether this interaction occurs in a vascular setting.

Currently there is nothing in the literature exploring the possible link between CaMKIIδ and modulation of NF-kB activity during the ageing process. Importantly, this is true for both cardiac and vascular settings. Given that NF-κB signalling is important in modulating ED associated with ageing, and that ROS (which is significantly increased during ageing) can directly activate CaMKII; it may be possible that the NF-kB-induced ED observed with advanced age is in fact partially initiated by increased CaMKII activation. Since CaMKIIδ is now known to be expressed within vascular ECs, there is potential that any interaction between CaMKIIδ and NF-κB specifically within the endothelium of the vasculature could serve as a potential target for dampening the pro-inflammatory and pro-oxidant phenotype in the elderly. Targeted inhibition of CaMKIIδ or indeed a CaMKII-substrate/binding partner interaction within the NF-κB signalling pathway could present a novel route for preventing ED and thus, relieve the chronic inflammation and associated negative consequences which are evident among older individuals; therefore reducing the likelihood of developing age-related conditions such as CVD.

1.7 Hypothesis and aims

The overall hypothesis of this project is that CaMKIIδ expressed in the vascular endothelium is up-regulated and hyperactive during ageing as a result of enhanced oxidative stress. This 'active' CaMKIIδ, acts to stimulate NF-kB pro-inflammatory signalling in the vascular endothelium via direct protein-protein interaction with IKKβ of the IKK complex and thus, contributes to the development of chronic inflammation which is apparent with advanced ageing, via endothelial dysfunction. We also hypothesise a similar increase in CaMKIIδ expression and activity in the hearts of

aged animals, mirroring what has already been well established in the diseased scenario.

The aims of this PhD study are to:

1. Demonstrate the co-existence of CaMKIIδ and NF-kB signalling in vascular ECs and define whether CaMKIIδ can modulate NF-kB activation using cells from two vascular beds and two species, i.e. primary human umbilical vein endothelial cells (HUVECs) and Aortic ECs from the rat respectively.

2. Provide evidence of cardiovascular and endothelial cellular dysfunction during ageing and show that an increased inflammatory phenotype is observed, using young and aged rats to demonstrate a parallel between *in vivo* and *in vitro* alterations.

3. Define whether CaMKIIδ expression and activation (by autophosphorylation and oxidation) is up-regulated in the myocardium and endothelium of the vasculature during ageing and whether there is a parallel increase in NF-kB activation.

Chapter 2: Materials and Methods

2. 1 Materials

Abcam

Anti-Glyceraldehyde-3-phosphate dehydrogenase (GAPDH) mouse monoclonal antibody, Anti-IKKβ mouse monoclonal antibody, 2', 7'-dichlorofluorescein diacetate (DCFDA)-cellular reactive oxygen species detection assay kit. Anti-CD31 (PECAM) rabbit polyclonal antibody, Sheep polyconal antibody to von Willebrand factor (vWF), Alexa fluor 488 conjugated donkey anti-sheep immunoglobin G (IgG), Goat anti-rabbit IgG TRITC, Goat anti-mouse IgG FITC.

BioRad Laboratories

Tween-20.

BD Biosciences

Mouse anti-rat CD45 polyclonal antibody

Calbiochem

Anti-IKKβ mouse monoclonal antibody.

Cell Signalling

Anti-IκBα rabbit polyclonal antibody, Phospho-NF-κB p65 (Ser536) rabbit polyclonal antibody, 4'6-diamidino-2-phenylindole (DAPI).

Concord Pharmaceuticals

Isoflurane.

Corning Costar

All tissue culture plastics including graduated pipettes, flasks and plates.

Eurogentec

Custom made anti-CaMKIIδ rabbit polyclonal antibody.

eBioscience

Rat tumour necrosis factor (TNF)-α and rat interleukin (IL)-1β ELISA Ready-SET-Go!® kits.

Fischer Scientific

Anti-phospho-threonine-286 CaMKII mouse monoclonal antibody, Novex® sharp pre-stained protein standard, Histoclear, Shandon histoplast paraffin wax.

Fine Science Tools

Aortic clamps.

GE Healthcare

Anti-mouse horseradish peroxidase (HRP)-linked whole antibody.

Gibco Life Technologies Ltd.

Dulbecco's Modified Eagle Medium (DMEM), Penicillin/Streptomycin antibiotics, Foetal Calf Serum (FCS), L-Glutamate, 100x non-essential amino acids, 100x sodium pyruvate.

GeneTex

Anti-Ox-CaMKII rabbit polyclonal antibody.

Insight Biotechnology Ltd.

TNF-α and IL-1β recombinant proteins.

Integrated DNA Technologies (IDT)

TriFECTa® kit DsiRNA duplex (rn. Ri. CaMK2d. 13.1, 13.2 and 13.3), Negative control DsiRNA and TYE[563] transfection control DsiRNA.

Leo Laboratories

Heparin (5000 IU/ml).

Lonza, U.K.

Endothelial growth basal medium (EBM-2), Foetal Bovine Serum (FBS), hydrocortisone, recombinant epidermal growth factor (rhEGF), ascorbic acid, gentamicin sulphate, fibroblast growth factor, heparin, vascular endothelial growth factor (VEGF) and insulin-like growth factor (IGF).

Merck Chemical Ltd.

Protein inhibitor cocktail set V ethylenediaminetetraacetic acid (EDTA) free, Phosphatase inhibitor cocktail set V (50x), Calmodulin, Autocamtide-II related inhibitory protein (AIP).

Millipore

P81 phosphocellulose squares, Autocamtide II substrate, protein kinase A (PKA) inhibitor peptide, PKC inhibitor peptide, Recombinant CaMKIIδ active 10ug, Millicell® EZ slides.

MIUS

Ultrasound transmission gel.

Perkin Elmer

$[\gamma\text{-}^{32}P]$ ATP [3000 Ci/mmol].

Pierce Biotechnology

Coomassie Plus® Reagent.

Promega UK Limited.

FuGENE® transfection reagent.

Qiagen

HiPerfect transfection reagent.

Reckitt Benckiser

Veet (topical depilatory cream).

Santa Cruz Biotechnology Inc.

Anti-IKKβ (C-20) goat polyclonal antibody, Ultracruz autoradiography film.

Sigma-Aldrich Co. Ltd

Adenosine triphosphate (ATP), Ethyleneglycerol-bis-(β-aminoethylether)-N, N, N'-tetraacetic acid (EGTA), Ethylenediaminetetra-acetic acid (EDTA), 4-(2-Hydroxyethyl) piperazine-/- ethaesulfonic acid (HEPES), Taurine, Creatine, Minimum 98% bovine serum albumin (BSA) for electrophoresis, Potassium chloride (KCl), Sodium dihydrogen orthophosphate (Na_2HPO_4), Dithiothreitol (DTT), Potassium dihydrogen orthophosphate (KH_2PO_4), Sodium orthovanadate (Na_3VO_4), Triton X-100, Sodium Dodecyl Sulphate (SDS), Sodium chloride (NaCl), Glycine, Acrylamide, Tris-base, TEMED, Anti-rabbit IgG-peroxidase conjugate whole molecule antibody, Glycerol, Angiotensin-II, Mowiol, Endothelial cell growth supplement (from bovine neural tissue) (ECGS), Haematoxylin, Eosin, Duolink In Situ PLA® probes (anti-rabbit PLUS and anti-mouse MINUS), Duolink polymerase (10 u/µl), ligase (1 U/µl), ligation buffer (5x) and amplification orange buffer (5x).

Worthington Ltd.

Collagenase type II (351 u/mg).

2.2 Human umbilical vein endothelial cell culture

Human umbilical vein endothelial cells (HUVECs) were cultured in EBM-2 supplemented with FBS (2%), hydrocortisone (0.04%), rhEGF (0.4%), ascorbic acid (0.1%), gentamicin sulphate (0.1%), fibroblast GF (0.4%), heparin (0.1%), VEGF (0.4%) and IGF (0.1%). Cells were grown to ~80% confluency at 37˚C in an atmosphere of 5% CO_2 and media changed every other day. Cells were passaged accordingly for required subsequent experiments.

2.3 Adult rat aortic endothelial cells

2.3.1 Isolation and culture

Adult male Sprague Dawley rats were used in these experiments at either 10-12 weeks (young) or 18-20 months (aged). Although aortic endothelial cells (ECs) are more commonly isolated by the mechanical 'scraping' technique (Bartov, Jerdan & Glaser, 1988), this procedure allows for more contamination with other cell types such as SMCs and fibroblasts. To reduce contamination and increase the purity and yield of ECs from aortae, an adapted version of the enzyme digestion method (Beijnum et al., 2008) was used.

Aortae were rapidly removed from rats following termination by intraperitoneal injection with pentobarbital sodium (10µl/g weight of animal; Euthatal) and heparin (0.1µl/g weight of animal; 5000 units/ml). The vessels were flushed gently with Ca^{2+}-free Krebs solution (120mM NaCl, 5.4mM KCl, 0.52mM NaH_2PO_4, 20mM HEPES, 11.1mM Glucose, 3.5mM $MgCl_2$, 20mM Taurine, 10mM Creatine, pH 7.4) and any surrounding tissue excised. A small aortic clamp was used at one end of the vessel to close the opening of the lumen. Using a 19G needle, Ca^{2+}-free Krebs solution containing 2 mg/ml collagenase type II was flushed inside the vessel as depicted by figure 2.1. Another clamp was used to close the opening of the lumen at the other end, allowing only the inner endothelial lining of the aorta to be exposed to the enzyme for subsequent digestion. The collagenase-filled vessel was incubated for 10 minutes at 37˚C in an atmosphere of 5% CO_2. Following digestion, both clamps were removed and 5ml of culture media consisting of DMEM supplemented with 20% (v/v) FCS,

1% (v/v), L-Glutamine and 2% Penicillin/ Streptomycin was added to the culture dish. The inside of the lumen was flushed through with the culture media using a 19G needle. The solution was then centrifuged at 1200 rpm for 5 minutes. The cell pellet was re-suspended in fresh media and the resulting cell mixture was plated in a T25 flask, incubated at 37˚C in an atmosphere of 5% CO_2 for 4 hours. After this time, remaining smooth muscle cells and fibroblasts were removed by replacement with EC specific Medium G (20% FCS, 1000 U/ml Penicillin-G, 100μg/ml Streptomycin, 2mM L-Glutamine, 1 x Non-essential amino acids, 1 x Sodium pyruvate, 25mM HEPES, 100μg/ml heparin, 60μg/ml ECGS (pH 7 – 7.6)). This medium was then changed every second day. Cells were cultured for approximately 7-10 days or until reaching 70-90% confluency before subsequent plating for required assays. All experiments were performed with cells from passage 1-3.

Tunica externa
(Connective tissue)

Tunica media
(Smooth muscle cells)

Tunica intima
(Endothelial cells)

Collagenase solution
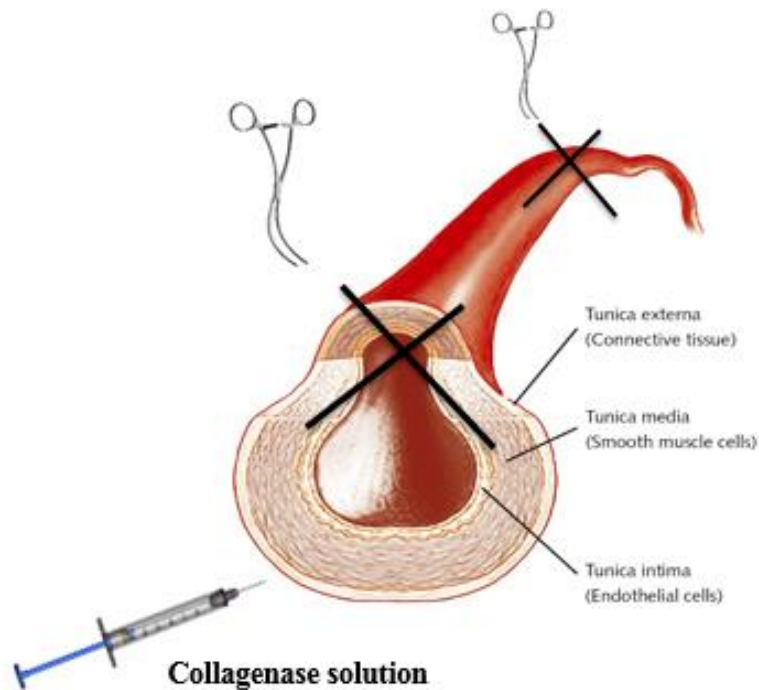
Figure 2.1 Adaptation of the enzyme digestion technique for isolating rat aortic ECs.

A schematic representation of the method used to fill the inner lumen of the aorta with collagenase-II solution following dissection from the rat. Both ends of the vessel are clamped shut allowing only the endothelial lining to be exposed to enzyme digestion, thus preventing contamination with other cell types such as smooth muscle cells. (Diagram adapted from Promocell, GmbH).

2.3.2 Characterisation of aortic ECs by immunofluorescence

Primary aortic ECs and HUVECs were grown on plain 13x13mm glass coverslips until they reached ~50% confluency (48h). Cells were fixed by aspirating the culture medium and applying ice cold methanol for 10 minutes. Coverslips were washed once with sterile phosphate buffered saline (PBS) (155mM NaCl, 2.7mM Na_2HPO_4, 1.5mM KH_2PO_4, pH 7.4) and then permeabilised using 0.01% triton X-100 (prepared in PBS) for 10 minutes. Non-specific binding was blocked using 1% (w/v) BSA in PBS for 1h at room temperature followed by direct addition and incubation of either CD31/Platelet endothelial cell adhesion molecule (PECAM)-1 or von Willebrand Factor (vWF) antibody overnight at 4°C. Both antibodies were prepared in 1% (w/v) BSA/ PBS at a concentration of 1:100. Following primary antibody incubation, coverslips were washed 3 times with sterile PBS and were then incubated with secondary antibody (alexa fluor 488 conjugated donkey anti-sheep IgG (1:200) for vWF staining. For cells stained with PECAM-1, no secondary antibody was required as the primary antibody is pre-conjugated to alexa fluor 488. All other controls were prepared in the absence of primary antibody. After washing 3 times in PBS, DAPI prepared in PBS (1:6000) was added to each coverslip for 5 minutes in the dark. This was used to stain the nuclei blue. A further wash step with PBS was conducted and coverslips were mounted using Mowiol® mounting agent. Slides were stored at 4°C in the dark until they were viewed and photographed. Pictures were taken using a Nikon Eclipse E600 Oil Immersion microscope connected to a photometrics (CoolSnap™ Fx) digital camera managed by MetaMorph™ software (Universal Imaging Corporation, West Chester, PA). Images were captured using a 10x objective lens.

2.4 Treatment of HUVECs and aortic ECs

For NF-κB stimulation experiments, both HUVECs and aortic ECs were passaged and plated at $1x10^5$ cells/well into 12-well culture dishes and grown until reaching ~80% confluence. Cells were exposed to either 10ng/ml TNF-α or 10ng/ml IL-1β over the course of 1h. For experiments using CaMKII inhibitors, cells were pre-incubated with

AIP (5µM) or KN93 (5µM) for 2h prior to TNF-α stimulation (1h). Vehicle control samples were treated with deionised H_2O (10µl). Following stimulation, cells were washed 3 times in PBS and then prepared in 1x lysis buffer (63mM Tris HCl (pH 6.8), 2mM $Na_4P_2O_7$, 5mM EDTA, 10% (v/v) Glycerol, 2% (w/v) SDS, 0.007% (w/v) Bromophenol Blue). Samples were then boiled and stored at -20˚C until their use for immunoblotting.

2.5 CaMKIIδ siRNA transfection of aortic ECs

2.5.1 Selection of appropriate transfection reagent

Initial experiments were performed to establish the best transfection reagent for all siRNA work. Cells were seeded at $5x10^4$ cells/well in a 24 -well culture plate for use the following day. Transfection reagents FuGENE® and HiPerfect® were used for these experiments and to assess their efficiencies, 1.5µl, 3µl or 4.5µl (ratios of 1.25:1, 5:1 and 7.5:1 respectively) of each of the reagents was pre-incubated with 75ng (10nM) of the fluorescent-labelled TYE^{TM} 563 DS control duplex (TriFecta®). Control mixtures contained either 75ng of the control duplex or 3µl FuGENE/HiPerfect® alone. 100µl of serum free endothelial specific medium (medium G) was then added to each mixture and vortexed gently before being left for 10 minutes at room temperature to allow the complexes to form. 100µl of media from each well was removed before adding each complex in a dropwise manner to the appropriate well. Cells were then incubated at 37˚C in an atmosphere of 5% CO_2 for 24h before being assessed by microscopy (ZOE^{TM} Fluorescent Cell Imager, BioRad). Cells which had been successfully transfected could be visualised using the rhodamine filter adopting a fluorescent red phenotype.

2.5.2 Determination of CaMKIIδ siRNA duplex efficiency

All subsequent siRNA experiments incorporated the HiPerfect® transfection reagent at a ratio of 5:1 with the appropriate siRNA as optimised in Section 2.5.1. The TriFecta® kits offer three target duplexes of the CaMKIIδ siRNA in order to assess

several variants and maximise the potential for efficient gene knockdown. Each of the three duplexes: (i) rn.Ri.Camkd2.13.1, (ii) rn.Ri.Camkd2.13.2 and (iii) rn.Ri.Camkd2.13.3, consisted of the following sequences respectively:

(i)

```
5'-GGGUAAAGAUAAACAACAAAGCCAA-3'
   | | | | | | | | | | | | | | | | | | | | | | | | |
3'-ACCCCAUUUCUAUUUGUUGUUUCGGUU-5'
```

(ii)

```
5'-CCAGUCAUUGUAUACAACAGAUUCT-3'
   | | | | | | | | | | | | | | | | | | | | | | | | |
3'-ACGGUCAGUAACAUAUGUUGUCUAAGA-5'
```

(iii)

```
5'-CAUUUGGGUCUUCUAAUUGUCAACA-3'
   | | | | | | | | | | | | | | | | | | | | | | | | |
3'-GUGUAAACCCAGAAGAUUAACAGUUGU-5'
```

Cells were seeded at 5×10^4 cells/well into a 12 well culture plate and on the following day treated with each of the siRNA:HiPerfect® duplexes at either 1nM, 10nM or 100nM final concentrations prepared as described previously in Section 2.5.1. Control samples were treated with a validated negative control duplex (NC1) provided by the TriFecta® kit that does not present in the human, mouse or rat genomes. All samples were then harvested at 72h post-transfection in 1x lysis buffer (63mM Tris HCl (pH 6.8), 2mM $Na_4P_2O_7$, 5mM EDTA, 10% (v/v) Glycerol, 2% (w/v) SDS, 0.007% (w/v) Bromophenol Blue) prior to analysis of CaMKIIδ expression by immunoblotting.

2.5.3 Assessment of NF-κB activation following CaMKIIδ silencing

A final concentration of 10nM siRNA was selected given it produced optimal knock down of CaMKIIδ expression at the 72h time-point. Subsequent experiments therefore incorporated transfection of cells with this concentration at the 5:1 ratio with HiPerfect® as described above before treating with or without 10ng/ml TNF-α over a 1h time course to assess NF-κB activation. Cells were then harvested in 1x lysis buffer as described in Section 2.4.

2.6 Proximity Ligation Assay (PLA)

The Duolink® Orange In Situ-Fluorescence PLA kit was purchased to assess and quantify potential intracellular interaction between CaMKIIδ and IKKβ. PLA technology allows the direct detection of protein-protein interactions with high specificity and sensitivity. It involves two antibodies raised in different species to recognise the proteins (antigens) of interest. Secondary antibodies are then directed against the constant regions of the different primary antibodies (the PLA probes). Each of the PLA probes has a unique oligonucleotide attached to it and if the probes are in close proximity (i.e. the proteins are interacting), rolling circle DNA synthesis occurs during ligation. The reaction causes a several hundred-fold amplification of the now fluorescently-labelled oligonucleotides, in which a signal can be easily detected as a fluorescent spot by fluorescence microscopy.

Initial immunofluorescence experiments were performed to optimise the conditions for the assay using the protocol as described in Section 2.3.2. Primary antibodies incubated overnight at 4°C included CaMKIIδ (rabbit polyclonal antibody, custom-made against the C-terminus of CaMKIIδ, Eurogentec), ox-CaMKII (rabbit polyclonal antibody, GeneTex) and IKKβ (mouse monoclonal, Abcam) at concentrations of 1:50, 1:50 and 1:200 respectively. Negative control samples were incubated with 1% BSA/PBS alone overnight also at 4°C. On the following day all samples (including negative control) were washed 3 times with sterile PBS and then incubated with the appropriate secondary antibody (goat anti-rabbit IgG TRITC or goat anti-mouse IgG FITC at dilutions of 1:200 in PBS). Nuclei were then counterstained with DAPI

(1:6000) for 5 minutes in the dark before slides were mounted onto coverslips and stored at 4°C in the dark until visualisation under the microscope as previously described in Section 2.3.2.

Once the best conditions had been selected, cells were seeded at 7×10^4 cells into individual wells of a culture chamber (Millicell® EZ slide, Millipore) and grown overnight to reach ~50% confluency. Day 1 of the Duolink® protocol followed the same method as day 1 of immunofluorescence where cells were incubated with the appropriate primary antibody overnight at 4°C after fixation, permeabilisation and blocking. In an attempt to optimise signals, a select number of wells were stimulated with either 10ng/ml TNF-α (for CaMKII experiments) or 30μM H_2O_2 (for ox-CaMKII experiments). Negative control samples were treated with antibody dilution buffer alone (1% BSA/PBS) or IKKβ antibody only (Figure 2.2). The following day, primary antibodies were removed and cells washed 2 times in PBS before incubation with the PLA probes. Each sample was treated with 8μl PLA MINUS + 8μl PLA PLUS + 24μl of the antibody dilution buffer used on day 1 for 1h at 37°C and an atmosphere of 5% CO_2 in a pre-heated humidity chamber. The PLA probes mixture was removed and cells were washed 2 times in wash buffer A (0.01M Tris, 0.15M NaCl, 0.05% Tween-20) (5 minute washes) under gentle agitation. The ligation mix was then added to each sample (8μl of 5x ligation stock + 31μl sterile water + 1μl ligase) and cells were incubated for 30 minutes at 37°C and an atmosphere of 5% CO_2 in a pre-heated humidity chamber. This was followed by two sets of washes with wash buffer A (2 minute washes) under gentle agitation and then the amplification mix was added to each sample (8μl amplification stock + 31.5μl sterile water + 0.5μl polymerase). The cells were incubated in the amplification buffer for 100 minutes at 37°C and an atmosphere of 5% CO_2 in a pre-heated humidity chamber. This step in the process is light sensitive therefore the chamber was wrapped in foil during the incubation and for all other subsequent steps. Cells were then washed two times in wash buffer B (0.2M Tris, 0.1M NaCl) (10 minute washes) before a final wash in diluted wash buffer B (1:100) for 1 minute. DAPI was added to stain the nuclei blue (1:6000 in PBS) for 5 minutes in the dark and then slides were mounted in Mowiol® onto coverslips and

left to dry overnight. Images were captured on a Leica 5P5 confocal microscope at 63x magnification at Exc. 554nm/Em. 579nm using an oil immersion dipping lens.
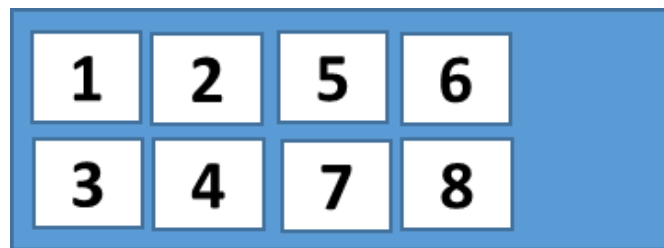
Figure 2.2 Typical Millicell® EZ chamber slide used for PLA.

A diagram illustrating the layout of a typical chamber slide into which cells are split for PLA experiments. Wells were numbered such that each assay consisted of either 4 or 8 wells using the following format: (1&5) Control, no antibody (antibody dilution buffer only); (2&6) Control, IKKβ antibody only; (3&7) IKKβ and CaMKII (or ox-CaMKII) antibodies (basal); (4&8) IKKβ and CaMKII (or ox-CaMKII) antibodies (treated with either 10ng/ml TNF-α or 30μM H_2O_2 for 10 minutes).

2.7 Measurement of endothelial cell impedance

2.7.1 Chamber manufacture and experimental set-up

All chambers used for impedance measurements were prepared beforehand by PhD student Ian Holland (Biomed Eng., University of Strathclyde). Cell culture chambers were manufactured by modifying a Lab-Tek cell culture 2 well chamber slide (Sigma Aldrich, Poole, United Kingdom) and a Falcon petri dish (Fisher Scientific, Loughborough, United Kingdom). A thin gold patterned layer was applied to the surface of the petri dish using a vacuum deposition process. The pattern comprised one large electrode and four smaller opposing electrodes as depicted in Figure 2.3. Wires were attached to the distal end of the electrodes with silver chloride paint (RS, Corby, United Kingdom). The chamber housing and silicone gasket was removed from the Lab-Tek slide cut to isolate a single cube. This was then adhered over the gold electrode pattern by applying double sided tape, recreating the seal between the housing and the slide.

For experiments investigating the effects that different electrode coatings have on cell growth, platinum black surface coatings were applied galvanostatically onto some of the chambers on top of the patterned gold layer. Other chambers were left with gold coated electrodes only. Combined coating of four small electrodes was applied using 3mA for platinum black over 3 seconds. The main electrodes were coated using 30mA over 3 seconds for platinum black where the coating processes used a Solartron SI-1287 Electrochemical interface (Solartron Analytical, Farnborough, United Kingdom). For all conditions, the electrodes were cleansed in ethanol and then 1.5ml of Chloroplatinic acid platinising solution (16.6ml distilled water, 5g Chloroplatinic acid hexahydrate, 0.5mg lead acetate) or 0.1M pyrrole/Sodium Salicylate solution (14.895ml distilled water, 104µl distilled pyrrole, 0.2415g Sodium Salicylate) was poured into the chamber.

Wires attached to distal end where current is applied.

Four platinum (or gold)-coated electrodes

One large electrode
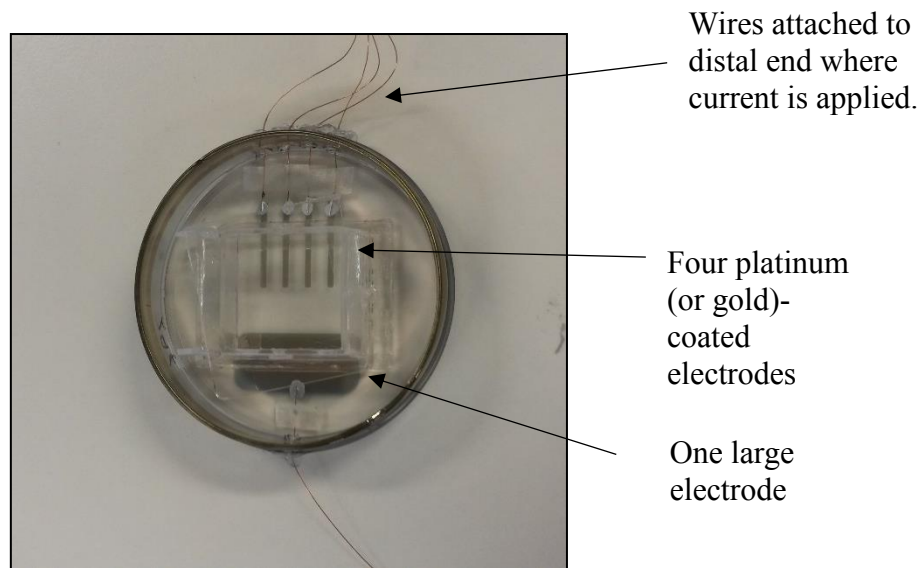
Figure 2.3 Image of modified cell culture chamber for impedance experiments.

A representative photograph of the typical chamber set up into which cells were seeded for optimisation and impedance experiments. Electrodes were either coated in platinum or gold and for control chambers, electrodes were taken out for cells to grow on plastic only.

2.7.2 Assessment of cellular growth and phenotype with different coatings

Initial experiments were performed to investigate differences in growth and phenotype of young aortic ECs grown on platinum or gold coated electrodes. Cells were isolated and maintained in culture as previously described (Section 2.3). Chambers were rinsed in distilled water and then ethanol before sterilisation for 1 hour under UV light. ECs were seeded at densities ranging from 5.5 to 10.5 x 10^4 cells per cm^2 (2ml/chamber) and at passage numbers in the range 2 to 3 for all experiments. Cells were viewed over a 72h time period using a Nikon Eclipse (TE300) Inverted microscope and images were taken at 10x magnification. Time-lapse imaging was also performed over 72h using a Moticam 10 microscope camera attached to an AE31 microscope (both Motic, China) to assess movement and growth of cells.

To further assess the impact different coatings had on cell phenotype, ECs grown on platinum and gold surfaces were fixed and subjected to immunofluorescence to measure activation of NF-κB signalling. Staining was performed similar to that as described in Section 2.3.2, where cells were exposed to primary antibody (phospho-NF-κB p65 (Ser536) rabbit polyclonal) at a concentration of 1:200 diluted in 1% BSA/PBS overnight at 4°C. On the following day cells were washed three times with sterile PBS and then incubated with goat anti-rabbit IgG FITC secondary antibody at a dilution of 1:200 in PBS. Nuclei were then counterstained with DAPI before mounting and imaging as previously described.

2.7.3 HUVEC and aortic EC impedance spectroscopy experiments

A 32 channel multiplexer circuit was used to autonomously switch an impedance measurement procedure between 8 of the previously detailed chambers (4 electrodes per chamber). The system comprised an ADG732BUZ 32:1 multiplexer chip (Analog devices, Norwood, Massachusetts, United States) an Arduino 2560 development board (Maplin, Glasgow) and an Autolab PGSTAT302N.FRA32M, (Metrohm, Herisau, Switzerland). The multiplexer was of the same architecture and manufacturer as used in previously published studies on impedance measurement (Sun & Morgan, 2010).

Bespoke software for integrating the disparate componentry was developed using LabView software (National Instruments, Texas, U.S.A). A voltage amplitude of 50mV with a frequency range of 1MHz to 1.2Hz at 10 frequencies per second was selected. The system was characterised for errors prior to use and these results were deemed to be within acceptable bounds. A further period of testing verified that the system was capable of performing measurements within an incubator environment for time periods typically used in cellular experimentation.

Both HUVECs and young rat aortic ECs were used for impedance experiments. Initial experiments investigated HUVECs alone to assess the impedance profile for this cell type and ensure reproducibility of such profiles. Chambers and cells were prepared as described above, with control chambers containing 2ml of media only. Impedance sweeps of each electrode were taken at approximately 2.5 hour intervals. Media changes were carried out every 48h. All EC tests were run for a period of 96h. Periodic 10x magnification images were taken at the time of impedance measurements using a Moticam 10 microscope camera attached to an AE31 microscope (both Motic, China).

2.8 Detection of intracellular reactive oxygen species (ROS) production

Intracellular ROS production was assessed in both young and aged EC cultures using a specially designed assay kit (Abcam, U.K.) which uses the cell permeant reagent DCFDA, a fluorogenic dye that measures hydroxyl, peroxyl and other ROS activity within the cell.

Initial optimisation experiments were performed in young ECs only to determine the efficiency of the assay. Cells were plated in 96-well black-sided culture dishes at a seeding density of 2.5×10^4 cells/well. The ROS assay was then conducted 48h after initial plating. Cells were incubated with or without $25\mu M$ of the cell permeant reagent DCFDA (prepared in 1x dilution buffer (Hanks Balanced Saline Solution (HBSS)) diluted from the 10x stock supplied in the kit) ($100\mu l$/well) for 45 minutes in the dark at $37°C$ in an atmosphere of 5% CO_2. They were then washed in $100\mu l$ 1x dilution buffer briefly before being treated with either of the following ($100\mu l$/well), prepared in 1x supplemented buffer (10% FCS (v/v) diluted in 1 x dilution buffer):

50μM Tert-Butyl Hydrogen peroxide (TBHP) (positive control)

10μM Hydrogen Peroxide (H_2O_2)

30μM H_2O_2

100μM H_2O_2

300μM H_2O_2

Background wells were treated with or without 25μM DCFDA prepared in 1x supplemented buffer only. All treatment conditions were for a total of 3h in the dark at 37˚C and an atmosphere of 5% CO_2.

Following this, young and aged cells were both assessed for intracellular ROS activity at baseline and after 10μM Angiotensin (Ang)-II (prepared in 1x supplemented buffer) stimulation (3h). A similar protocol was followed as above where cells were either pre-incubated with or without 25μM DCFDA for 45 minutes prior to appropriate treatment. Signals were then read at Excitation 485nm/ Emission 535nm using a Polarstar^{TM} plate reader and fluorescence intensities determined following background subtractions and expressed as arbitrary units (a.u.).

2. 9 Echocardiography

All experiments involving live animals were carried out under licence from the British Home Office. Procedures conformed to the *Guide for the Care and Use of Laboratory Animals* published by the US National Institutes of Health (NIH Publication No. 85-23, revised 1996) and Directive 2010/63/EU of the European Parliament. Animals were all bred in-house, with aged rats kept as ex-breeders until reaching the appropriate age. Animals were group housed in conditions of a 12h light-dark cycle with ad-lib feeding (standard rat chow) and water.

In preparation for echocardiography rats were briefly anaesthetised in a perspex chamber with 3% Isoflurane in the presence of 100% oxygen at a flow rate of 2L/min. After 2-3 minutes, rats were placed supine on a facemask and were maintained with 1.5-2% Isoflurane in the presence of 0.5-1L/min oxygen. Fur was removed by

application of a topical depilatory cream from the neck and upper chest area. For echocardiography of the heart, two-dimensional short axis views and M mode images were recorded at the level of the papillary muscle with the use of a MIUS HDI 3000CV echocardiography system, a 13MHz linear array transducer and ultrasound transmission gel. Systolic and diastolic LV wall measurements (including anterior wall (AW) and posterior wall (PW) measurements, LV end systolic dimension (LVESD), LV end diastolic dimension (LVEDD) and fractional shortening (%FS) were assessed from M mode traces. Fractional shortening is expressed as [LVEDD – LVESD/ LVEDD] x 100. An average of three measurements of each variable was used for each animal.

For measurements of blood flow through the ascending aorta, a short axis view of the heart was obtained initially. The linear probe was then slowly turned ~70-80° clockwise to obtain a clear longitudinal axis of the heart and to allow a clear view of the vessels to be visualised. Brightness mode (B mode) ultrasound was used to measure vessel diameter and colour Doppler mode to visualise the direction of blood flow. Pulsed wave Doppler mode (PWDM) was used to measure the velocity of blood passing through the ascending aorta. From these traces, the velocity time integral (VTI) and heart rate (HR) could be assessed. At least three measurements were recorded for velocity in the vessel per animal and an average taken. The blood flow was then calculated using the following formula:

$$Flow\ (ml/min) = VTI(Velocity\ Time\ Integral)\ x\ \pi r^2\ x\ HR\ (Heart\ Rate)$$

2.10 Post Mortem Analysis

2.10.1 Rat left ventricular heart homogenisation

Young and aged rats were euthanised as described in Section 2.3.1. The midline of the abdomen was incised and the thorax opened to expose the heart and lungs. Hearts were rapidly removed then washed in ice cold Ca^{2+}-free Krebs solution, blotted dry and

weighed. Left ventricular tissue was then dissected and tissue was cut into fine pieces in ice-cold homogenisation buffer (20 mM Tris-base buffer, 1 mM DTT, 1X protease inhibitor cocktail (500 μM AEBSF, 150 nM Aprotinin, 1 μM E-64, and 1 μM Leupeptin)] (5 x ventricular weight) and was then homogenised using an ultra-turrax T8 (IKA®, U. K.). Samples were then aliquoted and stored at -80°C until required for immunoblotting.

2.10.2 Rat aorta dissection and solubilisation

Following termination of animals, aortae were excised by dissecting out from the aortic arch down to the abdominal aorta. Once removed, vessels were immediately immersed in ice-cold Ca^{2+} -free Krebs solution and the lumen flushed through to remove any remaining blood. Any fat or connecting tissue was also removed from the vessels using fine forceps. Tissues were blotted dry and weighed before being pulverised in liquid nitrogen until a fine, white powder was formed. The frozen vessel was then solubilised by adding the required volume of solubilisation buffer (50mM Tris pH 7.5, 50mM NaCl, 1% Glycerol, 1mM EDTA, 1mM DTT, 1% Triton X, 1x protease inhibitors (Merck), 1 x phosphatase inhibitors (Merck), 10x aortic weight)) and transferring solution containing the tissue to an eppendorf tube. This was left to mix end-over-end for 10 minutes at 4°C before centrifugation at 13,000rpm for 5 minutes, also at 4°C. The supernatant was then removed and aliquots stored at -80°C until used for immunoblotting.

2.11 Protein quantification

Total protein concentrations for both whole ventricular and aortic homogenates were quantified using a Bradford assay (Bradford, 1976). BSA samples (0mg/ml, 0.1mg/ml, 0.25mg/ml, 0.5mg/ml, 0.75mg/ml and 1.0mg/ml) were used to generate a standard curve. Ventricular homogenates were then prepared at 1:20, 1:40 and 1:50 dilutions, while aortic homogenates at 1:5, 1:10 and 1:20 dilutions to ensure they fell within the linear range of the protein BSA standard curve. Each standard and sample was loaded

in triplicate into a 96 well plate with one row loaded in appropriately diluted homogenisation buffer (ventricular tissue) or solubilisation buffer (aortic tissue) to serve as a blank background. Coomassie Plus^{TM} Protein Reagent (200µl) was then added to each well and the plate was read at 595nm using a microplate reader (Model 680, BioRad). Standards were plotted using a sigmoidal fit and only samples with absorbance readings within the linear range of the curve were used for quantification.

2.12 Quantitative immunoblotting and densitometry

Tissue samples were prepared in 1 x lysis buffer (63mM Tris HCl (pH 6.8), 2mM Na$_4$P$_2$O$_7$, 5mM EDTA, 10% (v/v) Glycerol, 2% (w/v) SDS, 0.007% (w/v) Bromophenol Blue) containing 75mM DTT as a reducing agent and were heated to 100°C for 5 minutes prior to loading into 10% (v/v) acrylamide gels and subjecting to electrophoresis using the BioRad system. To minimise inter-gel variations, comparisons between young and aged tissues were initially made by loading a range of protein amounts (2.5µg - 10µg) onto the same gel. Once a suitable amount had been optimised, subsequent experiments used the same total protein load per sample (5µg for ventricular and 10µg for aortic tissue preparations). For comparisons between young and aged cell preparations, cells were equally seeded at 1×10^5 cells/well into a 12 well culture plate and grown to ~80% confluence before harvesting in 1 x lysis buffer containing 75mM DTT as before. A total of 10µl from each sample was then loaded onto the acrylamide gels for electrophoresis to be performed. Similar volumes of cell preparations were used for comparisons between control and stimulated/transfected cell lysates as described in Sections 2.4 and 2.5.

Electrophoresis was performed at a constant voltage of 130V in running buffer (25mM Tris-base, 192mM Glycine, 1% (w/v) SDS) for 90 minutes. This was followed by transfer of proteins onto nitrocellulose membranes using transfer buffer (25mM Tris-base, 192mM Glycine, 20% (v/v) Methanol) for 105 minutes at 0.3A. Subsequently, non-specific binding sites on the membranes were blocked with 5% (w/v) non-fat dry milk diluted in Tris buffered saline solution containing Tween-20 (TBST) buffer (20mM Tris-base, 137mM NaCl and 0.1% (v/v) Tween-20, pH 7.6) for 1h at room

temperature. Following this the membrane was then incubated overnight at 4°C with the appropriate primary antibody (Table 2.1) prepared in 5% (w/v) non-fat dry milk in TBST buffer. On day 2 of the protocol, membranes were washed for 5x 5minute washes with TBST buffer and then incubated for 2h at room temperature with the appropriate secondary antibody (Table 2.1) in 5% (w/v) non-fat dry milk in TBST. Blots were then washed again as above (5x 5 minute washes) with TBST buffer before signals developed by enhanced chemiluminescence (ECL) and visualised on autoradiography film. Membranes were developed by the X-Omat (Kodak M35-M X-Omat processor) and signals then quantified by densitometry using a GS800 densitometer and Quantity One Image Software (version 4.5.2, BioRad). Blots were then subsequently stripped of their antibodies by incubating in 15ml stripping buffer (1.5% glycine (w/v), 0.1% SDS (w/v), 1% Tween-20 (v/v), pH 2.2) for 1h at 60°C on a shaking platform. Membranes were then washed for 5x 5 minutes in TBST buffer before incubating with GAPDH primary antibody which was used as an internal standard (refer to table) overnight at 4°C. Day 2 of the immunoblotting protocol was then followed (as above) and signals were quantified by densitometry analysis. All previous proteins investigated were then normalised to their counterpart GAPDH signals in order to generate all histogram data.

Protein	Molecular Weight (kDa)	Primary Antibody	Secondary Antibody	Company
IκBα	37	Rabbit polyclonal (1:1500)	Goat anti-rabbit IgG (whole molecule)-peroxidase conjugated (1:7500)	Cell Signalling Technology
pp65	65	Rabbit polyclonal (1:1500)	Goat anti-rabbit IgG (whole molecule)-peroxidase conjugated (1:7500)	Cell Signalling Technology
CaMKIIδ	56	Rabbit polyclonal (1:1000)	Goat anti-rabbit IgG (whole molecule)-peroxidase conjugated (1:7500)	Eurogentec (Custom made)
phosphoThr286-CaMKIIδ	56	Mouse monoclonal (1:500)	Donkey anti-mouse IgG-HRP (1:7500)	Thermo Fisher Scientific
Oxidised-CaMKII	56	Rabbit polyclonal (1:1000)	Goat anti-rabbit IgG (whole molecule)-peroxidase conjugated (1:7500)	GeneTex
IKKα	85	Mouse monoclonal (1:1500)	Donkey anti-mouse IgG-HRP (1:7500)	Calbiochem
IKKβ (i)	87	Goat polyclonal (1:1500)	Rabbit anti-goat IgG-HRP (1:7500)	SantaCruz
(ii)	87	Mouse monoclonal (1:1500)	Donkey anti-mouse IgG-HRP (1:7500)	Calbiochem
(iii)	87	Rabbit polyclonal (1:1500)	Rabbit anti-goat IgG-HRP (1:7500)	Abcam
GAPDH	40	Mouse monoclonal (1:100,000)	Donkey anti-mouse IgG-HRP (1:7500)	Abcam

Table 2.1 Primary and secondary antibodies for immunoblotting

2.13 CaMKII activity assay

The CaMKII activity assay was used to measure the phosphotransferase activity of CaMKII in aortic and cardiac tissue homogenates from both young and aged animals, based on the phosphorylation of a specific substrate peptide (autocamtide-II) by the transfer of $[\gamma\text{-}^{32}P]$ ATP by CaMKII.

All assay components, consisting of CaMKII substrate cocktail (500µM autocamtide-II and 40µg/ml calmodulin), PKA/PKC inhibitor cocktail (2µM PKA peptide inhibitor + 2µM PKC peptide inhibitor) and the source of CaMKII enzyme (recombinant CaMKII or aortic homogenates) diluted to the desired concentration, were prepared on ice to a final volume of 40µl in assay dilution buffer (ADB)-I (20mM MOPS, pH 7.2, 25mM β-glycerol phosphate, 1mM sodium orthovanadate, 1mM dithiothreitol, 75mM $MgCl_2$, 1mM $CaCl_2$. In Ca^{2+} free controls, ADB-I was substituted for ADB-II (20mM MOPS, pH 7.2, 25mM β-glycerol phosphate, 1mM sodium orthovanadate, 1mM dithiothreitol, 75mM $MgCl_2$, 5mM EGTA). Reactions were initiated by the addition of 10µl $[\gamma\text{-}^{32}P]$ ATP diluted to 1µCi $µL^{-1}$ with Mg^{2+}/ATP cocktail (75mM Mg/Cl_2, 500µM ATP prepared in ADB-I). Samples were assayed in triplicate and incubated at 30°C for 10 minutes under constant agitation. The reaction was then terminated by spotting 25µl of each sample on to individual squares of P81 phosphocellulose paper. These were then washed 3 times (2 minute washes) with 0.75% (v/v) phosphoric acid containing 0.1% (v/v) Tween-20, followed by a single 2 minute rinse in acetone. Phosphocellulose squares were left to air dry before transfer to scintillation vials containing 3ml scintillation fluid. Samples were read by a scintillation counter and associated radioactivity quantified as bound phosphorylated substrate.

The specific radioactivity (S.R) of the Mg^{2+}/ATP-hot mixture was determined by adding 5µl of the mixture directly in to 3ml scintillation fluid and counting. Background counts were taken from samples in which there was no CaMKII source (i.e. no tissue or recombinant protein sample). CaMKII activity in each sample could then be calculated from the following equation:

$$\frac{Sample\ counts - background\ counts}{S.R.\,x\ incubation\ time}$$

Individual activity values were then converted to pmol of phosphate incorporated min^{-1} μg protein^{-1} and normalised to the calculated activity of an untreated sample included in every assay.

2.14 Histological sectioning and staining of rat aortae and heart tissues

2.14.1 Fixation, wax embedding and cutting of tissues

Aortae and hearts were isolated following termination as described in Section 2.3.1 and flushed through with Ca^{2+}-free Krebs buffer to remove any remaining blood. Tissues were then fixed in 10% formaldehyde (v/v) for 24h prior to processing in a Citadel 1000 (Thermo Shandon, UK) processor overnight under the following conditions:

- 70% ethanol: 3h

- 90% ethanol: 3.5h

- 100% ethanol: 2h

- 1:1 (v/v) of ethanol: histoclear: 1h

- 100% histoclear: 1h

- 100% histoclear:1h

- Paraffin wax: 2h

- Paraffin wax: 2h.

Following this tissues were embedded in paraffin wax using a Leica EG1140H (Leica Microsystems, UK) embedder and 5μm sections cut using a Leica RM2125RTF (Leica Microsystems, UK) microtome. Tissue sections were floated onto silanated

slides using a water bath at 60˚C. On their day of use, the slides were placed again in the oven at 60-65˚C for 15 minutes.

Prior to histological staining, tissue sections were rehydrated using the following solutions:

- Histoclear: 10 minutes

- Histoclear: 10 minutes

- Histoclear: 10 minutes

- 100% ethanol: 5 minutes

- 100% ethanol: 5 minutes

- 100% dH2O: 5 minutes

2.14.2 Haematoxylin and eosin staining

Tissue sections were placed into metal racks following rehydration for staining by haematoxylin and eosin (H&E) using the following protocol:

- Haematoxylin: 6 minutes

- dH$_2$0: 1 minute

- Acid: alcohol (1%): 3 seconds

- dH$_2$O: 1 minute

- Scots tap water substitute: 2 minutes

- dH$_2$O: 1 minute

- Eosin: 1 minute

- dH$_2$O: 1 minute

At the end of staining slides were dehydrated in the following:

- 100% ethanol: 10 minutes

- 100% ethanol: 10 minutes

- 100% ethanol: 10 minutes

- Histoclear: 5 minutes

- Histoclear: 5 minutes

- Histoclear: 5 minutes

2.14.3 CD45 Staining

To examine infiltration of lymphocytes, following rehydration of tissues (as above) slides were subjected to antigen retrieval to break the formalin bonds which form in fixed tissue. This was performed using Sodium Citrate buffer (10mM Sodium Citrate, 0.05% Tween-20, pH 6.0), which was pre-heated in a pressure cooker. The slides were placed in the cooker and heated in a 900watt microwave for 7 minutes. After depressurisation and cooling, slides were washed in PBS. Slides were then incubated with buffered 1.5% H_2O_2 for 10 minutes to block endogenous peroxidase activity, followed by a PBS wash. To block non-specific binding, 10% serum (from a source compatible with the antibodies) was added to the tissue sections for 1h at room temperature. Slides were then probed with an anti-CD45 rat polyclonal antibody (1:250) prepared in 10% serum overnight at 4°C. The slides were washed in three changes of PBS before adding the anti-mouse biotinylated secondary antibody (1:500) prepared in PBS at room temperature for 1h. Slides were then washed as before and diaminobenzidine (DAB) added for 10 minutes to allow visualisation of the staining. Tissue sections were also counterstained with Haematoxylin to visualise the nuclei before being dehydrated following the same procedure as outlined in Section 2.14.2

Thereafter, slides were mounted using histomount and 24 x 50mm coverslips. Slides were left to dry overnight before microscopic analysis.

A total of 5 random sections per tissue sample and 5 areas of interest per sample were photographed at 10x magnification (H&E staining) and 40x magnification (CD45 staining) using a Leica DFC 320 camera (Leica Microsystems, Germany). Mean

vessel width (µm) was calculated from images of H&E staining of aortae. Quantification of CD45 staining was performed on Image J software, where the percentage of positive stained nuclei within a field of view was calculated.

2.15 ELISA

Whole serum taken from young and aged rats were assayed for levels of TNF-α and IL-1β proteins using commercially available ELISA kits (ELISA Ready-SET-Go!® kit, eBioscience). Animals were euthanised as described in Section 2.3.1. Once the rat became unresponsive, whole blood was collected by cardiac puncture and was left to clot by leaving the sample undisturbed at room temperature for 20 minutes. Clots were then removed by centrifugation at 2000 x g for 10 minutes at 4°C. The resulting supernatant (serum) was immediately aliquoted into clean polypropylene tubes and stored at -80°C until future use. Small aliquots were taken instantaneously for assessment of total protein concentration using a NanoDrop 2000c Spectrophotometer. Each sample was then prepared to a final concentration of 30mg/ml in PBS.

TNF-α and IL-1β ELISAs were performed according to manufacturer's instructions. Briefly, ELISA plates were coated with 100µl/well of capture antibody and incubated overnight at 4°C. Wells were then washed 5 times with 250µl/well wash buffer (PBS containing 0.05% (v/v) Tween-20) to remove capture solution. Any residual wash buffer in the wells was removed by blotting the plate on absorbent paper. To prevent non-specific protein binding, plates were blocked in 200µl/well 1x ELISA/ELISPOT buffer (assay diluent) for 1h at room temperature, followed by 5 times washes as previous. Both TNF-α and IL-1β protein standards (recombinant proteins) were prepared to generate a standard curve with top concentrations of 2000pg/ml and 5000pg/ml respectively. A total volume of 100µl of standard or sample was then added to the appropriate wells. Plates were sealed with adhesive plastic and incubated overnight at 4°C. Subsequent washes were performed as described above before 100µl of detection antibody (biotin-conjugated antibody) diluted in 1x ELISA/ELISPOT buffer was added to each well and incubated for 1h at room temperature. The detection antibody was then removed and plates were washed as described, followed by addition

of 100µl/well avidin-HRP diluted in 1x ELISA/ELISPOT diluent and incubation at room temperature for 30 minutes. Wells were then washed 7 times with 250µl/well wash buffer before being incubated with 100µl/well 3, 3', 5, 5'-tetramethylbenzidine (TMB) substrate solution for 15 minutes at room temperature. Finally, 50µl of stop solution (2M H_2SO_4) was added to each well and the plate was read at 450nm using a BioTek EPOCH plate reader and Gen5 software. Standards were plotted using log-log linear fit and only samples with absorbance readings falling within the linear range of the curve were quantified.

2.16 Data analysis

All data and associated statistics were analysed using GraphPad prism® software with resultant graphical data and values presented as mean ± standard error of the mean (S.E.M) of the total number of experiments (n). All statistical analysis was performed using either unpaired or paired Student's t-tests or one-way and two-way ANOVA analysis with the appropriate post-test as outlined in each figure. Values of $p<0.05$ were considered to be statistically significant and where no p value is shown, $p>0.05$.

Chapter 3: Investigating an interaction between CaMKIIδ and NF-κB signalling in endothelial cells

3.1 Introduction

Endothelial dysfunction (ED) is a key feature of the stressed/injured endothelium associated with ageing and enhanced NF-κB signalling is an important factor contributing towards this phenotype (Csiszar et al., 2008; Donato et al., 2009). In both the myocardium and vasculature, NF-κB is well known to promote CVD through its pro-inflammatory, pro-adhesion and pro-oxidant gene transcription properties. Furthermore, there is now a considerable amount of evidence highlighting a link between CaMKIIδ and NF-κB specifically within the heart (Singh & Anderson 2011; Luczak & Anderson, 2014) and evidence suggests that this interaction contributes to pathological outcome. In spite of this link in the heart, a similar link within the endothelium of the vasculature and in particular during ageing, remains elusive regardless of the strong evidence of a role for NF-κB in mediating ED. CaMKII is known to be expressed within ECs and it is has been established that the δ isoform (along with its splicing variants) is indeed the predominant isoform expressed in this cell type (Wang et al., 2010) similar to that which is expressed within cardiac-specific cells. Thus the possibility of an interaction between CaMKII and NF-κB seems likely in stressed endothelium such as the stress we observe during ageing.

Previous studies have indicated that CaMKII may interact directly with specific components of the canonical NF-κB signalling pathway. Initial observations by Hughes et al., (1998) suggested that inhibition of CaMKII could prevent degradation of IκBα. A few years later, this finding was supported when the same group published reports that expression of a constitutively active form of CaMKII resulted in NF-κB activation and that inhibition of CaMKII resulted in decreased IKK phosphorylation (Hughes et al., 2001). Altogether these results suggest that CaMKII modulates the NF-κB pathway upstream of, or at the level of, the IKK complex, interacting with IKKα, IKKβ and/or IKKγ (refer to Figure 3.1). Novel findings from our own research group have built upon this work by showing via Surface Plasmon Resonance (SPR) that CaMKII can directly interact with the IKKβ subunit of the IKK complex (Martin, 2011). This finding suggested for the first time that direct protein-protein interaction between CaMKIIδ and NF-κB signalling at the level of IKKβ exists.

Taking all of these findings into account, we hypothesise that CaMKIIδ may modulate the NF-κB pathway within ECs and therefore contribute to the pro-inflammatory and pro-oxidative state of the endothelium during advanced ageing. Given the previous data generated by our group suggesting direct interaction between CaMKIIδ and IKKβ in the heart, we hypothesise that the same interaction exists at the level of the vasculature. Experimental results presented in this chapter have thoroughly investigated this hypothesis by initially defining activation of both CaMKII and NF-κB pathways in HUVECs. These cells were used in order to optimise all stimulation and immunoblotting conditions before moving on to using more physiologically relevant primary aortic ECs. Following successful characterisation of activation of both pathways in primary ECs, the possibility of an interaction between CaMKII and NF-κB was then explored using several different approaches. These included the use of different tools to inhibit CaMKII signalling and examine the resultant effect upon NF-kB signalling as well as investigating whether a direct interaction between CaMKIIδ and IKKβ might exist. CaMKII was inhibited via : (i) Use of selective CaMKII inhibitors (AIP and KN93) prior to NF-κB activation and (ii) Knock down of CaMKIIδ gene expression by siRNA transfection and assessing subsequent NF-κB activation following stimulation. The potential for direct CaMKIIδ - IKKβ interaction at the cellular level was explored using Proximity Ligation Assay (PLA) technology.
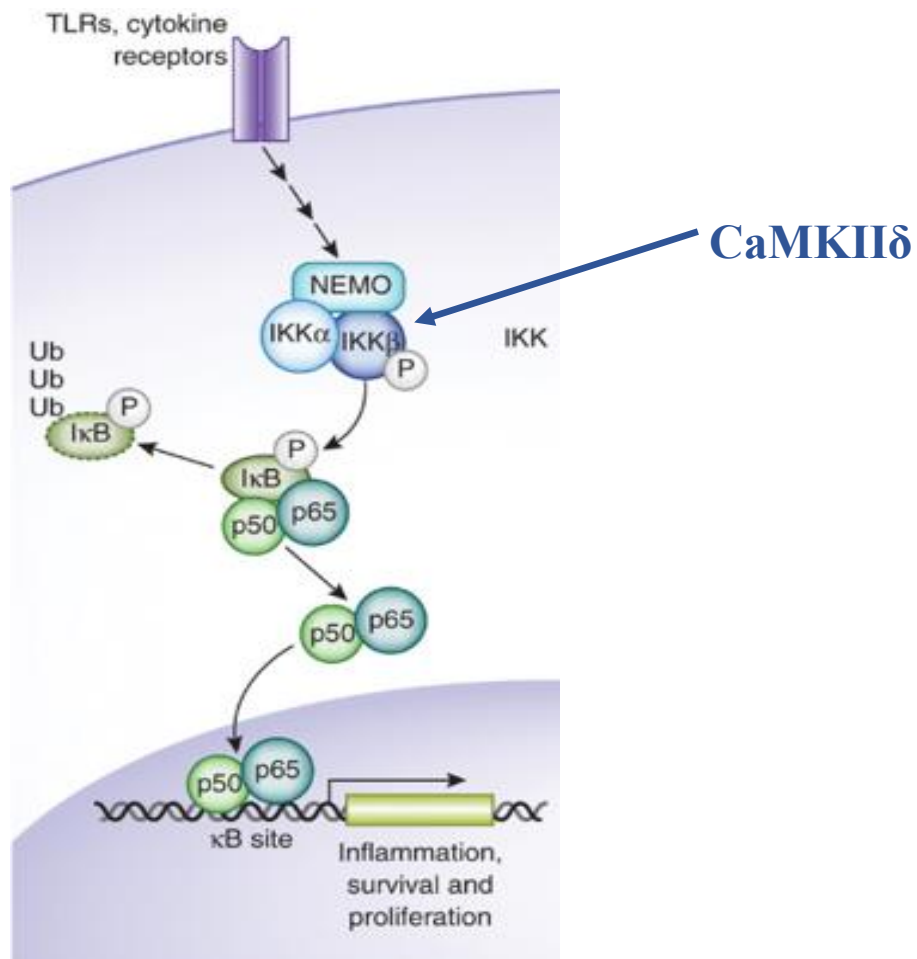
Figure 3.1 Potential modulation of NF-κB by CaMKIIδ.

Schematic diagram of the canonical NF-κB signalling pathway highlighting where CaMKIIδ may directly interact to exert its effects: the IKKβ subunit of the IKK complex. Interaction here would have downstream effects on IκBα degradation and p65 phosphorylation (adapted from Gerondakis et al., 2014).

3.2 *CaMKIIδ expression in HUVECs*

Preliminary work was performed to examine the CaMKIIδ expression profile in HUVECs and to determine specificity of the antibody used for future experiments. By comparing CaMKIIδ expression levels to those in mouse cardiac whole homogenate and cardiac fibroblast (CF) preparations, where it is known to be highly expressed, it is evident that CaMKIIδ is present in HUVECs, as detected by immunoblotting (Figure 3.2). A characteristic feature of CaMKIIδ detection by immunoblot analysis is the presence of distinct bands which represent different splice variants of the δ isoform. This feature is apparent from our findings depicted in Figure 3.2, therefore it can be confirmed that CaMKIIδ is present in HUVECs and it may suggest the presence of different splice variants within these cells. The predominant isoform expressed in ECs is the δ_6 splice variant (Wang et al., 2010), whereas in cardiac cells δ_2 and δ_3 are more commonly expressed, hence the reason for different immunoblot profiles between cell types and homogenates. A custom-made antibody raised to the C terminus specific to CaMKIIδ gives a clear signal and was therefore used for all subsequent immunoblot experiments.
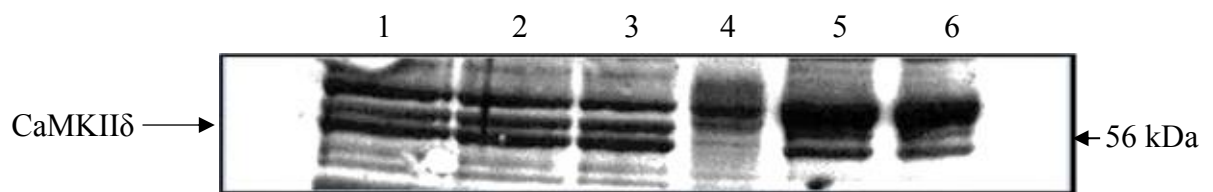
Figure 3.2: CaMKIIδ is expressed in HUVECs. Typical immunoblot showing CaMKIIδ expression across a range of protein loads of HUVECs. Cells were grown to confluence in individual wells of a 12-well culture plate and harvested in 1x lysis buffer. Final volumes of 30µl (lane 1), 20µl (lane 2) and 10µl (lane 3) were tested for total CaMKIIδ expression. Mouse cardiac ventricular whole homogenate (5µg) (WH) (lane 4) and rat cardiac fibroblasts (5µg and 10µg) (lanes 5 and 6) served as positive controls for CaMKIIδ expression. Blot is representative of n=3 experiments.

3.3 NF-κB activation in HUVECs

NF-kB signalling within HUVECs was assessed by measuring two key markers for identifying activation of the pathway, including IκBα degradation and phosphorylation of p65 at the Ser536 residue, both examined following exposure to TNF-α (10ng/ml) or IL-1β (10ng/ml) over a 1h time course. These cytokines are well known activators of the NF-κB pathway and are also pivotal signalling mediators involved in the chronic inflammation associated with advanced ageing, therefore were extremely relevant for this project. Representative time-courses for IκBα degradation and p65 phosphorylation, both markers of activation of NF-κB signalling in the presence of TNF-α are shown in Figures 3.3A and B respectively. Maximal IκBα degradation was observed at 15 minutes TNF-α stimulation and p65 phosphorylation at 5 minutes stimulation, as would be expected based on previous observations (Alkalay et al., 1995; Sakurai et al., 1999). Similar results were also observed in response to IL-1β stimulation (10ng/ml) with regard to IκBα degradation and phosphorylation of p65 (Figure 3.4). It was essential that these conditions were optimised in HUVECs initially before moving onto primary aortic ECs (due to the sensitive nature of these cells) and prior to pre-treatments with any CaMKII inhibitors (as will be discussed later).

(A)

(B)

Figure 3.3 TNF-α stimulated NF-κB activation in HUVECs. HUVECs were exposed to TNF-α (10ng/ml) for the indicated periods of time. IκBα (**A**) and pp65 (**B**) expression were assessed by immunoblot analysis and quantified by normalising to GAPDH. Representative immunoblots are shown for each protein of interest. Un-stimulated cells served as a control and cells exposed to PBS as vehicle controls at 15 min time-point. Densitometric analysis of immunoblots was performed, with data from 3 independent experiments expressed as mean ± S.E.M. Values compared to control were considered significant if $p<0.05$, ** represents $p<0.01$.

(A)

(B)

Figure 3.4 IL-1β stimulated NF-κB activation in HUVECs. HUVECs were exposed to IL-1β (10ng/ml) for the indicated periods of time. IκBα (**A**) and pp65 (**B**) expression were assessed by immunoblot analysis and quantified by normalising to GAPDH. Representative immunoblots are shown for each protein of interest. Un-stimulated cells served as a control and cells exposed to PBS as vehicle controls at 15 min time-point. Densitometric analysis of immunoblots was performed, with data from 3 independent experiments expressed as mean ± S.E.M. Values compared to control were considered significant if *p<0.05, ** represents p<0.01.

3.4 CaMKII is activated by phosphorylation following TNF-α stimulation

Phosphorylated (active) CaMKIIδ was also analysed following stimulation of HUVECs with TNF-α (10ng/ml) to assess whether the same pro-inflammatory cytokines known to activate the NF-kB signalling cascade would have any effect on CaMKII activation. Findings from this experiment indicate evidence to suggest that upon exposure to TNF-α, autophosphorylation of CaMKIIδ in HUVECs occurs after 10 minutes of exposure. This increase in phosphorylated CaMKII expression is short-lived however as levels (assessed by immunoblotting) appear to decrease back to baseline again by 15 minutes (Figure 3.5). Nonetheless, this finding shows that both pathways are capable of activation over the same time-period in ECs.
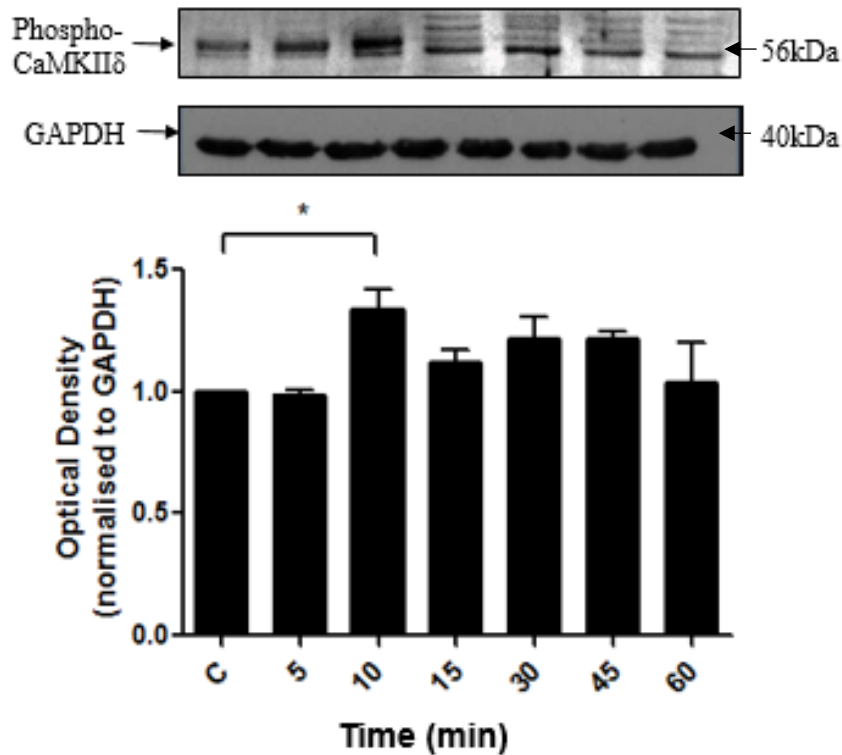
Figure 3.5: CaMKIIδ is activated by phosphorylation in response to TNF-α.
HUVECs were exposed to TNF-α (10ng/ml) for the indicated periods of time.
Expression of phosphorylated (activated) CaMKIIδ at threonine 286 was measured by
immunoblotting and normalising to GAPDH. A representative immunoblot is shown,
where un-stimulated cells served as a control. Densitometric analysis of immunoblots
was performed, with data from 3 independent experiments expressed as mean ±
S.E.M. Values compared to control were considered significant if p<0.05, *.

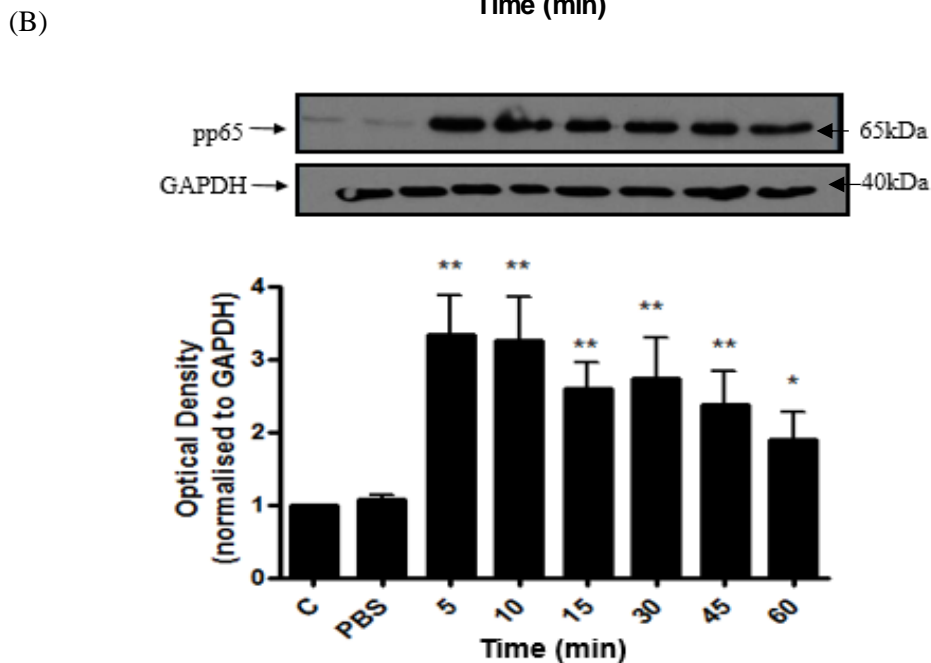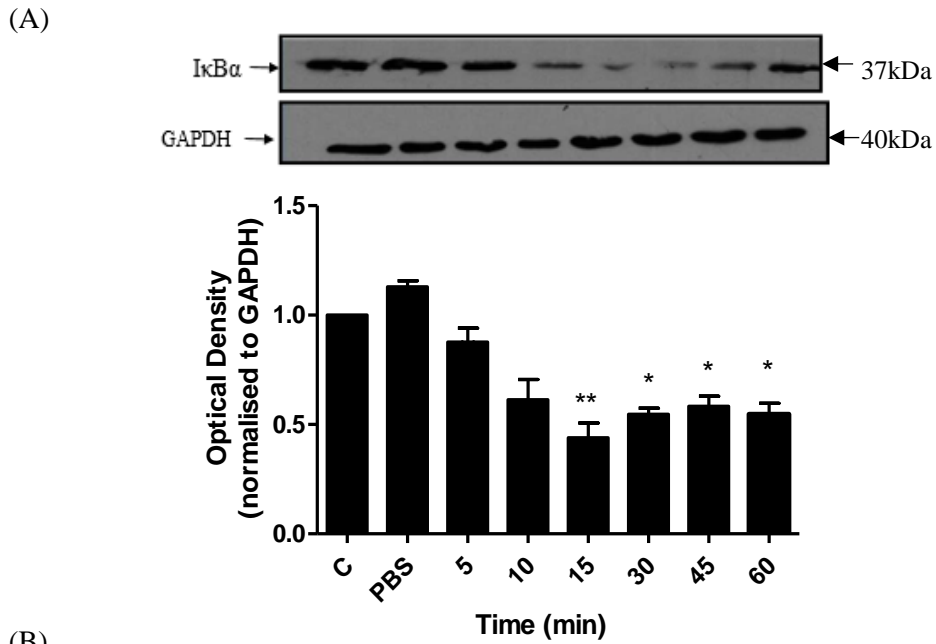### 3.5 Isolation and characterisation of aortic endothelial cells

Despite initial experiments in HUVECs show promising results in terms of NF-kB signalling and CaMKIIδ expression/activation, this is a relatively artificial system and does not necessarily translate to what would be observed in primary ECs from other organs. Importantly, HUVECs are from veins and not arteries, the latter being the key focus of this project, therefore ECs from the aorta were used for all further experiments. These cells were isolated from the adult rat aorta under sterile conditions using an in-house enzyme digestion method adapted from a previous study (Kobayashi et al., 2005). Primary cells were cultured at 37°C in 5% CO_2 as described in the Methods section 2.3.1. Confirmation of a pure culture of ECs was initially obtained by visually investigating their morphology. ECs characteristically appear in culture as fairly small, round cells and are typically described as exerting a 'cobblestone-type' phenotype as they become more confluent. This appearance can be clearly seen from Figure 3.6, where images show the cells growing from day 2 to day 8 in culture. Following initial isolation, cells were found to take around 8-10 days to reach confluence, which is similar to that reported previously (Kobayashi et al., 2005). Immunofluorescence staining for two EC specific markers, CD31/PECAM-1 and vWF were used to verify that the isolated cells were indeed predominantly ECs and that cultures were free from contamination by other cell types, such as smooth muscle cells. Initially, PECAM-1 was selected as the only EC marker for use as this is commonly used in the literature for characterising ECs. However, early staining results showed CF cells (which were used as a negative control as they are documented not to express PECAM-1) also displayed positive expression of PECAM-1 (data not shown) therefore vWF was also used as a second marker for increased stringency. As illustrated in Figure 3.7, ECs in culture express both PECAM-1 (panel A) and vWF (panel B), with similar expression levels as that detected in HUVECs (panels C and D). Negative controls used for each marker show no positive staining, with only DAPI staining of the cell nuclei apparent, thus confirming that we have a pure culture of ECs. Both PECAM-1 and vWF are not expressed in smooth muscle cells therefore indicating that there is no contamination with these cells. It should be noted that cells

used in these staining experiments were used between passages 1 and 3 as these are the passages which would be used for all other EC experiments.
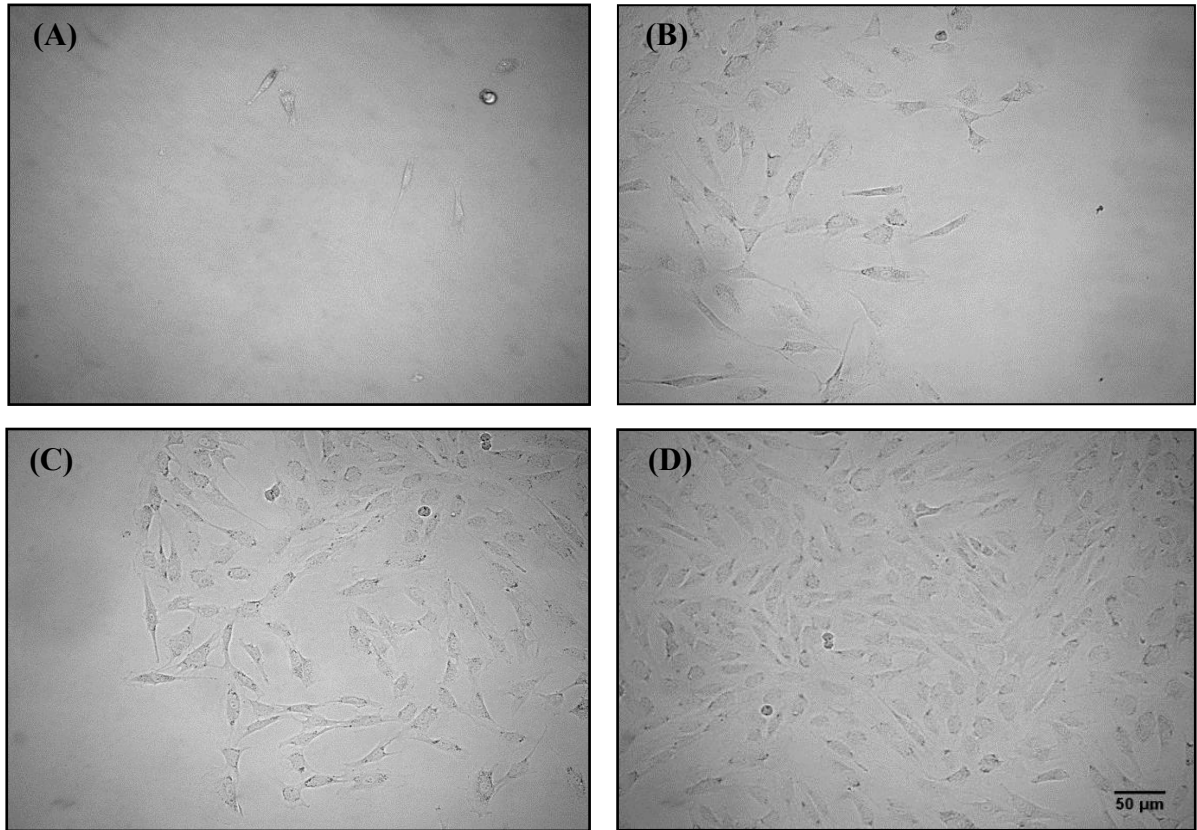
Figure 3.6 Isolation of primary rat aortic endothelial cells. Endothelial cells were isolated using an adapted version of the enzyme digestion method and were maintained in culture at 37°C in an atmosphere of 5% CO_2. Panels A-D show representative photographs of cells growing in T25 flasks at days 2, 4, 6 and 8 respectively. Images were taken using an epifluorescent inverted microscope (Nikon, Eclipse TE300) (10x objective lens). Scale bar represents 50µm for all images.
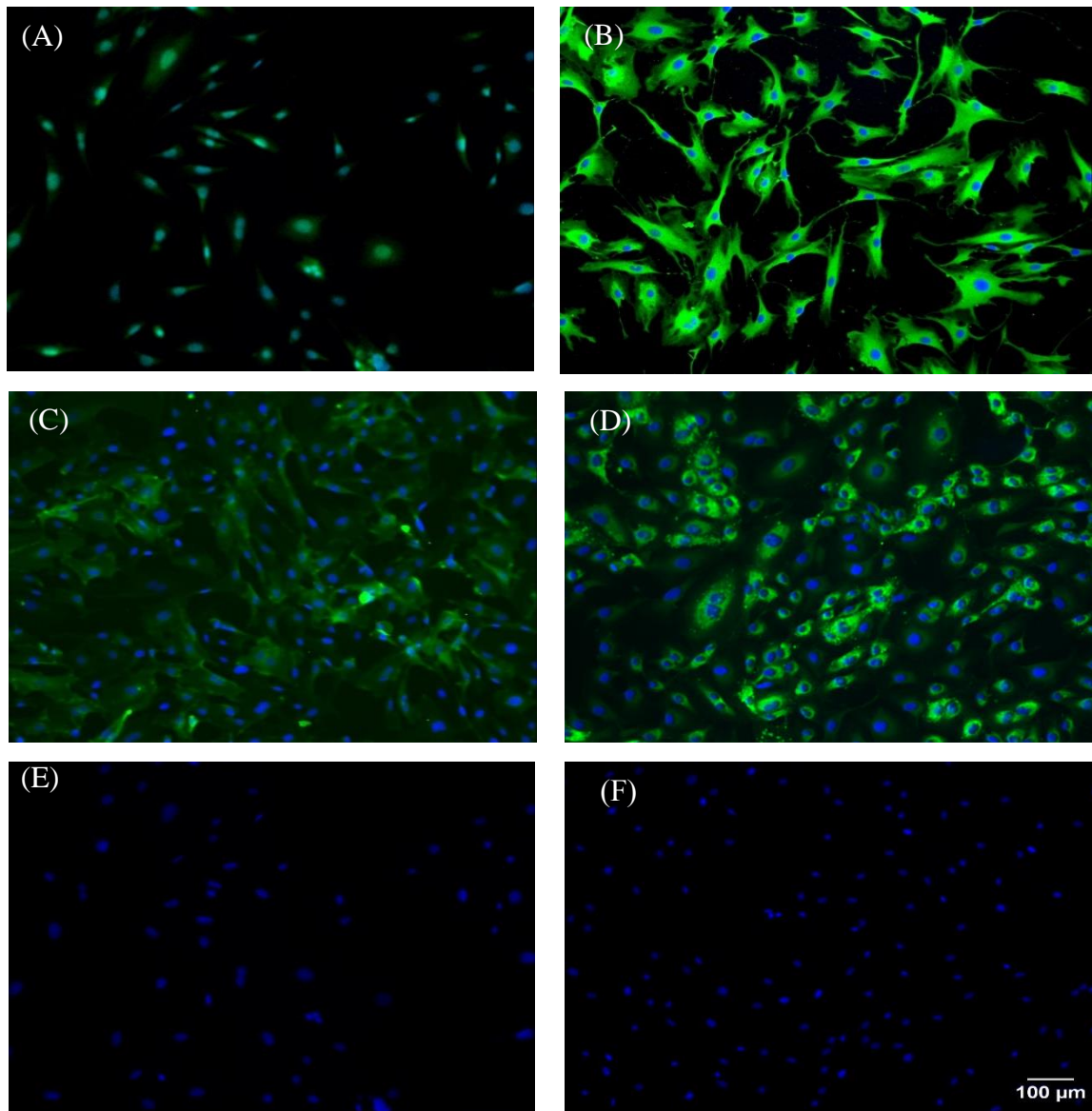
Figure 3.7 Characterisation of rat aortic endothelial cells by immunofluorescence. Primary rat aortic endothelial cells were grown on plain coverslips in 12 well culture dishes until ~50% confluency reached. Cells were stained for two endothelial cell-specific markers CD31/PECAM-1 (A) and vWF (B). HUVECs were used as a positive control for both CD31/PECAM-1 (C) and vWF staining (D). Panels E and F show aortic endothelial cells incubated with alexa fluor 488 secondary antibody alone to show no positive green FITC staining, serving as a negative control. DAPI was used in all experiments to label the nucleus as blue. Images of fluorescent cells were taken using a Nikon Eclipse 600 Oil Immersion microscope with the 10x objective lens. Scale bar represents 100µm for all images. Data are from an individual experiment, typical of 2 others.

3.6 Expression of CaMKIIδ and activation of the NF-κB pathway in aortic endothelial cells

Similar experiments to those previously performed in HUVECs as in Section 3.1 were conducted in rat aortic ECs in terms of investigating CaMKIIδ expression levels and NF-kB signalling following cytokine stimulation. A representative immunoblot showing CaMKIIδ expression across increasing protein loads of cell lysates is shown in Figure 3.8. The characteristic appearance of three distinct bands with immunoblotting, representing different splice variants of the δ isoform (including δ_6) is clearly evident, thus confirming it is indeed the δ isoform of CaMKII present in these cells as the profile is extremely similar to that observed in HUVECs (Section 3.2).

To assess NF-κB activation, primary aortic ECs were treated with TNF-α (10ng/ml) over a 1h time course as previously (Section 3.3). Maximal degradation of IκBα occurred at 15 minutes and protein levels then returned close to basal levels by 60 minutes stimulation, mirroring what we also observed in HUVECs (Figure 3.9A). Phosphorylated p65 levels were also monitored over the course of 60 minutes TNF-α stimulation and showed a slight increase, however this was found to be non-significant (Figure 3.9B). Overall however, these findings suggest activation of the NF-kB signalling cascade by pro-inflammatory cytokine stimuli, in ECs derived from the aorta, similar to that reported in HUVECs.
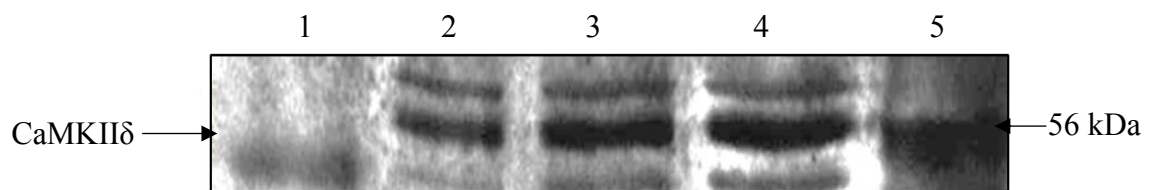
Figure 3.8 CaMKIIδ expression in rat aortic endothelial cells. Typical immunoblot showing CaMKIIδ expression across a range of protein loads in rat aortic primary endothelial cells. Cells were grown to confluence in individual wells of a 12-well culture plate and harvested in 1x lysis buffer. Final volumes of 10µl (lane 2), 20µl (lane 3) and 30µl (lane 4) were tested for total CaMKIIδ expression. Rat cardiac ventricular whole homogenate (10µg) (lane 5) served as a positive control for CaMKIIδ expression. Molecular weight markers are shown in lane 1. Blot is representative of n=3 experiments.

(A)

(B)
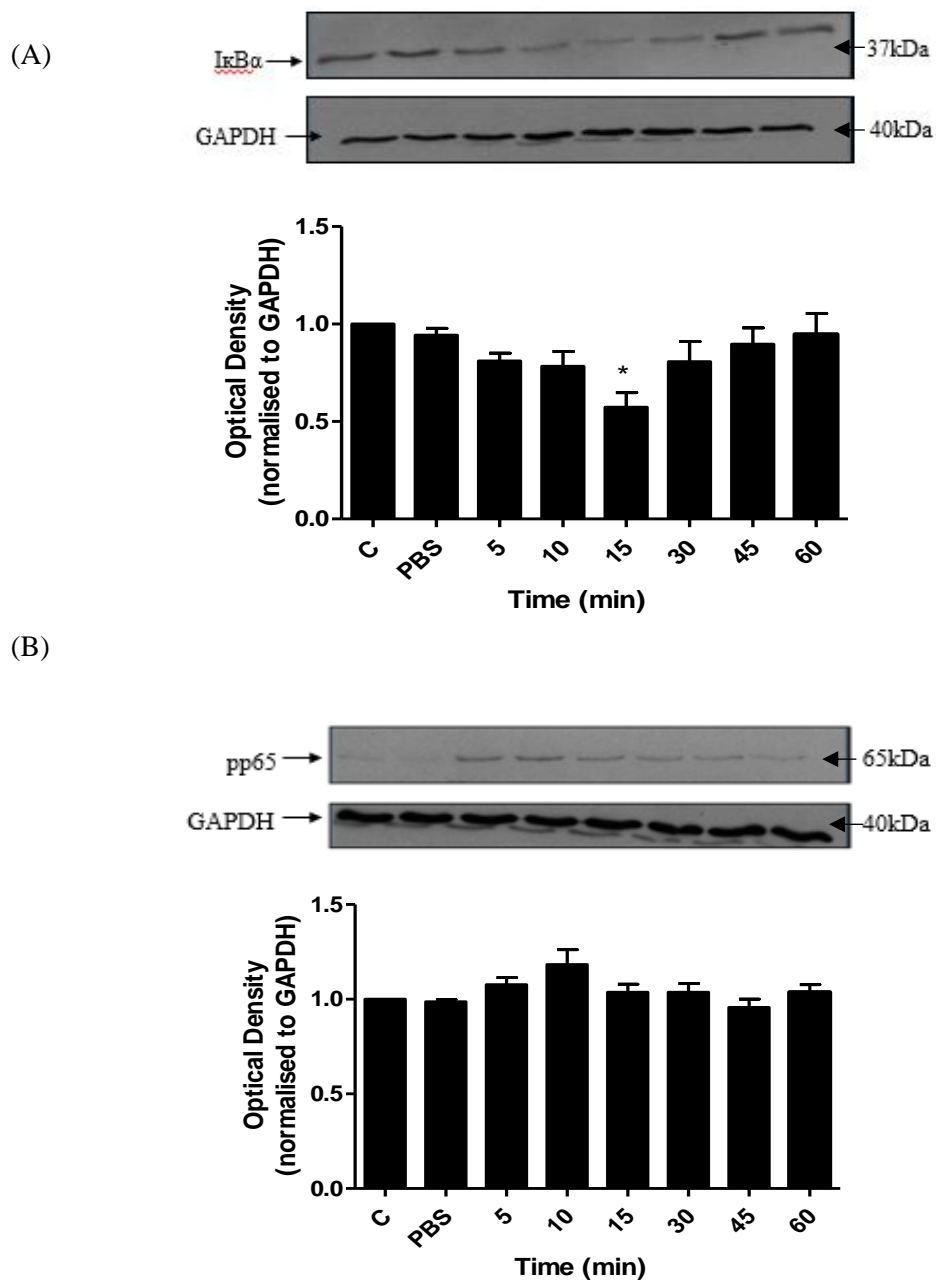
Figure 3.9 NF-kB activation in TNF-α stimulated rat aortic endothelial cells. Cells were exposed to TNF-α (10ng/ml) for the indicated periods of time. IκBα (**A**) and pp65 (**B**) expression were assessed by immunoblot analysis and quantified by normalising to GAPDH. Representative immunoblots are shown for each protein of interest. Un-stimulated cells served as a control and cells exposed to PBS as vehicle controls at 15 min time-point. Densitometric analysis of immunoblots was performed, with data from 3 independent experiments expressed as mean ± S.E.M. Values compared to control were considered significant if $p<0.05$ *.

3.7 A functional role for CaMKII in NF-κB signalling – the effect of CaMKII inhibition on IκBα degradation

In order to establish whether CaMKII plays a role in the regulation of vascular endothelial NF-κB signalling, the effect of CaMKII inhibition upon agonist-induced IκBα degradation was assessed. As mentioned in Section 3.1, previous work from our research group has already examined this within the cardiac setting using CFs and produced some interesting novel findings (Martin, 2011). These will initially be described below as it provided a basis for work carried out specifically in ECs. For all of the experiments in CFs the CaMKII peptide inhibitor autocamtide-2-inhibitory peptide (AIP) was used to explore the potential involvement of CaMKII in modulation of the NF-κB pathway. A final concentration of 5μM was used as this has previously been shown to induce 95-100% inhibition of CaMKII activity in rabbit cardiac preparations (Currie et al., 2004).

3.7.1 Effect of AIP in adult cardiac fibroblasts

Adult CFs stimulated with 5μg/ml lipopolysaccharide (LPS) over a 2h time course resulted in significant degradation of IκBα as would be expected. As shown in Figure 3.10, pre-treatment of these cells with AIP caused the degradation of IκBα in response to LPS to be significantly inhibited at 30 minutes stimulation and this effect was maintained until 45 minutes. Some level of variation among cell preparations was evident, as with the representative immunoblot shown in Figure 3.10A, where inhibition of IκBα degradation was still in fact evident at 60 minutes stimulation. These data presented by Martin et al., (2011) demonstrated for the first time that CaMKII may play a potential role in regulating agonist-induced IκBα degradation and therefore corresponding activation of the NF-κB signalling pathway.
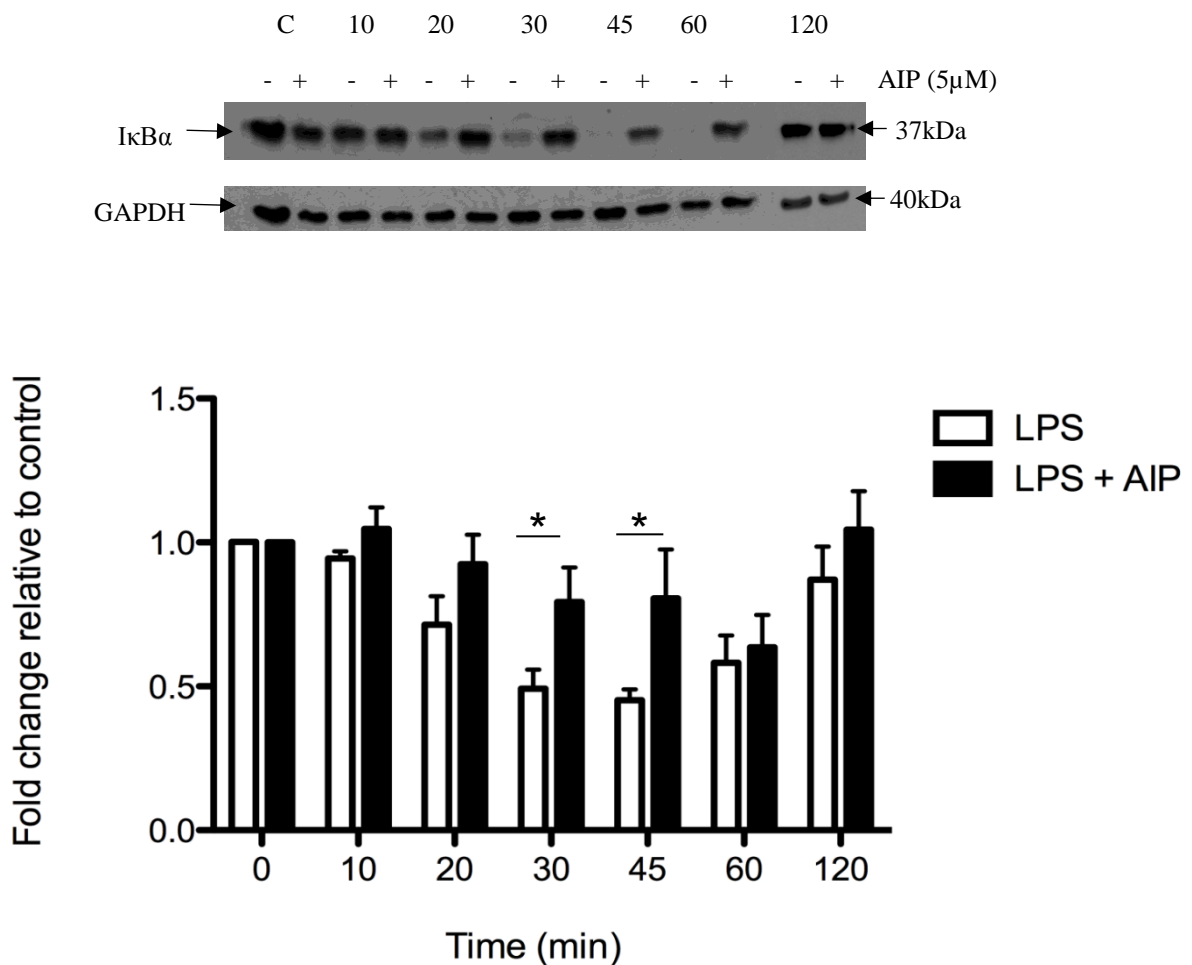
Figure 3.10 LPS-induced IκBα degradation in cardiac fibroblasts is reversed following CaMKII inhibition. Cardiac fibroblasts were exposed to LPS (5µg/ml) for the indiciated periods of time. Stimulations were performed in the presence and absence of pre-treatment with AIP (5µM) and reactions stopped in 1x lysis buffer. IκBα degradation was assessed by immunoblotting and quantified against GAPDH. A representative immunoblot is shown. Densitometric analysis of immunoblots was performed, with data from 4 independent experiments expressed as means ± S.E.M. *$p<0.05$ from the non-inhibited control reaction (Martin, 2011).

3.7.2 Effect of AIP in aortic endothelial cells

Having established that CaMKII plays a functional role in activation of NF-κB signalling in cardiac cells, similar agonist-induced IκBα degradation experiments were performed in the presence or absence of 5µM AIP in primary aortic ECs. TNF-α (10ng/ml) was selected as the agonist for these experiments as TNF-α has previously been shown to induce sufficient degradation of IκBα (Section 3.6) and is a more physiologically relevant stimulator of the pathway than LPS in the context of this work. A representative time course for this is shown in Figure 3.11 where it can be seen that TNF-α induced IκBα degradation was only very slightly inhibited by AIP at 10 minutes stimulation, however this was non-significant and there were no more differences at any other time-points. Another CaMKII inhibitor (KN-93) was chosen to further explore the potential involvement of CaMKII in modulation of the NF-κB pathway given the insignificant result with AIP. However, this also revealed no inhibition of IκBα degradation following TNF-α stimulation (data not shown).
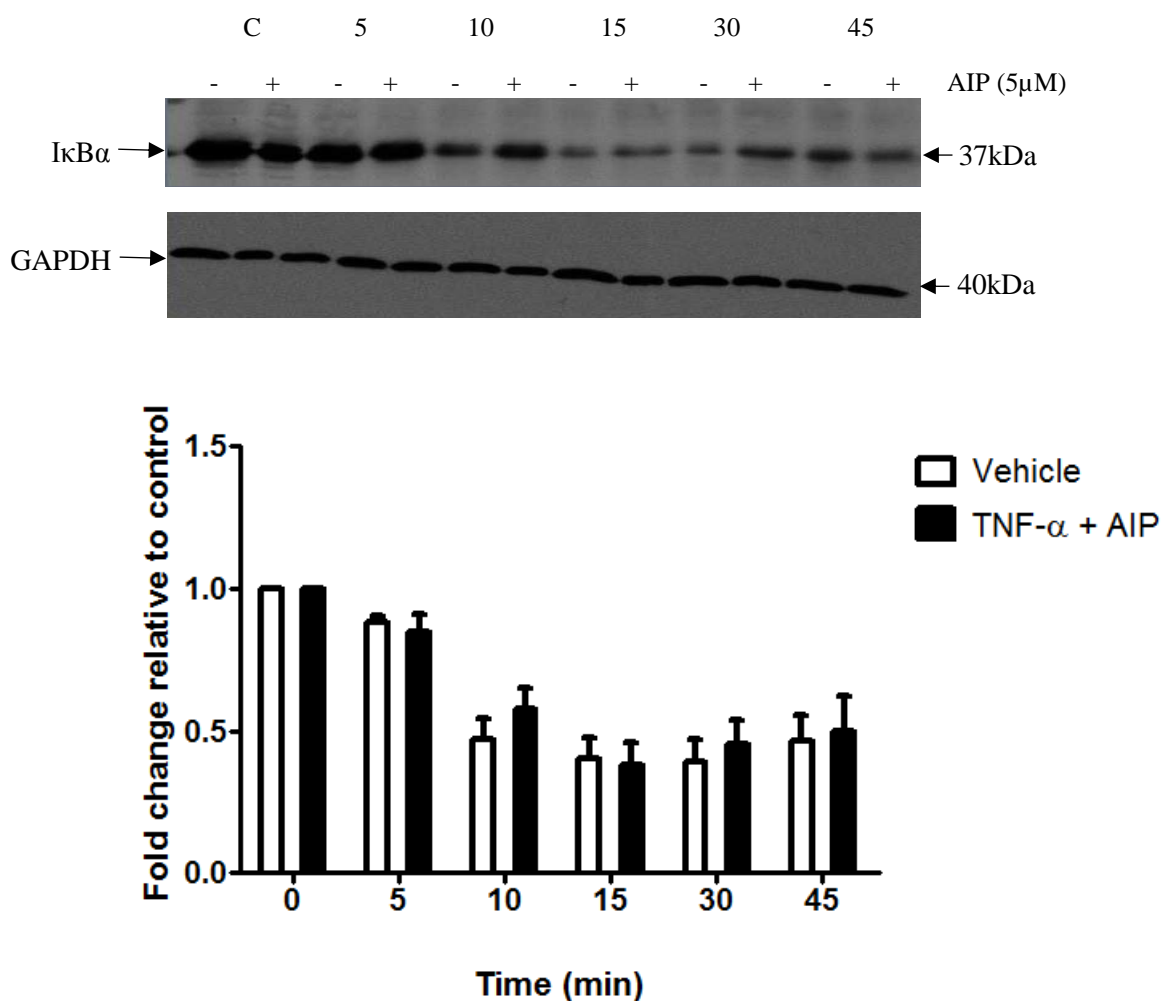
Figure 3.11 TNF-α induced IκBα degradation in endothelial cells is not reversed following CaMKII inhibition with AIP. Aortic endothelial cells were exposed to TNF-α (10ngg/ml) for the indiciated periods of time. Stimulations were performed in the presence and absence of pre-treatment with AIP (5μM) and reactions stopped in Laemmli sample buffer. IκBα degradation was assessed by immunoblotting and quantified against GAPDH. A representative immunoblot is shown. Densitometric analysis of immunoblots was performed, with data from 3 independent experiments expressed as means ± S.E.M. Values were compared to the non-inhibited control reactions.

3.8 A functional role for CaMKII in NF-κB signalling – the effect of silencing CaMKIIδ

Given the fact that inhibition of CaMKII activity by treatment with specific inhibitors AIP and KN-93 had no obvious effects on NF-κB signalling within ECs, an alternative approach at assessing this modulation was utilised in the form of small interfering RNA (siRNA) gene silencing. This is a useful technique in terms of evaluating the functional role of a protein as the expression of the protein of interest (in this case CaMKIIδ) is knocked down (silenced) and any subsequent effect this silencing may have on specific signalling pathways (canonical NF-κB pathway activation) can be measured. This approach works such that the siRNA interferes with the expression of the CaMKIIδ gene by degrading messenger RNA (mRNA) after transcription, thus resulting in no translation of the CaMKIIδ protein. For such experiments to be performed, initial optimisation steps had to be conducted to ensure maximal efficiency for future work.

3.8.1 Optimisation of the best transfection reagent for aortic endothelial cells

In order to successfully introduce siRNA genes into cells, it is essential that a suitable transfection reagent is selected to ensure maximal delivery of siRNA to the nucleus of cells. There are a vast number of different transfection reagents commercially available, therefore selecting the best one for a specific cell type can be challenging. For simplicity, two different transfection reagents were selected and analysed for their efficiencies in primary aortic ECs: FuGENE® and HiPerfect®. FuGENE® was selected given its previously reported efficiency in HUVECs (Hunt et al., 2010) and HiPerfect® for its reported effective transfection using low siRNA concentrations and specifically in primary cells where sensitivity can be an issue. It was also of prime importance than an optimal ratio of transfection reagent:siRNA was chosen in early experiments as the volume of transfection reagent required for optimal performance can vary depending on a number of factors, including cell type and gene target; thus it is always strongly recommended a range of ratios are tested prior to initiation of experimentation.

To do such optimisation, cells were seeded at 5×10^4 cells/ml in 24 well culture plates and treated with 10nM fluorescent-labelled TYE^{TM} 563 DS control duplex in the presence of either HiPerfect® or FuGENE® transfection reagents at the ratios as described in Chapter 2, Section 2.5.1. As can be clearly observed in Figure 3.12 HiPerfect® successfully transfected the ECs with the fluorescent control duplex, made evident by the cells fluorescing under the rhodamine (red) filter of the microscope 24h-post transfection. Note the stronger signal in the cells treated at a HiPerfect®:duplex ratio of 5:1, which provided evidence that this would be a suitable ratio to perform future siRNA experiments. Cells treated under identical conditions with FuGENE® transfection reagent showed no positive fluorescence at any of the tested ratios (Figure 3.13). These findings highlight the critical importance of optimisation prior to siRNA techniques being performed and provide evidence to suggest that even cells of the same type (in this case endothelial - HUVECs and aortic ECs) can react very differently under the same conditions.

Brightfield	Rhodamine	Combine
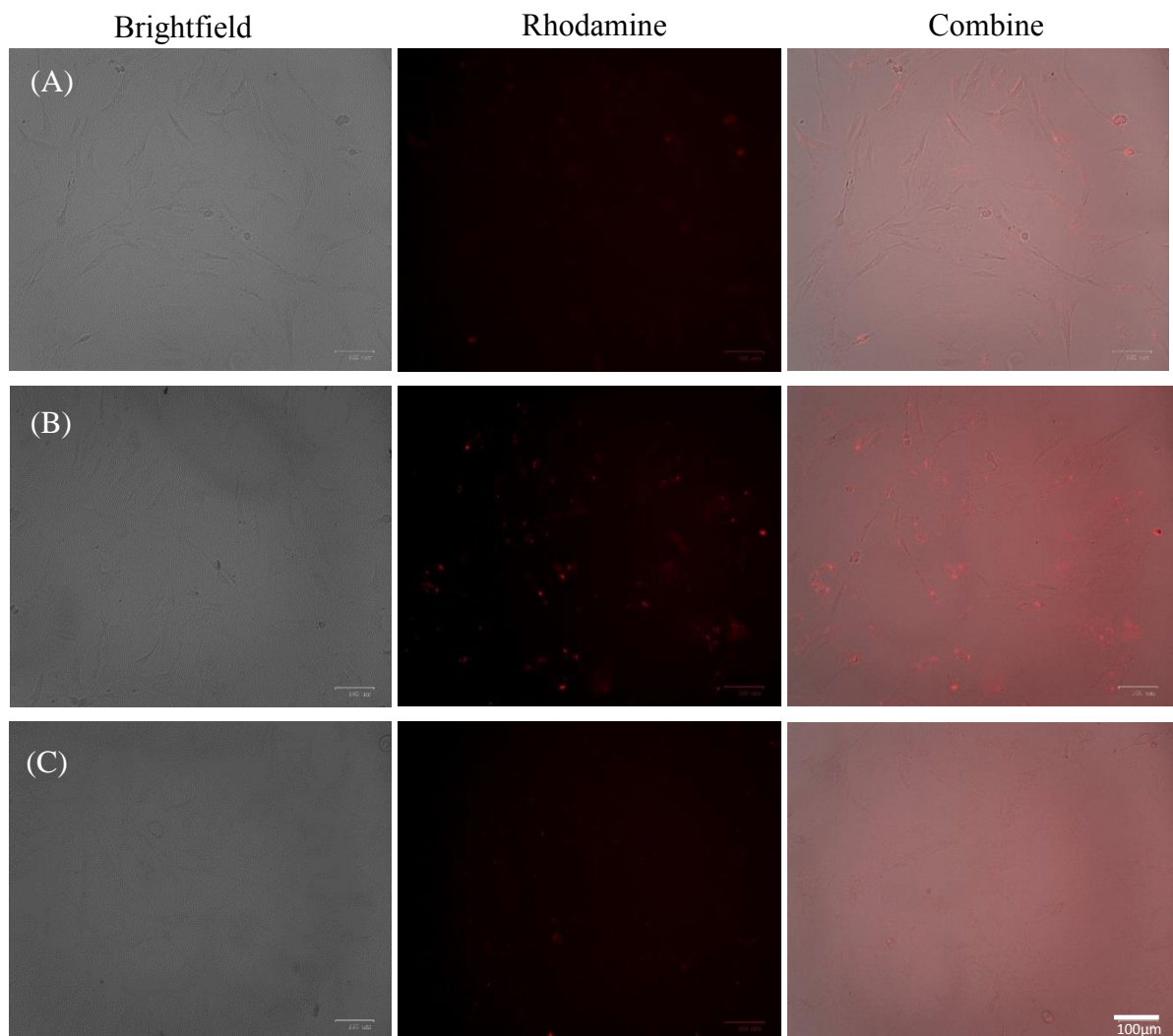
Figure 3.12 HiPerfect® transfection reagent can successfully transfect endothelial cells. Rat aortic endothelial cells were treated with HiPerfect® transfection reagent pre-incubated with 75ng fluorescent-labelled TYE^{TM} 563 DS control complex at ratios of 2.5:1 (A), 5:1 (B) and 7.5:1 (C) for 24h. Images were taken (10x magnification) of the cells on brightfield and rhodamine filters to assess fluorescence as a measure of successful transfection. Pictures were then merged to show transfection within the cells. Scale bar represents 100µm for all images.

| | Brightfield | Rhodamine | Combine |
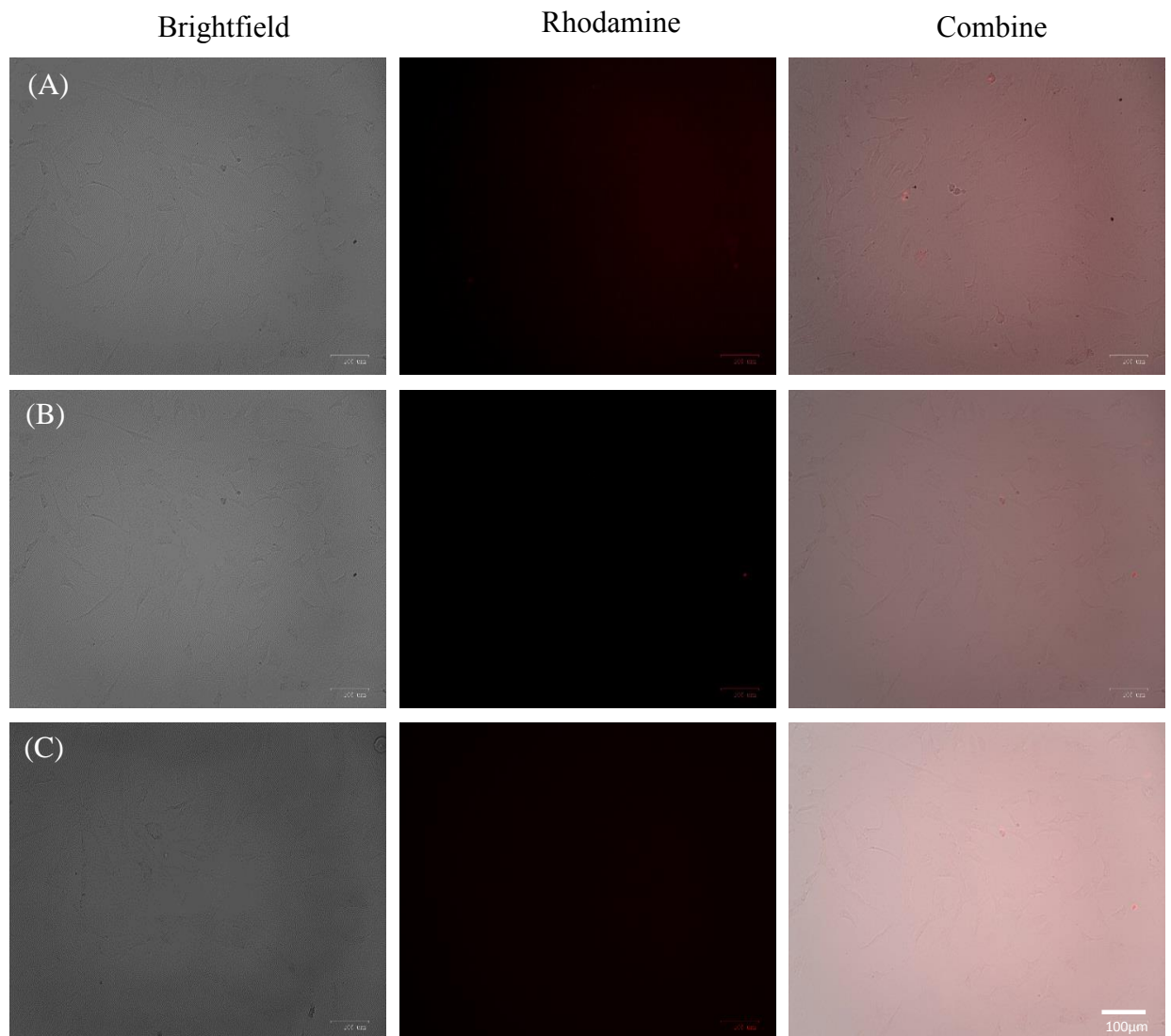
Figure 3.13 FuGENE® transfection reagent cannot transfect endothelial cells.
Rat aortic endothelial cells were treated with FuGENE® transfection reagent pre-incubated with 75ng fluorescent-labelled TYE^{TM} 563 DS control complex at ratios of 2.5:1 (A), 5:1 (B) and 7.5:1 (C) for 24h. Images were taken (10x magnification) of the cells on brightfield and rhodamine filters to assess fluorescence as a measure of successful transfection. Pictures were then merged to show lack of transfection within the cells. Scale bar represents 100µm for all images.

3.8.2 Optimisation of the best CaMKIIδ siRNA duplex and concentration

As outlined in Chapter 2 Section 2.5.2, the TriFecta® kits used for siRNA experiments in this project offer three target duplexes of the CaMKIIδ siRNA in order to assess several variants and maximise the potential for efficient gene knockdown. Cells were therefore treated with each of the duplexes at a ratio of 1:5 with HiPerfect® to determine which, if any, produced the highest knock down of protein expression. As can be seen in Figure 3.14 there was no obvious reduction in CaMKIIδ expression using all three of the duplexes at a final concentration of 1nM. When cells were exposed to 10nM of each of the duplexes, only DsiRNA 13.3 produced 50% knockdown of CaMKIIδ expression when compared to control samples. This is however only representative of 2 independent experiments and variation will indeed exist between cells from different animals and passages. Cells were also treated with 100nM siRNA however this caused complete cell death by the 72hr time point and therefore were not analysed by immunoblotting. This is a high, yet commonly used concentration for siRNA experiments however ECs tend to be much more sensitive than other cell types and since they are also primary cells, this may suggest good reason for their death at this concentration. A negative control duplex was also used in each of the experiments (as outlined in Section 2.5.2) to confirm that any reduction in protein expression was not due to the transfection technique itself and this did indeed have no obvious effect on CaMKIIδ expression.
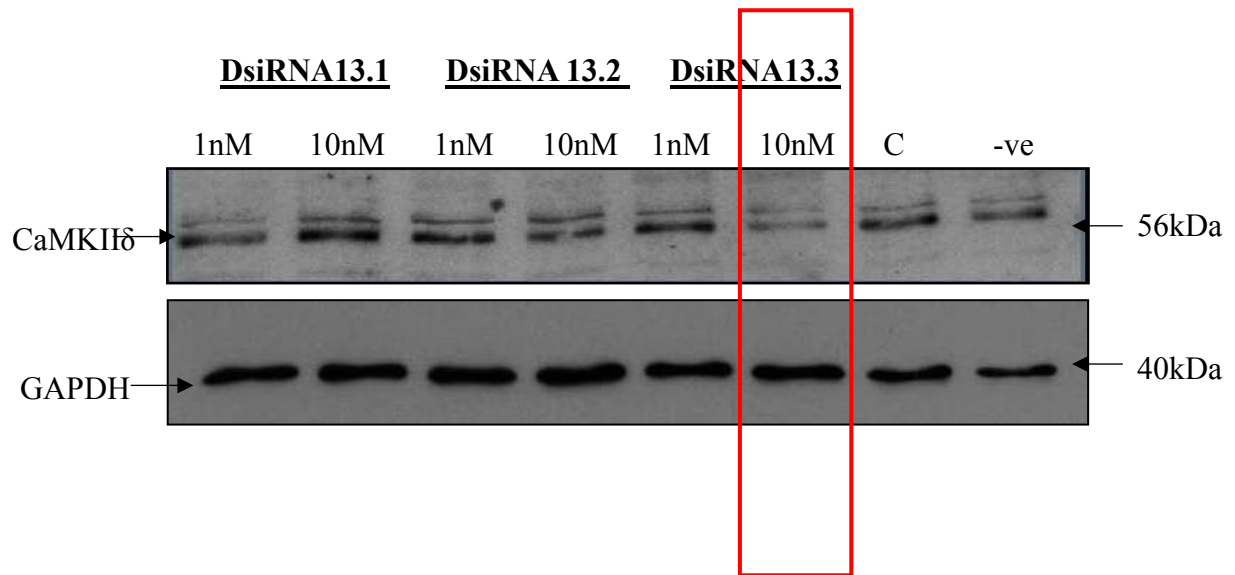
Figure 3.14 Optimisation of the best CaMKIIδ siRNA duplex. Rat aortic endothelial cells were treated with HiPerfect® transfection reagent pre-incubated with each of the siRNA duplexes (DsiRNA 13.1, 13.2 and 13.3) at 1 and 10nM final concentrations. Control samples were left un-treated and negative (-ve) control cells treated with a validated NC1 duplex provided by the TriFecta® kit. Reactions were stopped after 72h in 1x lysis buffer and CaMKIIδ expression was assessed by immunoblotting and quantified against GAPDH. An immunoblot is shown, representative of 2 independent experiments. A red box has been used to highlight successful knockdown of CaMKIIδ by 50%.

3.8.3 IκBα degradation is inhibited following CaMKIIδ silencing

In spite of not producing as high a level of CaMKIIδ knockdown as would have been preferred, DsiRNA 13.3 was selected as the most suitable siRNA duplex to go forward with experiments investigating CaMKIIδ and its role in potentially modulating NF-κB signalling. In order to establish this, cells were pre-treated with or without 10nM CaMKIIδ siRNA for 72hrs as previously and then TNF-α (10ng/ml)-induced IκBα degradation was assessed. A representative time course for this is shown in Figure 3.15 where it can be clearly seen that IκBα degradation in response to TNF-α stimulation was significantly inhibited by silencing CaMKIIδ expression. This was apparent even at 10 minutes TNF-α exposure and maintained until 45 minutes. As mentioned in Section 3.8.2 a marked level of variation exists between cell passages and those isolated from different animals, thus producing a range of findings. Here, a total of 3 independent experiments were performed using different batches of cells and as a result, not all outcomes were quite as significant. Data from 2 other experiments showed no obvious inhibition of IκBα degradation at any time point (data not shown) hence the reason why the collective data shown in Figure 3.15 displayed significance only at one time point (15 minutes). Nonetheless, this finding highlights for the first time that there may be a potential role for CaMKIIδ in regulating agonist-induced IκBα degradation and corresponding activation of NF-κB signalling in aortic ECs.
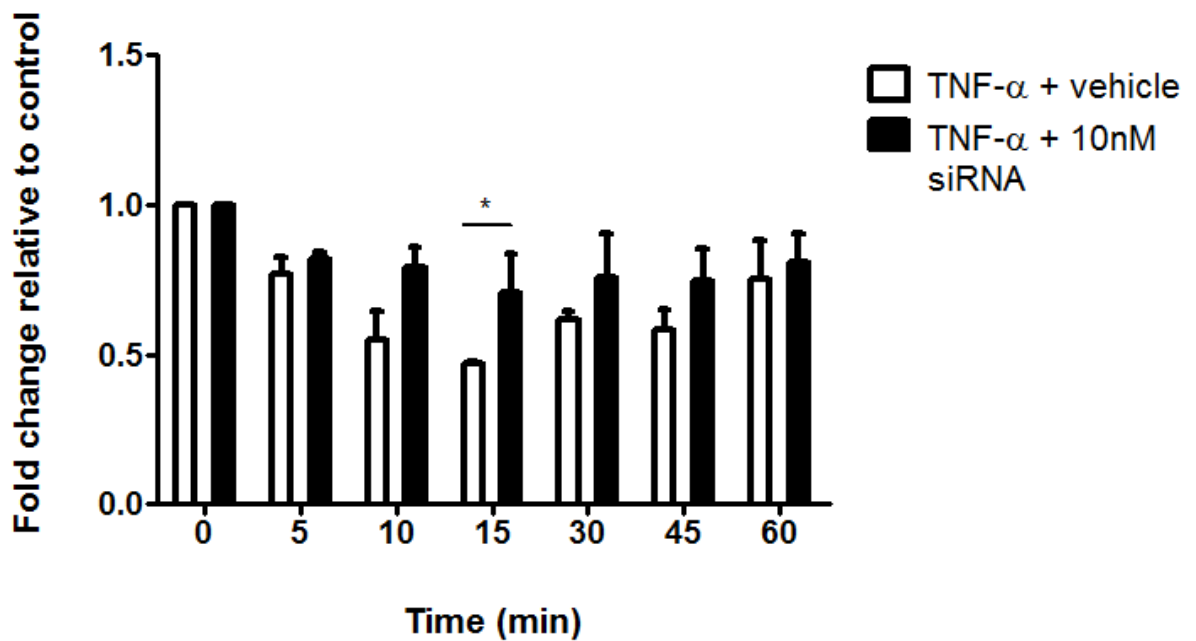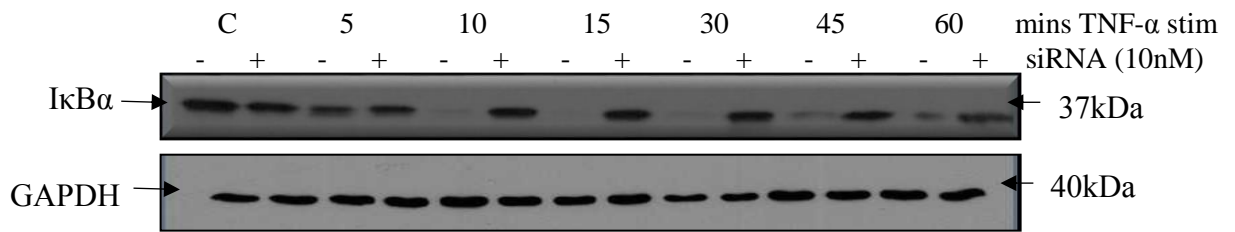
Figure 3.15 TNF-α-induced IκBα degradation in endothelial cells is inhibited following CaMKIIδ knockdown. Rat aortic endothelial cells were treated with or without 10nM CaMKIIδ siRNA (DsiRNA 13.3) for 72h before being exposed to TNF-α (10ng/ml) for the indicated periods of time. IκBα degradation was assessed by immunoblotting and quantified against GAPDH. A representative immunoblot is shown. Densitometric analysis of immunoblots was performed with data from 3 independent experiments, expressed as means ± S.E.M. Values were compared to the non-transfected control reactions.

3.9 Investigation of CaMKII interaction with the IKKβ component of the NF-κB signalling pathway using PLA technology

Having established that CaMKIIδ plays a functional role in activation of NF-κB signalling, investigation of specifically how this functional interaction may occur was important. As previously stated, data generated by our group has already highlighted a potential interaction between CaMKIIδ and IKKβ in the heart however this has yet to be established in the vascular endothelium. Here, we sought to investigate this interaction in primary aortic ECs using a PLA approach.

3.9.1 Introduction to PLA

The proximity ligation assay (PLA) is a technology which enables the detection, visualisation and quantification of direct protein-protein interactions in cell samples prepared for microscopy. Detection is facilitated using two primary antibodies against the two proteins of interest (CaMKII and IKKβ). A pair of oligonucleotide labelled secondary antibodies (PLA probes) generate a signal when the two PLA probes have bound in close proximity (30-40nm) indicating that the two primary antibodies have bound i.e. are interacting. The signal can be clearly visualised using fluorescence microscopy therefore this is a simple, yet extremely effective method for investigating protein-protein interaction within individual cells.

3.9.2 Optimisation of conditions

Prior to conducting the PLA in our ECs, it was of fundamental importance that conditions for each of the antibodies (CaMKII and IKKβ) were optimised in order to achieve the best signals. Sample pre-treatment for the PLA technique is identical to pre-treatment used for immunofluorescence staining therefore working assays for each antibody were determined by this method in the first instance.

3.9.2.1 IKKβ

For IKKβ staining, ECs were fixed, permeabilised and subjected to immunofluorescence as described in Section 2.6 using an Abcam mouse monoclonal

anti-IKKβ primary antibody at a 1:200 dilution as recommended in the manufacturers' instructions. Figure 3.16 shows representative images of positive IKKβ staining in the ECs under these conditions. A negative control was included where cells were incubated with FITC-conjugated anti-mouse secondary antibody alone and this showed no positive green staining. This result confirmed that these conditions for IKKβ were indeed suitable to move forward with for the PLA.
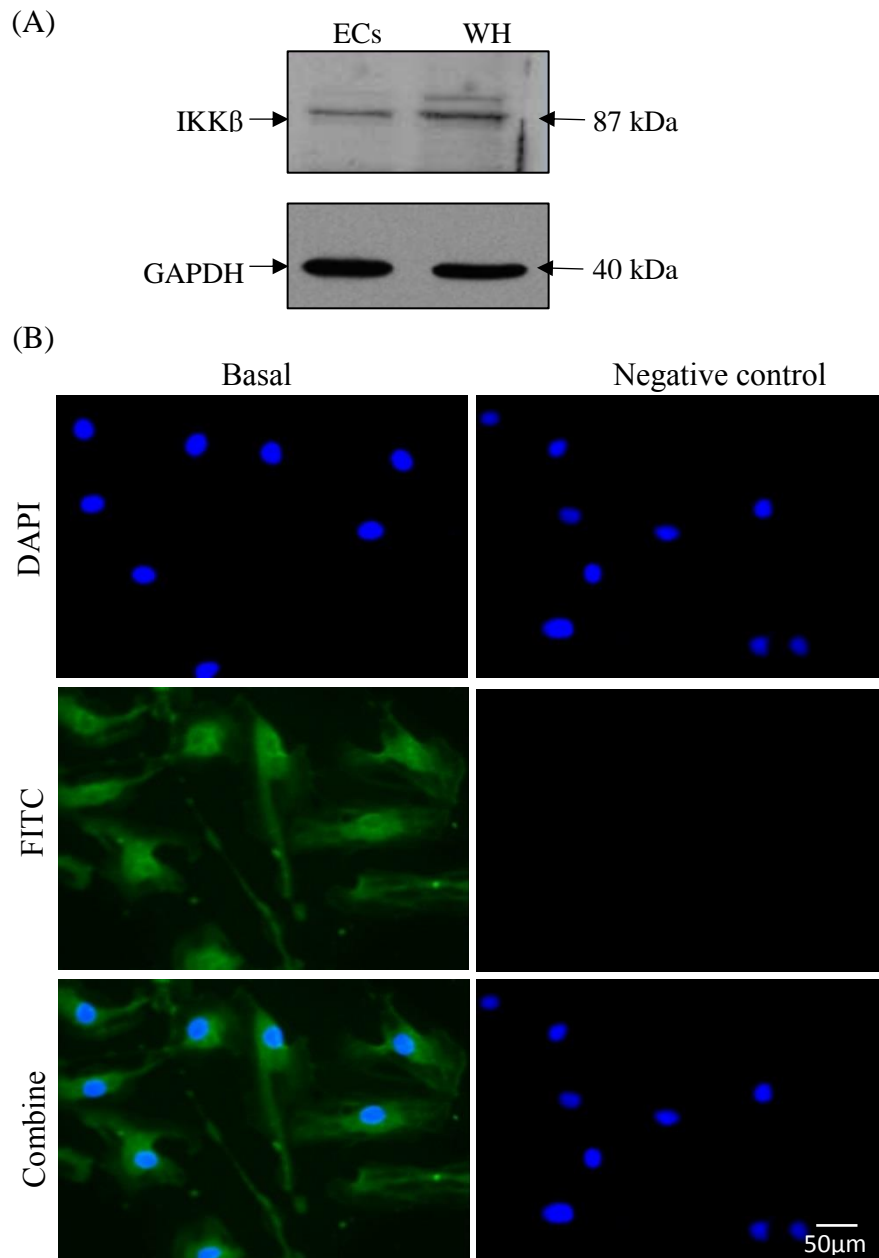
Figure 3.16 Optimisation of IKKβ antibody conditions for PLA. Rat aortic endothelial cells were harvested in lysis buffer and subjected to quantitative immunoblotting to show anti-IKKβ antibody specificity and compared with that of aorta WH (A). Cells were also grown on coverslips and subjected to immunofluorescence with the same anti-IKKβ antibody (1:200) overnight at 4°C. Anti-mouse FITC conjugated secondary antibody (1:200) was added to show positive IKKβ staining under basal conditions as green. Cells stained with secondary antibody only were used as a negative control. DAPI was used in all experiments to label the nucleus as blue. All images were taken using the 20x objective lens. Scale bar represents 50µm for all images. Data are from an individual experiment, typical of 2 others.

102

3.9.2.2 CaMKIIδ

For a PLA to successfully work, the two primary antibodies used for each protein of interest are required to be raised in different species. Given that a clear signal for IKKβ was obtained in ECs by immunofluorescence using an anti-mouse primary antibody, an anti-rabbit antibody was selected for CaMKIIδ staining. Cells were subjected to staining as previously, however as can be depicted from Figure 3.17, a positive signal for CaMKIIδ was extremely weak despite using a high concentration of antibody (1:50). An alternative approach was therefore sought using an antibody against the activated form of CaMKII as described in the following section.
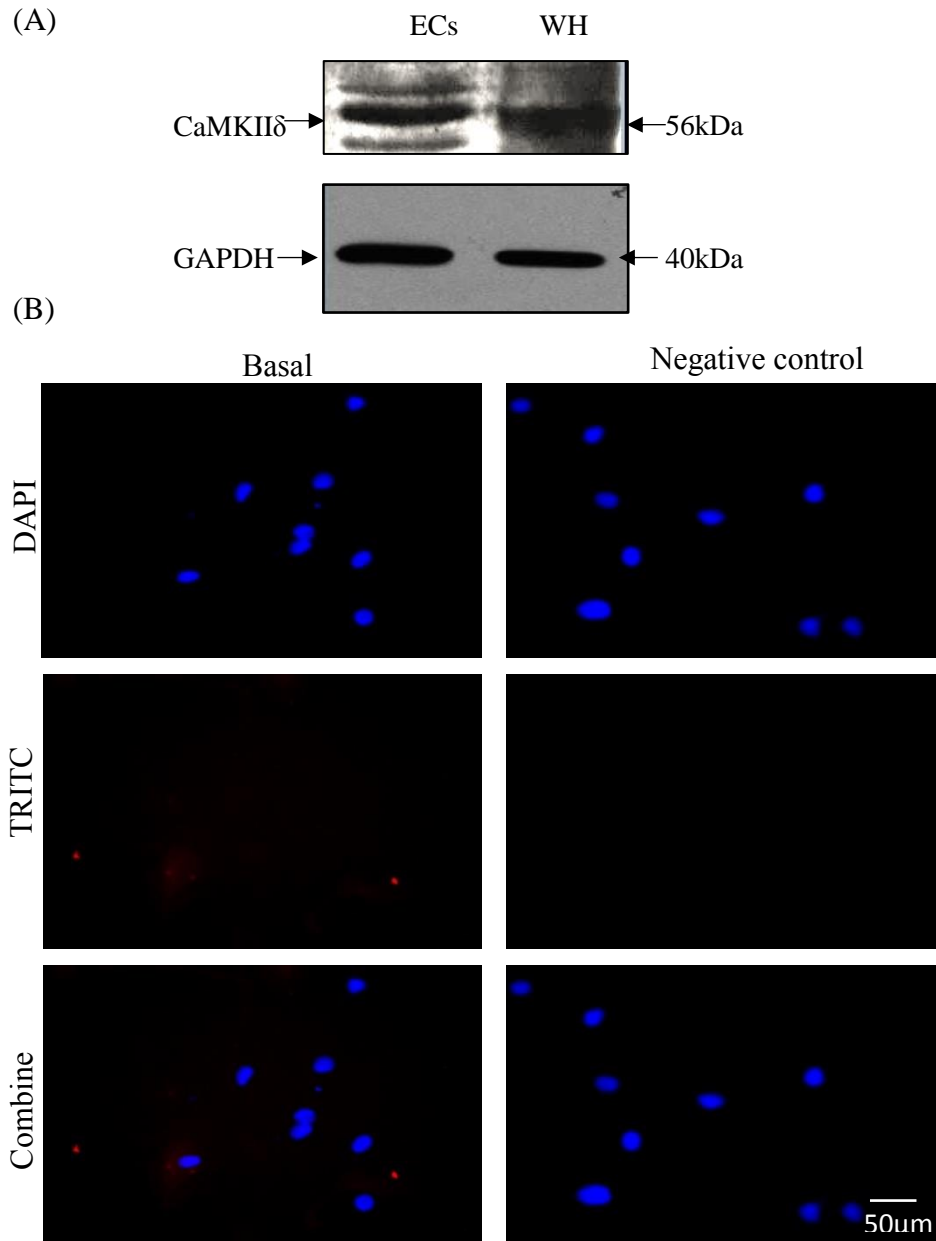
Figure 3.17 Optimisation of CaMKIIδ antibody conditions for PLA. Rat aortic endothelial cells were harvested in lysis buffer and subjected to quantitative immunoblotting to show anti-CaMKIIδ antibody specificity and compared with that of aorta WH (A). Cells were also grown on coverslips and subjected to immunofluorescence with the same anti-CaMKIIδ antibody (1:50) overnight at 4°C. Anti-rabbit TRITC conjugated secondary antibody (1:200) was then added to show positive CaMKIIδ staining under basal conditions as red. Cells stained with secondary antibody only were used as a negative control. DAPI was used in all experiments to label the nucleus as blue. All images were taken using the 20x objective lens. Scale bar represents 50µm for all images. Data are from an individual experiment, typical of 2 others.

3.9.2.3 ox-CaMKII

The ox-CaMKII was selected as it has been reported to show good results using immunofluorescence from the manufacturers' datasheet and since it was raised in rabbit, should potentially work in the subsequent PLA experiments with the anti-mouse IKKβ antibody. One important point to note is that ox-CaMKII is not specific to the δ isoform and therefore will show a positive result for all CaMKII isoforms activated by oxidation of Met 281/282. In spite of this, as mentioned in Chapter 1, the δ isoform is predominantly expressed in ECs and therefore a positive signal for activation is likely due to oxidation of CaMKIIδ.

Given that the ox-CaMKII antibody detects an active form of CaMKII, it was of key importance to assess the efficacy of the antibody at baseline and following stimulation to ensure an optimal signal is detected. Cells were therefore treated with varying concentrations of H_2O_2 (10-300μM) for 3h and ox-CaMKII protein expression assessed and compared to that of control (un-stimulated) cells by immunoblotting (Figure 3.18). ox-CaMKII expression appeared low in control samples and was significantly increased following treatment with 10μM H_2O_2. This result indicates that ox-CaMKII expression is low at baseline in ECs and that the antibody can detect increased expression due to activation of CaMKII following agonist stimulation. Using an immunofluorescence approach, ox-CaMKII expression also appeared to increase following H_2O_2 stimulation (15 minutes) when compared to un-stimulated cells (Figure 3.19). Overall these findings strongly suggest that in order to achieve optimal results with the ox-CaMKII antibody for PLA experiments, exposure of cells to an agonist is essential in order to capture any interaction between IKKβ and active CaMKII.
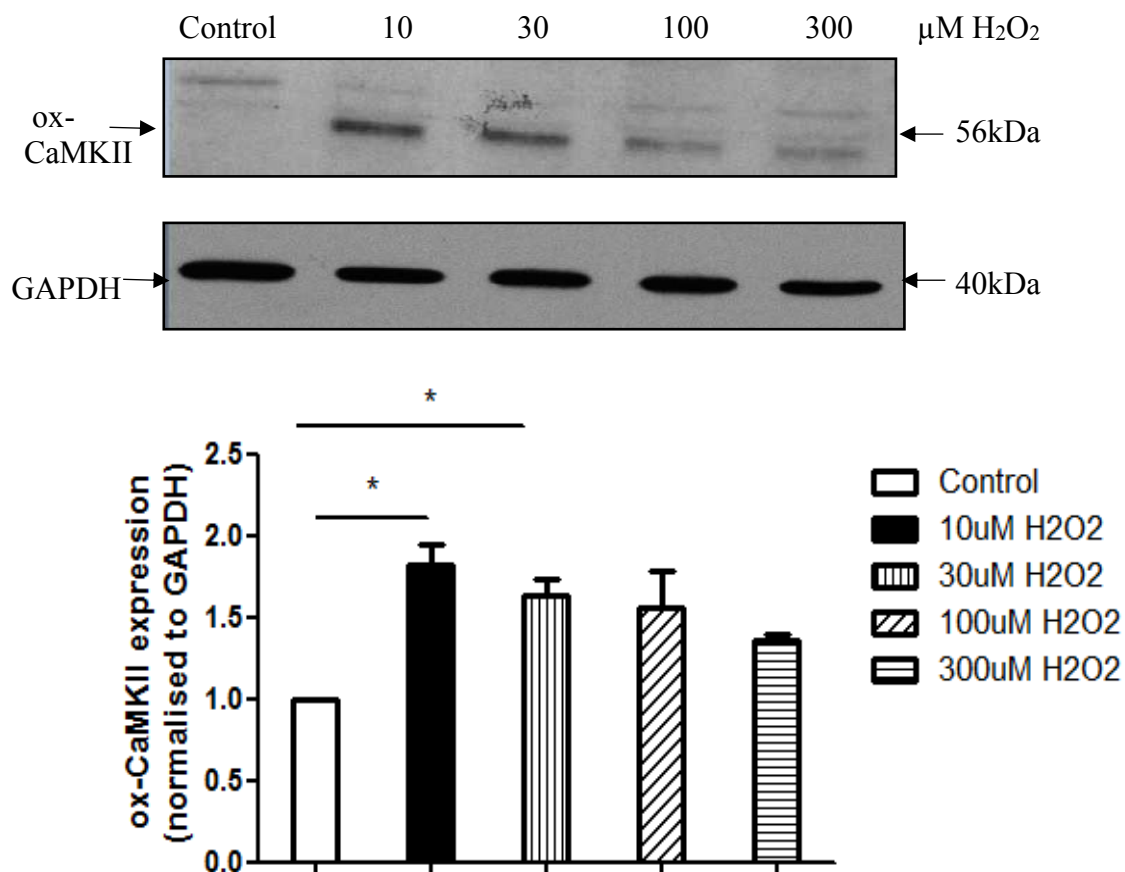
Figure 3.18: CaMKII is activated by oxidation following exposure to H_2O_2. Rat aortic endothelial cells were grown in individual wells of a 12 well culture plate and exposed to varying concentrations of H_2O_2 (10, 30, 100 or 300µM) in supplemented buffer for 3h. Control cells were exposed to supplemented buffer only. Ox-CaMKII expression was assessed in cell preparations by immunoblot analysis and quantified by normalising to GAPDH. Densitometric analysis of immunoblots was performed, with data from 3 independent experiments expressed as mean ± S.E.M. Values compared to control were considered significant if p<0.05 *.
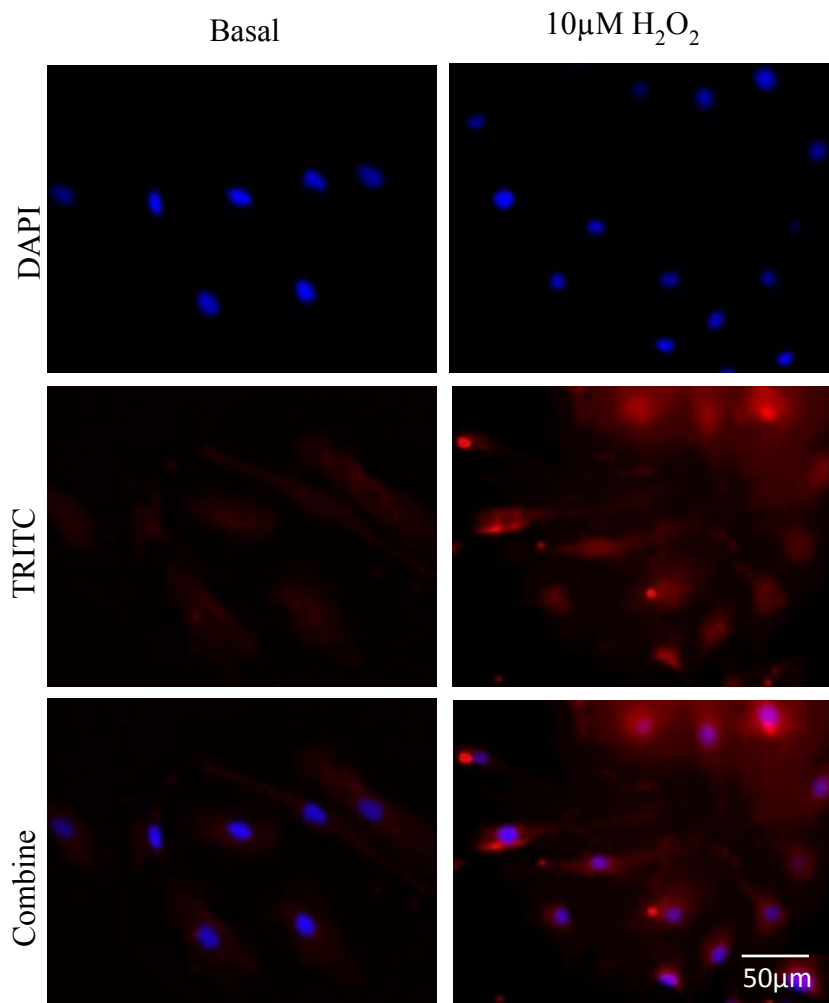
Figure 3.19 Optimisation of ox-CaMKII antibody conditions for PLA. Rat aortic endothelial cells were grown on plain coverslips in 12 well culture dishes until ~50% confluency reached. Cells were fixed, permeabilised and incubated with anti-ox-CaMKII antibody (1:50) overnight at 4°C. Anti-rabbit TRITC conjugated secondary antibody (1:200) was then added to show positive ox-CaMKII staining under basal conditions as red. Cells pre-treated for 15 minutes with 10μM H_2O_2 prior to fixation were used as a positive control. Cells stained with secondary antibody only were used as a negative control. DAPI was used in all experiments to label the nucleus as blue. All images were taken using the 20x objective lens. Scale bar represents 50μm for all images. Data are from an individual experiment, typical of 2 others.

3.9.3 CaMKII specifically interacts with IKKβ following oxidation and activation

The main objective of this chapter was to investigate a functional interaction between active (oxidised) CaMKII and IKKβ in ECs. Having fully optimised conditions for both IKKβ and active ox-CaMKII antibodies for immunofluorescence, this objective was then fully explored using the PLA approach.

Treatment conditions for each experiment included: (i) Control (no primary antibodies); (ii) IKKβ antibody only (negative control); (iii) ox-CaMKII and IKKβ (measured at baseline) and (iv) ox-CaMKII and IKKβ (after 15 minutes H_2O_2 stimulation). As illustrated in Figure 3.20, cells exposed to both ox-CaMKII and IKKβ antibodies showed a higher signal at baseline and after H_2O_2 stimulation compared to control suggesting an interaction. Importantly however there was a marked level of variation in signals amongst different batches of cells, with some experiments displaying higher signals in control and negative control samples, as represented by Figure 3.21. Quantification of all signals however revealed there to be a significant increase in signal within the stimulated cells (Figure 3.22). This highlights for the first time that CaMKII specifically interacts with IKKβ and in doing so, may potentially modulate NF-κB signalling in aortic ECs.
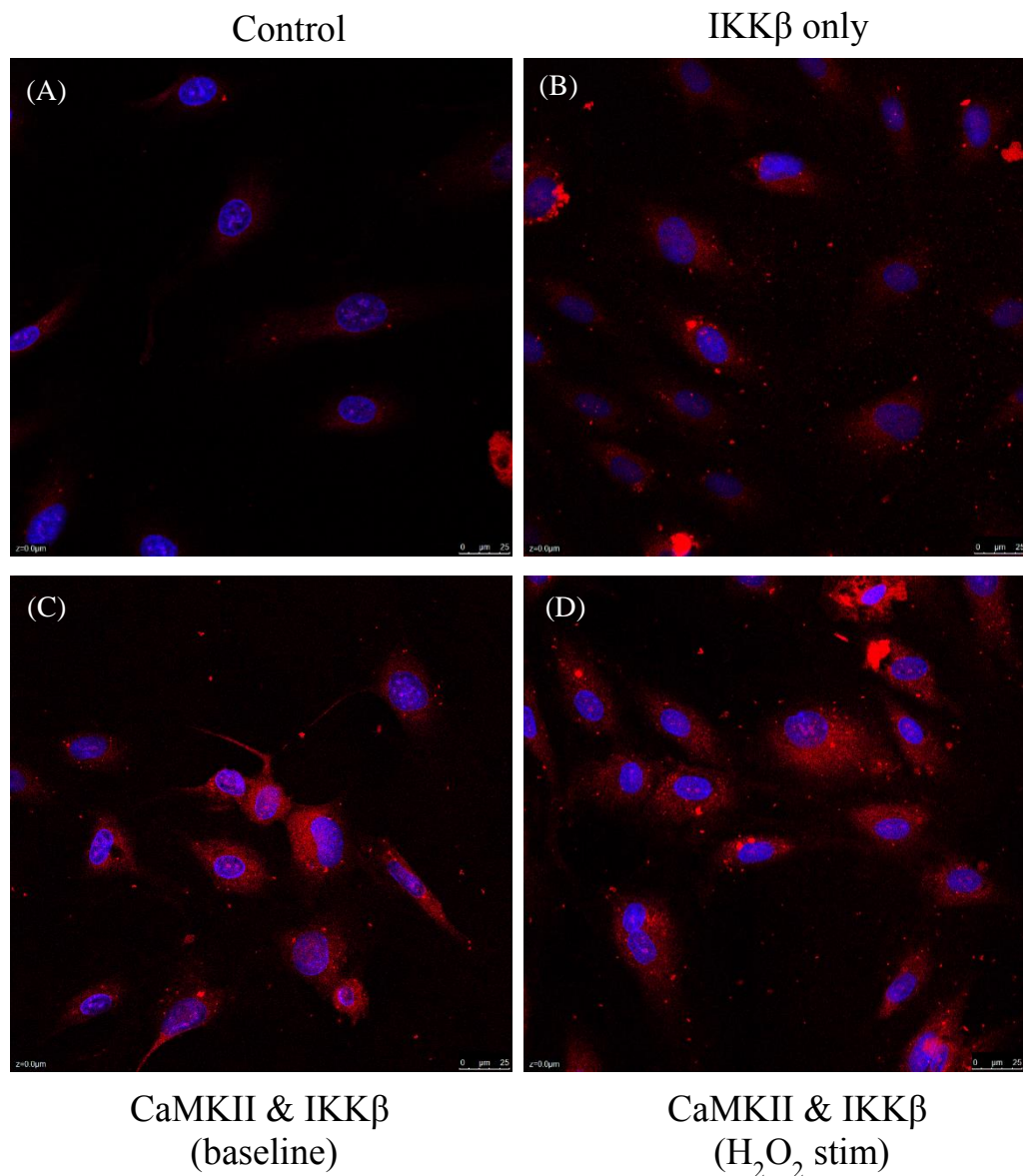
Figure 3.20 CaMKII interacts with IKKβ following H₂O₂ stimulation. Rat aortic endothelial cells were grown in PLA culture chambers and treated with or without 10μM H₂O₂ for 15 minutes. The Duolink® Orange PLA was performed on each sample using IKKβ (1:200) and ox-CaMKII (1:50) antibodies. Panel A shows cells exposed to 1% BSA/PBS only; Panel B – IKKβ antibody only; Panel C – IKKβ and ox-CaMkII antibodies at baseline; Panel D – IKKβ and ox-CaMKII antibodies after H₂O₂ stimulation. Images are shown, representative of 3 independent experiments.

Control   IKKβ only

(A)   (B)

(C)   (D)

CaMKII & IKKβ   CaMKII & IKKβ
(baseline)   (H₂O₂ stim)
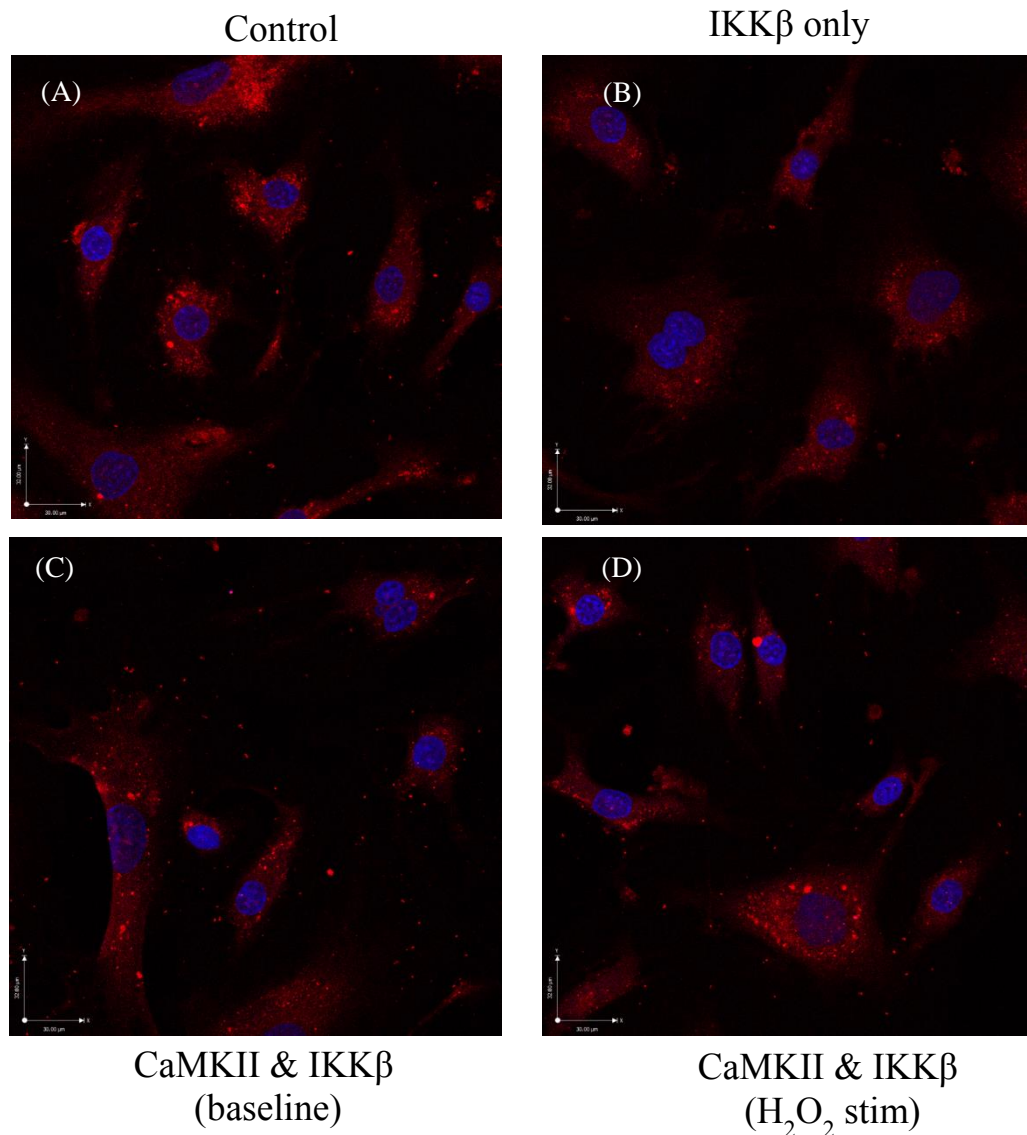
Figure 3.21 Variation in PLA signals across different experiments. Representative images of the variation in signals observed in PLA experiments across different cell batches. Rat aortic endothelial cells were grown in PLA culture chambers and treated with or without 10μM H_2O_2 for 15 minutes. The Duolink® Orange PLA was performed on each sample using IKKβ (1:200) and ox-CaMKII (1:50) antibodies. Panel A shows cells exposed to 1% BSA/PBS only; Panel B – IKKβ antibody only; Panel C – IKKβ and ox-CaMKII antibodies at baseline; Panel D – IKKβ and ox-CaMKII antibodies after H_2O_2 stimulation. Images are shown, representative of 3 independent experiments.
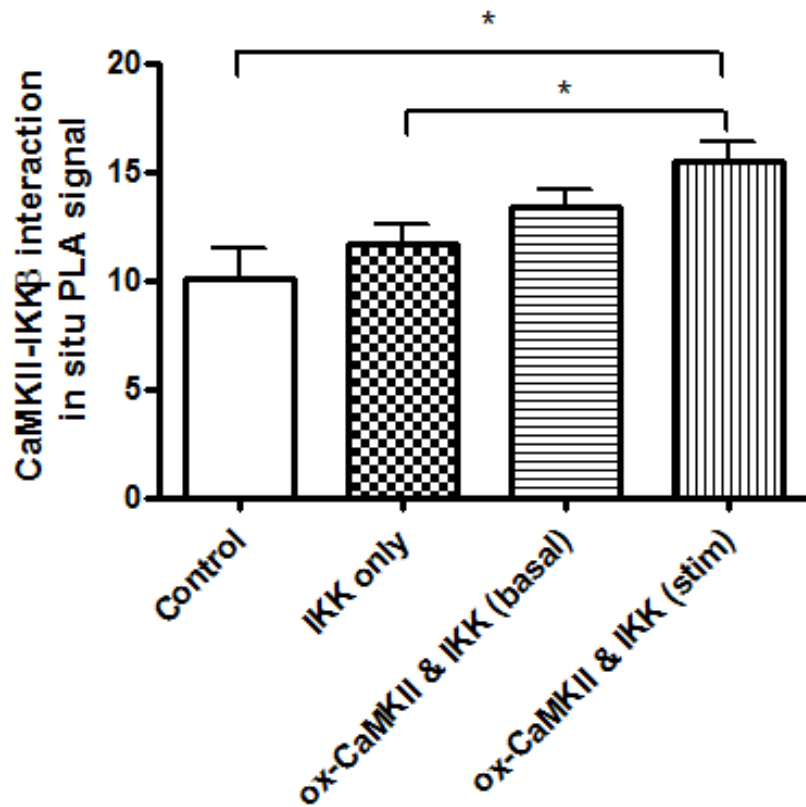
Figure 3.22 Quantification of CaMKIIδ-IKKβ interaction. Histogram shown quantitative analysis of all PLA experiments. 5 images were taken of each sample (control, no antibody; IKKβ antibody only; ox-CaMKII & IKKβ at baseline and ox-CaMKII & IKKβ after 15 minutes 10μM H_2O_2 stimulation) and from each image 5 cells were selected for quantification. Data are presented as mean ± S.E.M of fluorescent dots/cell. Statistical analysis was performed using a one-way ANOVA and Tukey's multiple comparison post-test to compare each individual group. Data were considered significant if $P<0.05*$, n=3.

3.10 Discussion

The main aim of this chapter was to explore the potential for modulation of the NF-κB signalling pathway by CaMKIIδ and to determine whether this may occur via direct protein-protein interaction in primary aortic ECs. A number of studies have indeed already suggested a link between CaMKIIδ and NF-κB signalling in the cardiovascular system, however this is limited specifically to the heart and a similar link is yet to be established within the vasculature. Furthermore, the potential for direct protein-protein interactions between CaMKIIδ and NF-κB signalling remains elusive.

As discussed in Chapter 1, NF-κB signalling plays an important role in contributing towards endothelial dysfunction (ED) associated with ageing. ED is a hallmark of most vascular diseases including atherosclerosis and coronary artery disease (Deanfield et al., 2005) and given the strong correlation between advanced ageing and the development of cardiovascular diseases, NF-κB could potentially serve as a useful therapeutic target for such conditions. Previous studies have shown that targeting NF-κB signalling in the endothelium protects against the development of atherosclerosis and other vascular disorders (Gareus et al., 2008). As mentioned in Chapter 1 however, NF-κB activation is also involved in the resolution of inflammation and therefore may exert positive or negative effects on inflammatory processes depending on cell type and disease phase (Lawrence et al., 2001). Taking this into account, it may be more beneficial to target a specific regulation part of the larger NF-κB signalling network, e.g. a specific modulator of the pro-inflammatory NF-κB pathway. This would allow control over diminishing the overactive inflammatory signalling without compromising the host defence response. One such modulator is CaMKIIδ, given the vast amount of evidence supporting a role for the kinase in NF-κB-mediated cardiac inflammation.

3.10.1 Isolation of aortic endothelial cells

Initial experiments were performed in the preliminary stages of this project using readily available and easy to use endothelial cells (HUVECs). This allowed for optimisation of various conditions including agonist treatments and

antibody/immunoblotting protocols as will be discussed in the following section. In order to obtain more physiologically relevant results however, primary ECs derived from the rat aorta were used. As discussed in Chapter 1, the aorta is the largest of the arteries and undergoes pathogenesis and remodelling in comparison to other smaller arteries during vascular disease, with ED being a key feature (Wind et al., 2010). These cells are therefore more clinically relevant for this project and thus, were isolated using an adapted version of the standard enzyme digestion method. The enzyme digestion method for isolation is commonly used, where the full vessel is submerged and digested in enzyme buffer before separating out the ECs from all other cell types (Kobayashi et al., (2005). Another common method is the 'scraping' technique in which the inner endothelial lining is mechanically broken down manually (Bartov et al., 1988). Both of these techniques however can often lead to contamination with other cell types, particularly smooth muscle cells. We have slightly adapted the enzyme method, allowing for only the inner endothelial lining to be exposed to collagenase digestion buffer for a very short period of time (10 minutes). This minimises the likelihood of subsequent cell layers (tunica media and adventitia) from also being digested and contaminating our cultures. Immunofluorescence was performed using two EC specific markers, PECAM-1 and vWF, both of which were identified in our isolated primary cells (Figure 3.7). PECAM-1 is expressed on the surface of vascular ECs and at their junctions between adjacent cells. It is an efficient signalling molecule, primarily playing a fundamental role in regulating leukocyte migration through the vascular wall via direct interaction with the ECs (Woodfin et al., 2007). Although PECAM-1 is also expressed on most leukocyte sub-types (Woodfin et al., 2007), it is not expressed on smooth muscle cells, which are the most common cell type to contaminate an endothelial culture following the enzyme digestion method of isolation. Experiments also revealed positive expression of PECAM-1 in CF preparations however, where it should not be expressed. As a result of this false positive, it was essential that a second EC marker (vWF) was also confirmed as it was. This, combined with their characteristic phenotype in culture (Figure 3.6), provided confidence in our adapted isolation technique in that we were obtaining pure cultures of ECs.

3.10.2 CaMKIIδ and NF-κB activation following pro-inflammatory cytokine stimulation in ECs

Until fairly recently, it remained unclear which isoform of CaMKII was expressed in endothelial cells, however research performed by Wang et al., (2010) revealed that it is indeed the δ_6 isoform which is predominantly expressed in the endothelium. The present study has shown that CaMKIIδ is highly expressed in HUVECs (Figure 3.2) and importantly that it is also present in primary aortic ECs (Figure 3.8). Key markers of NF-κB activation were also assessed and found to exist within both EC types following pro-inflammatory cytokine stimulation (Figures 3.3, 3.4 and 3.9). These early results confirmed that all components required for any potential interaction between CaMKIIδ and NF-κB signalling were present in ECs. We have also provided evidence that CaMKIIδ activity increases in these cells in response to the age-associated, NF-kB stimulating TNF-α cytokine (Figure 3.5). This may have been caused following an initial increase in intracellular Ca^{2+} and subsequent Ca^{2+}/CaM binding to CaMKII, initiating autophosphorylation of the threonine in the 286/287 position and rendering the enzyme active and independent of further Ca^{2+}/CaM binding (Cai et al., 2008). These results may not truly reflect the activation capacity for CaMKIIδ following inflammatory cytokine stimulation however, as cells were only exposed to TNF-α for 1h. Activation of CaMKIIδ by autophosphorylation occurs during chronic cardiovascular disease as a result of prolonged Ca^{2+}/CaM elevations, thus promoting a chronic activation state of the kinase as autonomous activity is achieved (Hudmon & Schulman, 2002). In addition to this, ageing also represents a chronic inflammatory state as previously discussed, therefore exposing ECs to pro-inflammatory cytokines for a maximum of 1h may not accurately represent CaMKIIδ activation during a chronic diseased or aged setting. In spite of this, these preliminary findings set up the next stage of this chapter which was to specifically investigate an interaction between CaMKIIδ and NF-κB.

3.10.3 A functional role for CaMKIIδ in NF-κB signalling in ECs

In the present study, initial experiments examining the potential for interaction between CaMKIIδ and the NF-κB signalling pathway were performed by measuring IκBα degradation in the presence and absence of a selective CaMKII inhibitor AIP. AIP inhibits CaMKII by binding to the substrate binding site on the enzyme, therefore preventing it from exerting its kinase effects (Ishida et al., 1998). Previous studies, including that conducted by Martin, (2011), have shown that selective inhibition of CaMKII (using AIP pre-treatment) prevents IκBα degradation and subsequent NF-κB activation in adult CFs. We did not however find this same result when ECs were pre-treated with AIP and exposed to TNF-α stimulation (Figure 3.11). LPS was used as the agonist of choice to activate the NF-κB pathway in the study mentioned above (Martin, 2011) which may explain the differences with our work as it is a much more potent activator of NF-κB signalling. The use of such an agonist in this study however offers no physiological relevance to the ageing context, given the fact (as outlined in Chapter 1) we hypothesise that it is circulating pro-inflammatory stimuli and ROS which are the underlying activators of NF-kB signalling in the endothelium. An alternative approach to explore a functional role for CaMKIIδ in NF-κB signalling was therefore sought.

Using siRNA technology is an effective strategy for assessing a functional role of a protein of interest by inducing its gene knockdown and subsequently analysing downstream consequences. We therefore used this method to further assess a potential role for CaMKIIδ in modulating NF-κB signalling in ECs. Results from this experiment showed that by knocking down CaMKIIδ gene expression, IκBα degradation was prevented and therefore subsequent NF-κB activation inhibited (Figure 3.15). This suggests for the first time that CaMKIIδ may play a role in modulating pro-inflammatory NF-κB activation in ECs and therefore may serve as a useful target for preventing ED. In reaching this conclusion however, a great deal of optimisation was required for such siRNA experiments, which itself took several months to conduct. Early experiments had to be performed to assess a suitable transfection reagent that could be used. As mentioned in Section 3.8.1, there are a large number of transfections reagents which are commercially available which can make selecting the most appropriate one extremely difficult. The first transfection reagent

which we decided to use was FuGENE® given the fact it successfully transfected HUVECs (data not shown) and it had also been previously shown to work well with other primary ECs including coronary artery and microvascular ECs (Ziouzenkova et al., 2003). In spite of this, we did not find FuGENE® to successfully transfect the primary aortic ECs (Figure 3.13) therefore this would not be deemed as suitable to use when transfecting these cells for siRNA purposes. HiPerfect® transfection reagent was therefore also investigated as it has also been previously shown to work well with primary EC cultures (Cortese et al., 2008). Here, we established good transfection efficiency using HiPerfect® (Figure 3.12) similar to that which has been previously reported at the same ratio (Alabi et al., 2012) therefore this was selected to use in our subsequent siRNA experiments. In terms of assessing a suitable concentration of siRNA to use, 3 concentrations were initially selected to cover a wide range: 1nM, 10nM and 100nM. The manufacturers' protocol in the TriFecta® kits which were used suggested starting concentrations of 0.1nM, 1nM and 10nM, however when comparing this to other studies in the literature successful knockdown of gene expression was more significant at higher concentrations up to, and including 100nM. When the ECs were transfected with such high concentrations however it induced cytotoxicity and therefore no protein expression was analysed. This mirrors what has been reported in other studies using such a high concentration (Liu et al., 2004) where by 48h post-transfection, 80% cell detachment had occurred. Optimal CaMKIIδ knockdown was only achieved at a final concentration of 10nM and using only one of the DsiRNA duplexes provided in the kit (Figure 3.14). As detailed in Chapter 2, Section 2.5.2, the TriFecta® kit provides three different siRNA duplexes all of which target different regions of the CaMKIIδ gene. This greatly increases the likelihood of inducing successful knockdown as variation can exist between different cell types. In earlier experiments different siRNA kits were used however these only included one duplex and therefore knockdown of CaMKIIδ expression was unsuccessful (data not shown). Overall however, results from these siRNA experiments have shown novel evidence that CaMKIIδ does play a functional role in NF-κB signalling in aortic ECs and importantly, may therefore also play a role in modulating age associated ED which will be further investigated in future chapters.

3.10.4 Analysis of the CaMKII-IKKβ interaction

Having established that CaMKIIδ does indeed play a functional role in NF-κB modulation in ECs, the final aim of this chapter was to assess CaMKII-NF-κB interactions at the level of the IKK complex – specifically the IKKβ subunit. Despite the fact it was established nearly 10 years ago that CaMKIIδ can modulate NF-κB signalling in the heart (Singh et al., 2009), no subsequent studies have yet investigated how the two pathways specifically interact. As mentioned earlier, previous work from our own research group has built upon that reported in the literature and shown via SPR that CaMKIIδ can directly interact with the IKKβ subunit of the IKK complex (Martin, 2011). This work initially investigated whether CaMKIIδ could potentially interact with any of the IKK proteins (IKKα, IKKβ and IKKγ), however the SPR analysis revealed there to only be a direct protein-protein interaction between CaMKIIδ and IKKβ. No such findings were reported with IKKα and IKKγ. This discovery provided an excellent starting point for this work in terms of investigating the modulation of NF-κB by CaMKIIδ in ECs.

Initial plans to investigate this protein-protein interaction between CaMKIIδ and IKKβ were to use immunoprecipitation of native proteins from solubilised aortae whole homogenates and solubilised EC extracts. This is a very commonly used technique for investigating protein-protein interactions, however due to the poor quality and specificity of the commercially available IKKβ antibodies for immunoprecipitation such experiments were unsuccessful (data not shown). An alternative approach was therefore sought and from this, the relatively novel PLA technique was selected. As mentioned, PLA enables the detection, visualisation and quantification of direct protein-protein interactions in cell samples using immunofluorescence and is therefore a relatively straight-forward technique. From these experiments, it was clear that CaMKII interacts with IKKβ following activation by oxidation (Figure 3.20 and 3.22). There was however quite a wide degree of variation in terms of the signal produced, with some control samples showing higher positive signals than that of stimulated samples containing both CaMKIIδ and IKKβ antibodies (Figure 3.21). Due to time constraints, these experiments were only performed 3 times therefore it is not unusual for such a range of results to be observed in cells isolated from different animals. In spite of this however, when analysis was performed on all of the combined data, the

level of positive signal and therefore corresponding CaMKII-IKKβ interaction was significantly higher in the H_2O_2 stimulated cells compared to control. This shows important novel evidence, which supports our earlier work that CaMKII can specifically interact with the IKKβ subunit of the IKK complex following activation by oxidation. As mentioned earlier, the ox-CaMKII antibody is not specific to the δ isoform of CaMKII and therefore it is important to note that this PLA result also does not show specifically a CaMKIIδ-IKKβ interaction. Nonetheless, the SPR data produced by Martin, (2011) and the siRNA results from earlier in this chapter do provide strong evidence to suggest the δ isoform of CaMKII does modulate the NF-κB signalling pathway. Furthermore, given the strong role for ROS in advanced ageing of the endothelium, the fact that an interaction exists between active (oxidised) CaMKII and NF-κB in ECs only further supports our overall hypothesis: Not only does CaMKIIδ interact with and modulate NF-κB signalling; it is over-expressed and hyper-activated, thus it may contribute to the chronic inflammatory and oxidative phenotype of the endothelium during advanced ageing – all of which will be investigated in more detail in the forthcoming chapters of this thesis

3.11 Conclusions

In summary, data presented in this chapter shows novel evidence that an interaction exists between CaMKIIδ and the canonical NF-κB signalling pathway in primary adult aortic ECs and importantly, that this interaction exists following activation of CaMKII by oxidation. These findings suggest that targeting/inhibiting CaMKIIδ could be a strategy for reducing ED associated with ageing and therefore the following chapters will investigate CaMKIIδ and NF-κB in the context of ageing.

Chapter 4: Ageing – cardiovascular and endothelial cell dysfunction

4.1 Introduction

As discussed in Chapter 1, advanced age is the greatest risk factor for the development of cardiovascular diseases (CVD) including myocardial infarction (MI), hypertension and atherosclerosis (Gordon et al., 1989; Kannel, 1998). Cardiovascular ageing is a complex and dynamic process involving both structural and functional alterations to the heart and vasculature. In humans, left ventricular (LV) diastolic filling rate significantly declines after the age of 60 (Olivetti et al., 1991) and LV systolic function, measured by ejection fraction (EF), is also severely compromised (Cheng et al., 2009). During even healthy ageing, cardiac hypertrophy develops, similar to that observed in diseased animal models (Nakou et al., 2016) demonstrating that cardiac dysfunction is inevitable with increased age. The arterial system also undergoes significant alterations as we age with the large arteries, including the aorta, becoming stiff and rigid in structure and the vessel walls thickening over time. This enhances inelasticity which in turn, potentiates systolic pressure as more strain is placed on the heart, thus augmenting the risk of developing disease not only in the myocardium, but also in the vasculature itself (Lakatta & Levy, 2003).

Numerous adaptations to the arteries are likely to contribute to the development of age-associated CVD, however one of the most clinically important of these is the development of vascular endothelial dysfunction (ED) (Brandes, Fleming & Busse, 2005; Lakatta & Levy, 2003). In its healthy state, the endothelium plays a fundamental role in regulating various processes in maintaining the health of the arterial system. This includes the synthesis and release of an array of biologically active molecules to modulate vasodilatory, thrombolytic or vasoprotective functions (Seals, Jablonski & Donato, 2011). During arterial ED a chronically 'activated' phenotype develops and normal homeostatic function is lost (Deanfield et al., 2007). Damage to the endothelium enhances endothelial permeability and leukocyte adhesion and these infiltrating immune cells can then potentiate the development of a pro-inflammatory environment. Thus, a chronic low grade inflammatory phenotype is apparent in aged individuals and significantly increases the risk of illness and/or death (Csiszar et al., 2008; Edirisinghe & Burton-Freeman, 2014). Additionally, the pathogenesis of ED associated with ageing is also extensively mediated by reactive oxygen species (ROS).

ROS, in particular superoxide (O_2^-) and hydrogen peroxide (H_2O_2), are known to be significantly elevated in aged individuals causing oxidative stress and damage to tissues. They reduce the bioavailability of the endothelium-derived relaxing factor nitric oxide (NO), therefore contributing to impaired endothelium dependent dilation (EDD), which is often considered the first sign of adverse cardiovascular events (Li et al., 2017; Yoon et al., 2010). Furthermore, ROS play a role in activating various signal transduction pathways within vascular cells mediating the production of numerous pro-inflammatory transcription factors such as NF-κB (Csiszar et al., 2008). Activation of the NF-κB-mediated inflammatory cascade by such mechanisms further potentiates the chronic inflammatory phenotype which manifests during ageing and thus, it is now generally accepted that both inflammation and oxidative stress work in parallel contributing to age-associated cardiovascular ailments.

Taking all of the above information into account, the second main objective of this project was to examine both structural and functional alterations to the heart and vasculature in aged rats, as well as investigating whether inflammation and oxidative stress are increased during ageing. *In vivo* transthoracic echocardiography was performed on live animals to assess functional abnormalities during ageing and post-mortem analysis examined structural differences using an immunohistochemical approach. The endothelium from aged animals was then specifically investigated for phenotypic abnormalities and differences in ROS production compared with young, control cells. Conventional methods for assessing ED include *ex vivo* wire myography and *in vivo* studies, where in both cases the delivery of vasoactive agents such as acetylcholine can be used to assess endothelial dependent dilation (Seals et al., 2014). For this project however, we have attempted to develop a completely novel method for assessing dysfunctional ECs by analysing differences in cell impedance profile. This could hopefully be used in future studies as an alternative approach to those listed above.

4.2 Cardiac dysfunction is apparent with ageing

Transthoracic echocardiography was used to functionally assess cardiac contractility and left ventricular remodelling. Typically, echocardiography was performed on a lightly anaesthetised animal placed in the supine position. Heart rate (HR) was monitored throughout to ensure the well-being of the animal was maintained and analysis from this revealed a 20% reduction HR in aged animals (Figure 4.1), indicating compromised cardiac function within this group. For cardiac measurements, a two dimensional short axis view was obtained such that the LV, contracting papillary muscles (PM), posterior (PW) and anterior wall (AW) were clearly visible. This was obtained initially in young animals (Figure 4.2A (i)) and from these, motion mode (M-mode) traces could be recorded at the level of the papillary muscle (Figure 4.2A (ii)). Once the reproducibility of the method was established, cardiac contractility was assessed during systole and diastole by taking measurements of LV wall dimensions including, PW, LV end systolic dimension (LVESD) and LV end diastolic dimension (LVEDD) from M-mode traces. This was then repeated in aged rats with representative images of short axis views and M-mode traces shown in Figure 4.2B (i) and (ii). Analysis of these LV measurements is shown in Figure 4.3 and revealed no significant difference in LVPW during diastole and LVEDD between young and aged groups. LVPW during systole and LVESD were however significantly increased in aged animals. Some of these results contradict what has been shown in previous studies of CVD, where both LVESD and LVEDD are lower in diseased hearts compared to healthy (Parfrey et al., 1996; Martin, 2011), however given the finding that the difference between LVESD-LVEDD is markedly reduced in aged animals, this suggests altered LV function.
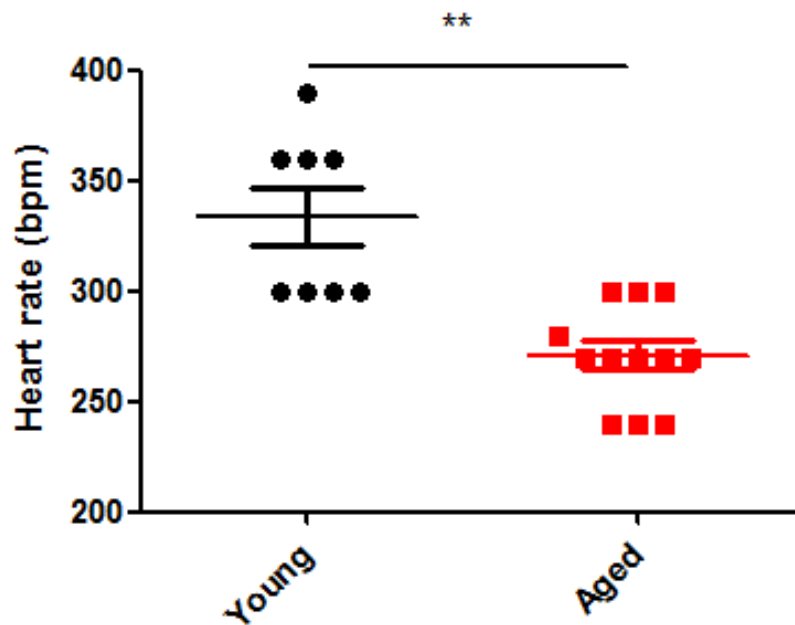
Figure 4.1 Heart rate is decreased in aged rats. Heart rate was measured in young and aged male Sprague Dawley rats from pulse wave traces on echocardiography machine as beats per minute (bpm). Data are shown as mean ± S.E.M and statistical analysis was performed using an unpaired student's t test; p<0.01, **; n=8 for young and n=12 for aged rats.
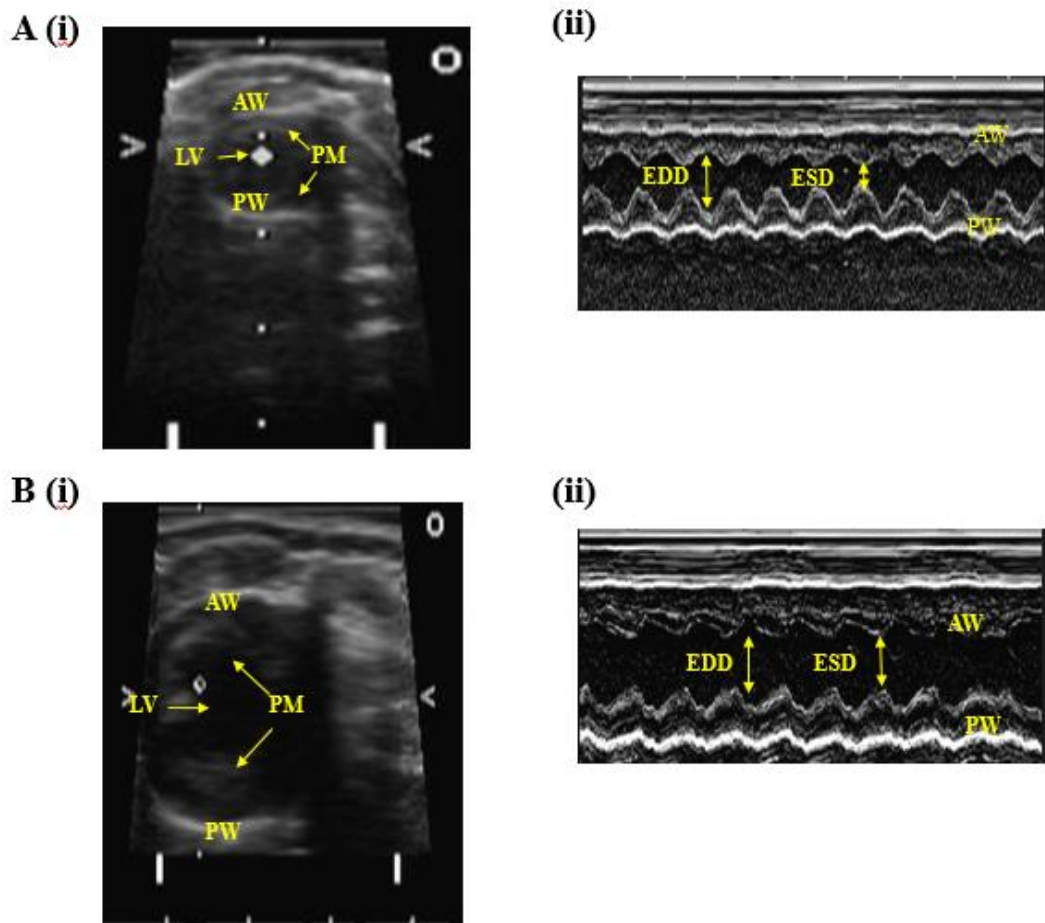
Figure 4.2 In vivo echocardiography of hearts from young and aged rats. Two-dimensional short axis views of the hearts were obtained in both young (A (i)) and aged (B (i)) rats. From this, images clearly show structures including the left ventricle (LV), anterior (AW) and posterior wall (PW) and the papillary muscles (PM). M mode traces could then be recorded at the level of the papillary muscle in young (A (ii)) and aged (B (ii)) animals, where systolic and diastolic wall measurements could be assessed (LV end systolic dimension (LVESD), LV end diastolic dimension (LVEDD). Images are representative of n=8 young and n=12 aged animals.
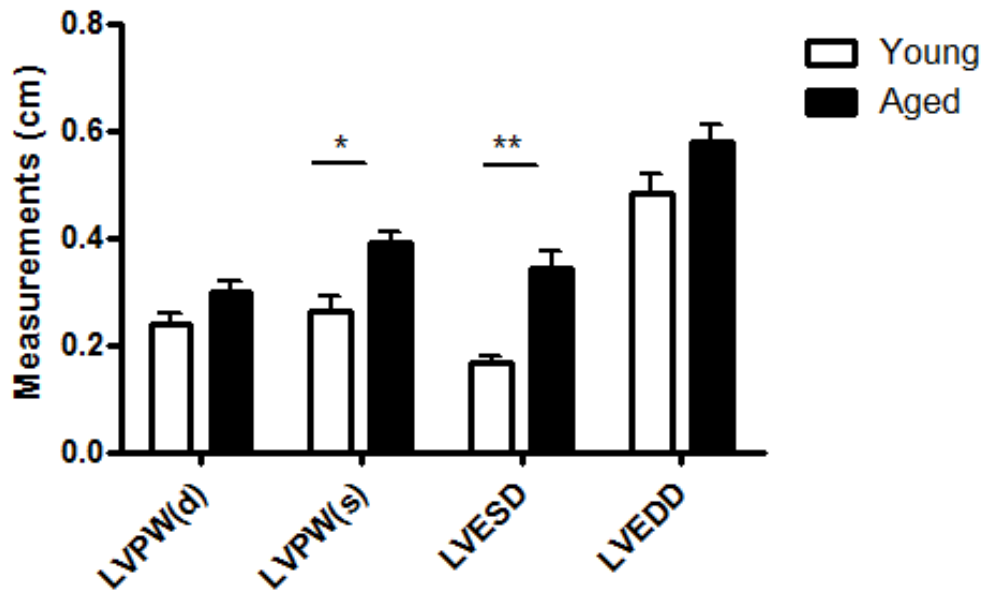
Figure 4.3 Echocardiography left ventricle measurements. Left ventricular posterior wall thickness (LVPW) was measured during diastole (d) and systole (s) in both young and aged rats. Left ventricular end systolic dimensions (LVESD) and eft ventricular end-diastolic dimensions (LVEDD) and were also assessed. Values are presented as mean ± S.E.M. Statistical analysis was performed using a two-way ANOVA followed by Bonferroni's post-test, $p<0.05^*$, $p<0.01^{**}$; n=8 for young and n=12 for aged.

4.2.1 Cardiac hypertrophy develops in aged rat hearts

LV function was then quantitatively assessed by fractional shortening (%FS) which can be calculated using the following equation: [LVEDD – LVESD/ LVEDD] x 100. It can be clearly seen from Figure 4.4A that FS was markedly decreased in aged animals compared to young (63.2 ± 1.3 vs. 50.6 ± 1.9, young vs. aged, $p<0.01$), indicating compromised contractile function in aged hearts. In correlation with this, post-mortem analysis revealed an increase in heart weight: body weight ratio (HW:BW) with ageing (2.68 ± 0.2 vs. 3.63 ± 0.1, young vs. aged, $p<0.01$; Figure 4.4B), thus suggesting a hypertrophic phenotype in LV tissue with ageing. This is similar to that already reported in diseased models (Karamanlidis et al., 2014; Martin et al., 2012) and these alterations likely reflect a number of physiological changes occurring in both the heart and vasculature during the ageing process that contribute to deterioration of cardiac function.

A
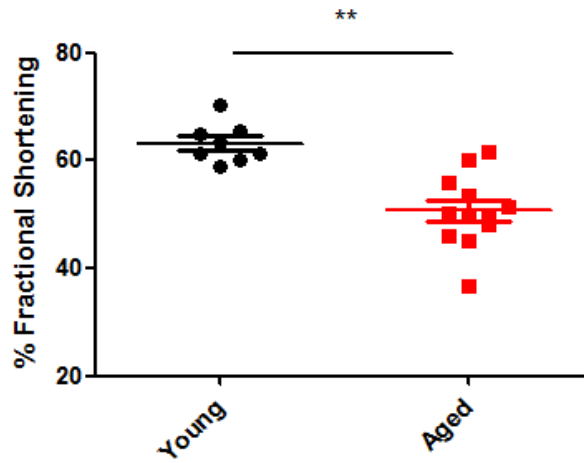
B
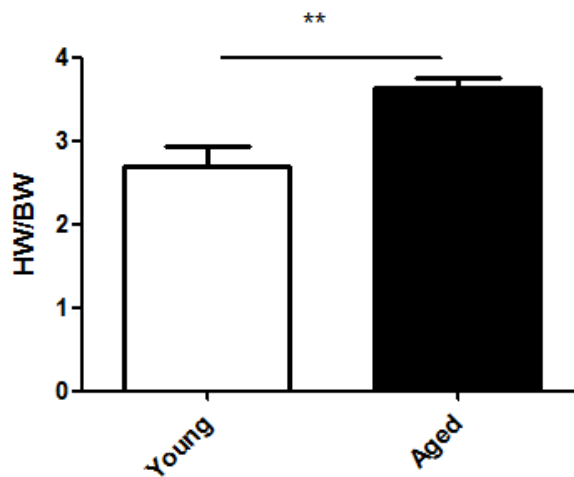
Figure 4.4 Ageing induces a hypertrophic phenotype in heart. M mode traces recorded at the level of the PM enabled measurements of the LVESD and LVEDD to be taken in young and aged rats (cm) (A). Fractional shortening (%FS) was determined using the equation [LVEDD – LVESD/ LVEDD] x 100 in both young and aged animals (B). Heart weight (HW) and body weight (BW) of rats was recorded post-mortem and HW: BW ratio calculated. Data are shown as mean ± S.E.M and statistical analysis was performed using a student's unpaired t test, $p<0.01$**; n=8 for young and n=12 for aged.

*4.3 Assessment of aortic (vascular) dysfunction during ageing*

As well as cardiac dysfunction, ageing is also associated with vascular dysfunction as previously discussed. Both structural and functional changes such as hypertrophy, extracellular matrix deposition and plaque formation accompany vascular ageing (Seals, Jablonski & Donato, 2011). Echocardiography can also be used to effectively assess vascular function. In the present study this approach was used to measure any differences in aortic function between young and aged rats. For such experiments animals were again placed in a supine position with the linear array probe angled in a clockwise manner to obtain an image of the parasternal long axis view (PLAX). The transducer was angled such that the aortic valve (AV) and LV could be visualised as well as the ascending aorta (AA). These images were initially obtained in young animals (Figure 4.5A (i)) and from this, Pulsed Wave Doppler Mode (PWDM) was used to measure the velocity of blood passing through the AA. Representative images of PW traces from young animals are shown in Figure 4.5A (ii). These measurements were then repeated in aged animals (Figure 4.5B (i) & (ii)) and from this, blood flow could be calculated using the formula: Flow (ml/min) = VTI x πr^2 x HR. Overall blood flow (ml/min) was found to be faster in aged vessels (76.7±4 vs. 104±9.7, young vs. aged, p=0.05; Figure 4.6) which can also be observed from the representative PW traces in Figure 4.5. Turbulence in blood flow was also greater in the aged vessels, which is reflected in the spread of normalised flow measurements. This correlates with previous work where aortofemoral PWV was shown to increase with age and to be a predictor of future cardiovascular events (Strait & Lakatta, 2012).
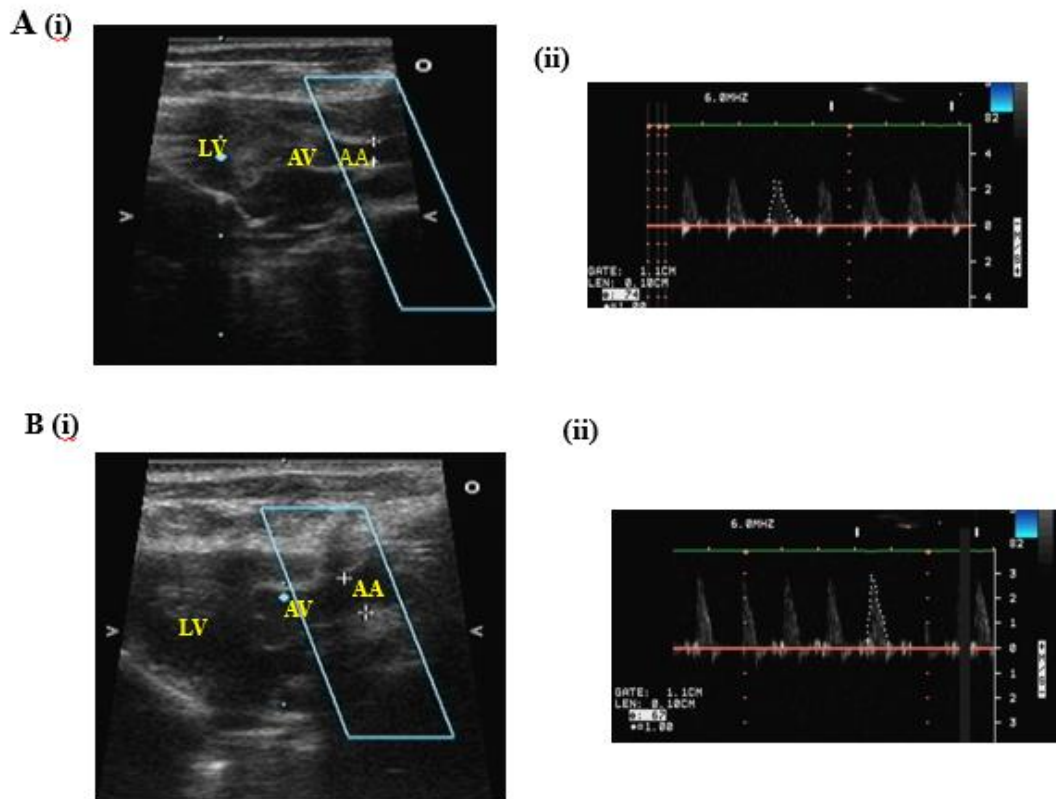
Figure 4.5 in vivo echocardiography of aortae from young and aged rats. A parasternal long axis view (PLAX) was obtained by rotating the probe ~80˚ clockwise from the initial short axis position to allow a clear image of the ascending aorta (AA) and aortic valve (AV) as depicted in panel A(i) (young) and panel B(i) (aged). The left ventricle (LV) is also seen from this position. For blood flow measurements, settings can be changed from brightness mode (B mode) to Pulsed wave Doppler mode (PW) to measure velocity of blood passing through the AA. The velocity time integral (VTI) can be calculated from tracing around each velocity peak. Velocity traces were taken from both young (panel A(ii)) and aged (panel B(ii)) rats. All images are representative for n=9 young and n=9 aged animals.
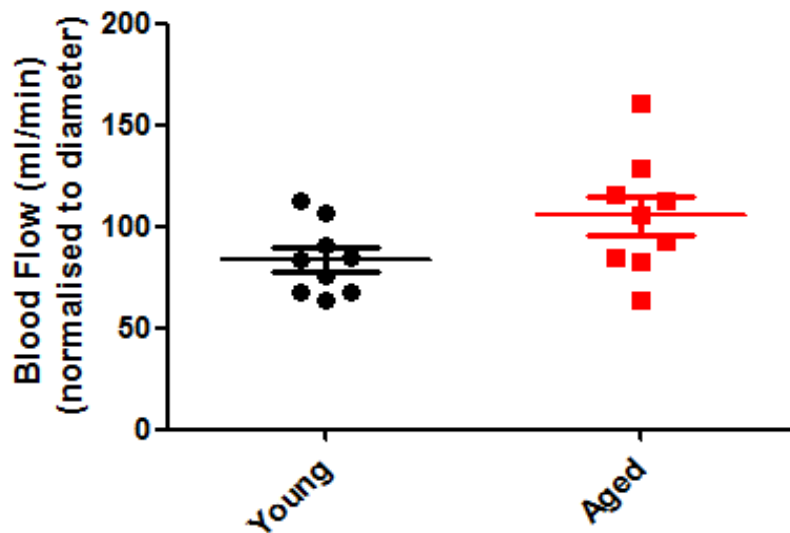
Figure 4.6 Variations in blood flow through the ascending aorta during ageing. Velocity time integral (VTI) values and heart rate (HR) were calculated from traces as shown in Figure 4.5 and from this, blood flow through the ascending aorta (AA) was determined using the formula Flow(ml/min) = VTI x πr^2 x HR. All values were normalised to AA diameter. Data are shown as mean ± S.E.M and statistical analysis was performed using a student's unpaired t test, $p < 0.05$*; where no * is displayed $p > 0.05$; n=9 for young and n=9 for aged.

4.4 Post-mortem assessment of aortic phenotypic alterations with ageing.

Physiological changes to the aorta with ageing were investigated post-mortem to assess whether the functional alterations presented above correlated with structural abnormalities. Following dissection of the thoracic aorta, photographs were taken to observe any obvious differences between young and aged animals. Representative photographs are shown in Figure 4.7 from young (A) and aged (B) rats, depicting the difference in sheer size between the two groups. Thoracic aortae taken from aged animals were more than double the length of that from young animals, which is not surprising given the difference in BW between young and aged rats ((g) 303.4 ± 0.4 vs 525.1 ± 1.2, young vs aged). Furthermore, when fixed and wax embedded aortae were subjected to immunohistochemical examination, more striking phenotypic differences were exposed. The aged vessels showed obvious signs of hypertrophy with increased lumen diameter and increased medial wall thickness ((μm) 16.4 ± 0.9 vs. 28 ± 1.5, young vs. aged, p=0.003; Figure 4.7 C, D & G). The formation of atherosclerotic plaques also seems apparent in aged aortic sections, shown by the deposition of fatty streaks on the inner lining of the vessel wall which is not observed in young aortae (Figure 4.7 E & F). Taken together, these results provide evidence that significant adaptive changes occur in the aorta of aged animals that will ultimately contribute to overall cardiovascular dysfunction.
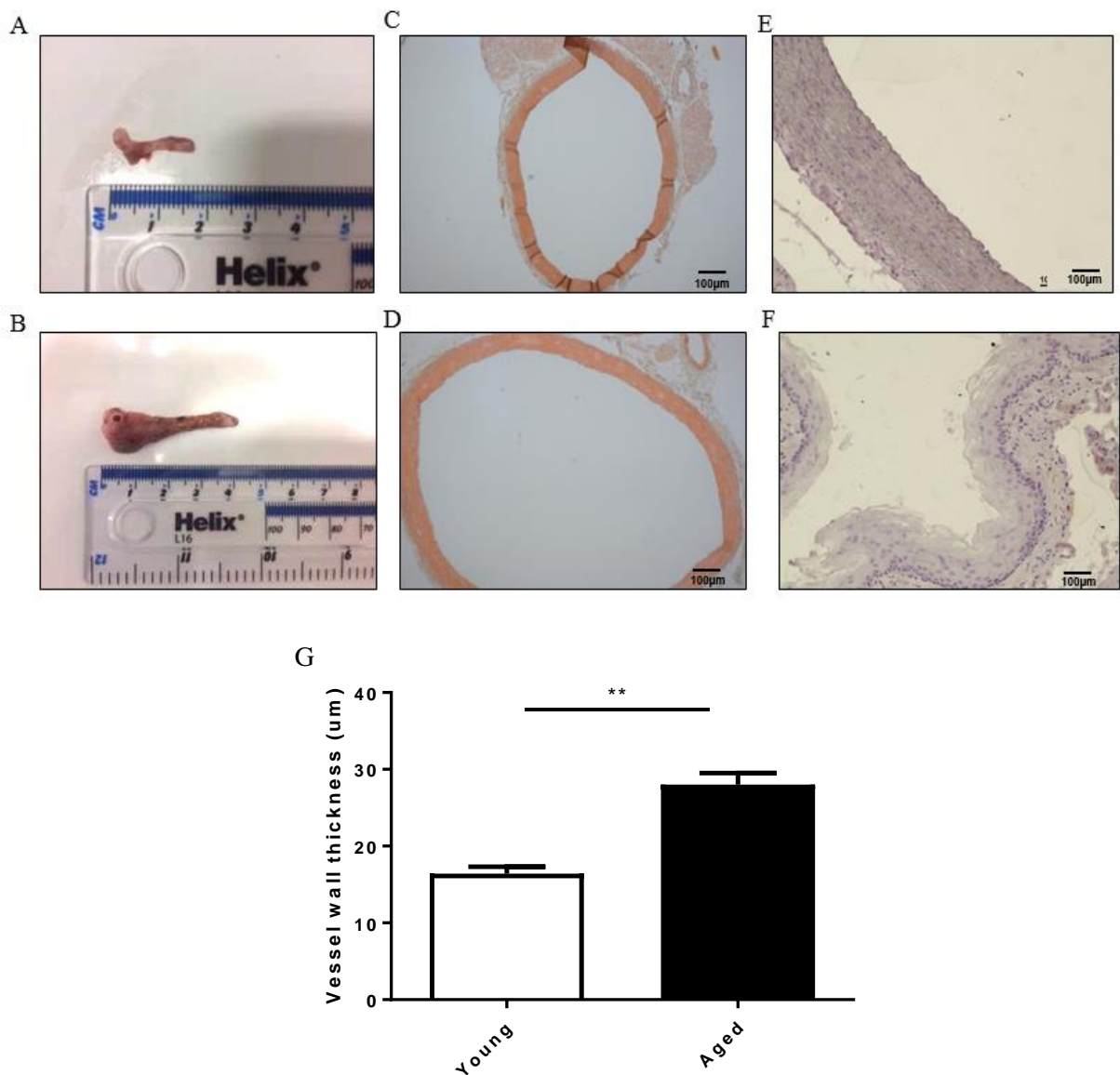
Figure 4.7 Phenotypic alterations during ageing of the aorta. Representative photographs of the dissected thoracic aorta were taken from both young (A) and aged (B) rats to show size differences. Aortae were processed and wax embedded before being subjected to H&E staining (panel C – young, panel D – aged) and immunohistochemical examination (panel E – young, panel F – aged) to depict structural differences. Vessel width was then calculated and plotted as mean ± S.E.M (G). Statistical analysis was performed using a student's unpaired t test, $p < 0.01$**; n=6 young and n=8 aged.

4.5 Assessment of an increased inflammatory phenotype during ageing of the cardiovascular system

As outlined in Chapter 1, previous studies have indicated that ageing is associated with an increase in pro-inflammatory signalling and importantly, this occurs predominantly within the CVS (Csiszar et al., 2008). As such, a key objective of this chapter was to establish this chronic inflammatory phenotype in both the heart and aorta from aged rats. Initial experiments examined circulating inflammatory mediators, including cytokines TNF-α and IL-1β as they have previously been shown to play a key role in promoting inflammation during ageing (Bruunsgaard et al., 1999; Dinarello, 2006; Tha et al., 2000). Importantly, increased systemic inflammatory activity in the elderly does indeed reflect age-related pathological processes (Bruunsgaard et al., 1999) therefore measuring serum levels of such inflammatory mediators is a good predictor for onset of disease.

Figure 4.8 shows expression of both TNF-α (A) and IL-1β (B) in terminal sera from young and aged rats as measured by ELISA. Levels of TNF-α were increased in the blood of aged animals when compared with young ((pg/ml) 0.002 ± 0.002 vs. 22.05 ± 12.9, p=0.2; Figure 4.8A). Note the considerable spread in the aged data however, which reflects the labile nature of TNF-α and variation across animals. This caused no significant differences to exist between young and aged, however the trend towards an increase in aged animals is evident, in spite of the low sample numbers. Interestingly, no such differences were recorded in levels of circulating IL-1β between young and aged rats (Figure 4.8B). Expression of this cytokine remained exceptionally low in both groups suggesting no differences with ageing. This contradicts what has been reported previously in the literature in that IL-1β is up-regulated in the ageing CVS and may play a role in the development of myocardial infarction (Deten et al., 2005). The release of IL-1β is in fact delayed following synthesis however, and large pools of precursor IL-1β accumulate within cells before it is released (Hazuda et al., 1988). Therefore it is extremely difficult to specifically capture peaks in circulating IL-1β levels during ageing, given the low-level transient pro-inflammatory state which exists with advanced ageing.

A
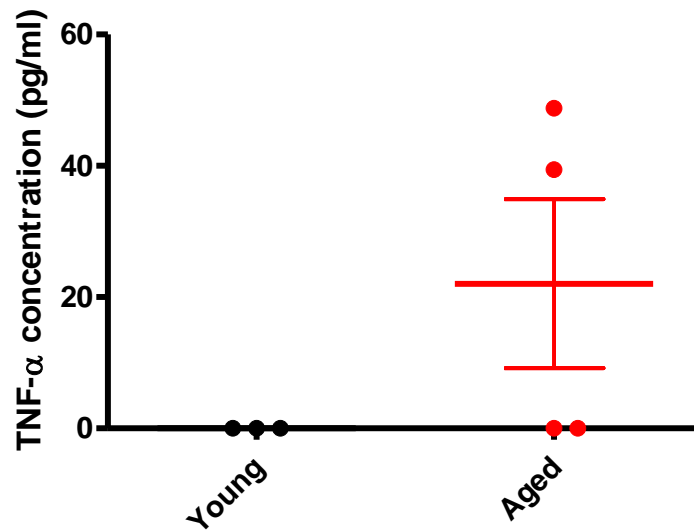
B
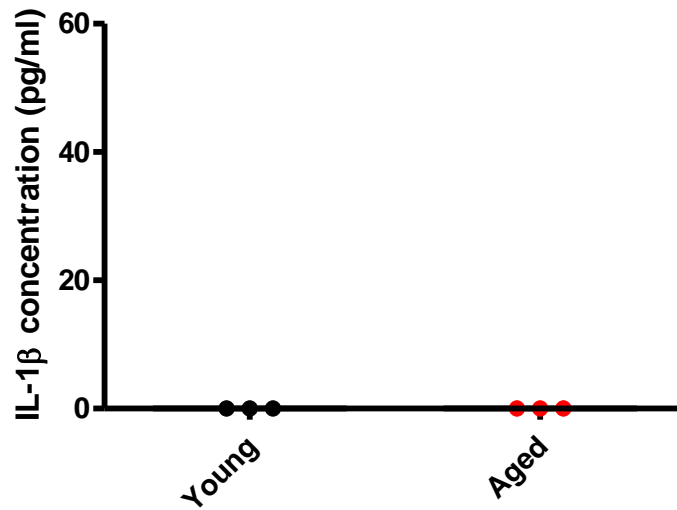
Figure 4.8 Pro-inflammatory cytokine expression in young and aged blood serum samples. Terminal sera from animals was assessed for TNF-α (A) and IL-1β levels by ELISA. Individual results are plotted and mean ± S.E.M (pg/ml). Statistical analysis was performed using a student's unpaired t test, $p < 0.05$*; where no * is shown $p > 0.05$; n=3 young and n=4 aged.

4.5.1 CD45 staining in aged cardiovascular tissues

To further assess the existence of a chronic inflammatory phenotype in aged cardiovascular tissues, sections of heart and aorta were examined for expression of CD45 as an indicator of leukocyte infiltration. Leukocyte count is clinically an independent risk factor for CVD (Madjid et al., 2004) and therefore a useful predictor for the development of a diseased phenotype in our aged rats. Levels of positive CD45 cells (as detected by DAB (brown) staining) increased significantly in aged LV sections (Figure 4.9) and aortic sections (Figure 4.10) indicating increased inflammatory leukocyte infiltration. This mirrors what has already been reported in models of CVD (Sin et al., 2015) suggesting the onset of disease in the aged rats. This result also correlates with the increased levels of TNF-α shown above, as TNF-α is an early mediator involved in the recruitment of leukocytes during inflammatory reactions (Morley & Baumgarter, 2004).

Overall, the combined findings from Figures 4.8, 4.9 and 4.10 suggest a chronic pro-inflammatory phenotype is evident in the ageing cardiovascular system. This, coupled with altered function of both the heart and aorta during ageing (as indicated by the *in vivo* studies), suggests a general pathological state is adopted as we age, independent of other risk factors for onset of CVD. The next section of this chapter will specifically investigate the endothelium of the vasculature by assessing its dysfunction and altered phenotype during ageing.
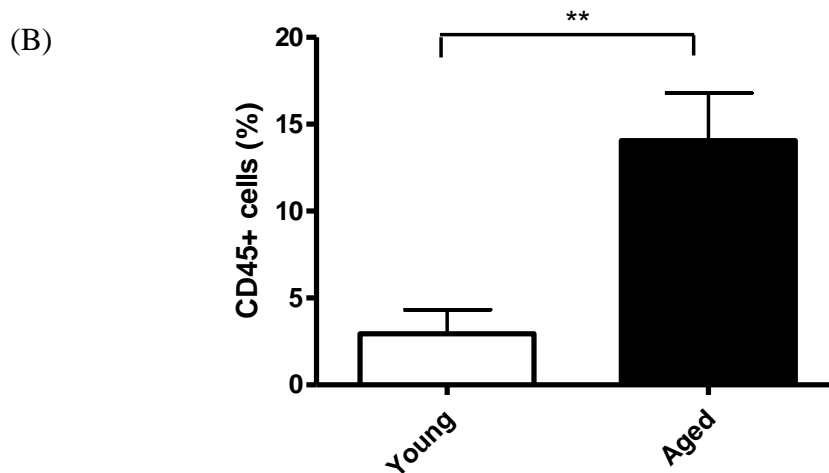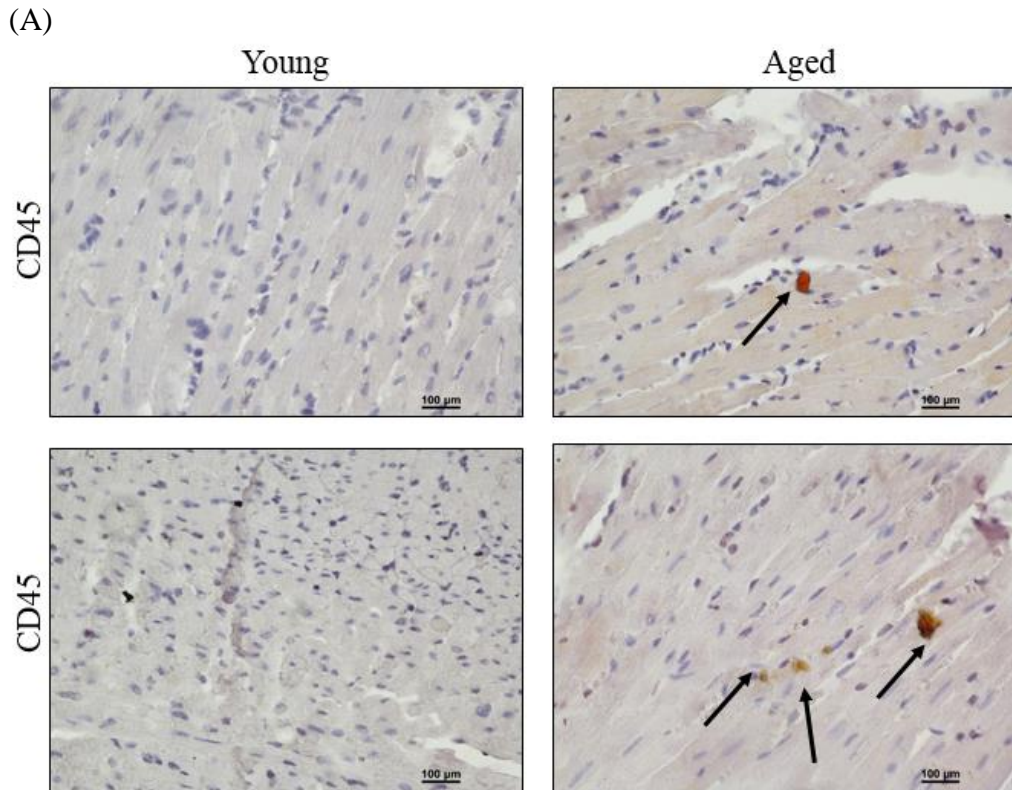
Figure 4.9 Immunohistochemistry for CD45 positive staining in young and aged LV heart sections. Typical images of LV sections showing expression of common lymphocyte antigen CD45 in young and aged samples as detected by DAB (brown) staining (indicated by arrows). Scale bar = 100µm (A). Quantification was performed showing % of CD45 positive cells and data analysed using a student's unpaired t test; n=6 for both groups, p<0.01** (B).
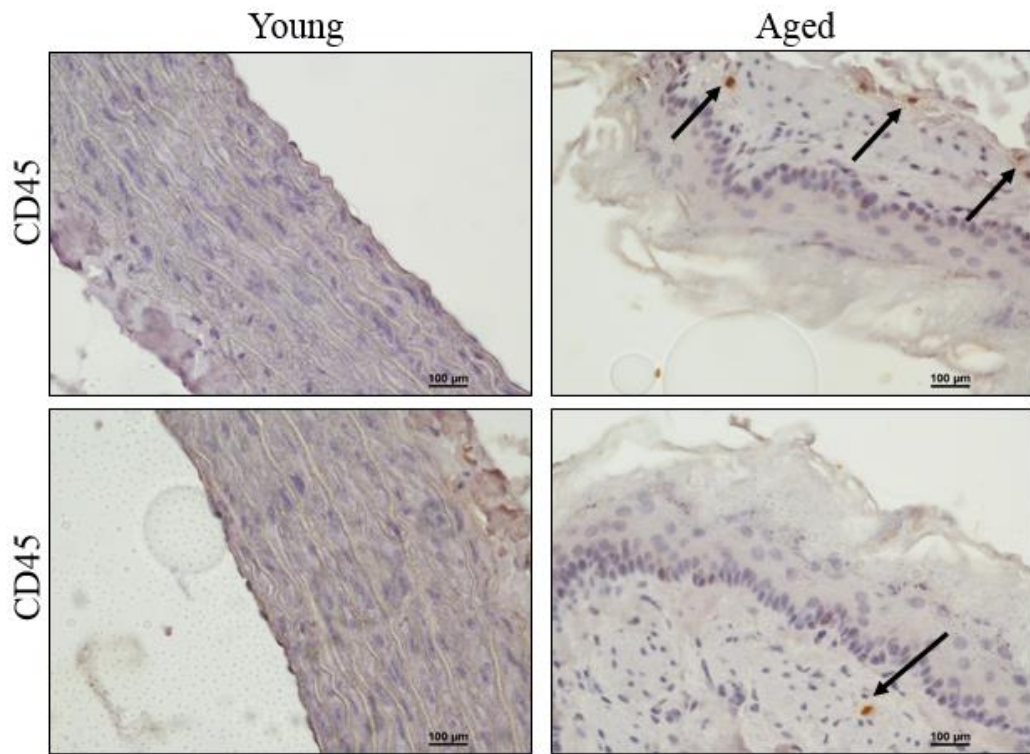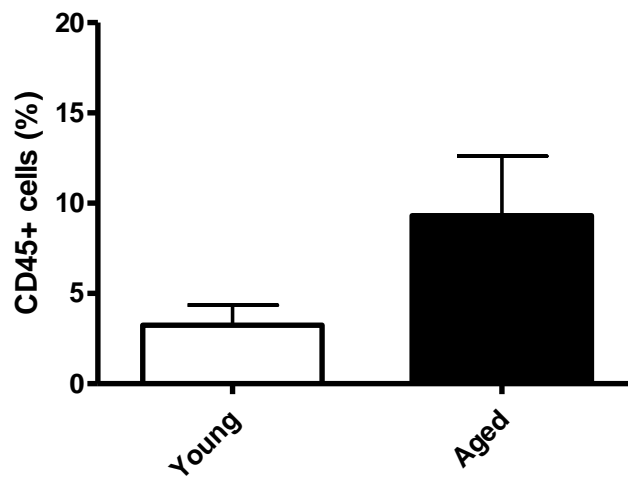
Figure 4.10 Immunohistochemistry for CD45 positive staining in young and aged aorta sections. Typical images of aortic sections showing expression of common lymphocyte antigen CD45 in young and aged samples as detected by DAB (brown) staining (indicated by arrows). Scale bar = 100µm (A). Quantification was performed showing % of CD45 positive cells and data analysed using a student's unpaired t test; n=6 for both groups, p<0.05**; where no * is shown, p>0.05 (B).

4.6 Assessment of an altered phenotype in aged aortic endothelial cells

Another key objective of this chapter was to establish if modifications also exist at the cellular level, specifically the endothelium of the vasculature, given the overall hypothesis of this work is that targeting the CaMKII-NF-κB interaction in ECs of the ageing vasculature may serve some therapeutic potential for diminishing age-associated inflammation. As mentioned previously, ageing is associated with ED where a chronically 'activated' phenotype is adopted, causing expression of inflammatory mediators, oxidative modifications and cell permeability all to be up-regulated (Donato et al., 2007; Esper et al., 2006). An improved understanding of the factors that may contribute to ED and ultimately vascular dysfunction is therefore crucial for preserving vascular health in ageing.

Having established that aged aortae exhibit significant changes functionally and physiologically (Sections 4.3, 4.4 and 4.5), initial experiments were performed to simply examine phenotypic differences between ECs isolated from young and aged rats and grown in culture. As can be seen in Figure 4.11 the characteristic EC shape was lost in aged cells, where they appeared significantly larger in size, more rounded and stressed. There was also the appearance of dark granules or vacuoles in the cytoplasm and around the nucleus of aged cells. Due to time constraints these were not examined in detail, therefore it is difficult to predict what they represent. It is however likely that they are associated with cell damage given the fact they are not present in the young, healthy cells. Aged cells also on average took longer to reach confluency (~14 days compared with ~10days for young, control cells) therefore it could be suggested that cell growth rate was stunted in the ECs isolated from aged animals. Overall, these findings show for the first time, that primary ECs isolated from aged animals maintain their dysfunctional phenotype in culture, similar to that observed with diseased or damaged cells exposed to stress induced senescence (Farhat et al., 2008; Jelonek et al., 2011) as previously reported.

A
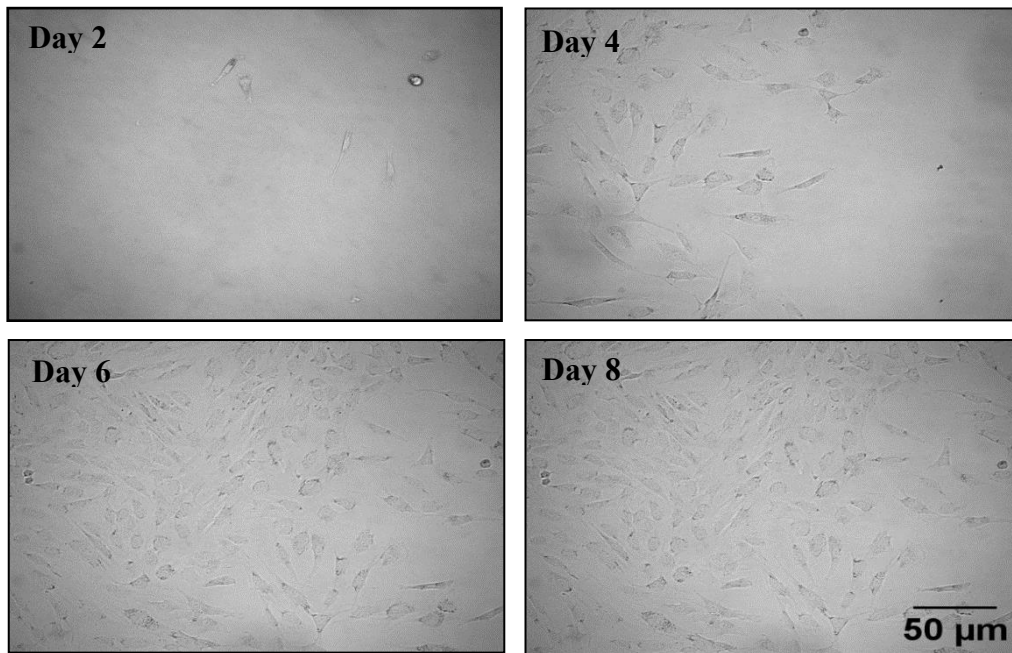
B
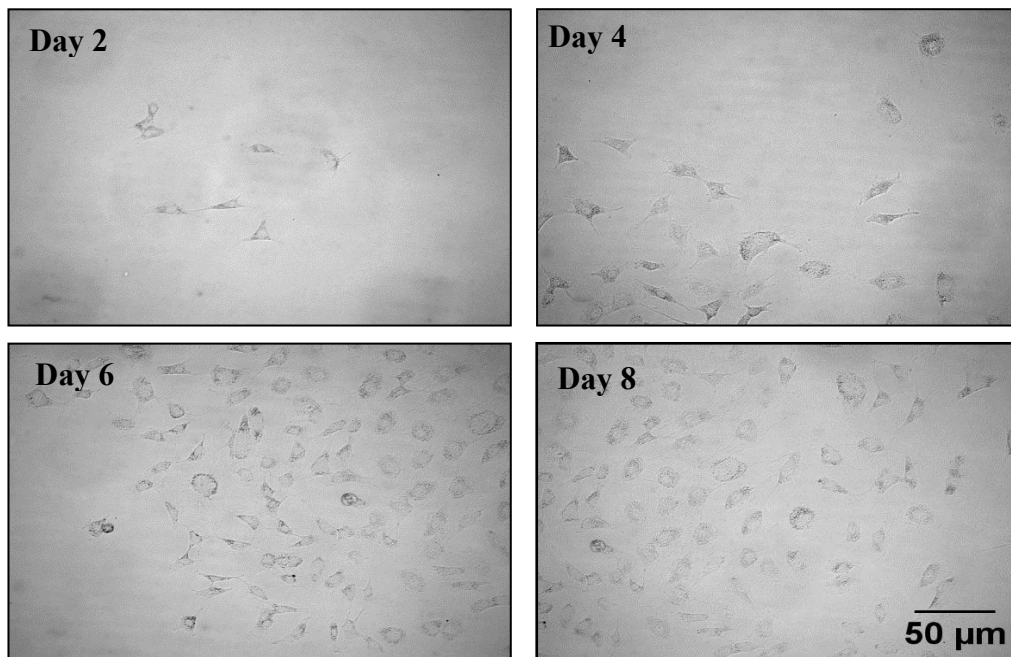
Figure 4.11 Young and aged endothelial cell growth in culture. Typical photographs of aortic endothelial cells isolated from young (A) and aged (B) rats and grown in culture for up to eight days (10x magnification) showing striking phenotypic differences. Images are representative of n=3 experiments. Scale bar = 50µm for all images.

4.6.1 Aged aortic endothelial cells show increased levels of ROS

To confirm that aged ECs were indeed stressed in culture, it was important to measure this quantitatively by assessing production of ROS by the cells. Oxidative stress is a key feature of the aged vasculature and plays a fundamental role in promoting ED due to the multifunctional capacity for ROS to induce damage (Higashi et al., 2009).

For such experiments, cell permeant DFCDA was used to assess intracellular ROS activity as outlined in Chapter 2, Section 2.8. DFCDA is converted to a highly fluorescent compound dichlorofluorescein upon oxidation and can therefore be used to quantify total intracellular ROS activity as a fluorescent signal generated in cells where ROS activity is present. As depicted in Figure 4.12 aged ECs had significantly higher levels of intracellular ROS than young cells under basal conditions (1556 ± 365 vs. 4065 ± 915 (a.u.), young vs. aged, p=0.03). To verify that the DFCDA assay could detect changes in intracellular ROS production upon stimulation of cells, both groups of cells were also treated with 10μM angiotensin II (Ang-II) for 3h. As would be expected, in response to stimulation both young and aged groups showed increased levels of intracellular ROS. Interestingly however, aged cells still produced higher levels than young cells following stimulation, correlating with what is observed under basal conditions (4856 ± 2754 vs. 8047 ± 2095 (a.u.), young vs. aged, p=0.04) and suggesting for the first time that aged primary ECs in culture maintain a stressed, pro-oxidative phenotype.
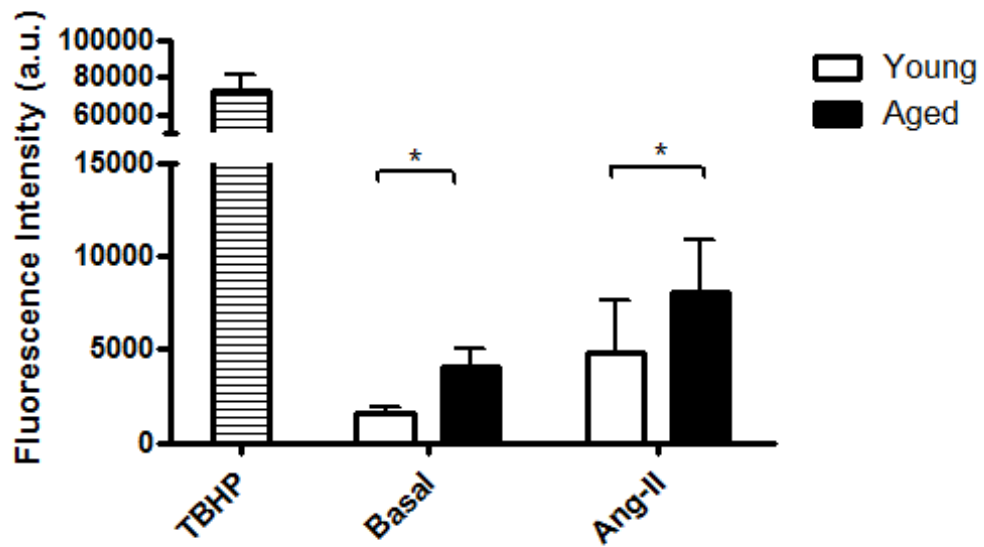
Figure 4.12 Increased ROS production by aged aortic endothelial cells. Histogram showing intracellular ROS production in young and aged endothelial cells with and without 10µM Ang-II (3h) stimulation. Young cells treated with 50µM TBHP (3h) served as a positive control for the assay. All data are expressed as mean (a.u.) ± S.E.M, n=3. Statistical analysis was performed using a two-way ANOVA and Tukey's post-test; *p<0.05.

4.6.2 Measuring cell impedance as a novel method of characterising endothelial dysfunction with ageing

The most commonly used techniques for assessing ED include *ex vivo* wire myography and *in vivo* studies, where in both cases the delivery of vasoactive agents such as acetylcholine can be used to assess endothelial dependent dilation (EDD), a key marker for evaluating healthy endothelial function (Seals et al., 2014; Schuler et al., 2014). More invasive approaches are also used routinely including coronary epicardial vasoreactivity or Flow-Mediated-Dilation (FMD), however these are often challenging and expensive to actually perform (Flammer et al., 2012). As such, the development of a simple yet effective strategy for measuring ED at the single cell level is needed.

Here, we have collaborated with the Department of Biomedical Engineering (University of Strathclyde) in an attempt to develop a novel method for assessing dysfunctional ECs in culture. For such experiments, a technique for measuring individual cell impedance has been optimised by PhD student, Ian Holland (BioMed Eng.). The system is set up such that, when a voltage is applied to cells growing on electrodes in culture, it generates an impedance profile which is dependent upon various phenotypic factors such as intracellular structures, cell-cell junction formation and membrane permeability (Lisdat & Schiffer, 2008). Any alterations in cell phenotype would consequently have an effect on impedance and thus, this platform may serve as a novel tool for characterising ED via phenotypic changes not only from aged animals, but additionally in models of disease where ED also plays a role.

4.6.2.1 Characterisation of technique in HUVECs

Initial impedance experiments were performed using the same HUVECs as in previous experiments (Chapter 3) to ensure reproducibility of EC impedance profiles could be captured. Cells were cultured on platinum coated electrodes in modified culture dishes, allowing electric currents to pass through each individual cell. Figure 4.13 illustrates a representative image of cells growing as a healthy monolayer on a single platinum coated electrode. When a voltage amplitude of 50mV was applied to the

cells, with a frequency range of 1MHz to 1.2Hz, a steady rise in impedance across all cells on all electrodes occured, as shown in Figure 4.14. This increase continued until approximately 60-70hrs following which it gradually declined as the cells became overconfluent. This result was found to be consistent across different cell culture chambers (Chambers 1&3 shown) and varies to that seen in control chambers (Chambers 2&4) where media alone is added and no increase in impedance is observed. All of the data was then collected to construct impedance profiles of the cells (Figure 4.15). This creates a 3D representation of the impedance measurements of endothelial cells. As depicted in Figure 4.15A & B, reproducibility of similar impedance profiles for HUVECs can be produced using different batches of cells and thus, suggests that similarities exist between these populations of cells in terms of phenotype and intracellular structures, as would be expected. Additional experiments were performed with smooth muscle cells (SMCs) to provide further evidence that measuring impedance is an efficient method for showing phenotypic and functional differences between cells (Figure 4.15D). These cells produced a markedly different impedance profile to HUVECs when subjected to exactly the same conditions. For SMCs impedance actually declines and then begins to increase again as the cells grow and proliferate.

Overall these preliminary findings collectively demonstrate that by measuring the impedance of cells, this can not only provide a novel method for characterising different cell types but can also distinguish between structural alterations which may occur in dysfunctional cells from the same lineage (i.e. during ageing).
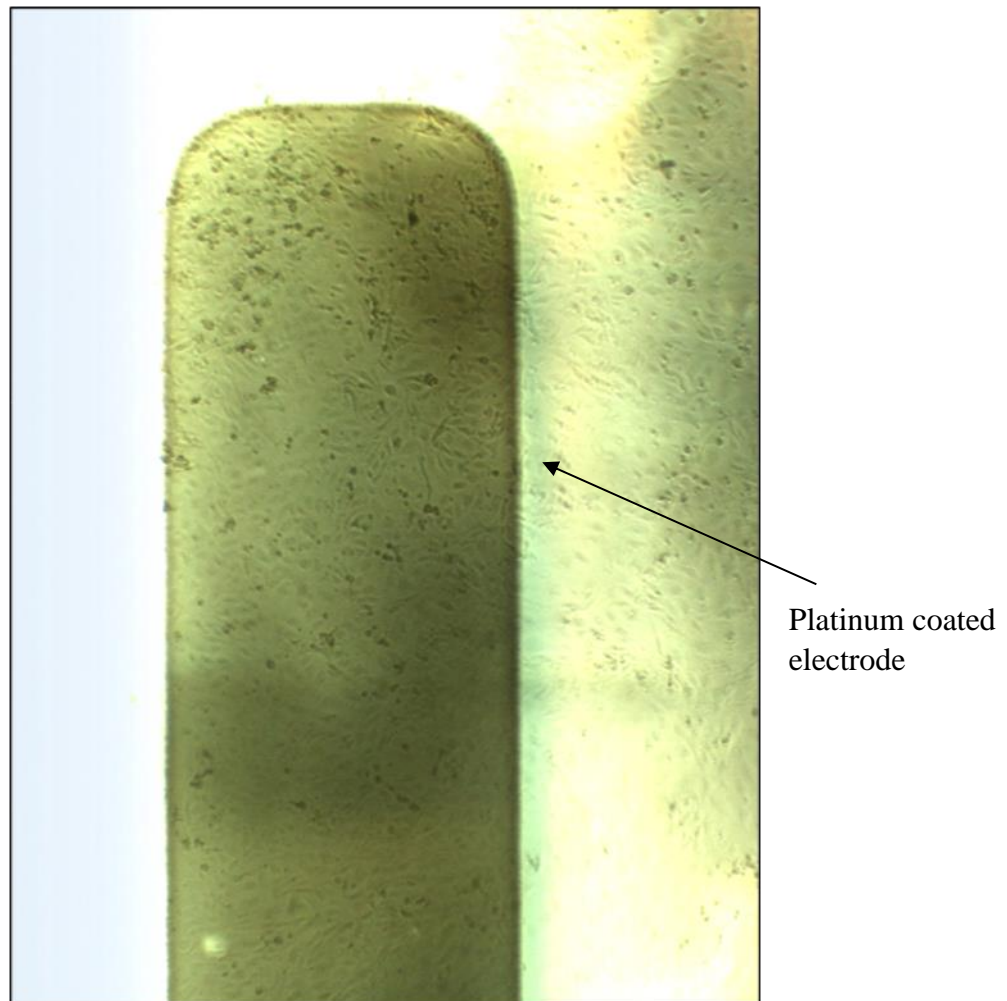
Figure 4.13 Growth of HUVECs on platinum coated electrodes for impedence experiments. Typical photograph of HUVECs grown on platinum coated electrodes for impedance experiments. Pictures were taken using a Moticam 10 microscopic camera attached to an AE31 microscope at 10x magnification. Photograph is representative of n=4.
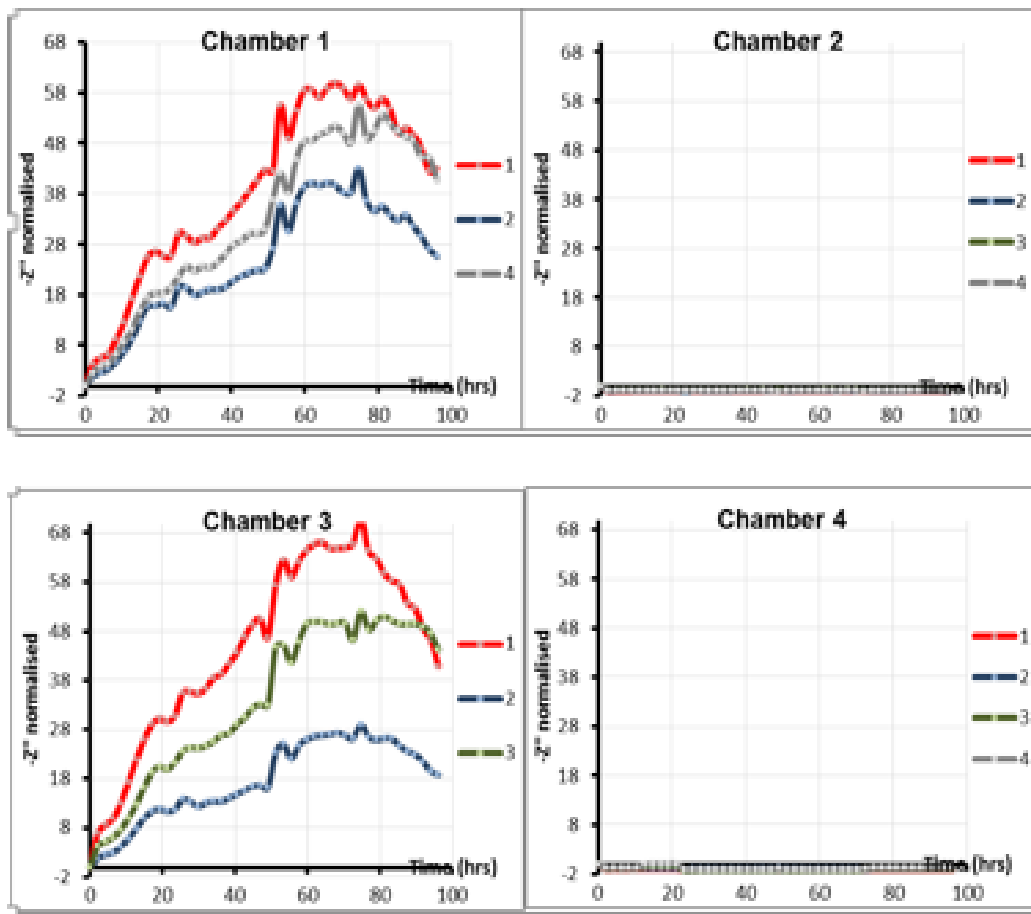
Figure 4.14: Impedence measurements in HUVECs. Cells were seeded at densities ranging from 5.5 to 10.5 x 10^4 cells/cm^2 and grown on platinum coated electrodes in chambers. Each chamber had 3 electrodes in which cells were grown to confluence (chambers 1 and 3), shown by coloured numbered lines (1-4) on graphs. Impedence sweeps of each electrode were taken at approximately 2.5h intervals. Control chambers contained media alone (chambers 2 and 4). All tests were run for 96h and for each set of experiments, 8 chambers were used: 3 control and 5 containing cells.
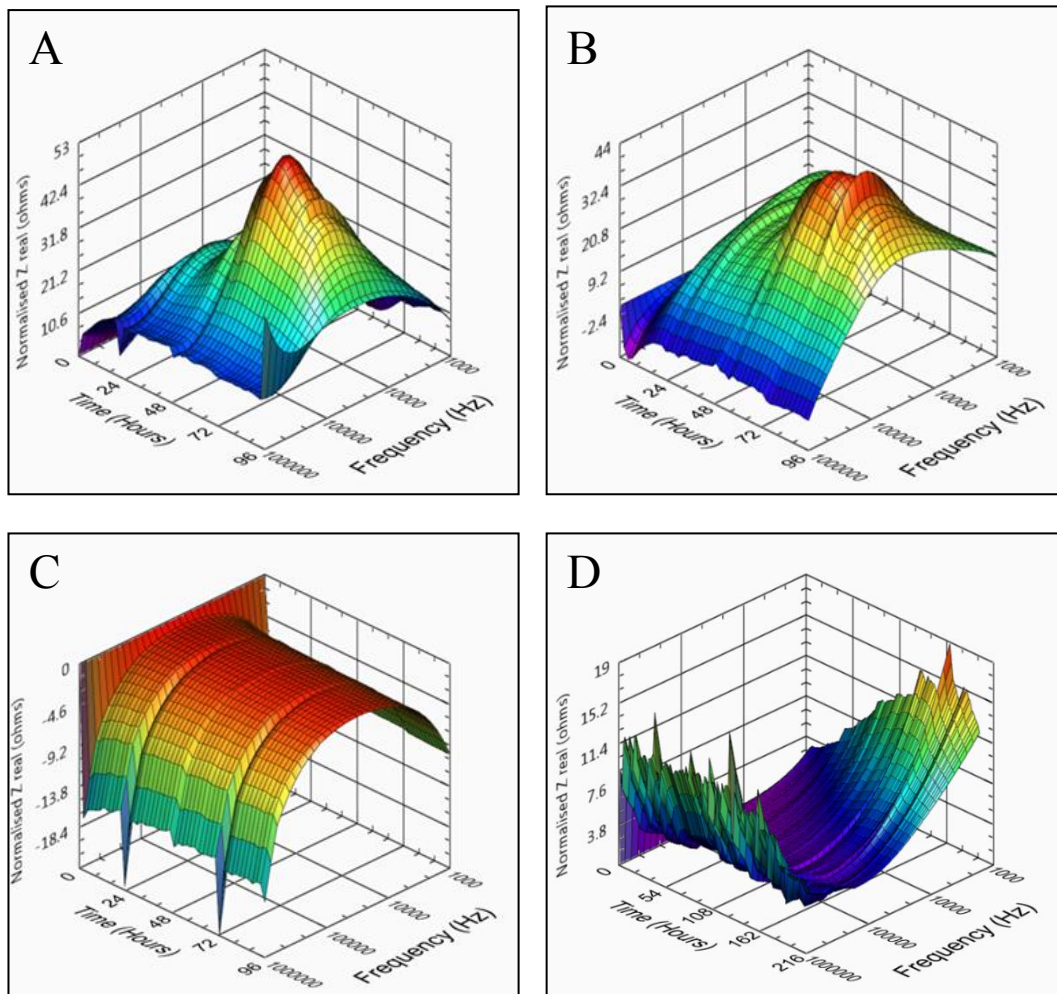
Figure 4.15: Different cell types show different impedence profiles. Impedence sweeps from all electrodes within each chamber were collated and profiles obtained over a frequency range of 1,000-1,000,000Hz. Panels A and B show impedence profiles for two separate chambers containing HUVECs. Panel C shows a typical profile for control chambers with no cells. Similar experiments were conducted with porcine smooth muscle cells (Panel D).

4.6.2.2 Optimisation of conditions for primary aortic endothelial cells

The next step was then to apply this technique to the primary aortic ECs to ensure that similar impedance profiles were obtained to that as the HUVECs. Initially, experiments were performed under exactly the same conditions as previously, with cells growing on platinum coated electrodes. Interestingly, when seeded at similar densities as the HUVECs, the primary aortic ECs showed no signs of cell growth over the measured 72h time period and also appeared to form clusters on the electrodes as depicted in Figure 4.16. This experiment was repeated 3 times and on each separate occasion, similar results were obtained. A time lapse video was recorded over the 72h to show this in more detail (attached on DVD, video 1). In an attempt to overcome this problem, similar chambers were constructed, however these contained gold coated electrodes instead of platinum as this is another commonly used material for such impedance experiments. Despite cell growth being improved on the gold coatings (as can be observed on DVD, video 2), the aortic ECs adopted an unusual phenotype under these conditions. The typical endothelial characteristic morphology was lost, with processes extending out from the cells and some appearing more elongated in shape (Figure 4.16), suggesting the cells were not healthy. This finding was further validated when cells grown on both gold and platinum electrodes were fixed and stained for pp65 to show activation of inflammatory signalling pathways (Figure 4.17). Cells grown on gold coated electrodes showed obvious signs of inflammatory activation as evident by the positive FITC (green) staining. On the other hand, only a slight green signal was detected in cells grown on platinum surfaces, however it is again clear that cell growth is halted under these conditions. This suggests that although activation of inflammatory pathways is significantly lower here than compared to the gold coatings, something about the platinum environment is having a detrimental impact on the health of the cells and therefore is not a suitable material to use for future experiments.
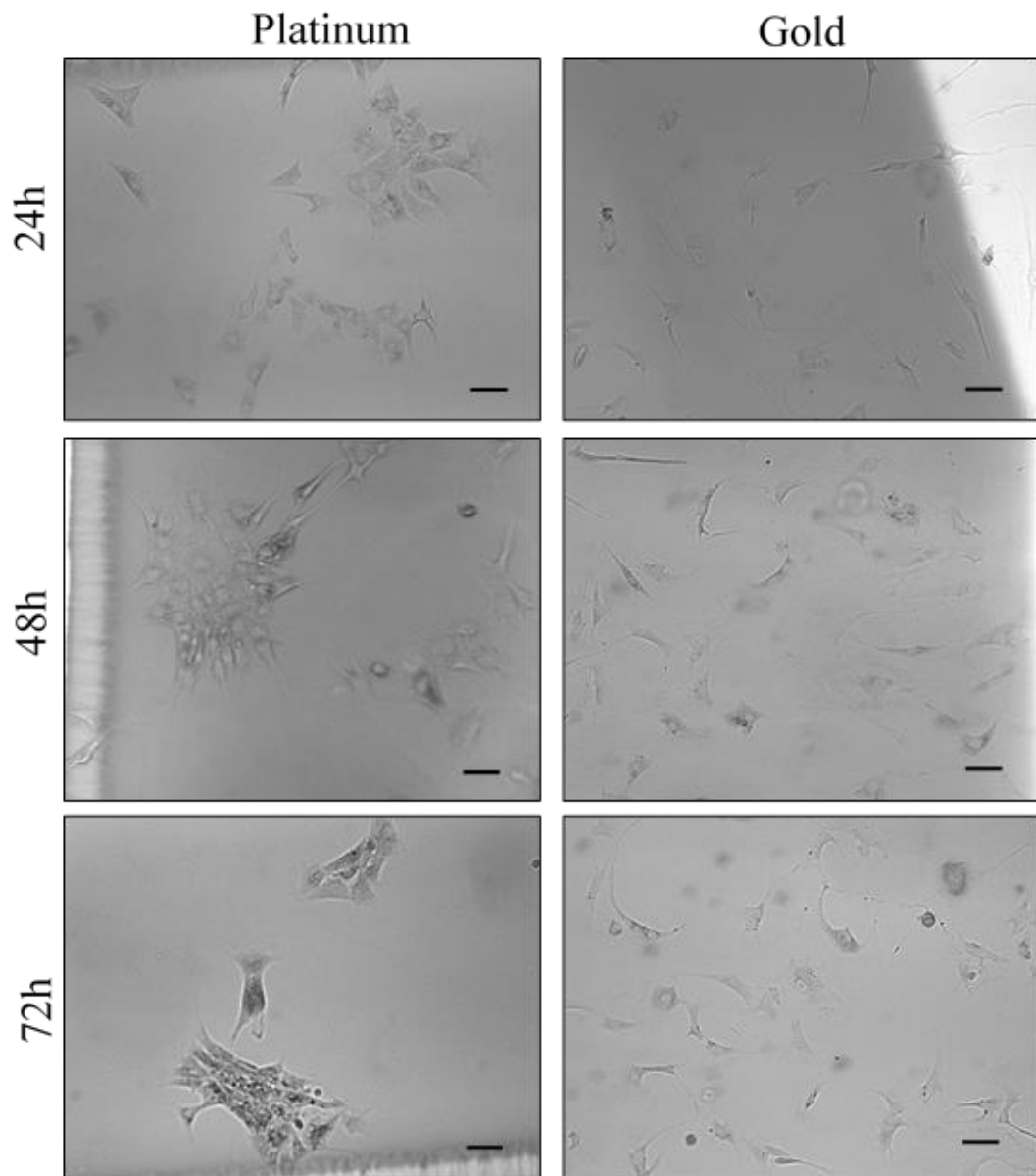
Figure 4.16 Growth of aortic endothelial cells on platinum and gold coated electrodes. Cells were seeded at densities ranging from 5.5 to 10.5 x 10^4 cels/cm^2 into chambers containing either platinum or gold electrodes and photographs taken over a period of 72h to monitor cell growth. Representative images are shown (10x magnification) depicting striking differences between cell phenotype on the two surfaces. Scale bar = 100µm for all images, typical of n=3 experiments.
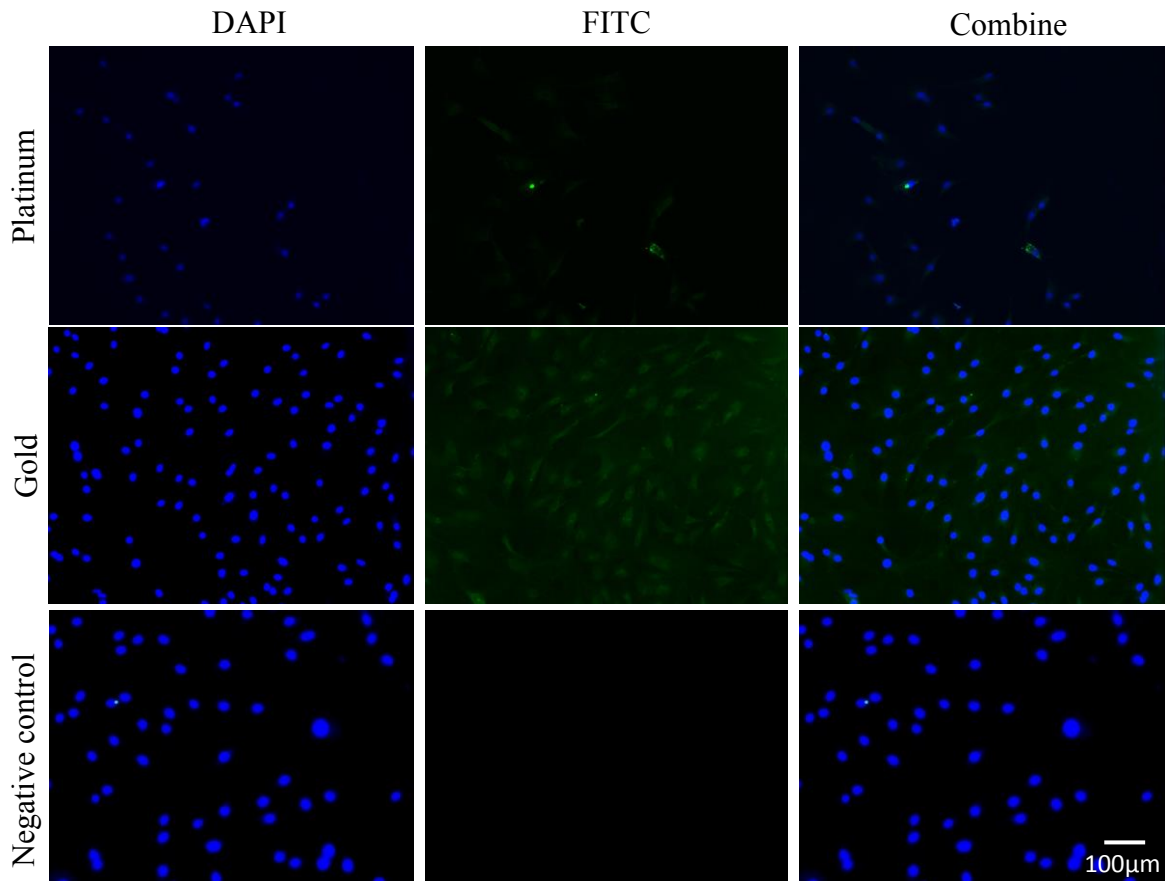
Figure 4.17 Increased inflammatory activation of aortic endothelial cells grown on platinum and gold coated electrodes. Cells were seeded at densities ranging from 5.5 to 10.5 x 10^4 cels/cm^2 into chambers containing either platinum or gold electrodes and at 72h fixed and stained with rabbit anti-pp65 to show inflammatory activation. Nuclei were conterstained with DAPI and FITC conjugated anti-rabbit secondary antibody alone was used to serve as a positive control. Images were all taken at 10x magnification, typical of n=3 experiments. Scale bar = 100µm for all images.

Overall, despite initially promising results in the HUVEC experiments and due to time constraints with the project, no further experiments were conducted to assess impedance profile differences between ECs isolated from young and aged rats. Given the findings that both commonly used surface coatings (platinum and gold) were inducing altered phenotypes in the cells isolated from young animals, further optimisation tests would be required. This does not however mean that measuring cell impedance is not a useful novel method for assessing ED in aged or even diseased cells. Logically if phenotypic and structural differences are evident in ECs isolated from aged animals (as we have already shown in Figure 4.11) then impedance should in theory be altered as a direct result. Thus, if further experiments can be performed to successfully optimise this approach, it may still serve as a simple and useful strategy as an alternative to the more commonly used methods for measuring ED.

4.7 Discussion

CVD remains as the leading cause of morbidity and mortality in the developed world, despite reductions in the prevalence over the past three decades (Roth et al., 2015). Advanced age is the primary causal factor for the development of CVD (North & Sinclair, 2012), therefore the central aim of this chapter was to investigate structural and functional alterations to both the heart and vasculature during ageing. The endothelium of the vasculature was then specifically examined in young and aged rats to assess dysfunctional alterations known to exist clinically in aged individuals.

4.7.1 Cardiac hypertrophy and dysfunction with ageing

Initial findings from echocardiography studies revealed that aged rats displayed significantly lower heart rates than that of young (Figure 4.1). This likely reflects physiological changes occurring at the level of the SA node where there may be cell loss and/or damage and is in agreement with previous studies, where it has been documented that advanced ageing is associated with alterations in pacemaker tissue, reduced responsiveness of autonomic cardiovascular reflexes and intrinsic heart rate (Kostis et al., 1981). Some studies contradict this finding however, where they report that although resting heart rate does not change with age, the maximum attainable heart rate is indeed reduced (Murray & Dodds, 2004). In addition to this, the induction of anaesthesia in aged individuals may itself cause a reduction in heart rate (Jin & Chung, 2001). This is however, usually underpinned by the fact that elderly individuals display aspects of myocardial abnormalities and dysfunction and therefore supports our conclusion that decreased cardiac function is evident in the aged group.

Further evidence of altered cardiac physiology is shown in Figures 4.3 and 4.4. Although analysis of LV measurements revealed LVEDD to be slightly higher in aged animals compared to young, which is the opposite to what has been reported in other studies investigating the aged and diseased heart (Hu et al., 2003; Nakamura et al., 2001); the degree of shortening of the LV diameter between end-diastole and end-systole is markedly lower in the aged group. This can be clearly seen when comparing the individual LVESD and LVEDD columns for each group in Figure 4.3 and was

indeed confirmed when %FS was calculated as being significantly lower in the aged animals (Figure 4.4A). This suggests that the aged hearts have developed a compensated concentric hypertrophic phenotype which was further evidenced by the significant increase in heart size, reflected as increased heart weight:body weight ratio (HW/BW) (Figure 4.4B). These findings support what has already been well reported in terms of ageing cardiac tissue and is likely a result of a compensatory physiological response to the altered stress the heart is under during ageing. To assess this in more depth, further investigations could have been performed to assess other parameters, including LV ejection fraction which is another gold standard marker for determining heart failure (Fonarow & Hsu, 2016).

4.7.2 Ageing induces aortic dysfunction

As well as cardiac dysfunction, ageing is associated with vascular dysfunction. Both structural and functional changes such as hypertrophy, extracellular matrix deposition and development of plaques, accompany vascular ageing (Seals, Jablonski & Donato, 2011); thus aortic function in young and aged animals was also assessed *in vivo*. Figures 4.5 and 4.6 show the functional changes in aortic blood flow that accompany ageing.

Stiffness of the large elastic arteries, including the aorta is a prominent feature of ageing and the gold standard clinical measurement of this aortic stiffness is an increase in PWV (Seals et al., 2014). As discussed previously, aortic PWV is the velocity at which a pulse wave generated by left ventricular contraction travels down the aorta, where the stiffer the artery, the faster the velocity (Seals et al., 2014). As depicted in Figure 4.5, traces of ascending aortic PWV appear to be substantially higher in aged animals in comparison to young, therefore suggesting some degree of stiffness has developed. Interestingly, there was no significant difference in blood flow between young and aged (Figure 4.6) however there was a substantially higher level of variation in measurements within the aged group. This suggests turbulence in flow is a factor during ageing of the vasculature and mirrors what has been reported previously, where aged individuals display increased turbulent flow patterns which can contribute to the development of atherosclerosis (Chiu & Chien, 2011).

In addition to functional alterations in the aged vasculature, the physiology of the aorta was also found to be significantly altered in aged animals. The vessels appeared to adopt a hypertrophic phenotype as medial wall thickness was significantly increased in the aged sections (Figure 4.7). This is not surprising given that numerous vascular ageing studies have also produced similar findings, reporting that the aortic wall becomes substantially thicker with advanced age, as well as the development of other structural changes becoming more evident. These include increased collagen deposition, leading to fibrosis, fragmentation of elastin filaments, calcification and formation of advanced glycation end-products (AGEs) (Seals et al., 2014). Furthermore, we show evidence that aged vessels display signs of intraluminal fat deposition (Figure 4.7E & F) which is a key feature in the development of atherosclerotic plaque formation in diseased arteries. These findings suggest overall significant adaptive changes occur in the aorta of aged animals and this may ultimately contribute to the overall development of cardiovascular dysfunction.

As mentioned previously, CVD within the aged population is a fundamental problem within the developed western world (North & Sinclair, 2012). In addition to age being a contributing factor, diet clearly also plays a role due to the fact there is such a high prevalence within areas where diet is influenced by a large amount of processed and 'fast' foods. Since all animals in this study were maintained on a similar standard chow diet however, this highlights the possibility that ageing alone is sufficient to induce such alterations in both cardiac and vascular structure and function independent of other risk factors.

4.7.3 Inflammation and ageing of the cardiovascular system

Levels of inflammatory mediators are known to typically increase with advancing age and two key cytokines which have been reported to play a role are TNF-α and IL-1β (Bruunsgaard et al., 1999; Dinarello, 2006; Tha et al., 2000). TNF-α is a multifunctional pro-inflammatory cytokine released by both cardiac and vascular cells (including ECs) in response to stress to stimulate an inflammatory response (Ranta et al., 1999; Sato et al., 2003). Both circulating and tissue levels of TNF-α have been

reported to increase during ageing (Bruunsgaard et al., 1999; Pedersen et al., 2003) and importantly, this is also apparent in numerous cardiovascular diseases such as myocardial infarction, dilated cardiomyopathy and LV pressure overload (Deswal et al., 2001; Kassiri et al., 2005; Satoh et al., 2000). Furthermore, clinical studies in aged individuals showed that blood TNF-α was significantly up-regulated during ageing and that this correlated with increased prevalence of atherosclerosis (Bruunsgaard et al., 1999). This was likely due to the fact that TNF-α stimulates the production of other pro-inflammatory, atherosclerotic associated mediators, including IL-6, C-reactive protein (CRP) and up-regulation of intracellular adhesion molecule (ICAM)-1. Thus, measuring expression of TNF-α is a useful predictor of the development of age-related pathological processes. In the present study, blood levels of TNF-α from young and aged rats were assessed by ELISA following termination. As shown in Figure 4.8A levels of circulating TNF-α appeared to be higher in blood serum from aged animals compared to young, reflecting what has been reported in previous studies. There was a marked degree of variation between individual data points which caused no significance between groups to be obtained. This is likely due to the low sample numbers for this experiment as animal studies often require larger sample sizes since variation is an important factor. However similar findings in terms of variation in blood TNF-α levels have been reported in the literature, irrespective of age (Mozes et al., 2011).

IL-1β levels were also assessed in blood serum samples from young and aged rats. IL-1β is another pro-inflammatory cytokine which is has been associated with ageing and also participates in the pathogenesis of vascular diseases such as atherosclerosis (Dinarello, 2006). The endothelium itself is a prime target for IL-1-mediated inflammation since IL-1 receptors on the surface of ECs can be triggered by systemic IL-1β, resulting in prostaglandin E production, release of neutrophils from the bone marrow and IL-6 production, all mediators associated with ageing (Daynes et al., 1993; Dinarello, 2006; Eilati et al., 2012). In spite of this, when IL-1β levels were assessed in the present study, there were no differences between young and aged (Figure 4.8B). There may have been a number of reasons for this unexpected result, including again that small n numbers is an issue, similar to the TNF-α samples. The

total number of animals examined in each group was low (n=3) and therefore may not be a true representation of what actually happens during ageing. Another important factor to consider is that blood samples were taken from the animals at one time point only. Literature has suggested that chronic inflammation associated with ageing is in fact subclinical and therefore levels of pro-inflammatory mediators are not expressed as highly as they are during disease, e.g. rheumatoid arthritis where increased inflammatory cytokines are used as biomarkers for disease progression (Selaas et al., 2015). Thus, it may have been difficult to know exactly when to take blood samples from the animals in terms of capturing when levels of IL-1β would have been at their highest given the transient nature of cytokine production and release. Interestingly, it has also been reported that even in patients with certain diseases such as sepsis, circulating levels of IL-1β can remain extremely low (Cannon et al., 1993; Yentis, Rowbottom & Riches, 1995). Furthermore, contradictory evidence exists in the literature with some studies reporting increased IL-1β while others show no change or in fact a decrease in levels during ageing (Roubenoff et al., 1998). It may therefore be beneficial to assess other markers for inflammation to give a true representation of what occurs during the ageing process. As already discussed, IL-6 has been shown to be up-regulated systemically during ageing, even in the absence of any disease (Maggio et al., 2006). IL-6 also plays an important role in pathogenesis associated with cardiovascular conditions (Kanda & Takahashi, 2004; Song et al., 2010), therefore it would be useful to assess this in our aged rats. In addition, CRP could also be assessed given the strong evidence for its role in ageing of the CVS (Assuncao et al., 2012) and monocyte chemoattractant protein (MCP)-1 which has additionally been shown to increase substantially in aged rat aortic tissues (Spinetti et al., 2004).

In order to examine whether inflammation was present specifically within the cardiovascular tissues, expression of leukocyte common antigen (CD45) was assessed in both cardiac and aortic tissue sections. The CD45 antigen is expressed on almost all hematopoietic immune cells and is therefore a useful marker for leukocyte infiltration and thus, inflammation in tissues. As mentioned previously, leukocyte count is clinically an independent risk factor for CVD (Madjid et al., 2004) and therefore a useful predictor for the development of a diseased phenotype during ageing. As shown

in Figures 4.9 and 4.10, positive staining for CD45 was obtained in aged tissue sections compared to young. The level of brown DAB staining appears to be relatively low, however literature also shows this low-level positive staining even in models of CVD (Esaki et al., 2008). Furthermore, there was virtually no brown staining in young tissues even though total cell count (shown by haematoxylin staining) was markedly higher here (demonstrated when quantification was performed). This strongly suggests increased inflammatory cell migration into cardiovascular tissues during ageing, as expected. A recent study also provided evidence that specific immune cell populations are increased in aged myocardial tissues, including $CD4^+$ T lymphocytes (Ramos et al., 2017). They showed that aged mice had accumulated levels of activated $CD4^+$ T cells in heart draining lymph nodes and therefore concluded that with ageing, spontaneous immune responses directed against the heart arise even in the absence of previous myocardial damage. It may therefore have been useful to also assess this in our aged rat models as an additional marker for enhanced activation of inflammatory activation. Furthermore, expression of cell adhesion molecules (CAMs) themselves on aged aortic tissues could be assessed in future work. There is now an abundance of evidence suggesting that both ICAM-1 and VCAM-1 are significantly up-regulated in expression during ageing of the vasculature and in disease models (Scioli et al., 2014; Tousoulis et al., 2006). This makes sense given the increased inflammatory cell migration which has also been reported with ageing and overall, supports the theory that chronic inflammation contributes to cardiovascular dysfunction associated with advanced age.

4.7.4 Endothelial dysfunction with ageing

Once dysfunction and altered phenotype had been established at the level of the vasculature, the next key objective of this chapter was to assess this specifically in the endothelium itself. As previously discussed in Chapter 1, damage to the endothelium during ageing contributes to the overall chronic inflammatory phenotype associated with advanced age, given that it enhances endothelial permeability and leukocyte adhesion.

To date, only very few of studies have used isolated ECs from young and aged patients to assess differences with ageing (Donato et al., 2007; Williamson et al., 2013). In spite of this, nothing has been reported about basic phenotypic differences between ECs isolated from young and aged subjects in culture. In the present study, we show for the first time that cells from aged rats display striking phenotypic alterations, where the characteristic 'cobblestone' morphology is lost and cells appear significantly enlarged and stressed looking compared to young ECs (Figure 4.11). This is relatively similar to what has been observed previously in ECs isolated from atherosclerotic chronic smokers (Farhat et al., 2008) however this was not shown by brightfield imaging as the data presented in the current study is. Cell growth rate also appeared to be slower in the EC cultures from aged aortae. This was only assessed by measuring the time taken to reach confluency following initial isolation however and therefore it would have been useful to analyse this more quantitatively by for example performing cell proliferation assays.

In addition to displaying visual signs of stress, ECs isolated from both young and aged rats were subjected to assays to detect production of intracellular ROS – a useful marker of a stressed environment. Increased oxidative stress impairs endothelial function and there is now a plethora of evidence supporting a role for ROS contributing to vascular diseases associated with ageing (Donato et al., 2007; Ungvari et al., 2011). As can be seen from Figure 4.12, upon stimulation with Ang-II, aged cells produced significantly higher levels of ROS than young. Ang-II was selected as a suitable agonist for such experiments given that it is a pro-hypertensive factor well-known for inducing ROS production in vascular cells (Harvey et al., 2015). This suggests that an enhanced capacity for ROS production exists in ECs isolated from aged animals, and that theory was confirmed when a significant increase in basal levels of ROS was detected in the aged group (Figure 4.12). Previous studies support this finding, where other markers of increased oxidative stress have been reported in aged cells. An abundance of nitrotyrosine – a modified amino acid marker of oxidative stress – was reported to be significantly higher in ECs obtained from brachial arteries of aged men compared to young (Donato et al., 2007). In addition to this, EC expression of the oxidant enzyme NAD(P)H oxidase-p47^{phox}, primarily involved in

superoxide production, was also enhanced in aged individuals (Li et al., 2002; Donato et al., 2007). These findings, combined with our own, support the free radical theory of ageing (as outlined in Chapter 1), where endothelial oxidative stress develops significantly with ageing. There is now a considerable amount of evidence published that in addition to the NAD(P)H oxidase system serving as a key source of ROS production; mitochondrial production of ROS plays a fundamental role in the overexpression of ROS with ageing, particularly in both the heart and vasculature (Judge et al., 2005; Ungvari et al., 2007). As a future extension of the work performed here it would be of interest to assess mitochondrial production of ROS in ECs derived from the aged rats and compare with young counterparts. Techniques have now been developed to routinely isolate mitochondria from tissues and cells and with specific relevance to this work, mitochondria have been isolated from ECs (Koziel et al., 2015). Thus, measuring the rates of mitochondrial ROS emissions between young and aged ECs could allow us to distinguish specifically the source of enhanced ROS production.

4.7.4.1 Developing a novel approach for assessing endothelial dysfunction with ageing

As mentioned in Section 4.6.2, the development of vascular ED is primarily indicated in the clinic by reduced peripheral artery EDD. It is the reduced bioavailability of the endothelial-derived dilating molecule nitric oxide (NO) (as a result of oxidative stress) that is primarily responsible for the increased ED associated with advanced age. Thus, measuring each of these parameters are typically useful methods for evaluating endothelial function and dysfunction in the clinic. In humans, EDD is assessed by two primary methods: (i) the brachial flow-mediated dilation (FMD) model and (ii) the forearm blood flow model (Seals, Jablonski & Donato, 2011). Each method comes with its own advantages and disadvantages as discussed below:

The brachial FMD model involves a non-invasive approach using ultrasound analysis of the brachial artery. It is therefore much safer than more invasive techniques and blood flow itself is a physiological stimulus for vasodilation therefore there is no need for agonist infusion. In spite of this, resolution of images can be poor relative to arterial size and variability in measurements is a common issue given that it is highly operator-

dependent (Widlansky et al., 2003). The forearm blood flow model, also known as venous occlusion plethysmography is another straightforward technique in which the rate of swelling of the forearm during venous occlusion is used to assess the rate of arterial inflow. Usually, local infusion of agonists or antagonists into the brachial artery allows assessment of vascular tone between healthy control subjects and patient populations (Benjamin et al., 1995). Furthermore, it allows for examination of basal endothelial function (with NOS antagonist infusion) between groups therefore is a good method for assessing the presence or absence of ED (Widlansky et al., 2003). The main disadvantage of this technique however is that it is invasive and therefore there is a risk of median nerve injury, infection and vascular injury. It is also important to note that with either of these methods, they are not feasible to perform on small animal models. In addition to this, neither of these methods allow for assessing ED at the single cellular level. In an attempt to identify an alternative approach for assessing ED, we have set up a collaboration with our Biomedical Engineering department to examine alterations in cell impedance that could directly reflect alterations in cell phenotype.

These types of assays were first introduced in the 1980s, however only in recent years has this method found increasing application (McGuinness, 2007). As described previously, when a voltage is applied to cells growing on electrodes in culture, it generates an impedance profile which is dependent upon various phenotypic factors such as intracellular structures, organelles, cell-cell junction formation and membrane permeability (Lisdat & Schiffer, 2008). Any modifications to these factors would consequently have an effect on impedance and thus, this may serve as a novel tool for characterising dysfunctional ECs as opposed to the traditional methods listed above. The aged endothelium has been reported to exert numerous physiological modifications including increased 'leakage' or permeability to infiltrating immune cells. Furthermore, following cellular senescene (a model for ageing) dysfunction of cell-cell junctions has also been observed in human ECs (Krouwer et al., 2012). Taking all of this into account, one would expect this novel approach presented here to show such differences between young and aged ECs.

To date, preliminary experiments have been performed in HUVECs and reproducibility of EC impedance profiles were successfully obtained (Figure 4.15). In addition to this, when similar studies were performed in SMCs, a completely different profile was recorded but was consistent between different SMC populations (Figure 4.11). This suggests that different cell types display different impedance profiles given their structural and functional dissimilarities which is line with what previous studies have reported (Reiss & Wegener, 2015; Sun, Green & Morgan, 2008). When such experiments were performed in primary ECs isolated from young rats however, issues arose with the growth of cells on the platinum coated electrodes (Figure 4.16). Platinum was chosen as the material of choice as it is highly biocompatible, biorobust and highly conductive (Geninatti et al., 2015). It is also commonly used on the surface of medical stents, which was another area that our Biomedical Engineering department were interested in, therefore it was compatible for both projects. No such issues were reported with their preliminary stent work using EC lines and primary SMCs. Additionally, there appears to be no evidence in the literature suggesting ECs do not grow well on platinum surfaces. We performed further investigations with cells grown on gold electrodes instead (Figure 4.16) however, analysis of these findings showed cells exerting altered phenotypes on these surfaces as well as showing an increased inflammatory profile (Figure 4.17). Gold is another common surface material used in impedance analysis of EC monolayers (Wegener et al., 1996) where no issues have been reported in terms of cell growth. However, research has shown that in clinical studies there is increased risk of restenosis and reduced revascularisation after placement of gold-coated stents in patients (Kastrati et al., 2000). While this may be due in part to the endovascular procedure of inserting the stent itself; the evidence presented here that ECs grown on the gold surface show signs of increased inflammatory activation may also provide some reasoning as to why gold is not a suitable surface for stents and may contribute to the detrimental physiological response associated with restenosis. In spite of this, simple factors such as low n numbers and also the fact that primary cells, which are generally more fragile than cell lines, are being used for such experiments, may also explain why the initial optimisation experiments could not be concluded from this study. It may be useful for future experiments to be performed using higher initial seeding densities of cells on

platinum coated electrodes. ECs grown under these conditions still maintained their characteristic phenotpye despite slow growth rate and clustering, therefore starting at higher densities may overcome this.

4.8 Conclusions

The overall findings from this chapter have shown that advanced ageing is accompanied by increased cardiac and aortic dysfunction, as assessed in a rat model of ageing *in vivo*. This correlates with physiological alterations to cardiovascular tissues and an increased inflammatory profile, in line with what has previously been reported in the literature. Furthermore, endothelial dysfunction is apparent in aged animals as shown by altered phenotype of ECs following isolation and enhanced ROS production.

In the next results chapter, findings from the aged rat model presented here will be built upon to specifically investigate potential modifications in CaMKIIδ and NF-κB signalling during ageing of the CVS . Given what is already well established in models of cardiac disease in tems of altered CaMKII and NF-κB signalling pathways, and since we have already demonstrated the potential for CaMKII modulation of the NF-κB pathway in Chapter 3; it will be of interest to examine whether similar alterations also exist with ageing, where a dysfunctional phenotype is evident.

Chapter 5: Alterations in CaMKII and NF-κB signalling with ageing

5.1 Introduction

Having previously established that CaMKIIδ modulates NF-κB signalling in rat aortic ECs (Chapter 3), the final aim of this project was to explore whether both signalling systems were altered during ageing. Given the potential for interaction/modulation between pathways, alterations in aged vasculature could affect this relationship with subsequent implications for any potential intervention strategies. In CVD models, both CaMKIIδ and NF-κB activity have been shown to be up-regulated in cardiac cells and tissues (Kirchhefer et al., 1999; Sossalla et al., 2010) however whether this occurs during ageing remains unknown, nor do we appreciate whether any changes occur at the level of the vasculature.

As discussed in detail in Chapter 1, a plethora of evidence now supports a role for elevated CaMKIIδ signalling in the failing or diseased heart. Studies have shown that increased expression of CaMKIIδ correlates with increased incidence of cardiac hypertrophy (Singh & Anderson, 2011) and that animal models of myocardial infarction (MI) also show associated increased activity of CaMKIIδ (Erickson et al., 2008; McKinsey, 2007). This has also been shown using transgenic overexpression of CaMKIIδ which causes the development of myocardial pathological alterations and increased incidence of MI in mice (Maier et al., 2003; Zhang et al., 2002). Crucially, inhibition of CaMKII significantly improves myocardial contractility in failing human hearts (Sossalla et al., 2010). This list is not exhaustive and provides strong evidence that up-regulated CaMKIIδ expression and activity plays a detrimental role in myocardial diseases. In spite of this, there is limited information to date on whether CaMKIIδ may modulate impaired cardiac function that accompanies the ageing process. As previously discussed, ageing is the greatest risk factor for the development of CVD and research has shown that advanced age does indeed correlate with the development of cardiac hypertrophy and onset of heart failure (Dai et al., 2012). Thus, the likelihood that CaMKIIδ expression and activity are also enhanced in the aged heart is extremely probable, yet previously unreported. Importantly, since it is now recognised that CaMKII can be activated by a number of routes, including via oxidation of Met281/282, and since oxidative stress is a key feature of ageing, it seems

likely that CaMKII may play a role during ageing of the heart via up-regulated activation by ROS.

In spite of the extensive research conducted to investigate the role of CaMKIIδ in myocardial dysfunction and disease, nothing is known about the role of CaMKII in dysfunctional vasculature. As shown in the previous chapter of this thesis, and in line with what others have reported, cardiovascular ageing is a complex process involving not only changes to the heart muscle but also significant adaptations to the vasculature, some of which appear similar to what would be observed during disease progression. Thus, it seems plausible that CaMKIIδ may play a role in ageing of the vascular system, similar to what we observe in disease. Indeed, since we have shown CaMKIIδ is highly expressed within the endothelium of the aorta (Chapter 3, Figure 3.8) a role in the ED associated with ageing seems possible, especially since ROS play such an important role in mediating ED and could lead to increased levels of oxidised CaMKII. Additionally, and as highlighted in Chapter 3, CaMKII can contribute to the inflammation associated with CV disease likely via its ability to modulate pro-inflammatory NF-κB signalling (Singh & Anderson, 2011) in cardiomyocytes and CFs (Frantz et al., 2009; Martin, 2011; Singh et al., 2009). Crucially, we have presented novel evidence of how CaMKII regulates this NF-κB signalling (specifically via IKKβ interaction) within the endothelium in Chapter 3. It will be important to understand how this relationship may be affected under pathological conditions such as the ED associated with ageing. In order to understand more about the relationship, we first need to ascertain whether either or both of these signalling networks are altered in expression and/or activation within the endothelium of aged animals.

The overall aims of this final chapter were to assess whether total CaMKII expression and activation (by phosphorylation and oxidation) are altered in both hearts and aortae from aged animals in line with what we would anticipate to occur in pathophysiological conditions. Assessment of expression was performed by quantitative immunoblotting for CaMKIIδ. In order to assess activation of CaMKII, phosphoThr286/7 (p)-CaMKII and ox-CaMKII were measured in tissue samples along with the use of kinase assays to strengthen the significance of the overall data. Specific focus was then placed on aortic ECs isolated from young and aged animals. It was

important to determine whether the vascular dysfunction and in particular the EC dysfunction and phenotypic abnormalities reported in Chapter 4, correlated with altered CaMKIIδ expression and activation. Finally, given that we previously observed a functional role for CaMKII in terms of modulating NF-κB signalling in ECs (Chapter 3), it was also of interest to examine if activation of this pathway was altered during ageing. This was assessed by measuring phospho-p65 nuclear translocation and comparing with that of young cells to study any differences in pro-inflammatory signalling, similar to that reported in diseased cardiac cells (Maier et al., 2012; Martin, 2011).

5.2 Altered CaMKIIδ expression and activity in aged cardiac and aortic preparations

Whole cardiac ventricular and aortic homogenates obtained post-mortem from both young and aged animals were analysed for expression of total CaMKIIδ protein expression by immunoblotting, using a custom-made antibody against the C terminus of the enzyme, as described in Chapter 2, Section 2.12. As shown in Figure 5.1A, quantitative immunoblotting using densitometry analysis demonstrated that CaMKIIδ expression was significantly increased in aged hearts ((CaMKIIδ:GAPDH) 1.03 ± 0.04 vs. 1.71 ± 0.26, young vs. aged, p=0.03). This is similar to what has been reported in diseased hearts (Currie & Smith, 1999; Martin et al., 2014) and suggests that ageing alone triggers alterations in CaMKIIδ which may in turn, contribute to disease progression associated with ageing of the heart. When aortic tissue preparations were examined, only a slight increase in expression of CaMKIIδ was observed in aged animals (1.03 ± 0.07 vs. 1.26 ± 0.1, young vs. aged, p=0.09) (Figure 5.1B). However, upon examining each of the δ variants (individual bands) shown in the blot, it appears there is a greater increase in certain variants over others in the aged aorta. This was apparent across several of the experiments (n=7) and may suggest certain variants play more of a role than others during ageing of the vasculature.

Assessment of the activation of CaMKII in cardiac and aortic homogenates was measured by quantifying expression of autophosphorylated CaMKII, using a site-specific antibody generated against the phospho-Thr 286/287 site. Immunoblotting revealed a significant increase in the phosphorylation of CaMKII in both aged hearts and aortae when compared to young (Figure 5.2) ((pCaMKII:GAPDH) 0.85 ± 0.09 vs. 1.19 ± 0.12, young vs. aged (heart), p=0.04 and 1.16 ± 0.13 vs. 1.82 ± 0.2, young vs. aged (aorta), p=0.04). Interestingly, visual examination of individual blots revealed very striking differences in expression of p-CaMKII between young and aged aortae (Figure 5.2B) suggesting activation of CaMKII by autophosphorylation may play a fundamental role in ageing of the vasculature. Overall, these combined findings suggest that CaMKII activity is up-regulated during ageing in both the heart and vasculature; two key observations which have previously never been reported in the literature.
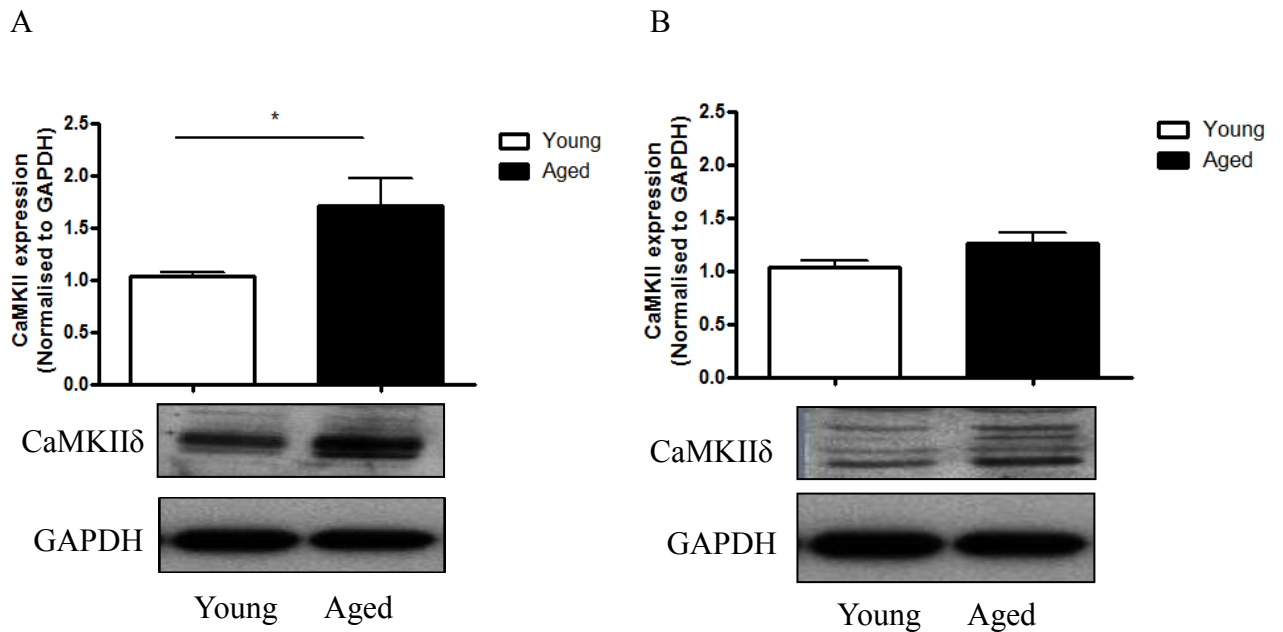
Figure 5.1: Expression of total CaMKIIδ in young and aged cardiac and aortic homogenates. Immunoblot analysis of total CaMKIIδ expression in young and aged whole heart (5µg total protein) (A) and aortic (10µg total protein) (B) homogenates. Representative immunoblots are shown of each in addition to expression of the loading control GAPDH. Densitometry analysis was performed and data normalised to GAPDH. Mean normalised data are shown ± S.E.M. Statistical analysis was performed using a student's unpaired t test; p<0.05*; n=7 for each group.
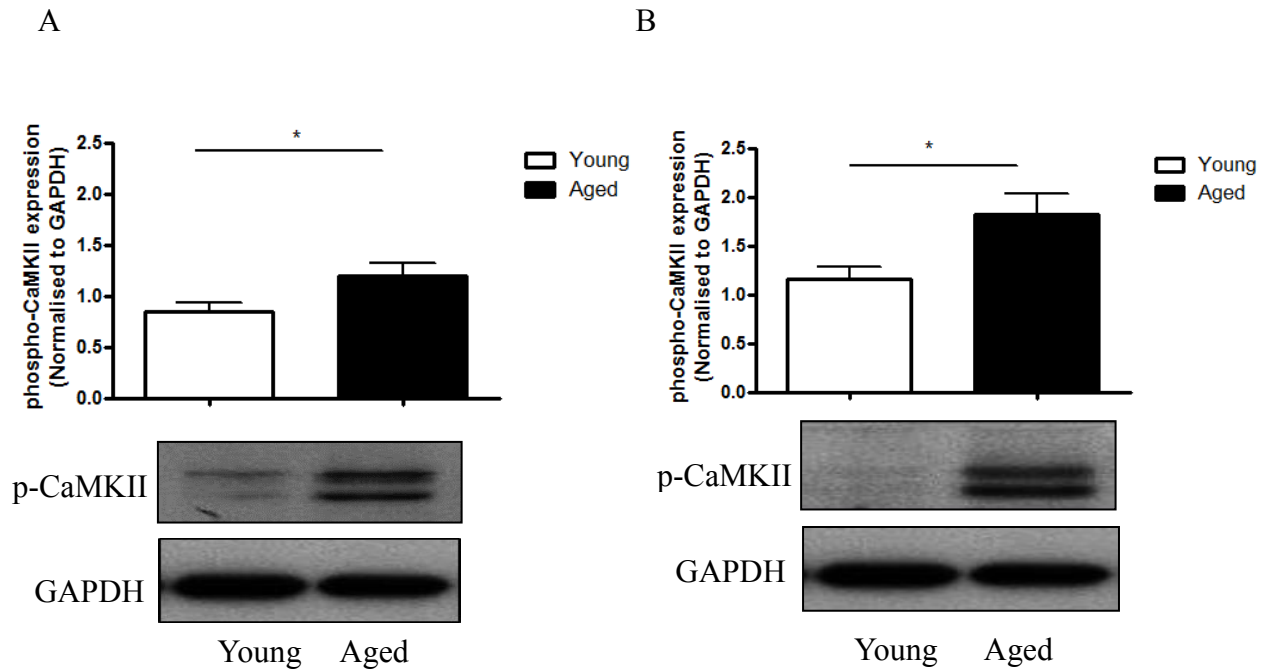
Figure 5.2: Increased activation of CaMKII by autophosphorylation in aged cardiac and ventricular homogenates. Immunoblot analysis of phosphoThr286/7 (p)-CaMKII expression in young and aged whole heart (5µg total protein) (A) and aortic (10µg total protein) (B) homogenates. Representative immunoblots are shown of each in addition to expression of the loading control GAPDH. Densitometry analysis was performed and data normalised to GAPDH. Mean normalised data are shown ± S.E.M. Statistical analysis was performed using a student's unpaired t test; p<0.05*; n=7 for each group.

Further analysis of the activation state of CaMKII was performed using a radioactive kinase assay. Cardiac and aortic homogenates were measured for total protein content and 10μg of homogenate preparation was used as a source of CaMKII to measure the incorporation of [^{32}P]ATP into autocamtide II (a CaMKII peptide substrate) in the presence of PKA and PKC inhibition, as described in detail in Chapter 2, Section 2.13. Each experiment used recombinant (R) CaMKII (50ng) as a positive control alongside samples containing no enzyme source as a negative control. As shown in Figure 5.3A, samples containing RCaMKII showed significantly higher levels of CaMKII activity to all other groups as would be expected ((pmol PO$_4^-$inc/min) 131.5 ± 3 (RCaMKII), 5.95 ± 1.9 (young aortae), 8.21 ± 1.4 (aged aortae), 4.9 ± 0.4 (young hearts), 4.8 ± 0.16 (aged hearts), 2.31 ± 0.56 (control no enzyme) p=0.0008). When aortic tissues were assessed only, it was shown that there was increased CaMKII activity associated with aortic homogenates from aged animals when compared with control (Figure 5.3B) ((pmol PO$_4^-$inc/min) 2.31 ± 0.56 (control no enzyme), 5.95 ± 1.9 (young), 8.21 ± 1.4 (aged), p=0.03). There were no significant differences in CaMKII activity between control and young aortic homogenates ((pmol PO$_4^-$inc/min) 2.31 ± 0.56 (control no enzyme), 5.95 ± 1.9 (young) p=0.05). Thus, despite no significant differences being reported between young and aged aortic homogenates ((pmol PO$_4^-$inc/min) 5.95 ± 1.9 (young), 8.21 ± 1.4 (aged) p=0.2); this finding does suggest altered CaMKII activity during ageing of the vasculature and supports the evidence for increased activity as assessed by post-translational modifications shown in Figure 5.2B.

Interestingly, when similar experiments were performed investigating CaMKII activity in young and aged cardiac homogenates, no differences were observed between any group (Figure 5.3C) ((pmol PO$_4^-$inc/min) 4.9 ± 0.4 (young), 4.8 ± 0.16 (aged), 2.31 ± 0.56 (control no enzyme) p=0.3). As shown earlier (Figure 5.3A), 50ng RCaMKII did indeed cause significant activation of the enzyme for all experiments, confirming specificity of the assay. Thus, it appears activity of CaMKII within these samples were extremely low, which is different to what has been reported in failing hearts where CaMKII activity is increased (Schulman & Anderson, 2010) and also with our earlier results showing increased activation of CaMKII by

autophosphorylation (Figure 5.2A). In spite of this, findings from this assay did reveal alterations in the activation state of CaMKII at the level of the vasculature, further supporting our hypothesis that CaMKIIδ is altered during ageing and may play a role in ageing of the cardiovascular system.
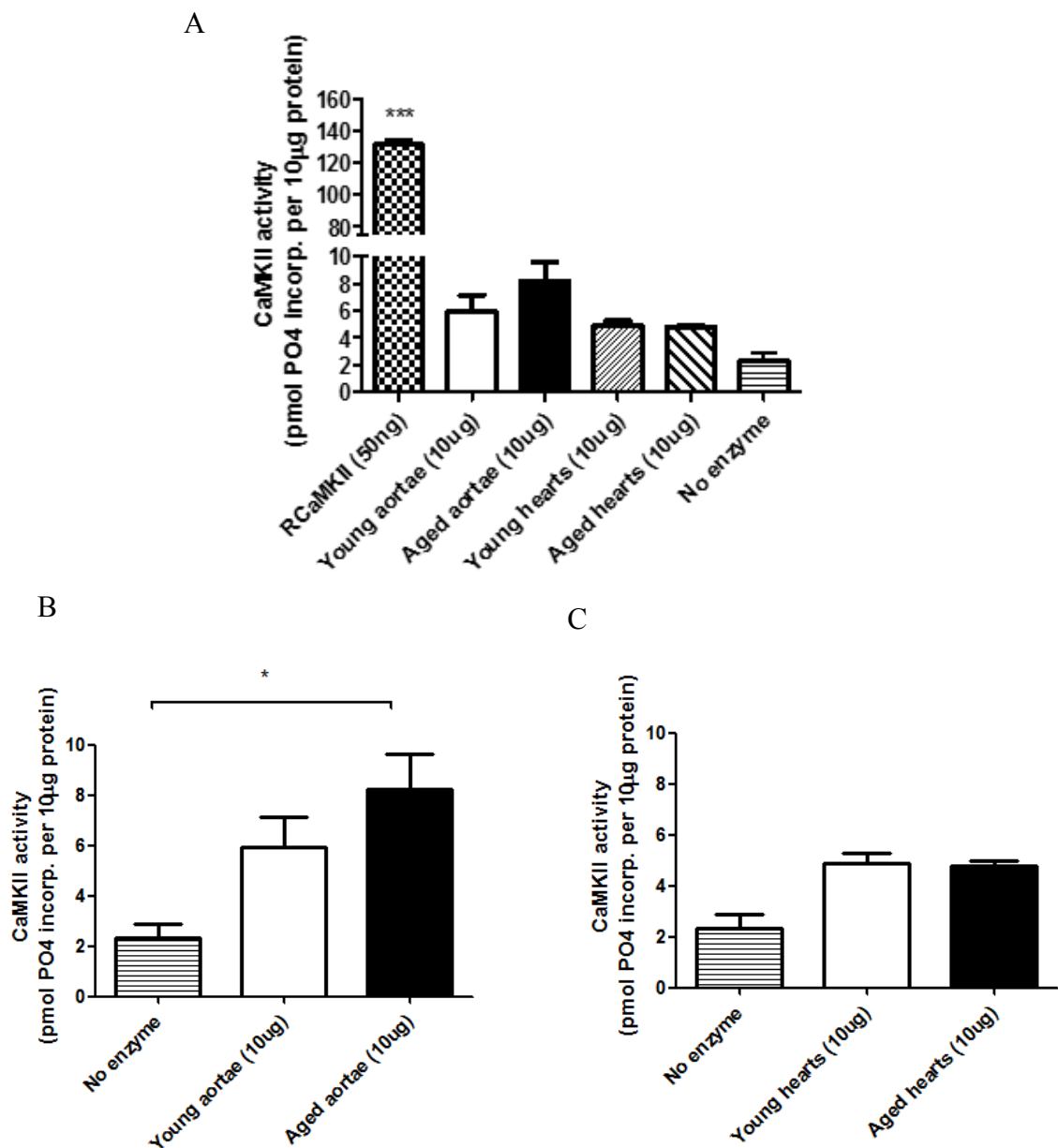
Figure 5.3: Assessment of phosphotransferase activity of CaMKII in cardiac and aortic homogenates. CaMKII activity in young and aged whole aortic and cardiac homogenates (10μg total protein) when compared with background activity (no source of enzyme) and recombinant (R) CaMKII (50ng) (positive control) (A). Separate histograms showing CaMKII activity in aortic (B) and cardiac (C) homogenates alone compared with background. Activity was measured as described in the methods section and is shown as [^{32}P] incorporated into specific autocamtide II peptide substrate/min /10μg protein. All data are expressed as mean ± S.E.M. Statistical analysis was performed using a one-way ANOVA and Tukey's post-test; $p<0.05$*; $p<0.001$ ***; n=3 for each group.

5.3 Activation of CaMKII by oxidation is increased in aged cardiac and aortic tissues

Similar quantitative immunoblotting experiments as those in Section 5.1 were performed on ventricular and aortic homogenates from both young and aged animals, however samples were now subjected to analysis of expression of oxidised (ox)-CaMKII. In addition to autophosphorylation of Thr286/287, activation of CaMKII is also achieved by oxidation of the Met 281/282 site of the kinase and given the link between increased oxidative stress and ageing, this seemed a highly relevant pathway for activation of CaMKII in our aged animals. Representative immunoblots and accompanying histograms are displayed in Figure 5.4 and show levels of ox-CaMKII were significantly increased in both aged hearts and aortae when compared with young ((oxCaMKII:GAPDH) 0.9 ± 0.08 vs. 1.14 ± 0.04, young vs. aged (heart), p=0.03 (Fig 5A) and 1.02 ± 0.01 vs. 1.3 ± 0.07, young vs. aged (aorta), p=0.01 (Fig 5B)). This mirrors what has been documented in recent years in diseased hearts (Singh et al., 2012), however is the first time anything has been reported with regard to a role for ox-CaMKII in the vasculature and more specifically, during ageing.
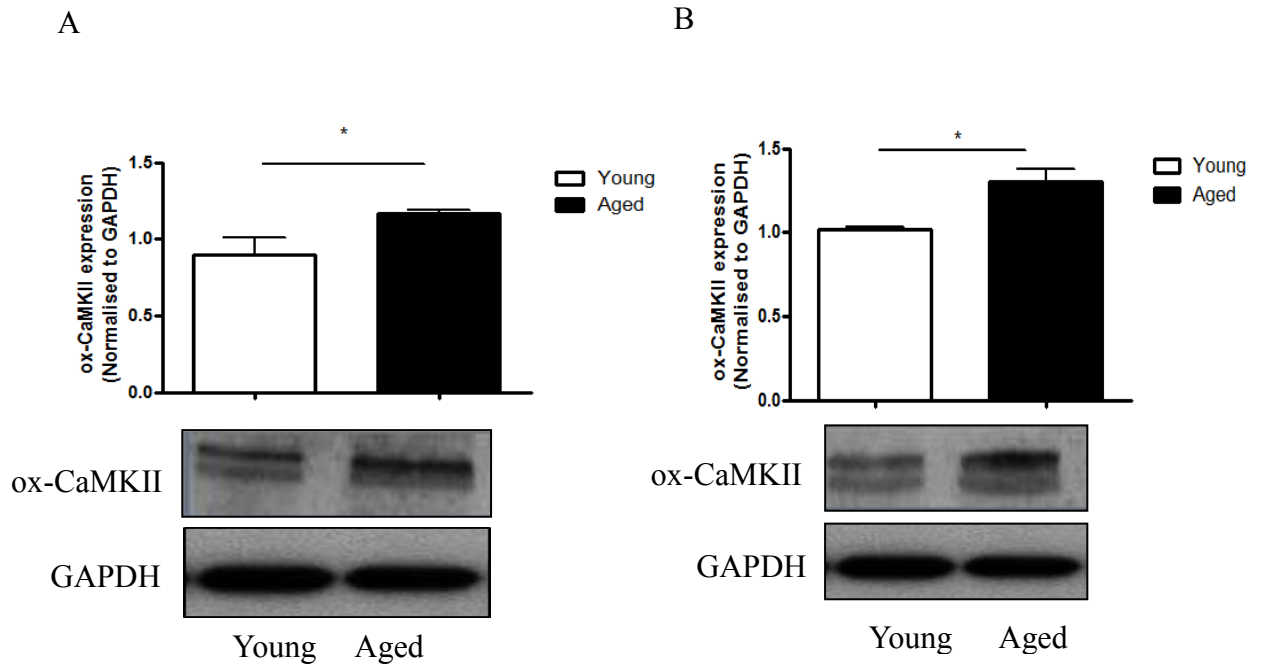
Figure 5.4: Increased activation of CaMKII by oxidation in aged cardiac and aortic homogenates. Immunoblot analysis of oxidised (ox)-CaMKII expression in young and aged whole heart (5µg total protein) (A) and aortic (10µg total protein) (B) homogenates. Representative immunoblots are shown of each in addition to expression of the loading control GAPDH. Densitometry analysis was performed and data normalised to GAPDH. Mean normalised data are shown ± S.E.M. Statistical analysis was performed using a student's unpaired t test; p<0.05*; n=5 for each group.

5.4 Assessment of CaMKIIδ and ox-CaMKII protein expression and up-regulation in aortic endothelial cells from aged rats

Having established that aged aortae exhibit significant changes functionally and physiologically (Chapter 4) and that this correlates with a significant increase in CaMKIIδ expression and CaMKII activation (by phosphorylation and oxidation) (Figures 5.2B and 5.4B), it was of key interest to specifically examine potential alterations in CaMKII at the level of the endothelium. As already shown in Chapter 3, Figure 3.18, ox-CaMKII expression is up-regulated in ECs following treatment with H_2O_2; therefore since cells isolated from aged animals show an increased pro-oxidant environment (Chapter 4, Figure 4.12), this should in theory coincide with altered CaMKII activation by oxidation. Immunofluorescence experiments showed that both total CaMKIIδ (Figure 5.5A) and ox-CaMKII (Figure 5.6A) were highly expressed under basal conditions in aged ECs but there was little, if any, staining evident in cells isolated from young aortae. Cells from aged animals also visually appeared much larger than those from young following staining, which mirrors what was previously reported in Chapter 4. Quantitative immunoblotting of young and aged cell lysates also demonstrated similar findings, where expression levels of both total CaMKIIδ and ox-CaMKII were significantly increased in aged cells when compared with young ((CaMKIIδ:GAPDH) 0.98 ± 0.14 vs. 1.92 ± 0.33, young vs. aged, p=0.04, Figure 5.5B and (ox-CaMKII:GAPDH) 0.85 ± 0.06 vs. 1.13 ± 0.02, young vs. aged, p=0.007, Figure 5.6B). Combined, these findings not only suggest that CaMKIIδ may play a role during ageing of the vasculature, but specifically activation of the enzyme by oxidation may also mediate the ED associated with advanced ageing, where oxidative stress is evident.
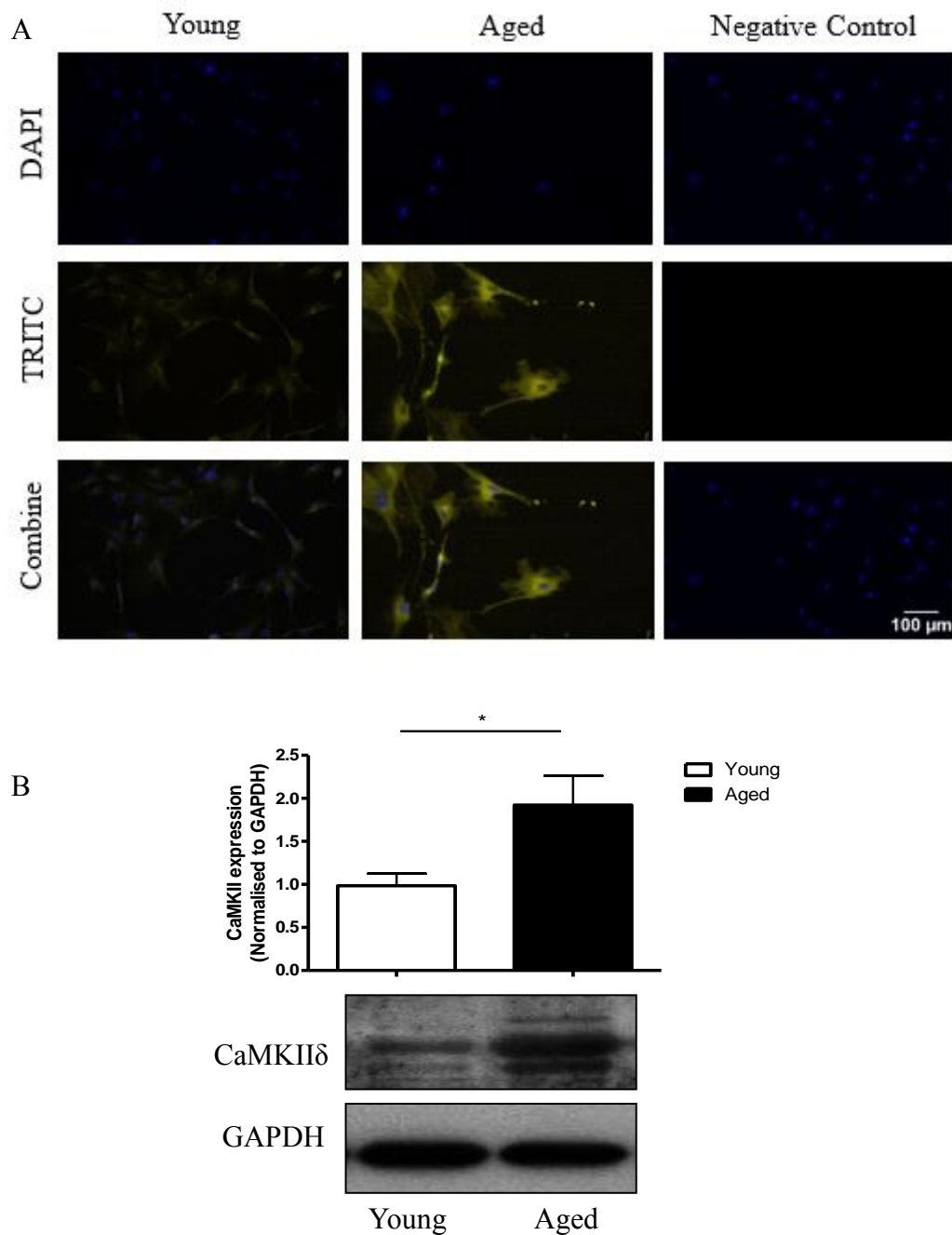
Figure 5.5: Aged aortic endothelial cells show increased CaMKIIδ expression.
Representative images of young and aged aortic endothelial cells stained for total
CaMKIIδ expression and measured by immunofluorescence (A). Cells stained with
secondary anti-rabbit IgG TRITC-conjugated antibody alone served as a negative
control. Images are representative of n=3 experiments, all at 10x magnification (scale
100μm). Immunoblot analysis of total CaMKIIδ in young and aged aortic endothelial
cells ($\sim10^4$ total cells) (B). Data were normalised to intrinsic GAPDH expression and
plotted as mean ± S.E.M in accompanying histograms. Statistical analysis was
performed using a student's unpaired t test; $p < 0.05$*; n=4 for each group.
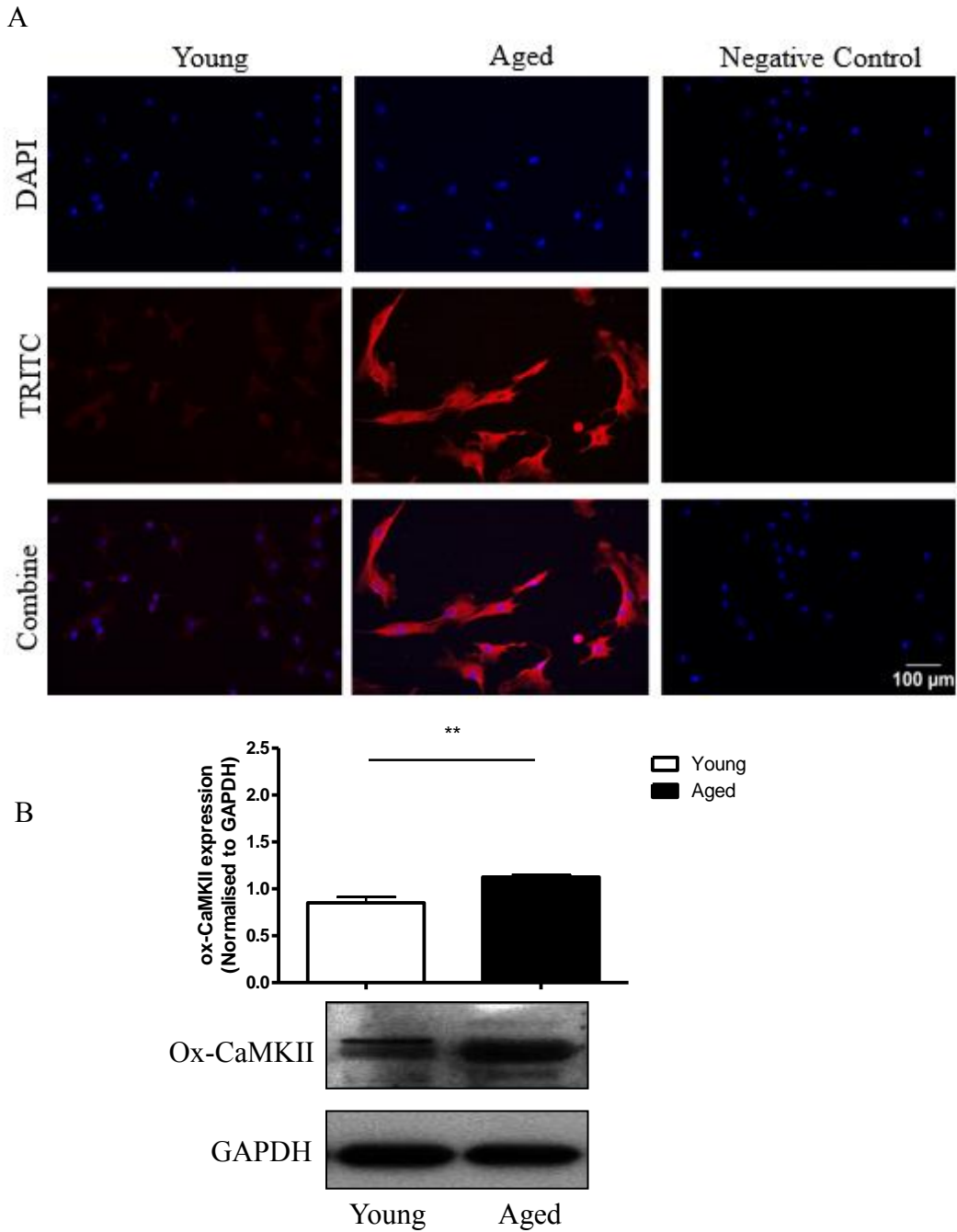
Figure 5.6: Activation of CaMKII by oxidation is increased in aged aortic endothelial cells. Representative images of young and aged aortic endothelial cells stained for ox-CaMKII expression and measured by immunofluorescence (A). Cells stained with secondary anti-rabbit IgG TRITC-conjugated antibody alone served as a negative control. Images are representative of n=3 experiments, all at 10x magnification (scale 100µm). Immunoblot analysis of ox-CaMKII in young and aged aortic endothelial cells ($\sim10^4$ total cells) (B). Data were normalised to intrinsic GAPDH expression and plotted as mean ± S.E.M in accompanying histograms. Statistical analysis was performed using a student's unpaired t test; p<0.01**; n=4 for each group.

5.5 Assessment of pro-inflammatory NF-κB signalling during ageing of the endothelium

There is now a large amount of evidence suggesting pro-inflammatory NF-κB signalling is up-regulated in cardiac cells from diseased hearts (Islam & Koch, 2012; Maier et al., 2012; Martin, 2011). Additionally, a number of studies also report a key role for NF-κB in diseases of the vasculature, where EC specific inhibition of NF-κB signalling protects mice from developing atherosclerosis (Gareus et al., 2008; Pamukcu, Lip & Shantsila, 2011). Given the obvious differences in EC growth and function between young and aged groups (Chapter 4, Section 4.6); it was important to also investigate altered NF-κB activity in these cells. Basal levels of inflammation in ECs isolated from both young and aged aortae were monitored by assessing phosphorylation (activation) of the pro-inflammatory mediator NF-κB sub-unit (p65). Results are shown in Figure 5.7 where there is a clear increase in phospho-p65 signal in aged cells, even in the absence of any external stimulus. In young cells, it can be clearly seen that there is no obvious basal signal for phospho-p65 (i.e. no obvious inflammatory status). To investigate this further, young cells (where there is no basal signal for phospho-p65) were stimulated with TNF-α for 10 minutes prior to staining, serving as a positive control for the experiment. Here, we can see there was a significant increase in phospho-p65 signal following stimulation of young cells, reflecting the potential for activation of this pathway in this cell type, as would be expected (Kempe et al., 2005). Interestingly, the levels of phospho-p65 in young cells following stimulation were almost equivalent to levels observed in aged cells without any stimulation. Furthermore, in both young ECs following stimulation and aged cells, the positive FITC staining appears to be more prominent in and around the nucleus, suggesting nuclear translocation of the phospho-p65 subunit and corresponding NF-κB activation. These findings overall suggest an intrinsic elevated inflammatory status in the aged ECs, possibly as a result of an 'activated' or 'stressed' phenotype and indeed, correlate with experiments performed in cardiac cells showing enhanced pro-inflammatory NF-κB activation in disease models (Martin, 2011).

(A)

(B)
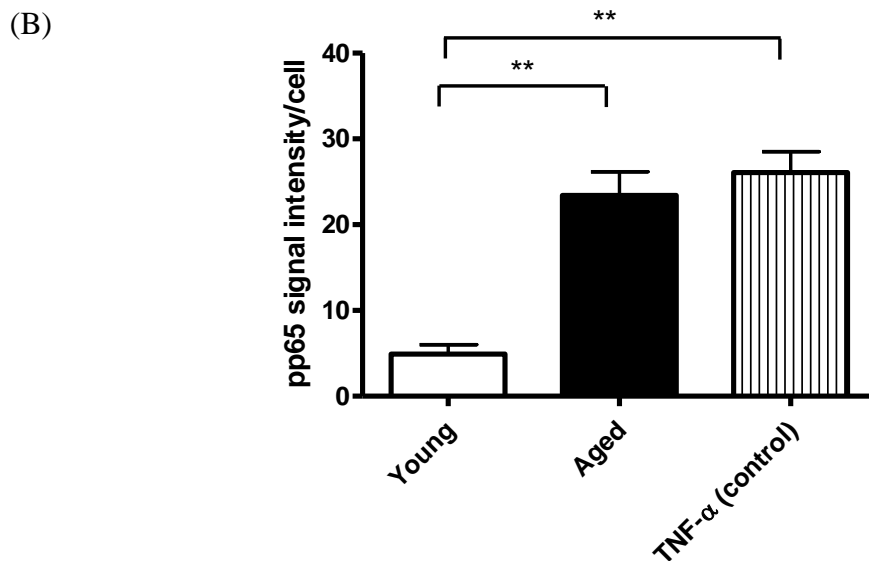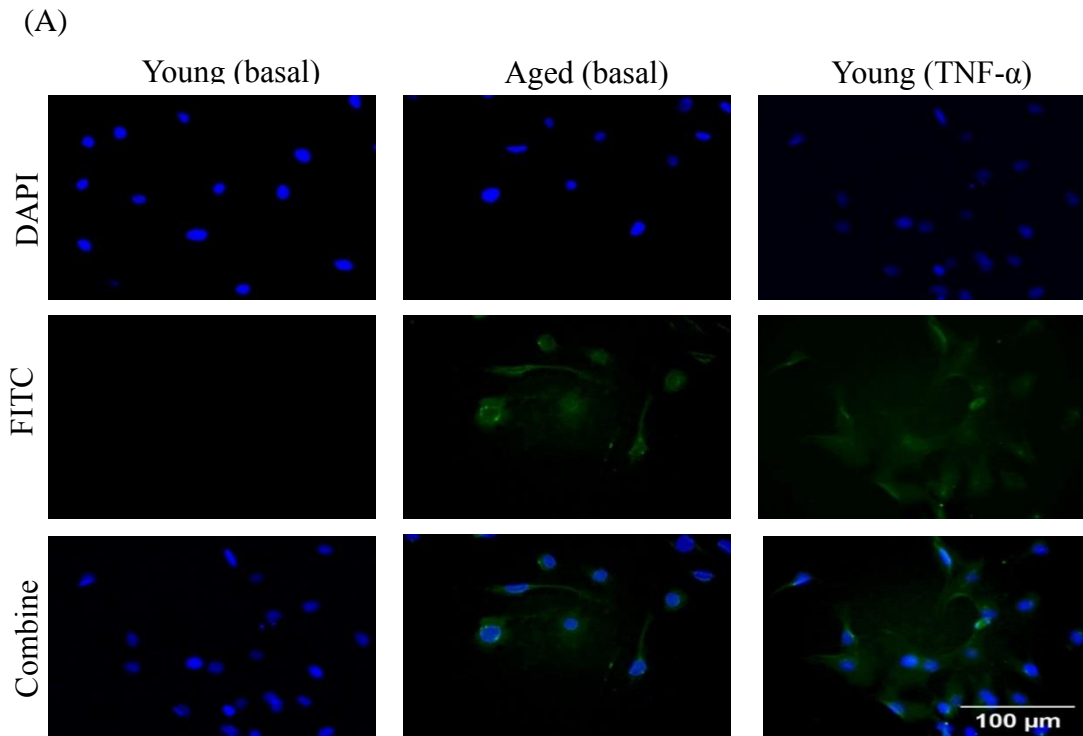
Figure 5.7: Increased NF-κB signalling in aged aortic endothelial cells.
Representative images showing positive staining for basal phospho-p65 expression in young and aged aortic endothelial cells. TNF-α (10ng/ml)-stimulated (10 minutes) young aortic endothelial cells served as a positive control for activation of NF-κB signalling pathway. Images are shown at 10x magnification (scale=100µm) (A). Quantification of pp65 signal intensity/cell was performed (B) and data analysed using a one-way ANOVA followed by Tukey's post-test; n=3 for each group; p<0.01**.

5.6 Discussion

The present study has provided evidence for the first time that CaMKII expression and activity are increased in both hearts and aortae from aged animals. Importantly, activation of CaMKII by oxidation appears to play a key role, not only in the vasculature as a whole, but specifically in the endothelium of the aged animals. This correlates with enhanced NF-κB activation in the aged cells and therefore, could suggest a connection between both signalling pathways, in line with what has already been reported in Chapter 1.

5.6.1 CaMKII expression and activity are increased in ageing of the heart

As discussed previously, CaMKIIδ has been extensively studied in the disease context, where up-regulated protein expression and activation by autophosphorylation have been reported in numerous studies (Colomer et al., 2003; Currie & Smith 1999; Martin et al., 2014). Additionally, the more recent route of CaMKII activation, by oxidation of Met 281/282, has also been shown to be significantly enhanced during myocardial injury due to the pro-oxidant environment known to exist in diseased myocardial tissue (Singh et al., 2012). Interestingly, experiments performed here have shown novel evidence that total CaMKIIδ expression is significantly increased in the hearts taken from aged animals (Figure 5.1A), as is activation of CaMKII by both phosphorylation and oxidation (Figures 5.2A and 5.4A respectively). These alterations to CaMKII activity are to a similar extent as those reported in cardiac disease models, where a 2-3-fold increase in kinase activity has been shown in pressure overload-induced LV failure (Wang et al., 2008; Kreusser & Backs, 2014) as well as in animal models of MI and cardiac hypertrophy where phosphorylated CaMKII is elevated significantly (Meyer et al., 2003; Zhang et al., 2003). CaMKII activation by oxidation constitutes a second pathway for sustained activation, as oxidation of the Met281/282 residues 'locks' CaMKII into an open configuration (Wang & Anderson, 2012). ROS are known to trigger activation of CaMKII by this mechanism and these include H_2O_2 and superoxide anion (O_2^-), both of which are increased in MI and ageing (Munzel & Harrison, 1999; Tsay et al., 2000). Thus, it is not surprising that we observed such an

increase in ox-CaMKII in the aged hearts, however this has previously not been documented in the literature. When radioactive kinase assays were performed to provide further evidence that CaMKII activity is increased during ageing of the heart, results did not support those obtained earlier as no increase was observed in aged samples (Figure 5.3C). As mentioned, the use of RCaMKII as a positive control in these experiments confirmed that the assay itself was working, therefore suggesting the issue must be due to the samples themselves. Perhaps activity of CaMKII within both young and aged samples were just extremely low, however previous studies using this technique to assess activation state of CaMKII in diseased hearts have shown very different results, where kinase activity is significantly greater compared to control (Ashpole et al., 2012). Furthermore, given the earlier findings that activation of CaMKII assessed by phosphorylation and oxidation mirrored what has been reported in disease, then similar results would be expected using this approach also. The answer may lie simply in that low sample numbers were used for these assays (n=3) and since physiological and functional variations exist between animals, larger group sizes may be required to perform further experiments in the future. In spite of this, the combined findings from this section of the project correlate with earlier findings that ageing induces structural and functional changes to the heart (Chapter 4). This may indicate that CaMKII plays a fundamental role in the compromised cardiac function associated with advanced ageing.

5.6.2 CaMKII expression and activity are increased in ageing of the vasculature

A fundamental aspect of this project was to investigate a role for CaMKIIδ in the aged vasculature. Despite the plethora of research conducted to investigate an involvement for CaMKIIδ in the heart, there remains a gap in the literature in terms of investigating similar mechanisms in the vasculature. A small number of studies have shown expression of CaMKIIδ in arterial preparations, however these have primarily been in the carotid arteries (Li et al., 2010; Scott et al., 2013). Furthermore, investigations into a role for CaMKIIδ in the arterial system have primarily focused on its expression in the tunica media and SMCs alone (House et al., 2007; Pfleiderer et al., 2004; Scott et

al., 2012) and even so, nothing has been reported in these tissues during ageing. Here, we show for the first time that expression of CaMKIIδ and activation of CaMKII are increased in aortae from aged animals. Despite total CaMKIIδ only slightly increasing in aged aortic preparations (Figure 5.1B), examination of the different δ variants shown in the blot, reveal that there is a greater increase in certain variants over others in the aged aorta. As previously mentioned, the δ isoform of CaMKII exists as two main variants in the CVS ($\delta_{2(B)}$ and $\delta3_{(C)}$), therefore it would be useful to analyse each of these separately in future experiments to determine which, if any variants play more of a role than others during ageing of the vasculature. In spite of this, activation of CaMKII by both phosphorylation of Thr286/287 and oxidation of Met281/282 were significantly increased in aged aortae when compared to young (Figures 5.2B and 5.4B). This finding was further supported when radioactive kinase assays were performed (Figure 5.3B) and suggests for the first time that increased CaMKII activation is associated with ageing of the aorta. Having established that aged aortae exhibit significant changes functionally and physiologically (Chapter 4), it is interesting that this coincides with altered CaMKII function and mirrors what we have shown in the aged heart, as well as what others have demonstrated so often in the diseased setting. This suggests that CaMKIIδ may present as a useful target for future therapeutic interventions to be developed, not only to treat myocardial diseases but also those affecting the vascular system such as atherosclerosis. As mentioned several times now, CVD is an extremely complex process affecting all parts of the cardiovascular system. The role of the vasculature is to transport blood, nutrients and oxygen to all areas of the body; therefore if it becomes damaged (as it does during ageing) it stands to reason that dysfunction and pathology would also develop in other organs, including the heart. Thus, a negative association exists and as ageing induces pathological alterations to the vascular network, this potentiates similar abnormalities elsewhere and an overall 'disease'-like phenotype develops. As such, it would be useful for future studies to investigate whether a correlation exists between increased vascular CaMKIIδ activity and other age-related conditions.

5.6.2.1 Increased expression and activation of CaMKII in aged endothelium

The endothelium of the cardiovascular system, although only a single cell layer thick, exhibits an extraordinary capacity for modulation of cardiovascular function. As discussed in Section 5.6.2, despite a number of studies previously investigating a role for CaMKIIδ in the diseased vasculature, their focus has primarily been on SMCs and the ' ability of CaMKII to regulate proliferation and motility within such cell populations, leading to vascular wall remodelling (House et al., 2007). To date, nothing has been reported of a similar role for CaMKIIδ in the endothelium of damaged vasculature. Additionally, there has been no previous work performed with regards to investigating a role for CaMKII in mediating dysfunctional aged endothelium.

Given our earlier findings that CaMKIIδ expression and activation were up-regulated in whole aortic homogenates from aged animals, the next aim was to investigate this specifically within the aged ECs themselves. Collectively, results from Figures 5.5 and 5.6 show that both total CaMKIIδ expression and activation by oxidation were significantly increased in ECs isolated from aged animals compared to young. This result was confirmed by using two independent approaches of assessment (immunofluorescence and quantitative immunoblotting). *In vivo*, ECs are continually subjected to shear stress from blood flow and evidence suggests that this flow is disturbed with ageing (Trinity et al., 2014), which is in line with what we also observed in our aged animals models (Chapter 4, Figure 4.6). As a result ECs adapt to these turbulences, inducing an altered phenotype and overall function to accommodate the environment (Potter et al., 2011). Additionally, vascular oxidative stress is amplified with advanced age as a consequence of greater ROS production and several lines of evidence now suggest that the development of this oxidative stress greatly contributes to the vascular ED associated with ageing. One particular study showed that brachial artery FMD (as outlined in Chapter 4, Section 4.7.4.1) is inversely related to circulating markers of oxidative stress (Eskurza, Kahn & Seals, 2006). Furthermore, acute administration of antioxidants such as vitamin C, have been reported to selectively improve EDD in elderly patients (Eskurza et al., 2004). Taking all of this into account, since earlier findings from this study have shown altered EC phenotype

and increased oxidative stress with ageing, it is not surprising that activation of CaMKII by oxidation is significantly increased in aged ECs. In spite of this, it is the first time a role for ox-CaMKII has been postulated in ED associated with advanced age. This may therefore serve as a useful marker for oxidative stress in future studies and furthermore, targeted inhibition of activation of CaMKII by oxidation may attenuate the adverse effects of ED, thus future experiments could investigate this further.

5.6.3 Increased NF-κB activity in the aged endothelium

As mentioned in Chapter 1, NF-κB signalling is a well-recognised pro-inflammatory pathway and a substantial amount of evidence now supports a crucial role for activation of the pathway contributing to age-associated ED (Csiszar et al., 2003; Csiszar et al., 2004; Donato et al., 2009). Findings from this study show that a pro-inflammatory EC phenotype is adopted in aged cells as measured by phosphorylation of the NF-κB p65 subunit (Figure 5.7). This was detected by immunofluorescent staining of the activated subunit and shows translocation to the nucleus in the aged cells, to a similar extent as is observed in young cells stimulated with TNF-α (positive control). Activation of the NF-κB pathway is triggered by various stimuli, including inflammatory cytokines (TNF-α) and ROS, both of which we have previously shown to be up-regulated in aged cells (Chapter 4). This triggers intracellular pro-inflammatory signalling, leading to phosphorylation and degradation of the inhibitor of NF-κB (IκBα) and subsequent translocation of the NF-κB dimer to the nucleus, where it binds to promoters of gene targets. Some of the potential gene targets include pro-inflammatory molecules, such as IL-6, TNF-α and MCP-1, as well as pro-oxidant enzymes including NADPH oxidase (Anrather et al., 2006; Harrison et al., 2007). Thus, activation of NF-κB and the consequent production of such mediators, predisposes the vasculature to ED as it connects both redox and inflammatory signalling in cells (Donato et al., 2009).

Other markers could have been assessed to show further activation of NF-κB signalling in the aged cells. Basal activity can be measured by a luciferase reporter

assay, where cultured cells are transfected with an NF-κB luciferase reporter vector containing a firefly luciferase gene under the control of the multimerised NF-κB responsive element. In addition to this, NF-κB binding to DNA could also have been assessed in cell nuclear extracts from young and aged animals, however due to time constraints this was not possible.

In the disease context, activation of NF-κB signalling induces the production of inflammatory cytokines and complement factors, further amplifying the inflammatory cascade (Singh & Anderson, 2011). Importantly, one particular study has shown that expression of complement factor B in cardiomyocytes is up-regulated in MI through activation of NF-κB, via CaMKII (Singh et al., 2009). Overall, this suggests that inflammatory activation associated with cardiac disease is modulated by NF-κB-CaMKII signalling. As mentioned previously, this link has not been established in the vasculature, nor during ageing. However, given earlier findings that CaMKII can modulate NF-κB signalling (via IKKβ interaction) in ECs and the evidence presented here suggesting that both pathways are up-regulated during ageing; this raises the question of whether up-regulation/activation of both CaMKII and NF-κB signalling pathways means greater potential for CaMKII-IKKβ interaction in the ageing context?

The final set of planned experiments for this project aimed to answer this by tying together results from both Chapter 3 and Chapter 5 and assess the interaction between CaMKII and NF-κB in ECs (by the PLA) and establish if this was altered during ageing. This was not however feasible as optimisation of conditions for the PLA (in Chapter 3) took substantially longer than originally anticipated. It would be important that future experiments investigate this further however to provide a strong argument that CaMKII does indeed play a role in ageing of the endothelium via modulation of NFκB pro-inflammatory signalling.

5.7 Conclusions

In summary, key findings from this chapter have shown for the first time that CaMKII expression and activity are increased during ageing in both the heart and vasculature. Importantly, this has also been demonstrated at the level of the vascular endothelium, where activation of CaMKII by oxidation may play a key role in mediating age-

associated ED. Interestingly, alterations in CaMKII correlate with enhanced NF-κB activity during ageing. Based on findings from Chapter 3, where a definitive link between both pathways was shown, these parallel changes in the aged CV system, could substantiate our findings suggesting activation of CaMKII in the aged system, results in pro-inflammatory NFκB activation. Although it was not possible to characterise this link in the aged setting, findings from this chapter combined with those from Chapter 3 strongly suggest an important relationship exists between CaMKII and NF-κB signalling in ECs, and that the interaction between these signalling systems may serve as a useful target for potential therapeutic intervention in the future.

Chapter 6: General Discussion

It is well established that the multi-functional CaMKIIδ plays an important role in normal cardiac function and is involved in contributing to dysfunction of the heart associated with disease. Much less however is known about a role for CaMKIIδ in the vasculature. Furthermore, it is apparent that both cardiac and vascular health deteriorates with advanced age, yet a role for CaMKIIδ in the cardiovascular dysfunction which accompanies ageing remains elusive. The present study has taken both an *in vivo* and *in vitro* approach to investigate for the first time whether CaMKIIδ may be associated with age-related cardiovascular deterioration and provides novel evidence of a mechanistic involvement in its modulation of inflammatory signalling pathways associated with ageing.

6.1 CaMKII-NF-κB interaction in the endothelium

Despite a number of previous studies reporting that CaMKII may modulate pro-inflammatory NF-κB signalling, this was primarily shown in lymphocytes (Ishiguro et al., 2006) and more recently, demonstrated in cells of the heart including cardiomyocytes (Singh & Anderson, 2011) and CFs (Martin, 2011). However, there is currently nothing in the literature suggesting a specific mechanism of how this modulation may occur. Additionally, a similar link has yet to be established in the vasculature. Given the well-documented role of NF-κB mediated inflammation in diseases of the vascular system (Gareus et al., 2008; Mallavia et al., 2013) and the fact that CaMKII is expressed within cells of the vasculature; it is surprising that no such work has yet been conducted to explore this possible link.

Here, we have shown for the first time that CaMKII may play a functional role in modulation of the NF-κB signalling pathway within ECs of the vasculature (Figure 3.15). The endothelium was specifically investigated as it has been well documented that it becomes dysfunctional during ageing, even in the absence of any disease (House et al., 2007; Wang et al., 2010). In addition, numerous studies now report activation of NF-κB pro-inflammatory signalling as being a key player in the development of this ED; thus investigating potential mechanisms of modulating this pathway may serve as a useful target for therapeutic intervention. Importantly, findings from this

study have also shown novel evidence that upon stimulation, CaMKII can specifically interact with IKKβ of the IKK complex in the NF-κB cascade (Figures 3.20 and 3.22). This supports previous observations from our own research laboratory, where experiments performed by Martin (2011) also demonstrated a direct interaction between CaMKIIδ and NF-κB signalling at the level of IKKβ using both autoradiography and SPR techniques. The interaction between CaMKII and IKKβ in ECs as detected by PLA was only shown in its active (oxidised) form as a result of low sensitivity of the CaMKIIδ antibody for immunofluorescence. It was however evident that differences in signal existed between cells under basal conditions and those exposed to H_2O_2, thus suggesting that CaMKII may only bind to IKKβ under these pro-oxidant conditions. This is extremely important in the context of ageing given the well-reported increase in intracellular oxidative stress and suggests a potential novel alternative mechanism for how NF-kB signalling may be increased during ageing of the endothelium. Nonetheless, it would be interesting that future studies are also performed to investigate any interaction between CaMKIIδ specifically and IKKβ using antibodies suitable for co-immunoprecipitation. It would also be of prime importance to examine whether CaMKII can phosphorylate unique sites of the IKKβ subunit. This could be achieved using experimental approaches such as site-directed mutagenesis or peptide array analysis to provide further insight into the mechanisms involved for an interaction between the two pathways to occur.

6.2 Characterisation of an aged phenotype

Given that the key objective of this study was to assess an involvement of CaMKIIδ in contributing to dysfunction of the CVS with ageing, it was essential that an 'aged' phenotype was successfully characterised within the cardiac and vascular systems of aged animals.

In vivo echocardiography was used to examine functional alterations to the CVS during ageing. Numerous parameters were measured and showed the development of cardiac hypertrophy (Figure 4.4), aortic stiffness (Figure 4.5) and blood flow turbulence (Figure 4.6). These results mirror what has been reported previously in

aged humans, where the prevalence of LV hypertrophy and arterial stiffening (as assessed by increased PWV during echocardiography) both correlated with increased incidence of developing cardiovascular diseases (Lakatta & Levy, 2003). Also, in line with previous work, post-mortem analysis of aortic tissues showed adaptations to vessel wall structure (Figure 4.7). Cross-sectional studies in humans have shown wall thickening and dilation are prominent structural changes that occur within large elastic arteries with ageing (Lakatta, 1993). These were obvious features in our aged animals, as was the deposition of fatty tissue within the lumen of the aortae, therefore suggesting the development of a disease-like phenotype similar to what occurs clinically.

As discussed in Chapter 1, ageing is associated with both increased inflammation and oxidative stress. This is true for within the CVS specifically, therefore assessing markers for each of these can serve as useful indicators of age-associated pathophysiology. Chronic inflammation was apparent with increased circulating TNF-α concentrations (Figure 4.8) and leukocyte infiltration up-regulated in aged animals (Figures 4.9 and 4.10). Examination of the endothelium of the vasculature also revealed enhanced levels of ROS as well as alterations in overall cell phenotype (Figures 4.11 and 4.12). These findings coincide with work conducted by Seals et al., (2011) where he also demonstrated that cells isolated from aged animals display a stressed phenotype, as measured by alterations in nitrotyrosine and eNOS expression & activity. These are alternative useful markers of cell damage and are also commonly used as methods of assessing ED *in vitro* (Gradinaru et al., 2015), therefore future experiments could also be conducted to evaluate expression of such proteins, particularly eNOS given the essential role it plays in regulating EDD as outlined in Chapter 1. This would provide a more detailed representation of the consequences of ED with ageing, and could be performed in combination with assessing differences in cell impedance profiles between young and aged ECs as discussed earlier.

6.3 CaMKIIδ and NF-κB pro-inflammatory signalling during ageing

Findings from this study have revealed for the first time that elevated expression and activity of CaMKIIδ exist in both aged cardiac and vascular tissues (Figures 5.1-5.4). Importantly, this was also established specifically in the endothelium of the vasculature (Figures 5.5 and 5.6) and correlated with increased NF-κB activity (Figure 5.7). These data suggest that CaMKIIδ may also play a role in contributing to ageing of the vasculature, given what has been demonstrated extensively in the heart where increased CaMKIIδ expression and activity is involved in mediating cardiac hypertrophy and disease progression (Sossalla et al., 2010; Schulman & Anderson, 2010). Furthermore, as there is now a plethora of evidence supporting a role for NF-κB pro-inflammatory signalling in mediating age-associated ED and that we have indeed demonstrated the ability of CaMKII to interact with IKKβ of the NF-κB pathway following oxidation; there is a strong possibility that these two signalling pathways could interact and further potentiate the development of ED with ageing. Anderson and his colleagues once asked the question if CaMKII serves as a link between inflammation and cardiac hypertrophy (Singh & Anderson, 2011). Here, we can ask a similar question - does CaMKII link oxidative stress and inflammation associated with ageing? Despite all of the evidence shown in this thesis pointing towards this likelihood, it is of fundamental importance that future experiments are performed to assess a functional role for CaMKIIδ in ageing of the vascular endothelium. This could be addressed by inhibiting CaMKII expression/activity within the aged ECs and measuring downstream consequences on NF-κB signalling. Additionally, as mentioned in Chapter 5, the interaction between CaMKII and IKKβ as assessed by PLA should also be quantified in aged ECs and compared with young. These experiments were not performed in this project due to time constraints, however would provide essential clarifications on whether there is a mechanistic implication for CaMKII in modulating NF-κB signalling during ageing.

6.4 CaMKIIδ-NF-κB as a target for therapeutic intervention

Overall, findings from this study demonstrate strong evidence to suggest that CaMKIIδ may play a role in contributing to age-related pathophysiology of the cardiovascular system. Inhibition of CaMKII has previously been suggested as a therapeutic approach for the treatment of various cardiomyopathies. However it is important to consider that inhibiting CaMKII activity will not only alleviate the unfavourable effects of elevated CaMKII during disease, it would also negatively affect its key role in normal cardiac function. Similarly, as mentioned in Chapter 1, targeting NF-κB activity has also been proposed as an effective therapeutic method for the treatment of both cardiac and vascular disorders, although activation of this signalling pathway plays other important roles including in the resolution phase of inflammation and in tissue repair. Selective targeting may therefore serve as a more valuable strategy for the treatment of such conditions. Here, we have identified CaMKIIδ as a novel modulator of NF-κB signalling in the endothelium of the vasculature. Targeting CaMKII-mediated activation of NF-κB specifically at the level of the endothelium could present as a novel therapeutic approach to reduce or prevent the development of ED, not only with ageing, but also in the context of vascular disease. This could be achieved as by precisely targeting the direct protein-protein interaction between CaMKII and IKKβ, it may relieve some of the inflammation associated with ED and therefore prevent the development of other age-related conditions in which ED plays a contributing role. Future experiments should be performed to map the CaMKII-IKKβ interaction in more detail. Once elucidated, this would allow for the development of selective novel peptide inhibitors targeting the site of interaction to be introduced and from here, both *in vitro* and *in vivo* experiments could be conducted to assess efficacy in the treatment of age-related cardiovascular disorders.

References

Alabi, C. A., Love, K. T., Sahay, G., Stutzman, T., Whitney, T., Langer, R., & Anderson, D. G. (2013). FRET-labeled siRNA probes for tracking assembly and disassembly of siRNA-nanocomplexes. *NIH Public Access*, **6** (7), 6133–6141.

Akbaraly, T. N., Hamer, M., Ferrie, J. E., Lowe, G., Batty, D., Hagger-Johnson, G., Singh- Manoux, A., Shipley, M. J., Kivimaki, M. (2013) Chronic inflammation as a determinant of aging phenotypes. *CMAJ*. **185**, E763-E770.

Alkalay, I., Yaron, A., Hatzubai, A. D. A., Oriani, A., & Ciechanovert, A. (1995). Stimulation-dependent IcBa phosphorylation marks the NF-κB inhibitor for degradation via the ubiquitin-proteasome pathway. *Proc Natl Acad Sci*, **92**, 10599–10603.

Anrather, J., Racchumi, G., & Iadecola, C. (2006). NF-κB Regulates Phagocytic NADPH Oxidase by Inducing the Expression of gp91 phox. *J Biol Chem*, **281** (9), 5657–5667.

Anderson, M. (2007) Multiple downstream proarrhythmic targets for calmodulin kinase II: Moving beyond an ion channel-centric focus. *Cardiovasc Res*. **73**, 657-666.

Ashpole, N. M., Song, W., Brustovetsky, T., Engleman, E. A., Brustovetsky, N., Cummins, T. R., & Hudmon, A. (2012). Calcium / Calmodulin-dependent Protein Kinase II (CaMKII) Inhibition Induces Neurotoxicity via Dysregulation of Glutamate / Calcium Signaling and Hyperexcitability. *J Biol Chem*, **287**(11), 8495–8506.

Assunção, L. G. S., Peixoto, S. V, Vidigal, P. G., Assunção, L. G. S., & Peixoto, S. V. (2012). High sensitivity C-reactive protein distribution in the elderly : the Bambuí Cohort Study , Brazil High sensitivity C-reactive protein distribution in the elderly : the Bambuí Cohort Study. *Brazil J Med Biol Res*, **45** (12), 1284-1286.

Backs, J., Backs, T., Neef, S., Kreusser, M. M., Lehmann, L. H., Patrick, D. M., Olson, E. N. (2009). The isoform of CaM kinase II is required for pathological cardiac hypertrophy and remodeling after pressure overload. *Proceedings of the National*

Academy of Sciences, **106** (7), 2342–2347.

Baldwin, A. S. (2001) The transcription factor NF-kB and human disease. *J Clin Invest*. **107**, 3-6.

Barbieri, M., Ferrucci, L., Ragno, E., Carsi, A., Bandinelli, S., Bonafe, M., Olivieri, F., Giovagnetti, S., Franceschi, C., Gurolnik, J. M., Paolisso, G. (2003) Chronic inflammation and the effect of IGF-1 on muscle strength and power in the older persons. *Am J Physiol Endocrinol Metab*. **284**, 481-487.

Bartov, E., Jerden, J. A., Glaser, B. M. (1988) A simple technique for isolating pure cell populations from mixed primary cultures. *J Tis Cul Meth*., **11** (4), 181-183.

Basak, S. and Hoffmann, A. (2008) Crosstalk via the NF-kB signalling system. *Cytokine growth rev*. **19**, 187-197.

Beckman, J. S., Carson, M., Koppenol, W. H. (1993) ALS, SOD and peroxynitrite. *Nature*. **364**, 548.

Beijnum, J. R., Rousch, M., Castermaris, K., Vander Linden, E., Griffioen, A. W. (2008) Isolation of endothelial cells from fresh tissues. *Nat protocol*, **3**, 1085-1091.

Benjamin, N., Calver, A., Collier, J., Robinson, B., Vallance, P., Webb, D. (1995) Measuring forearm blood flow and interpreting the responses to drugs and mediators. *Hypertension*, **25** (5), 918-923.

Bhatnagar, P., Wickramasinghe, K., Wilkins, E., & Townsend, N. (2016). Trends in the epidemiology of cardiovascular disease in the UK. *Heart*, **2015**, 1–8.

Biernacka, A., Frangogiannis, N. G., Cardiology, D., Einstein, A., & Ny, B. (2011). Aging and Cardiac Fibrosis. *Aging & Disease*, **2** (2), 158–173.

Brandes, R. P., Fleming, I., & Busse, R. (2005). Endothelial aging. *J Cardiores,* **66**, 286–294.

Brar, S. S., Corbin, Z., Kennedy, T. P., Hemendinger, R., Thornton, L., Bommarius, B., Amloid, R. S., Whorton, A. R., Sturrock, A. B., Huecksteadt, T. P.,

Quinn, M. T., Krenitsky, K., Ardie, K. G., Lambeth, J. D. and Hoidal, J. R. (2003) NOX5 NAD(P)H oxidase regulates growth and apoptosis in DU 145 prostate cancer cells. *Am J Phsiol Cell Physiol*. **285** (2), 353-369.

Brown, D. I., & Griendling, K. K. (2010). NOX proteins in signal transduction. *NIH Public Access*, **47**(9), 1239–1253.

Bruunsgaard, H., Anderson-Ranberg, K., Jeune, B., Pedersen, A. N., Skinhaj, P., Pedersen, B. K. (1999) A high plasma concentration of TNF-α is associated with dementia in centenarians. *J Gerentol A Biol Sci Med Sci*. **54** (7), 357-364.

Buffenstein, R., Edrey, Y. H., Yang, T., & Mele, J. (2008). The oxidative stress theory of aging : embattled or invincible ? Insights from non-traditional model organisms. *AGE*, **30**, 99–109.

Cai, H., Davis, M. E., Drummond, G. R., Harrison, D. G. (2001) Induction of endothelial NO synthase by hydrogen peroxide via a Ca2+/Calmodulin-dependent protein kinase II/janus kinase 2-dependent pathway. *Arterioscler Thromb Vasc Biol*. **21**, 1571-1576.

Cai, H., Liu, D., Garcia, J. G. N. (2008) CaM kinase-II dependent pathophysiological signalling in endothelial cells. *Cardiovasc Res*. **77**, 30-34.

Campisi, J. and Fagagna, F. (2007) Cellular senescence: when bad things happen to good cells. *Cell Biol*. **8** (9), 729-740.

Campos, G., Berg, A. Van Den, Nunes-silva, V., Weirather, J., & Peters, L. (2017). Myocardial aging as a T-cell – mediated phenomenon. *pnas*. **8**, 1254-1260.

Chaudhary, K. R., El-sikhry, H., & Seubert, J. M. (2011). Mitochondria and the aging heart. *J Ger Cardiol*, **8**, 159-167.

Cheitlin, M. D. (2003) Cardiovascular physiology - changes with aging. *Am J Gerant Cardiol*., **12** (1), 9-13.

Chen, L. F. and Grenne, W. C. (2004) Shaping the nuclear action of NF-kB. Mol
    Cell Biol. **5**, 392-401.

Christou, D. D., Seals, D. (2008) Decreased maximal heart rate with aging is related
to reduced B-adrenergic responsiveness but is largely explained by a reduction in
intrinsic heart rate. *J Apppl Physiol*, **105** (1), 24-29.

Chung, H. Y., Kim, H. J., Kim, K. W., Choi, J. S., Yu, B. P. (2002) Molecular
    inflammation hypothesis of aging based on the anti-aging mechanism of
    calorie restriction. *Microscopy Research and Technique*. **59**, 264-272.

Chung, H. Y., Sung, B., Jung, K. J., Zou, Y., Yu, B. P. (2006) The molecular
    inflammatory process in ageing. *Antioxidants and redox signalling*. **8**, 572-
    581.

Cohen, H. J., Pieper, C. F., Harris, T., Rao, K. K., Currie, M. S. (1997) The
    association of plasma IL-6 levels with functional disability in community
    dwelling elderly. *J Gerontol Med Sci*. **52**, 201-208.

Colbran, R. J. (2004) Targeting of calcium/calmodulin-dependent protein kinase II.
    Biochem J. **378**, 1-16.

Collins, K. and Mitchell, J. R. (2002) Telomerase in the human organism. *Oncogene*.
    21 (4), 564-579.

Colomer, J. M., Mao, L. A. N., Rockman, H. A., & Means, A. R. (2003). Pressure
    Overload Selectively Up-Regulates Ca2+/CaM-dependent protein kinase II in
    vivo. *Mol Endo*. **17** (2), 183–192.

Conti, V., Corbi, G., Simeon, V., Russomanno, G., Manzo, V., Ferrara, N., Fillippelli,
    A. (2015) Aging-related changes in oxidative stress response of human
    endothelial cells. *Aging Clin & Exp Res*., **27** (4), 547-553.

Corbisier, P. & Remacle, J. (1993) Influence of the energetic pattern of mitochondria
    in cell aging. *Eur J Cell Biol*., **51**, 173-182.

Cortese-krott, M. M., & Düsseldorf, H. (2017). Zinc protects endothelial cells from hydrogen peroxide via Nrf2-dependent stimulation of glutathione biosynthesis, *J freerad biomed*. **44**, 2002-2012.

Corson, M. A., James, N. L., Latta, S. E., Nerem, R. M., Berk, B. C., Harrison, D. G. (1996) Phosphorylation of endothelial nitric oxide synthase in response to fluid shear stress. *Circ Res*., **79**, 984-991.

Cristofalo, V. J., Pignolo, R. (1993) Replicative senescnece of human fibroblast-like cells in culture. *Physiol Rev*., **73** (3), 617-638.

Csiszar, A., Ungvari, Z., Edwards, J. G., Kaminski, P., Wolin, M. S., Koller, A., Kaley, G. (2002) Ageing-induced phenotypic changes and oxidative stress impair coronary arteriolar function. *J. Am. Heart Association*. **90**, 1159-1166.

Csiszar, A., Wang, M., Lakatta, E. G., & Ungvari, Z. (2008). Inflammation and endothelial dysfunction during aging: role of NF- B. *Journal of Applied Physiology*, **105** (4), 1333–1341.

Currie, S., Loughrey, C. M., Craig, M.-A., & Smith, G. L. (2004). Calcium/calmodulin-dependent protein kinase IIdelta associates with the ryanodine receptor complex and regulates channel function in rabbit heart. *Biochemical Journal*, **377**(2), 357–366.

Currie, S., & Smith, G. L. (1999). Calcium / calmodulin-dependent protein kinase II activity is increased in sarcoplasmic reticulum from coronary artery ligated rabbit hearts, *FEBS Letters*, **459**, 244–248.

Currie, S. (2009) Ryanodine receptor phosphorylation by CaMKII: getting the balance right. *Front Biosc.* **14**, 5134-5136.

Deanfield, J. E., Halcox, J. P., Rabelink, T. J. (2007) Endothelial function and dysfunction: Testing and Clinical relevance. *Circulation*. **115**, 1285-1295.

Deswal, A., Petersen, N. J., Feldman, A. M., Young, J. B., White, B. G., & Mann, D. L. (2002). Cytokines and Cytokine Receptors in Advanced Heart Failure. An

analysis of the cytokine database from the vesnarinone trial. *Circulation*, **103**, 2055-2059.

Dinarello, C. A. (2006). Interleukin 1 and interleukin 18 as mediators of inflammation and the aging process. *Am J Clin Nutri*, **83**, 447-454.

Donato, A. J., Eskurza, I., Silver, A. E., Levy, A. S., Pierce, G. L., Gates, P. E., & Seals, D. R. (2007). Direct Evidence of Endothelial Oxidative Stress With Aging in Humans Relation to Impaired Endothelium-Dependent Dilation and Upregulation of Nuclear Factor- κB. *Clin Res*, **100**, 1659-1666.

Donato, J., Pierce, G. L., Lesniewski, L. A., & Seals, D. R. (2009). Role of NF κ B in age - related vascular endothelial dysfunction in humans. *Impact Aging*, **1** (8), 678–681.

Durrant, J. R., Seals, D. R., Connell, M. L., Russell, M. J., Lawson, B. R., Folian, B. J., Lesniewski, L. A. (2009). Voluntary wheel running restores endothelial function in conduit arteries of old mice: direct evidence for reduced oxidative stress, increased superoxide dismutase activity and down-regulation of NADPH oxidase. *The Journal of Physiology*, **587** (13), 3271–3285.

Endrighi, R. (2016). Post-menopausal Women Exhibit Greater Interleukin-6 Responses to Mental Stress Than Older Men. *Annals of Behavioral Medicine*, **50**, 564–571.

Erickson, J. R., Joiner, M. A., Guan, X., Kutschke, W., Oddis, C. V, Bartlett, R. K., Anderson, M. E. (2009). NIH Public Access, **133** (3), 462–474.

Ershler, W. B., Sun, W. H., Binkley, N., Gravenstein, S., Volk, M. J., Kamoske, G., Klopp, R. G., Roecker, E. B., Daynes, R. A., Weindruch, R. (1993) Interleukin-6 and ageing: blood levels and mononuclear cell production increase with advancing age and in vitro production is modifiable by dietary restriction. *Lymphokine Cytokine Res*. **12**, 225-230.

Esper, R. J., Nordaby, R. A., Vilariño, J. O., Paragano, A., Cacharrón, J. L., & Machado, R. A. (2006). Endothelial dysfunction : a comprehensive appraisal.

Biomed Central, **18**, 1–18.

Fernandez-Ortiz, A., Badiman, J. J., Fuster, V. (1999) Pathogenesis of atherosclerosis. *Con Conc Cardiol*, **217**, 3-18.

Ferrari, A. U., Radaelli, A., Centola, M., Alberto, U., Radaelli, A., & In-, M. C. (2003). Invited Review : Aging and the cardiovascular system. *J Appl Physiol*, **95**, 2591–2597.

Flammer, A. J., Anderson, T., Celermajer, D. S., Mark, A., Deanfield, J., Ganz, P., … Vita, J. A. (2013). The assessment of endothelial function - from research into clinical practice. *Circulation*, **126** (6), 753–767.

Förstermann, U., & Münzel, T. (2006). Basic Science for Clinicians Endothelial Nitric Oxide Synthase in Vascular Disease. *Circulation*, **105**, 1708–1715.

Frantz, S., Bauersachs, J., & Ertl, G. (2009). Post-infarct remodelling : contribution of wound healing and inflammation. *Cardiovasc Res*, **292**, 474–481.

Fried, L. P., Tangen, C. M., Walston, J., Newman, A. B., Hirsch, C., Gottdiener, J., Seeman, T., Tracy, R., Kop, W. J., Burke, G., McBurnie, M. A. (2001) Frailty in older adults: evidence for a phenotype. *J gerontol A Biol Sci Med*, **56** (3), 146-156.

Gabay, C. & Kushner, I. (1999) Acute-phase proteins and other systemic responses to inflammation. *N Engl J Med.*, **340**, 448-454.

Gamble, C., McIntosh, K., Scott, R., Ho, K. H., Plevin, R., Paul, A. (2012) Inhibitory kappa B kinases as targets for pharmacological regulation. *Br J Pharmacol.* **165**, 802-819.

Gareus, R., Kotsaki, E., Xanthoulea, S., Made, I. Van Der, Gijbels, M. J. J., Kardakaris, R., Pasparakis, M. (2008). Article Endothelial Cell-Specific NF- k B Inhibition Protects Mice from Atherosclerosis. *Cell Metabolism*, **8**(5), 372–383.

Geninatti, T., Bruno, G., Barile, B., & Hood, R. L. (2015) Impedance characterisation, degradation and in vitro biocompatibiltiy for platinum electrodes on BioMEMS. *Biomed Microdevices*, **17** (1), 1–23.

Gerondakis, S., Fulford, T. S., Messina, N. L., Grumont, R. J. (2014) NF-kB control of T cell development. *Nat Immunol Rev*, **15**, 15-25.

Gill, R., Tsung, A., Billiar, T. (2010) Linking oxidative stress to inflammation: Toll-like receptors. *Free radical biology*. **48**, 1121-1132.

Ghosh, S., Karin, M., & Haven, N. (2002). Missing Pieces in the NF- κB Puzzle. *Cell Vol*, **109**, 81–96.

Goldspink, D. F., Burniston, J. G., & Tan, L. (2003). Cardiomyocyte death and the ageing and failing heart. *Experimental Physiology*, **88** (3), 447-458.

Gordon, D. J., Probstfield, J. L., Garrison, R. J., Neaton, J. D., Castelli, W. P., Knoke, J. D., … Tyroler, H. A. (1988). High-Density Lipoprotein Cholesterol and Cardiovascular Disease Four Prospective American Studies. *Circulation,* **79** (1), 8-15.

Gradinaru, D., Borsa, C., Ionescu, C., & Ioan, G. (2015). Oxidized LDL and NO synthesis — Biomarkers of endothelial dysfunction and ageing. *Mechanisms of Ageing and Development*, **151**, 101–113.

Haddad, J. J., Oliver, R. E., Land, S. C. (2000) Antioxidant/ pro-oxidant equilibrium regulates HIF-1α and NF-kB redox sensitivity: evidence for inhibition by glutathione oxidation in alveolar epithelial cells. *J Biol Chem*. **275**, 21130-21139.

Haddad, J. J. (2002) Redox and oxygen-sensitive transcription factors in the regulation of oxidant-mediated lung injury: role for nuclear factor-kB. *Critical Care*. **6**, 481-490.

Hafner, V., Dai, J., Gomes, A. P., Xiao, C. Y., Palmeira, C. M., & Sinclair, D. A. (2010). Regulation of the mPTP by SIRT3 - mediated deacetylation of CypD at lysine 166 suppresses age - related cardiac hypertrophy. *Impact Aging*, **2** (12), 914–923.

Harman, D. (1956) Ageing: A theory based on free radical and radiation chemistry.

J. Gerontol. **21**, 560-565.

Harman, D. (1981). The aging process. *Proc Natl Acad Sci*, **78** (11), 7124–7128.

Harrison, D. G., Gongora, M. C., Guzik, T. J., & Widder, J. (2007). Oxidative stress and hypertension. *J Am Soc Hypert*, **1** (1), 30–44.

Harvey, A., Montezano, A. C., & Touyz, R. M. (2015). Vascular biology of ageing — Implications in hypertension Young - Healthy Aged - Hypertension Media Normal Vascular Homeostasis M : L ratio. *Journal of Molecular and Cellular Cardiology*, **83,** 112–121.

Hayflick, L. (1965) The limited in vitro lifetime of human diploid cell strains. *Exp Cell Res.* **37**, 614-636.

Hazudas, D. J., Lees, J. C., & Youngsv, P. R. (1988). The Kinetics of Interleukin 1 Secretion from Activated Monocytes la and interleukin. *J Biol Chem*, **263** (17), 8473–8479.

Helenius, M., Hanninen, M., Lehtinen, S. K., Salminen, A. (1996) Changes associated with ageing and replicative senescence in the regulation of transcription factor-kappa B. *Biochem J*. **318**, 603-608.

Herscovitch, M., Comb, W., Ennis, T., Coleman, K., Yong, S., Kalaitzidis, D., … Gilmore, T. D. (2009). Intermolecular disulfide bond formation in the NEMO dimer requires Cys54 and Cys347. *Biochem Biophys Res Com*, **367** (1), 103–108.

Higashi, Y., Noma, K., Yoshizumi, M., & Kihara, Y. (2009). Endothelial Function and Oxidative Stress in Cardiovascular Diseases. *Circ J*, **73**, 411–418.

Hoch, B., Haase, H., Schulze, W., Hagemann, D., Morano, I., Krause, E. G., Karczewski, P. (1998) Differentiation-dependent expression of cardiac delta-CaMKII isoforms. *J Cell Biochem*. **68**, 259-268.

Horn, M. A., & Trafford, A. W. (2016). Journal of Molecular and Cellular Cardiology

Aging and the cardiac collagen matrix : Novel mediators of fi brotic remodelling. *Journal of Molecular and Cellular Cardiology*, **93**, 175–185.

Hosokawa, S., Haraguchi, G., Sasaki, A., Arai, H., Muto, S., Itai, A., … Isobe, M. (2013). Pathophysiological roles of nuclear factor kappaB (NF-kB) in pulmonary arterial hypertension : effects of synthetic selective NF-kB inhibitor IMD-0354. *Circ Res*, **2**, 35–43.

House, S. J., Ginnan, R. G., Armstrong, S. E., & Singer, H. A. (2007). Calcium / calmodulin-dependent protein kinase II- δ isoform regulation of vascular smooth muscle cell proliferation. *Am J Physiol Cell Physiol,* **3479**, 2276–2287.

Howe, C. J., Lahair, M. M., Mccubrey, J. A., & Franklin, R. A. (2004). Redox Regulation of the Calcium / Calmodulin-dependent Protein Kinases. *J Biol Chem*, **279** (43), 44573–44581.

Hu, P., Zhang, D., Swenson, L., Chakrabarti, G., Abel, E. D., Litwin, S. E., … Min-, S. E. L. (2003). Minimally invasive aortic banding in mice : effects of altered cardiomyocyte insulin signaling during pressure overload. *Am J Physiol Heart Circ Physiol*, **84132,** 1261–1269.

Hudmon, A and Schulman, H. (2002) Structure-function of the multifunctional Ca^{2+}/Calmodulin-dependent protein kinase II. *Biochem J*. **364**, 593-611.

Hudmon, A., Schulman, H., Kim, J., Maltez, J. M., Tsien, R. W., & Pitt, G. S. (2005). CaMKII tethers to L-type Ca 2+ channels, establishing a local and dedicated integrator of Ca 2+ signals for facilitation. *J Cell Biol*, **171** (3), 537–547.

Hughes, K., Edin, S., Antonssan, A., Grundstrom, T. (2001) Calmodulin-dependent kinase II mediates T cell receptor/CD3- and phorbol ester-induced activation of IκB kinase. *J Biol Chem*. **276**, 36008-36013.

Hughes, G., Murphy, M. P., & Ledgerwood, E. C. (2005). Mitochondrial reactive oxygen species regulate the temporal activation of nuclear factor κ B to modulate tumour necrosis factor-induced apoptosis : evidence from mitochondria-targeted

antioxidants. *Biochem J*, **89**, 83–89.

Hunt, M. A., Currie, M. J., Robinson, B. A., & Dachs, G. U. (2010). Optimizing Transfection of Primary Human Umbilical Vein Endothelial Cells Using Commercially Available Chemical Transfection Reagents. *J Biochem Tech*, **21**, 66–72.

Ishida, A., Shigeri, Y., Tatsu, Y., Uegaki, K., Kameshita, I., Okuno, S., Y, H. F. (1998). Critical amino acid residues of AIP , a highly speci ¢ c inhibitory peptide of calmodulin-dependent protein kinase II. *FEBS Letters*, **427,** 115–118.

Ishiguro, K., Green, T., Rapley, J., Wachtel, H., Xavier, R. J. (2006). Ca2+/ Calmodulin-dependent protein kinase II is a modulator of CARMA1 mediated NF-kB activation Ca 2+/Calmodulin-Dependent Protein Kinase II Is a Modulator of CARMA1-Mediated NF- κB Activation. *Mol Cell Biol,* **26** (14), 5497-5508.

Islam, K. N., & Koch, W. J. (2012). Involvement of Nuclear Factor κ B (NF-κB) Signaling Pathway in Regulation of Cardiac G Protein-coupled Receptor Kinase. *J Biol Chem*, **287** (16), 12771–12778.

Izzo, J. L. and Shykoff, B. E. (2001) Arterial stiffness: Clinical relevance, measurement and treatment. *Rev Cardiovasc Med*. **2** (1), 29-34.

Jang, M. K., Goo, Y. H., Sohn, Y. C., Kim, Y. S., Lee, S. K., Kang, H., Cheong, J., Lee, J. W. (2001) Ca2+/Calmodulin-dependent protein kinase IV stimulates nuclear factor-κB transactivation via phosphorylation of the p65 subunit. *J Biol Chem*. **276**, 20005-20010.

Jelonek, K., Walaszczyk, A., Gabryś, D., Pietrowska, M., Kanthou, C., & Widłak, P. (2011). Cardiac endothelial cells isolated from mouse heart - a novel model for radiobiology. *ABP*, **58** (14857).

Jenny, N. (2012) Inflammation in aging: Cause, effect or both? *Discov Med*., 13 (**73),** 451-460.

Jin, F., & Chung, F. (2001). Minimizing perioperative adverse events in the elderly. *British J Anasthesia*, **87** (4), 608–624.

Judge, S., Jang, Y. M., Smith, A., Hagen, T., & Leeuwenburgh, C. (2011). Age-associated increases in oxidative stress and antioxidant enzyme activities in cardiac interfibrillar mitochondria : implications for the mitochondrial theory of aging. *FASEB*, **19** (3), 419–422.

Kabe, Y., Ando, K., Hirao, S., Yoshida, M., Handa, H. (2005) Redox regulation of NF-kB activation: distinct redox regulation between the cytoplasm and the nucleus. *Antioxid Redox Signal*. **7**, 395-403.

Kadl, A., Leitinger, N (2005) The role of endothelial cells in the resolution of acute inflammation. *Antiox Redox Signal*, **7** (11-12), 1744-1754.

Kanda, T. K., & Akahashi, T. T. (2003). Interleukin-6 and Cardiovascular Diseases. *Jpn Heart J*, **45** (2), 183–193.

Kannel, W. B. (1998). Overview of Atherosclerosis. *Clin Therap*, **20**, 2-17.

Karamanlidis, G., Garcia-menendez, L., Kolwicz, S. C., & Lee, C. F. (2014). Promoting PGC-1 -driven mitochondrial biogenesis is detrimental in pressure-overloaded mouse hearts, *ajpheart* ,1307–1316.

Kashiwase, K., Higuchi, Y., Hirotani, S. Yamaguchi, O., Hikoso, S., Takeda, T., Watanabe, T., Taniike, M., Nakai, A., Tsujimoto, I., Matsumura, Y., Ueno, H., Nishida, K., Hori, M., Otsu, K. (2005) CaMKII activates ASK1 and NF-κB to induce cardiomyocyte hypertrophy. *Biochem and Biophys Res Commun*. **327**, 136-142.

Kassiri, Z., Oudit, G. Y., Sanchez, O., Dawood, F., Mohammed, F. F., Nuttall, R. K., Khokha, R. (2005). Matrix Metalloproteinase Inhibition Prevents Heart Failure After Pressure Overload in Tissue Inhibitor of Metalloproteinase-3 Knock-Out Mice. *Circ*

Res, **97**, 380-390.

Kastrati, A., Koch, W., Berger, P. B., Mehilli, J., Stephenson, K., Neumann, F., Scho, A. (2000). Protective Role Against Restenosis from an Interleukin-1 Receptor Antagonist Gene Polymorphism in Patients Treated With Coronary Stenting, *Interven Cardiol*, **36** (7), 2168-2173.

Kempe, S., Kestler, H., Lasar, A., & Wirth, T. (2005). NF- k B controls the global pro-inflammatory response in endothelial cells : evidence for the regulation of a pro-atherogenic program. *Nucelic Acids Res*, **33** (16), 5308–5319.

Kinugawa, S., Tsutsui. H., Hayashidoni, S., Ide, T., Suematsu, N. and Satoh, S. (2000) Treatment with dimethyliourea prevents left ventricular remodelling and failure after experimental myocardial infarction in mice: role of oxidative stress. *Circ Res*. **87**, 392-398.

Kirchhefer, U., Schmitz, W., Scholz, H., Neumann, J. (1999) Activity of cAMP-dependent protein kinase and Ca^{2+}/calmodulin-dependent protein kinase in failing and non-failing human hearts. *Cardiovasc Res*. **42**, 254-261

Kobayashi, M., Inoue, K., Warabi, E., Minami, T., & Kodama, T. (2005). A Simple Method of Isolating Mouse Aortic Endothelial Cells. *J Atheroscl & Thromb*, **12** (3), 138–142.

Kõks, S., Dogan, S., Guvenc, B., González-navarro, H., Potter, P., & Vandenbroucke, R. E. (2016). Mouse models of ageing and their relevance to disease. *Mechanisms of Ageing and Development*, **160**, 41–53.

Korhonen, P., Helenius, M., Salminen, A. (1997) Age-related changes in the regulation of NF-kB in rat brain. *Lett*. **225**, 61-64.

Kostis, J. B., Pietro, J. Di, Ed, M., Cosgrove, N., & Kuo, P. T. (1982). The Effect of Age on Heart Rate in Subjects Free of Heart Disease and Maximal Exercise Stress Test. *Circulation*, **65** (1), 141-145.

Koziel, A., Sobieraj, I., & Jarmuszkiewicz, W. (2015). Increased activity of mitochondrial uncoupling protein 2 improves stress resistance in cultured endothelial cells exposed in vitro to high glucose levels. *ajpheart,* **309**, 147–156.

Kreusser, M. M., Backs, J., & Menick, D. (2014). Integrated mechanisms of CaMKII-dependent ventricular remodeling, **5**, 1–8.

Krouwer, V. J. D., Hekking, L. H. P., Langelaar-makkinje, M., Regan-klapisz, E., & Post, J. A. (2012). Endothelial cell senescence is associated with disrupted cell-cell junctions and increased monolayer permeability. *Frontiers in Pharmacol*, **5** (36), 1–10.

Kwak, H. (2013). Effects of aging and exercise training on apoptosis in the heart. *J Exerc Rehab*, **9** (2), 212–219.

Kyi, K., Okuma, Y., Miyazaki, H., & Murayama, T. (2000). Changes in expressions of proinflammatory cytokines IL-1 b , TNF- a and IL-6 in the brain of senescence accelerated mouse. **885**, 25–31.

Lakatta, E. G. (1987) Cardiac muscle changes in senescence. *Am Rev Physiol*, **49**, 519-531.

Lakatta, E. G. and Levy, D. (2003) Arterial and cardiac ageing: Major shareholders in cardiovascular disease enterprises: Part 1: Ageing arteries 'set up' for vascular disease. *Circulation*. **107** (1), 139-146.

Lavrovsky, avrovsky, Y., Chatterjee, B., Clark, R. A., Roy, A. K. (2000) Role of redox-regulated transcription factors in inflammation, aging and age-related diseases. *Exp Gerontol,* **35** (5), 521-532.

Lambeth, J. D. (2004) NOX enzymes and the biology of reactive oxygen. *Nat Rev Immunol*. **4**, 181-189.

Lawrence, T., Gilroy, D. W., Colwille-Nash, P. R., Willoughby, D. A. (2001) Possible new role for NF-kB in the resolution of inflammation. *Nat med*, **7**, 1291-1297.

Lerman, A. and Zeiher, A. M. (2005) Endothelial function: cardiac events. *Circulation*. **111** (3), 363-368.

Li, Z., Froehlich, J., Galis, Z. S., Lakatta, E. G. (1999) Increased expression of matrix metalloproteinase-2 in the thickened intima of aged rats. *Hypertension*. **33**, 116-123.

Li, W., Li, H., Sanders, P. N., Mohler, P. J., Backs, J., Olson, E. N., Grumbach, I. M. (2011). The Multifunctional Ca 2+/Calmodulin-dependent Kinase II delta(CaMKIIδ) Controls Neointima Formation after Carotid Ligation and Vascular Smooth Muscle Cell Proliferation through Cell Cycle Regulation by p21. *J Biol Chem*, **286** (10), 7990–7999.

Linnane, A. W., Kios, M., Vietta, L. (2007) Healthy ageing: regulation of the metabolome by cellular redox modulation and pro-oxidant signalling systems: the essential roles of superoxide anion and hydrogen peroxide. *Biogerontology*. **8**, 445-467.

Lu, M., Yang, C. B. O., Gao, L., & Zhao, J. I. (2015). Mechanism of subclinical hypothyroidism accelerating endothelial dysfunction. *Exp Therap Med*, **9**, 3–10.

Luczak, E. D. & Anderson, M. E, (2014) CaMKII oxidative activation and the pathogenesis of cardiac disease. *J Mol Cell Cardiol*, **73**, 112-116.

Maack, C., Kartes, T., Kilter, H., Schafers, H. J., Nickenig, G., Bohn, M. and Laufs, U. (2003) Oxygen free radical release in human failing myocardium is associated with increased activity of Rac 1-GTPase and represents a target for statin therapy. *Circulation*. **108**, 1567-1574.

Madjid, M., Awan, I., Willerson, J. T., & Casscells, S. W. (2004). Leukocyte Count and Coronary Heart Disease Implications for Risk Assessment. *Journal of the American College of Cardiology*, **44** (10), 1945–1956.

Maggio, M., Basaria, S., Ble, A., Lauretani, F., Bandinelli, S., Ceda, G. P., Ferrucci, L. (2006). Correlation between Testosterone and the Inflammatory Marker Soluble Interleukin-6 Receptor in Older Men, *91*(1), 345–347. https://doi.org/10.1210/jc.2005-1097

Maier, L. S., Bers, D. M. (2002) Calcium, calmodulin and calcium-calmodulin kinase II: heartveat to heartbeat and beyond. *J Mol Cell Cardiol*, **34** (8), 919-939.

Maione, A. S., Cipolletta, E., Sorriento, D., Borriello, F., Soprano, M., Rusciano, M. R., Illario, M. (2017). Cellular subtype expression and activation of CaMKII regulate the fate of atherosclerotic plaque. *Atherosclerosis*, **256**, 53–61.

Mallavia, B., Recio, C., Oguiza, A., Ortiz-muñoz, G., Lazaro, I., Lopez-parra, V., Gomez-guerrero, C. (2013). Peptide Inhibitor of NF- k B Translocation Ameliorates Experimental Atherosclerosis. *The American Journal of Pathology*, **182** (5), 1910–1921.

Marganski, W. A., Gangopadhyay, S. S., Je, H. D., Gallant, C., & Morgan, K. G. (2005). Targeting of a novel Ca2+/calmodulin-dependent protein kinase II is essential for extracellular signal-regulated kinase-mediated signaling in differentiated smooth muscle cells. *Circulation Research*, **97** (6), 541–549.

Marin-Garcia, J., Ahkmedov, A. T., Moe, G. W. (2013) Mitochondria in heart failure: The emerging role of mitochondrial dynamics. *Heart Failure Rev*, **18** (4), 439-456.

Martin, T. P. (2011) The role of CaMKIIδ in modulation of NF-kB signalling in normal and hypertrophied mouse hearts. (Doctoral thesis, University of Strathclyde); Thesis no. T13040.

Martin, T. P., Robinson, E., Harvey, A. P., Macdonald, M., Grieve, D. J., Paul, A., & Currie, S. (2012). Surgical optimization and characterization of a minimally invasive aortic banding procedure to induce cardiac hypertrophy in mice. *Exp Physiol*, **7**; 822–832.

Martin, T. P., Lawan, A., Robinson, E., Grieve, D. J., Plevin, R., Paul, A., Currie, S.

(2014) Adult cardiac fibroblast proliferation is modulated by calcium/calmodulin-dependent protein kinase II in normal and hypertrophied hearts. *Pflugers Arch*. **466**, 316-330.

Mattila, P. S., Ullman, K. S., Fiering, S., Emmel, E. A., McCutcheon, M., Crabtree, G. R., Herzenberg, L. A. (1990) The actions of cyclosporine A and FK506 suggest a novel step in the activation of T lymphocytes. *EMBO J*. **9**, 4425-4433.

McCay, C., Crowell, M. F., Maynard, L. A. (1935) The effect of retarded growth upon the length of lifespan and upon the ultimate body size: One figure. *J Nutr*., **10** (1), 63-79.

Mcguinness, R. (2007). Impedance-based cellular assay technologies : recent advances. future promise. *Curr Opin Pharmacol*, **7** (5); 535-540.

Mckinsey, T. A. (2007). Derepression of pathological cardiac genes by members of the CaM kinase superfamily. *j.cardiores,* **73**, 667–677.

Meffert, M. K., Chang, J. M., Wiltgen, B. J., Fanselow, M. S., Baltimore, D. (2003) NF kappa B functions in synaptic signalling and behavious. *Nat Neurosci*. **6**, 1072-1078.

Merat, S., Freubis, J., Stutphin, M., Silvestre, M., Reaven, P. D. (2000) Effect of aging on aortic expression of the vascular cell adhesion molecule-1 amd atherosclerosis in murine models of atherosclerosis. *J Gerontol Biol Sci Med Sci*., **55** (2), 85-94.

Morgan, M. J., & Liu, Z. (2011). Crosstalk of reactive oxygen species and NF-κB signaling. *Cell Research*, **21** (1), 103–115.

Morley, J. E., & Baumgartner, R. N. (2004). Cytokine-Related Aging Process. *J Gerontol A Biol Sci Med Sci,* **59** (9), 924–929.

Nakamura, K., Robertson, M., Liu, G., Dickie, P., Nakamura, K., Guo, J. Q., Michalak, M. (2001). Complete heart block and sudden death in mice overexpressing calreticulin. *J Clin Invest*, **107** (10), 1223–1225.

Nakou, E. S., Parthenakis, F. I., Kallergis, E. M., Marketou, M. E., Nakos, K. S., &

Vardas, P. E. (2016). Healthy aging and myocardium: A complicated process with various effects in cardiac structure and physiology. *International Journal of Cardiology*, **209,** 167–175.

North, B. J. and Sinclair, D. A. (2012) The intersection between ageing and cardiovascular disease. *Circ Res*. **110** (8) 1097-108.

O'Rourke, M. F., Hashimoto, J. (2007) Mechanical factors in arterial aging: a clinical perspective. *J Am Cell Cardiol*, **50** (1), 1-13.

Olivetti, G., Melissari, M., Capasso, J. M., Anversa, P. (1991) Cardiomyopathy of the ageing human heart. Myocyte loss and reactive cellular hypertrophy. *Circ Res*. **68**, 1560-1568.

Pamukcu, B., Lip, G. Y. H., & Shantsila, E. (2011). The nuclear factor − kappa B pathway in atherosclerosis : A potential therapeutic target for atherothrombotic vascular disease. *Thrombosis Research*, **128** (2), 117–123.

Parfrey, P. S., Foley, R. N., Hornett, J. D., Kent, G. M., Murray, D. C., Barre, P. E. (1996) Outcome and risk factors for left ventricular disorders in chronic uraemia. *Nephrol Dial Transplant*, **11** (7), 1277-1285.

Pate, M., Damarla, V., Chi, D. S., Negi, S., Krishnaswamy, G. (2010) Endothelial cell biology: Role in the inflammatory response. *Adv Clin Chem*., **52**, 109-130.

Pedersen, M., Bruunsgaard, H., Weis, N., Hendel, H. W., Andreassen, U., Eldrup, E., … Pedersen, B. K. (2003). Circulating le v els of TNF-alpha and IL-6-relation to truncal fat mass and muscle mass in healthy elderly indi v iduals and in patients with type-2 diabetes. *Mech Aging Dev*, **124**, 495–502.

Pfleiderer, P. J., Lu, K. K., Crow, M. T., Keller, R. S., Singer, H. A., Paul, J., Singer, H. A. (2004). Modulation of vascular smooth muscle cell migration by calcium / calmodulin-dependent protein kinase II- δ2. *Am Physiol Soc*, **12208,** 1238–1245.

Phipps, M., & Petricevic, S. (2007). The tendency of individuals to transfer DNA to

handled items. *Forensic Sci Int*, **168**, 162–168.

Pierce, G. L., Lesniewski, L. A., Lawson, B. R., Beske, S. D., & Seals, D. R. (2010). NF-kB activation contributes to vascular endothelial dysfunction via oxidative stress in overweight/obese middle-aged and older humans, *Circulation*, **119** (9), 1284–1292.

Poljsak, B., Šuput, D., & Milisav, I. (2013). Achieving the Balance between ROS and Antioxidants : When to Use the Synthetic Antioxidants, *Ox Med Cell Long,* **2013**, 119-128.

Potter, C. M. F., Lundberg, M. H., Harrington, L. S., Warboys, C. M., Warner, T. D., Berson, R. E., Mitchell, J. A. (2011). Role of Shear Stress in Endothelial Cell Morphology and Expression of Cyclooxygenase Isoforms. *Arterioscler Thromb Vasc Biol,* **31** (2), 384-391.

Poyet, J. L., Srinivasula, S. M., Lin, J-H, Fernandes-Alhemri, T., Yamaoka, S., Tsicholis, P. N. and Alnemri, E. S. (2000) Activation of the IKβ kinases by RIP via IKKγ/NEMO-mediated oligomerisation. *J Biol Chem*. **275**, 37966-37977.

Quinn, M. T., Ammons, M. C. B., & Leo, F. R. D. E. (2006). The expanding role of NADPH oxidases in health and disease : no longer just agents of death and destruction, *Clin Sci Lon*, **20**, 1–20.

Rahman, A and Fazal, F. (2011) Blocking NF-κB: An inflammatory issue. *Pro Am Thorac Soc*. **6**, 497-503.

Ramirez, M. T., Zhao, X-L., Schulman, H. and Brown, J. H. (1997) The nuclear delta B isoform of calcium/calmodulin-dependent protein kinase II regulates atrial natriuretic factor gene expression in ventricular myocytes. *J Biol Chem.* **272**, 31203-31208.

Rauscher, F. M., Goldschmidt-clermont, P. J., Davis, B. H., Wang, T., Gregg, D.,

Ramaswami, P., Annex, B. H. (2003) Aging, progenitor cell exhaustion and atherosclerosis. *Circulation*, **108** (4), 457–463.

Reiss, B., & Wegener, J. (2015). Impedance Analysis of Different Cell Monolayers Grown on Gold-Film Electrodes, *IEEE*, 7079–7082.

Roth, G. A., Huffman, M. D., Moran, A. E., Feigin, V., Mensah, G. A., Naghavi, M., & Murray, C. J. L. (2015). Global Burden of Cardiovascular Disease Global and Regional Patterns in Cardiovascular Mortality From 1990 to 2013 Measuring the Global Cardiovascular. *Circulation*, **132** (17), 1667-1678.

Rubin, H. (1997) Cell aging in vivo and in vitro. *Mech Aging Dev.*, **98** (1), 1-35.

Sadowska-bartosz, I., & Bartosz, G. (2014). Effect of Antioxidants Supplementation on Aging and Longevity, *Biomed Res*, **2014.**

Sakurai, H., Chiba, H., Miyoshi, H., Sugita, T., & Toriumi, W. (1999). Communication IkB Kinases Phosphorylate NF- κB p65 Subunit on Serine 536 in the Transactivation Domain. *Oncogene*, **25** (51), 30353–30357.

Sato, S., Sanjo, H., Takeda, K., Ninomiya-tsuji, J., Yamamoto, M., Kawai, T., … Akira, S. (2005). Essential function for the kinase TAK1 in innate and adaptive immune responses, *Nat Immunol*, **6** (11), 1087–1095.

Satoh, M., Nakamura, M., Satoh, H., & Saitoh, H. (2000). Expression of Tumor Necrosis Factor-alpha – Converting Enzyme and Tumor Necrosis Factor-alpha in Human Myocarditis. *Journal of the American College of Cardiology*, **36** (4), 1288–1294.

Schulman, H., & Greengard, P. (1978). Ca2+-dependent protein phosphorylation system in membranes from various tissues, and its activation by "calcium-dependent regulator". *Proc Natl Acad Sci U S A*, **75** (11), 5432–5436.

Scioli, M. G., Stasi, M. A., Passeri, D., Doldo, E., Costanza, G., Camerini, R., Pace, S. (2014). Propionyl- L -Carnitine is Efficacious in Ulcerative Colitis Through its Action on the Immune Function and Microvasculature, **5** (3), e55-14.

Scott, J. A., Klutho, P. J., Accaoui, R. El, Nguyen, E., Venema, A. N., Xie, L.,

Grumbach, I. M. (2013). The Multifunctional Ca2+/Calmodulin-Dependent Kinase II d (CaMKII d) Regulates Arteriogenesis in a Mouse Model of Flow-Mediated Remodeling. *PLoS One*, **8** (8).

Seals, D. R., Jablonski, K. L., & Donato, A. J. (2012). Aging and vascular endothelial function in humans. *Clin Sci Lond*, **120** (9), 357–375.

Seals, D. R., Kaplon, R. E., Gioscia-ryan, R. A., & Larocca, T. J. (2014). You ' re Only as Old as Your Arteries : Translational Strategies for Preserving Vascular Endothelial Function with Aging. *Physiology (Bethesda)*, **29** (4), 250–264.

Selaas, O., Nordal, H. H., Halse, A., Brun, J. G., Jonsson, R., & Brokstad, K. A. (2015). Serum Markers in Rheumatoid Arthritis : A Longitudinal Study of Patients Undergoing Infliximab Treatment, *Int J Rheumatol*, **2015**.

Sengupta, P. (2013) The laboratory rat: relating its age with humans. *Int J Prev Med.*, **4** (6), 624-630.

Schmidt, C., Peng, B., Li, Z., Sclabas, G. M., Fujioka, S., Niu, J., Schmidt-Supprion, M., Evans, D. B., Abbruzzese, J. L. and Chiao, P. J. (2003) Mechanisms of pro-infammatory cytokine induced biphasic NF-kB activation. *Mol Cell*. **12**, 1287-1300.

Sen, R. and Baltimore, D. (1986) Multiple nuclear factors interact with the immunoglobulin enhancer sequences. *Cell*. **46**, 705-716.

Sherwood, L. (2003) Human Physiology: From cells to systems, 5th ed. Brooks. Cole.

Singer, H. A. (2012). Ca 2 + / calmodulin-dependent protein kinase II function in vascular remodelling. *J Physiol*, **6**, 1349–1356.

Singh, M. V, Kapoun, A., Higgins, L., Kutschke, W., Thurman, J. M., Zhang, R., Anderson, M. E. (2009). Ca 2 + / calmodulin-dependent kinase II triggers cell

membrane injury by inducing complement factor B gene expression in the mouse heart. *J Clin Invest*, **119** (4), 986-989.

Singh, M and Anderson, M. E. (2011) Is CaMKII a link between inflammation and hypertrophy in heart? *J Mol Med*. **89**, 537-543.

Singh, M. V., Swaminathan, P. D., Luczak, E. D., Kutschke, W., Weiss, R. M., Anderson, M. E. (2012) MyD88 mediated inflammatory signalling leads to CaMKII oxidation, cardiac hypertrophy and death after myocardial infarction. *J Mol Cell Cardiol*. **52**, 1135-1144.

Skelding, K. and Rostas, J. (2009) Regulation of CaMKII in vivo: The importance of targeting and the intracellular microenvironment. *Neurochem Res*. **34**, 1792-1804.

Spinetti, G., Wang, M., Monticone, R., Zhang, J., Zhao, D., & Lakatta, E. G. (2004). Rat Aortic MCP-1 and Its Receptor CCR2 Increase with age and alter vascular smooth muscle cell function, *Atheroscler Thromb Vasc Biol,* **24** (8), 1397-1402..

Soderling, T. R., Chang, B., Brickey, D. (2001) Cellular signalling through multifunctional Ca^{2+}/Calmodulin-dependent protein kinase II. *J Biol Chem*. **276**, 3719-3722.

Sohal, R. S. & Sohal, B. H. (1991) Hydrogen peroxide release by mitochondria increases during aging. *Mech Aging & Dev*., **57** (2) 187-202.

Solleveld, H. A. and Hollander, C. F. (1984) Animals in ageing research: requirements, pitfalls and a challenge for the laboratory animal specialist. The Veterinary Quarterly. *AGRIS*, **6**, 96-101.

Sun, T. A. O., Green, N. G., & Morgan, H. (2008). Single-cell microfluidic impedance cytometry: A review. *Microfluidics & nanofluidics*, **8** (4), 423-443.

Takeuchi, M. and Fujisawa, H. (1998) New alternatively spliced variants of calmodulin-dependent protein kinase II from rabbit liver. *Gene*. **221**, 107-115.

Terman, A., Kurz, T., Navratil, M., Arriaga, E. A., Brunk, U. T., Rossignol, R., & Sohal, R. S. (2010). Mitochondrial Turnover and Aging The Mitochondrial − Lysosomal Axis Theory of Aging. *Antioxid Redox Signal*, **12** (4), 503-535.

Tracy, R. P. (2003) Emerging relationships of inflammation, cardiovascular disease and chronic diseases of aging. *Int J Obes Relat Metab Disord.*, **27** (3), 29-34.

Trinity, J. D., Groot, H. J., Layec, G., Rossman, M. J., Stephen, J., Richardson, R. S., … City, S. L. (2015). Passive leg movement and nitric oxide-mediated vascular function: the impact of age. *Am Physiol Soc*, **308** (6), 1019–1025.

Tostes, R. C. A., Wilde, D. W., Bendhack, L. M. and Webb, R. C. (1997) Calcium handling by vascular myocytes in hypertension. *Brazillian Journal of Medical and Biological Research*. **30**, 315-323.

Tsay, H. J., Shyang-longwang, H. P. (2000). Age-Associated Changes of Superoxide Dismutase and Catalase Activities in the Rat Brain. *J Biomed Sci*, **7** (6), 466-474.

Turrens, J. F. (2003). Mitochondrial formation of reactive oxygen species. *J Physiol*, **2**, 335–344.

Ungvari, Z., Orosz, Z., Labinskyy, N., Rivera, A., Xiangmin, Z., Smith, K., Csiszar, A. (2007) Increased mitochondrial H_2O_2 production promotes endothelial NF-κB activation in aged rat arteries. *Am J Physiol Heart Circ Physiol*. **293**, 37-47.

Ureshino, R. P., Rocha, K. K., Lopes, G. S., Trindade, C. B., Smaili, S. S. (2014) Calcium signalling alterations, oxidative stress and autophagy in ageing. *Antiox and Redox Sign*. **21** (1).

Valen, G., & Yan, Z. (2001). Nuclear Factor Kappa-B and the Heart. *J Am Coli Cardiol*, **38** (2). 307-314.

Van der Loo, B., Lobugger, R., Skepper, J. N., Bachschmid, M., Kilo, J., Powell, J.
M., Palacios-Callender, M., Erusalmsky, J. D., Quaschning, T., Malinski, T.,
Gygi, D., Ulrich, V., Luscher, T. F. (2000) Enhanced peroxynitrite formation
is associated with vascular ageing. *J. Exp. Med*. **192**, 1731-1744.

Vander, A., Sherman, J. and Luciano, D. (1998) Chapter 14: Circulation, Section C:
The heart. Human Physiology: The mechanisms of Body Function.

Van der Loo, B., Schildknecht, S., Zee, R., Bachschmid, M. M. (2009) Signalling
processes in endothelial ageing in relation to chronic oxidative stress and
their potential therapeutic implications. *Exp Physiol*. **94**, 305-310.

Van der Heiden, K., Cuhlmann, S., Luong, L. A., Zakkar, M. and Evans, P. C.
(2010) Role of nuclear factor kappa B in cardiovascular health and disease.
Clin Sci. **118**, 593-605.

Vina, J., Borras, C., Miquel, J (2007). Critical Review Theories of Ageing. *Informa*,
59, 249–254.

Virmani, R., Avolio, A. P., Mergner, W. J., Robinowitz, M., Herderick, E. E.,
Cornhill, J. F., Guo, S. Y., Liu, T. H., Ou, D. Y., O'Rourke, M. (1991) Effect
of ageing on aortic morphology in populations with high and low prevalence
of hypertension and atherosclerosis. Comparison between occidental and
Chinese communities. *Arn J Pathol*. **139** (5), 1119-1129.

Walford, R. L., Weber, L., Panov, S. (1995) Caloric restriction and aging as viewed
from a Biosphere 2. *Receptor*, **5** (1), 29-33.

Walston, J., McBurnie, M. A., Newman, A. Tracy, R. P., Kop, W. J., Hirsch, C. H.,
Gottdiener, J., Fried, L. P. (2002) Frailty and activation of the inflammation and

coagulation systems with and without clinical comborbidities. *Arch Intern Med*, **162** (20), 2333-23.

Wang, Y., & Anderson, M. (2012). Intracellular Signaling Pathways in Cardiac Remodeling. Muscle: Fundamental Biology and Mechanisms of Disease (First Edition). *Elsevier Inc.*

Wang, Z., Ginnan, R., Abdullaev, I. F., Trebak, M., Vincent, P. A., & Singer, H. A. (2010). Calcium/calmodulin-dependent protein kinase II delta 6 (CaMKIIdelta 6) and RhoA involvement in thrombin-induced endothelial barrier dysfunction. *Journal of Biological Chemistry*, **285** (28), 21303–21312.

Wheeler, H. E., & Kim, S. K. (2011). Genetics and genomics of human ageing. *Physiol Trans R Soc Lond Biol Sci*, **366** (1561) 43–50.

Widlansky, M. E., Gokce, N., Keaney, J. F., & Vita, J. A. (2003). The Clinical Implications of Endothelial Dysfunction. *Journal of the American College of Cardiology*, **42** (7), 1149–1160.

Williamson, K. A., Hamilton, A., John, A., Sipos, P., Crocker, I., Stringer, S. E., & Alexander, Y. M. (2013). Aging Cell, (November 2012), 139–147.

Wind, S., Beuerlein, K., Armitage, M. E., Taye, A., Kumar, A. H. S., Janowitz, D., … Schmidt, H. H. H. W. (2010). Oxidative Stress and Endothelial Dysfunction in Aortas of Aged Spontaneously Hypertensive Rats by NOX1 / 2 Is Reversed by NADPH Oxidase Inhibition. *Hypertension*, **56** (3), 490-497.

Woodfin, A., Voisin, M., & Nourshargh, S. (2007). PECAM-1 : A Multi-Functional Molecule in Inflammation and Vascular Biology. *Atheroscler Thromb Vasc Biol*, **27** (12), 2514-2523.

Yentis, S. M., Rowbottom, A. W., Riches, P. G., & Cross, C. (1995). Detection of cytoplasmic IL-1beta in peripheral blood mononucelar cells from intensive care unit patients, *Clin Exp Immunol*, **100**, 330–335.

Zandi, E., Rothwarf, D. M., Delhase, M., Hayakawa, M., Karin, M. (1997) The IkB kinase complex (IKK) contains two kinase subunits, IKKα and IKKβ,

necessary for IkB phosphorylation and NF-kB activation. *Cell*. **91**, 243-252.

Zhang, R., Khoo, M. S. C., Wu, Y., Yang, Y., Grueter, C. E., Ni, G., Anderson, M. E. (2005). Calmodulin kinase II inhibition protects against structural heart disease. *Nature Medicine*, **11** (43), 409–417.

Zhang, T., & Brown, J. H. (2004). Role of Ca 2 +/calmodulin-dependent protein kinase II in cardiac hypertrophy and heart failure. *Cardiovasc Res*, **63**, 476–486.

Zhang, T., Maier, L. S., Dalton, N. D., Miyamoto, S., Ross, J., Bers, D. M., & Brown, J. H. (2003). The Delta c isoform of CaMKII is activated in cardiac hypertrophy and induces dilated cardiomyopathy and heart failure. *Circulation Research*, **92** (8), 912–919.

Zhang, G., Li, J., Purkayastha, S., Tang, Y., Zhang, H., Yin, Y., Li, B., Liu, G., Cai, D. (2013) Hypothalamic programming of systemic ageing involving IKK-β, NF-κB and GnRH. *Nature*. **497**, 211-218.

Zinovkin, R. A., Romaschenka, V. P., Galkin, I. I., Zakharova, V. V., Pletjushikina, O. Y., Chemyak, B. V., Popova, E. N. (2014) Role of mitochondrial reactive oxygen species in age-related inflammatory activation of endothelium. *Ageing*. **6** (8), 661-674.

Ziouzenkova, O., Perrey, S., Asatryan, L., Hwang, J., Macnaul, K. L., Moller, D. E., Plutzky, J. (2002). Lipolysis of triglyceride-rich lipoproteins generates PPAR ligands : Evidence for an antiinflammatory role for lipoprotein lipase. *Proc Natl Acad Sci*, **100** (5), 2730-2735.